



Molecular ecology of eukaryotic symbioses in the planktonic ecosystems of the oceanic photic zone

Nicolas Henry

► To cite this version:

Nicolas Henry. Molecular ecology of eukaryotic symbioses in the planktonic ecosystems of the oceanic photic zone. *Biodiversity and Ecology*. Université Pierre et Marie Curie - Paris VI, 2016. English.
NNT : 2016PA066181 . tel-01412337

HAL Id: tel-01412337

<https://theses.hal.science/tel-01412337>

Submitted on 8 Dec 2016

HAL is a multi-disciplinary open access archive for the deposit and dissemination of scientific research documents, whether they are published or not. The documents may come from teaching and research institutions in France or abroad, or from public or private research centers.

L'archive ouverte pluridisciplinaire **HAL**, est destinée au dépôt et à la diffusion de documents scientifiques de niveau recherche, publiés ou non, émanant des établissements d'enseignement et de recherche français ou étrangers, des laboratoires publics ou privés.



Université Pierre et Marie Curie

École doctorale Sciences de la Nature et de l'Homme : évolution et écologie

Adaptation et diversité en milieu marin UMR 7144 / Évolution des protistes et écosystèmes pélagiques

Écologie moléculaire des symbioses eucaryotes des écosystèmes planctoniques de la zone photique des océans

Par Nicolas Henry

Thèse de doctorat de Biologie marine

Dirigée par Colomban de Vargas et Stéphane Audic

Présentée et soutenue publiquement le 2 février 2016

Devant un jury composé de :

Dr Télesphore Sime-Ngando , Directeur de recherche, LMGE Université Blaise Pascal	Rapporteur
Pr. Jean-Louis Jamet , Professeur des universités, PROTEE-EBMA Université du Sud Toulon-Var	Rapporteur
Dr. Pascal Hingamp , Maître de conférences, IGS Aix Marseille Université	Examinateur
Dr. Yann Moalic , Maître de conférences, LM2E Université de Bretagne Occidentale	Examinateur
Pr. Bernard Kloareg , Professeur des universités, UPMC/CNRS Station Biologique de Roscoff	Examinateur
Dr. Stéphane Audic , Ingénieur de recherche, UPMC/CNRS Station Biologique de Roscoff	Co-directeur de thèse
Dr. Colomban de Vargas , Directeur de recherche, UPMC/CNRS Station Biologique de Roscoff	Directeur de thèse

Remerciements

Je tiens tout d'abord à remercier très chaleureusement mes directeurs de thèse, Colomban de Vargas et Stéphane Audic qui m'ont accompagné pendant ces trois ans.

Je remercie grandement Télesphore Sime-Ngando et Jean-Louis Jamet d'avoir accepté d'être les rapporteurs de ce manuscrit et également Pascal Hingamp, Yann Moalic et Bernard Kloareg d'avoir accepté de faire partie de mon jury de thèse en tant qu'examineurs.

Je remercie l'Université Pierre et Marie Curie qui a financé cette thèse.

Je remercie également tous les membres de l'équipe EPEP, anciens et actuels qui font le dynamisme de cette équipe et toutes les personnes de la station. Je remercie plus particulièrement Daniel, Cédric, Johan et Séb qui ont su m'accorder du temps, surtout en cette fin de thèse.

Merci Laetitia, Daniel (encore), Lionel, Bruno, Julie et Margaux pour tout ce que vous avez fait pour moi.

Je dédie ce manuscrit à mes parents.

Résumé

Les symbioses ont un rôle majeur dans le fonctionnement et l'équilibre des écosystèmes. Dans les océans, qui couvrent près de 70 % de la surface de la planète, vivent une multitude d'organismes incapables de lutter contre les courants et la plupart sont microscopiques, il s'agit du plancton. Les organismes du plancton, comme ceux d'autres écosystèmes, entretiennent des symbioses, mais la nature et l'ampleur de ces interactions sont encore mal connues dans le plancton du fait la petite taille de ces organismes et de la difficulté d'échantillonnage des écosystèmes planctoniques, surtout dans les zones les plus éloignées des côtes. Les principaux objectifs de cette thèse sont de donner un aperçu global de la place occupée par ces symbioses dans le plancton et de proposer des méthodes originales permettant leur détection. Les travaux présentés dans ce manuscrit s'appuient sur l'analyse des données générées lors de l'expédition *Tara Oceans* (2009-2013) pendant laquelle 210 stations océaniques ont été échantillonnées à travers le monde. Ils concernent plus précisément le jeu de données environnemental obtenu grâce au séquençage à haut débit (Illumina) de la région hypervariable V9 (130 nucléotides) de la sous-unité 18S de l'ADN ribosomique des organismes eucaryotes (metabarcoding). Dans un premier temps, un état des lieux de la diversité et de la structure des communautés du *pico-nano-micro-mesoplancton* (0,8-2000 µm) eucaryote de la zone photique des océans tempérés à tropicaux est réalisé. Il met en évidence la place importante occupée par les symbiotes au sein de ces communautés. Ensuite, l'étude de deux cas de symbiose (*Blastodinium*-Copépodes et *Symbiodinium*-*Tiarina*) montre les difficultés inhérentes à la détection de couples symbiotiques à partir d'un jeu de données issue d'études par metabarcoding du plancton (flexibilité de la spécificité des symbioses dans le plancton), mais aussi la possibilité de distinguer les différentes phases de vie des symbiotes (libres et symbiotiques) lorsque les échantillons étudiés ont été fractionnés. Enfin, un ensemble de méthodes est proposé afin d'améliorer l'efficacité de la détection de symbioses dans le cadre d'études par réseau de cooccurrences des communautés planctoniques. L'analyse de la distribution des metabarcodes le long des fractions de taille (*piconano-* (0.8-5 µm), *nano-* (5-20 µm), *micro-* (20-180 µm), et *meso-plancton* (180-2000 µm)) permet de différencier ceux provenant d'organismes symbiotiques de ceux d'organismes libres, sans a priori. De plus la comparaison de l'abondance de groupes génétiques définis à différents niveaux de résolution permet de détecter des associations symbiotiques peu spécifiques et d'apprécier leur niveau de spécificité.

Sommaire

Remerciements	1
Résumé	2
Sommaire	3
Introduction	4
La symbiose chez les protistes planctoniques	5
Étude du plancton océanique et des symbiotes qui le composent	10
Matériel et objectifs	13
Chapitre I	16
Eukaryotic plankton diversity in the sunlit ocean	22
Determinants of community structure in the global plankton interactome	52
Chapitre II	81
The symbiotic life of <i>Symbiodinium</i> in the open ocean within a new species of calcifying ciliate (<i>Tiarina</i> sp.)	85
Size-fractionated global DNA metabarcoding reveals ecological significance of the planktonic dinoflagellate parasite <i>Blastodinium</i> in sunlit oceans	125
Chapitre III	147
Unveiling photosymbiotic associations across phylogenetic gradients in world-wide marine plankton based on massive eukaryotic rDNA metabarcoding	153
Parasites diversity and abundance in the <i>Tara Oceans</i> dataset challenge classic views on marine plankton ecology	181
Conclusion et perspectives	206
Bibliographie	211
Liste des figures	218
Glossaire	219
Annexes	220
Liste des communications orales	220

Introduction

Les océans, qui couvrent 70 % de la surface la planète, constituent le plus grand écosystème de la planète. Les organismes les peuplant vivent pour la plupart en suspension dans la colonne d'eau et sont incapables de lutter contre les courants. Il s'agit du plancton qui est composé de virus, de bactéries, d'archées et d'eucaryotes (uni et multicellulaires). Les organismes photosynthétiques du plancton océanique (phytoplancton), regroupant des bactéries et des eucaryotes unicellulaires (protistes) sont à l'origine de près de la moitié de la production globale de dioxygène et initient la pompe biologique du carbone (Falkowski, 2012). Dans un contexte de changement globaux, l'étude du plancton, acteur majeur du cycle global du carbone, revêt une importance capitale. Il est en effet impossible d'anticiper les effets de l'élévation de la concentration du dioxyde de carbone atmosphérique sans avoir une connaissance fine de la structure et de la dynamique de ces écosystèmes.

Un écosystème, c'est un ensemble d'organismes vivants et de leur environnement physico-chimique interagissant en tant que système. Jusqu'à la naissance du concept de boucle microbienne (Azam *et al.*, 1983), la vue des écosystèmes planctoniques se limitait aux grandes espèces phytoplanctoniques (principalement des dinoflagellés et des diatomées), dont la croissance est dépendante de la lumière et des nutriments disponibles et qui servent de nourriture au zooplancton, principalement des copépodes (Steele, 1974). Depuis, l'étude du plancton a mis à jour une forte intensité d'interactions dans ces écosystèmes, où virus, bactéries, archées, protistes et métazoaires tiennent des rôles prépondérants (Worden *et al.*, 2015). Les protistes, du fait de leur large gamme de taille (4 ordres de grandeur de 10^{-2} à 10^6 m) et leurs modes de nutrition diversifiés (autotrophie, mixotrophie, hétérotrophie, symbioses) sont présents à tout les niveaux des écosystèmes planctoniques. Le développement de techniques moléculaires permettant de s'affranchir de la mise en culture des organismes étudiés (clonage, séquençage à haut débit, PCR quantitative) a permis de dévoiler une immense diversité de protistes du pico- et du nanoplancton aux modes trophiques diversifiés (Moon-van der Staay *et al.*, 2001; Diez *et al.*, 2001; López-García and Rodríguez-Valera, 2001). Cependant la biogéographie et la distribution des protistes du plancton reste assez peu connue du fait des difficultés inhérentes à leur étude, organismes microscopiques dans un environnement gigantesque et difficilement accessible. De plus, les connaissances actuelles de la diversité des interactions qui s'établissent entre ces protistes (symbiose, prédation, compétition), généralement acquises suite à la mise en culture de ces organismes, sont encore plus minces.

La symbiose chez les protistes planctoniques

La symbiose est une association intime et durable entre deux espèces différentes, selon la définition de Anton de Bary (de Bary, 1879). Elle englobe toutes les associations allant du parasitisme au mutualisme. Les symbioses (mutualisme, parasitisme et commensalisme) constituent avec la prédation et la compétition la majorité des interactions entre organismes. La description, l'analyse et la compréhension de ces interactions biotiques sont indispensables à l'étude de la structure et du fonctionnement des écosystèmes (Lidicker, 1979).

Dans le cas du parasitisme, un des partenaires (le parasite) tire profit de l'association aux dépens de l'autre (l'hôte). Le commensalisme caractérise une association dont l'un des partenaires tire profit sans que l'autre partenaire ne soit affecté ni positivement ni négativement. Lorsque les deux partenaires bénéficient de la symbiose, il s'agit de mutualisme. Il n'existe pas de frontières strictes entre ces différentes catégories, les symbioses s'inscrivent plutôt dans un continuum. La nature d'une symbiose entre deux organismes peut varier au cours du temps, soit du fait d'un changement des paramètres du milieu ou de l'état physiologique d'un des partenaires (Johnson *et al.*, 1997; van Ommeren and Whitham, 2002).

Alors que dans les environnements terrestres et aquatiques (benthiques) de nombreux travaux ont étudié l'écologie des symbioses au sens large, le rôle écologique des symbioses planctoniques marines est relativement peu étudié. Quelques travaux ont cependant souligné l'importance des photosymbioses dans les cycles biogéochimiques globaux, dont celui du carbone. Dans les déserts océaniques où l'accès aux nutriments est limité (zones oligotrophes), de grands protistes hétérotrophes (Acanthaires, Spumellaires, Collodaires) vivent en association avec des micro-algues (Haptophytes, Dinoflagellés, Chlorophytes). Cette association permet à ces méta-organismes de dominer ces environnements très pauvres où ils participent grandement à l'export de carbone vers les environnements profonds (Anderson, 1983; Lampitt *et al.*, 2009). Peu de symbiotes ont été caractérisés à la fois morphologiquement et génétiquement, empêchant ainsi une bonne compréhension de la dynamique de ces écosystèmes et de leur participation au cycle global du carbone. Les parasites semblent également tenir un rôle prépondérant dans le fonctionnement des écosystèmes planctoniques. Alors que les vrais parasites diminuent la valeur sélective de leur hôte comme le parasite de copépodes *Blastodinium* (Dinoflagellé) (Skovgaard *et al.*, 2012), les parasitoïdes quant à eux peuvent induire d'importantes mortalités chez les populations

d'hôtes. Certaines espèces du genre *Amoebophrya* (Syndiniales) peuvent avoir un impact important sur la dynamique des efflorescences de dinoflagellés jusqu'à dans certains cas les contrecarrer (Chambouvet *et al.*, 2008).

Phototrophie acquise

L'acquisition de la phototrophie par séquestration d'algues endosymbiotiques ou de leurs plastes est assez répandue parmi les protistes phagotrophes du plancton. La plupart de ces protistes sont alors capables de combiner hétérotrophie et phototrophie, ils sont alors mixotrophes. Les protistes mixotrophes, comprenant également les protistes ayant des chloroplastes permanents et acquérant une partie de leur énergie par phagotrophie, sont une composante majeure des protistes planctoniques. Leur abondance remet d'ailleurs en question l'application de la dichotomie phytoplancton-zooplancton, inspirée des écosystèmes terrestres (dichotomie plantes-animaux) (Flynn *et al.*, 2013), à l'écologie marine. Cependant, ces protistes sont encore peu connus, ce qui les rend difficiles à intégrer à des modèles écologiques. Seule une étude approfondie des différents modes de nutrition mixotrophes et de la biogéographie de ces organismes permettrait de réaliser des modélisations des écosystèmes planctoniques plus proches de la réalité que celles uniquement basées sur la dichotomie phytoplancton-zooplancton (Davidson, 2014).

Rétention d'organites

La rétention d'organites est un phénomène répandu chez les protistes mais est relativement limitée chez les métazoaires. Ce phénomène est plus fréquent dans les habitats marins que dans les habitats dulçaquicoles et est plus souvent observé dans les écosystèmes productifs (Stoecker *et al.*, 2009). La rétention d'organites, implique généralement l'enlèvement de plastides grâce à une modification du comportement de prédation et est alors appelée kleptoplastie. Ce mécanisme peut également impliquer l'assimilation de mitochondries, du cytoplasme, d'organites du système endomembranaires, voir du noyau des proies (Johnson *et al.*, 2007; Koike and Takishita, 2008). Parmi les protistes, les champions de la rétention d'organites sont les ciliés et les dinoflagellés, tous deux appartenant aux alvéolés. L'un des cas de rétention d'organites le plus emblématique est le complexe Cryptophyte - *Myrionecta rubra* - *Dinophysis* spp.. *Myrionecta rubra* dépend de l'ingestion de cryptophyte pour survivre. Suite à l'ingestion de proies, le cilié séquestre les plastes mais aussi le cytoplasme et les mitochondries en les entourant d'une membrane provenant de l'hôte. L'hôte

séquestre également un noyau permettant de réguler le fonctionnement des plastes. *Dynophysis* spp., qui est un dinoflagellé toxique, se nourrit de *Myrionecta rubra* par myzocytose. Il récupère alors les plastes de sa proie, à l'origine provenant de cryptophytes, pour les séquestrer à son tour (Nowack and Melkonian, 2010).

Endosymbiose

Dans les écosystèmes marins planctoniques, alors que la rétention d'organites chez les protistes est caractéristique des milieux eutrophes, les endosymbioses, pour la plupart photosynthétiques (on parle alors de photosymbioses), sont quant à elles caractéristiques des milieux oligotrophes (Stoecker *et al.*, 2009). L'endosymbiose est en général à l'origine d'une amélioration de la productivité de l'écosystème et d'une meilleure accumulation de la biomasse algale grâce à l'hôte qui fournit une protection contre la prédation et qui permet un recyclage plus efficace des métabolites (Trench, 1979). Les photosymbioses planctoniques impliquent généralement de grands protistes phagotrophes (Foraminifères et Radiolaires), hôtes de diverses micro-algues tels que des dinoflagellés, des haptophytes et des prasinophytes. Quelques espèces de dinoflagellés sont également connues pour être hôtes de micro-algues en milieu pélagique marin. C'est le cas d'*Amphisolenia* spp. en symbiose avec des pelagophytes (Daugbjerg *et al.*, 2013) et *Noctiluca scintillans* en symbiose avec un prasynophyte (*Pedinomonas noctilucae*). Ce dernier grâce à son symbiose peut former des efflorescences même dans des milieux oligotrophes (Madhu and Jyothibabu, 2012). Afin de maintenir de telles associations, l'hôte peut acquérir ses symbiotes par deux mécanismes. Soit par transmission verticale, c'est à dire que les symbiotes sont transmis à la cellule fille par la cellule mère lors des divisions mitotiques ou par le biais des gamètes, ou alors par transmission horizontale auquel cas les symbiotes sont directement acquis à partir du milieu environnant. La transmission horizontale serait le principal mode d'acquisition de symbiotes dans les écosystèmes planctoniques étant donné que de nombreux hôtes planctoniques ne possèdent pas de symbiotes au début et à la fin de leur cycle de vie (Shaked and de Vargas, 2006; Decelle *et al.*, 2012). Contrairement aux photosymbioses des habitats benthiques, comme celles entre les coraux et le dinoflagellé *Symbiodinium*, dans les habitats pélagiques oligotrophes, les populations de micro-algues symbiotiques en phase libre sont plus importantes que celles *in hospite*, très probablement pour faciliter la transmission horizontale dans un milieu où les chances de rencontre entre organismes sont faibles (Decelle, 2013). Les pressions de sélection sur les populations de micro-algues seraient donc plus importantes lorsqu'elles sont en phase libre. Ce qui expliquerait pourquoi la spécificité des

photosymbioses tend à être plus faible en milieu planctonique, où seules quelques espèces de micro-algues ont été décrites en symbiose avec une diversité importante d'hôtes (Decelle *et al.*, 2012; Probert *et al.*, 2014).

Parasitisme

Le parasitisme est considéré comme le mode de consommation le plus fréquent dans la nature et près de la moitié des espèces sur Terre pourrait être parasitaire (Meeûs and Renaud, 2002; Windsor, 1998). À l'échelle des écosystèmes, la biomasse de parasites est loin d'être négligeable et peut dépasser celle des superprédateurs dans les écosystèmes aquatiques (Kuris *et al.*, 2008). Alors que d'importants efforts ont été investis dans l'étude de l'écologie et de l'évolution des parasitoses du phytoplancton (Kagami *et al.*, 2007; Rasconi *et al.*, 2012) et du zooplancton (Burns, 1989; Decaestecker *et al.*, 2005) dulçaquicole, assez peu d'études ont abordé l'importance écologique du parasitisme dans le plancton marin à l'échelle des océans. Pourtant les protistes parasites y sont abondants, diversifiés et y infectent une large gamme d'hôtes (Skovgaard *et al.*, 2012; Jephcott *et al.*, 2016; Scholz *et al.*, 2016). On distingue généralement les vrais parasites, qui n'induisent pas directement la mort de leur hôtes, des parasitoïdes qui induisent systématiquement la mort de leur hôte pour achever leur cycle de vie.

Epibiontes

Dans les écosystèmes planctoniques, des protistes sont couramment observés vivant sur d'autres organismes, généralement des crustacés planctoniques. Il s'agit généralement de ciliés (*Zoothamnium* spp., *Paracineta* spp.) et de diatomées (*Pseudohimantidium* spp.). La densité d'épibiontes par hôte peut devenir très importante réduisant ainsi la motilité de ce dernier. Il est alors plus difficile pour l'hôte d'échapper à ses prédateurs.

Vrais parasites

Dans le plancton marin, les vrais parasites sont toujours associés à des métazoaires. Les copépodes qui sont d'important consommateurs de protistes planctoniques (diatomées, ciliés et dinoflagellés principalement), avec plus de 2500 espèces planctoniques marines (Razouls *et al.*, 2005), représentent un important réservoir d'hôtes pour ces parasites. Ils sont associés à une diversité élevée de protistes parasites (Ho and Perkins, 1985), principalement parmi les Alvéolés comme par exemple *Blastodinium* spp. (dinoflagellé) (Skovgaard *et al.*,

2012), les *Ellobiopsidae* (Protalveolata) (Walkusz and Rolbiecki, 2007), les ciliés apostomes (Ohtsuka *et al.*, 2004; Guo *et al.*, 2012) et *Cephaloidophora* spp. (Apicomplexe) (Gobillard, 1964). Alors que les espèces appartenant au genre *Blastodinium* ne sont associées qu'avec des copépodes planctoniques, les autres infectent d'autres crustacés planctoniques comme le krill (Euphausiacea) mais aussi des crustacés benthiques (*Balanus* spp.) dans le cas de *Cephaloidophora* spp.. Même si ces parasites n'induisent pas directement la mort de leur hôte, il diminuent la valeur sélective (fitness) de leur hôte, généralement en les privant d'une partie de leur énergie. Certains parasites sont qualifiés de castrateurs, c'est à dire qu'ils empêchent leur hôte de se reproduire. C'est le cas par exemple des femelles copépodes qui, lorsqu'elles sont infectées par *Blastodinium* spp., ne peuvent plus produire d'œufs.

Parasitoïdes

Les protistes parasitoïdes sont très abondants et très diversifiés dans le plancton. Ils peuvent être associés à des métazoaires et à d'autres protistes. Du fait de la vitesse de leur développement et de leur capacité à produire un nombre important de spores, ces parasites peuvent être très virulents et ont de ce fait un rôle très important dans la régulation des populations de protistes et de métazoaires planctoniques (principalement les copépodes). En environnement planctonique côtier, d'importants efforts ont été investis dans l'étude de la diversité et de la dynamique des protistes parasitoïdes infectant des micro-algues à l'origine d'efflorescences toxiques tel *Alexandrium* spp., *Karenia* spp. et *Dinophysis* spp. (Park *et al.*, 2004). Il a ainsi été démontré que *Amoebophrya* spp. (Syndiniales) et *Parvilucifera* spp. (Perkinsea) sont capables d'inhiber les efflorescences de leurs hôtes (Chambouvet *et al.*, 2008). Des parasites morphologiquement décrits comme appartenant au genre *Amoebophrya* sont également connus pour infecter d'autres protistes comme des radiolaires et des ciliés (Cachon, 1964). D'autres espèces de syndiniales ont été décrite en milieux planctonique. C'est le cas par exemple de *Syndinium turbo*, parasite de copépodes et le genre *Euduboscquella*, parasite de ciliés. De récentes analyses de séquences environnementales d'ADN ribosomique ont permis de dévoiler une importante diversité de ribotypes assignés à des syndiniales, ce qui suggère un rôle majeur de ces organismes dans les écosystèmes planctoniques à l'instar des virus (phages) régulant les populations de bactéries.

Étude du plancton océanique et des symbioses qui le composent

Contraintes de l'environnement pélagique

L'une des raisons expliquant une meilleure connaissance des symbioses des environnements terrestres et côtiers est la relative facilité d'échantillonnage des organismes les peuplant. Les écosystèmes planctoniques océaniques nécessitent des moyens importants pour être échantillonnés. Ainsi nous ne disposons généralement que de quelques instantanés de ces écosystèmes particuliers où les organismes sont très dilués. Ces derniers sont caractérisés par des taux métaboliques élevés et des durées de vie relativement courtes par rapport aux organismes terrestres. Les cellules phytoplanctoniques vivent quelques jours voir quelques semaines alors que les plantes terrestres vivent en général plusieurs mois (Smetacek, 2012). Il est donc relativement difficile dans le plancton d'observer des associations symbiotiques, durables à l'échelle des organismes impliqués, mais éphémères à notre échelle. La petite taille des organismes du plancton et parfois le manque de caractères morphologiques permettant leur identification sont également un frein à l'identification d'associations symbiotiques. Les symbioses le plus souvent observées dans le plancton impliquent des hôtes de grande taille, ayant une durée de vie relativement longue et/ou pour lesquels l'association est obligatoire (Rhizariens, copépodes).

Barcoding et metabarcoding

Le barcoding moléculaire (DNA barcoding) fut proposé en 2003 comme méthode permettant l'identification d'espèces (Hebert *et al.*, 2003). Cette méthode utilise de très courtes séquences génétiques d'une partie rigoureusement sélectionnée du génome (barcode) et les compare à des bases de données de référence afin de définir l'identité de l'organisme échantillonné. La région de gène utilisée comme barcode standard pour presque tous les animaux est une partie de 648 paires de bases du gène mitochondrial de la cytochrome c oxydase (COI). Chez les plantes, la COI n'évolue pas assez vite et des régions des gènes chloroplastiques de la maturase K (matK) et de la grande unité de la Rubisco (rbcL) sont alors classiquement utilisés. Avec l'avènement du séquençage à haut débit (454 et Illumina) le concept de metabarcoding fut formalisé (Taberlet and Coissac, 2012). Cette technique, à la différence du barcoding classique, vise à séquencer l'ensemble des barcodes d'un échantillon environnemental et non d'un organisme. Les protistes se caractérisent par une très importante

diversité phylogénétique, avec des lignées plus éloignées génétiquement entre elles que les plantes des animaux. Afin de couvrir l'ensemble des eucaryotes il est nécessaire de définir un marqueur génétique suffisamment conservé pour être présent chez tous les eucaryotes et assez résolutif pour différencier des genres voire des espèces. Il doit être également relativement court du fait de la faible taille des séquences obtenues par séquençage à haut débit (quelques centaines de nucléotides). Au début des années 2010, la région V9, une région hypervariable du gène ribosomique 18S, d'environ 130 nucléotides, est apparue comme un bon compromis pour étudier par metabarcoding les communautés eucaryotes provenant d'échantillons environnementaux (Amaral-Zettler *et al.*, 2009). Cet outil utilisable pour des échantillons anciens et actuels, a révolutionné le champ de l'écologie, et plus particulièrement les études de la biodiversité des micro-organismes. En plus de fournir une mesure de la richesse génétique des communautés étudiées, le metabarcoding permet, grâce au nombre de lectures associé à chaque metabarcode, d'obtenir leur abondance relative. Il est alors possible d'adapter les techniques d'écologie numérique à ce type de données afin d'en tirer des hypothèses sur la diversité et la dynamiques des communautés étudiées (Ji *et al.*, 2013).

Détection statistique des associations

Dans le contexte d'une étude de communautés naturelles par metabarcoding, il est possible, à partir des données d'abondance, de prédire des relations entre organismes en faisant le postulat que des patrons de distribution fortement non aléatoires sont induits par des processus écologiques (Faust and Raes, 2012). Prédire des associations à partir de ce principe est relativement aisé : quand deux espèces (ou entités génétiques) sont distribuées de manière similaire parmi différents échantillons, que leurs abondances sont positivement corrélées, il s'agit d'une association positive ; lorsque les distributions sont anti-corrélées, on parle d'association négative. Il est cependant difficile de faire le lien entre ces deux types d'association statistiques et les processus écologiques à leur origine. On peut cependant présumer, sans trop de risque de se tromper, que deux organismes en symbiose, c'est à dire formant une association intime et durable, devraient former une association statistiquement positive. Il semble cependant difficile de capturer des associations entre des parasitoïdes et leurs hôtes de cette manière car ils produisent un nombre considérable de propagules et leur association est relativement courte dans le temps. Ils peuvent donc être très abondants sous forme de propagules sans qu'il n'y ait d'hôtes à infecter. La comparaison des patrons d'abondance des entités génétiques issus d'études par metabarcoding apparaît, malgré ses

limites actuelles, comme étant une voie prometteuse pour la détection de nouvelles symbioses, en s'affranchissant d'une partie des contraintes de temps et d'argent inhérentes à l'étude des communautés planctoniques océaniques. Cependant ces techniques ne suffisent pas à elles seules à décrire de nouvelles symbioses. La description de nouvelles symbioses entre micro-organismes doit passer systématiquement par une observation directe du phénomène au microscope. Il est donc très important, lorsque l'on souhaite détecter de nouvelles symbioses à partir de données de metabarcoding, de disposer en parallèle d'échantillons biologiques fixés. La validation morpho-génétique d'une association statistique peut alors être exécutée rapidement en concentrant l'isolement et le séquençage des organismes correspondant à l'assignation taxinomique des metabarcodes corrélés dans l'échantillon où ces metabarcodes sont les plus abondants.

Matériel et objectifs

Le sujet de la thèse présentée dans ce manuscrit est l'étude de l'écologie des symbioses eucaryotes des écosystèmes planctoniques de la zone photique des océans. Ce vaste sujet a pu être abordé grâce aux données générées lors de l'expédition *Tara Oceans* (2009-2012) pendant laquelle 210 stations océaniques ont été échantillonnées à travers le monde. Les analyses ont été réalisées à partir des données obtenues à la suite du séquençage à haut débit (Illumina) de la région hypervariable V9 (~130 nucléotides) de la sous-unité 18S de l'ADN ribosomique des organismes eucaryotes (metabarcoding). Ce court fragment d'ADN, également appelé metabbarcode, a été séquencé à partir d'échantillons fractionnés par tailles d'organismes couvrant la majorité des protistes du plancton, c'est à dire le *piconano*, le *nano*, le *micro* et le *meso*-plancton correspondant respectivement aux gammes de taille 0.8-5, 5-20, 20-180 et 180-2000 µm. Les échantillons proviennent pour la plupart de deux profondeurs, la surface et la DCM (Deep Chlorophyll Maximum), cette dernière étant la profondeur, après la surface, à laquelle la concentration de chlorophylle est maximale. Quelques échantillons proviennent de la zone mésopélagique des océans, mais leur analyse ne sera pas abordée dans ce manuscrit. Pour chaque échantillon, le séquençage à haut débit a été réalisé de telle sorte qu'environ deux millions de lectures de metabarcodes (fragment V9) soient obtenues.

Il est communément accepté de partitionner les metabarcodes en groupes génétiquement homogènes (Blaxter *et al.*, 2005; Caron *et al.*, 2009) appelés OTUs (Operational Taxonomic Units) pour mesurer la diversité des organismes étudiés. Ce partitionnement est nécessaire car plusieurs metabarcodes peuvent être associés à une seule espèce du fait de leur variabilité naturelle et des erreurs générées lors du séquençage à haut débit. Les metabarcodes eucaryotes de l'expédition *Tara Oceans* ont été partitionnés en utilisant l'approche originale Swarm (Mahé *et al.*, 2014). Alors que les méthodes classiques de partitionnement génétique utilisent généralement un seuil global de partitionnement (*global clustering threshold*), incompatible avec la variabilité de la vitesse d'évolution des différentes lignées du vivant, Swarm assemble les OTUs itérativement en utilisant un seuil local de partitionnement jusqu'à atteindre leurs limites naturelles. Le nombre de copies du gène codant pour l'ARN ribosomique 18S dans le génome n'est pas le même dans toutes les espèces eucaryotes. Il est donc difficile de relier le nombre de lectures d'un metabbarcode ou d'une OTU à un nombre d'individus, d'autant plus que chez les métazoaires le nombre de cellules

constituant un individu est variable. Cependant nous avons observé qu'il existe une relation linéaire entre le nombre de copies de ce gène et le volume des cellules des organismes (de Vargas *et al.* 2015a). Le nombre de lectures d'un metabarcode est donc un indicateur du volume biologique (biovolume) de l'organisme associé. Par commodité, dans ce manuscrit, le terme abondance est utilisé pour faire référence au nombre de lectures.

Les travaux présentés dans les deux premiers chapitres de la thèse se basent sur l'analyse d'un jeu de données partiel, correspondant au séquençage de 334 échantillons provenant de 47 stations et rendu public lors de la publication des deux articles présentés dans le premier chapitre. Les deux articles en préparation, présentés dans le dernier chapitre de thèse, reposent sur l'analyse du même jeu de données étendu à 903 échantillons (126 stations).

Le DNA metabarcoding est une méthode majeure nous permettant d'appréhender la complexité des écosystèmes marins planctoniques. J'ai cherché pendant ma thèse à identifier des moyens permettant d'étudier spécifiquement la diversité et l'abondance des symbioses eucaryotes des écosystèmes marins planctoniques à partir de données de metabarcoding. J'ai dans un premier temps participé à la réalisation de deux articles publiés dans la revue *Science* dans le cadre d'un numéro spécial consacré à la présentation des premières données acquises suite à l'expédition *Tara Oceans* (2009-2012). Le premier article, « **Eukaryotic plankton diversity in the sunlit ocean** » décrit la diversité et la biogéographie des eucaryotes du plancton (0.8-2000 µm) des océans tempérés à tropicaux et le second article, « **Determinants of community structure in the global plankton interactome** », décrit la structure globale des communautés planctoniques des océans à partir d'un réseau de cooccurrences (interactome) intégrant eucaryotes, procaryotes, virus et paramètres abiotiques. Ma participation à ces deux articles, présentés dans le **chapitre I** de ce présent manuscrit, a particulièrement concerné l'étude des symbioses eucaryotes, parasites et mutualistes, et de leurs hôtes.

J'ai ensuite étudié l'écologie de la symbiose parasitaire entre les dinoflagellés appartenant au genre *Blastodinium* et leurs hôtes, les copépodes planctoniques : « **Size-fractionated global DNA metabarcoding reveals ecological significance of the planktonic dinoflagellate parasite *Blastodinium* in sunlit oceans.** ». En plus d'être la première étude concernant l'écologie de cette symbiose à l'échelle des océans, ce travail a permis de mettre en évidence le fait que le cycle de vie des symbioses expliquerait une distribution particulière des lectures des metabarcodes associés au travers des échantillons fractionnés par tailles

d'organismes. J'ai eu l'occasion de participer à l'étude d'un cas de mutualisme entre le cilié *Tiarina* sp. et la microalgue *Symbiodinium* sp.. Ces travaux ont été réalisés dans le cadre du stage de Master 2 de Solenn Mordret et publiés dans la revue The ISME Journal : « ***Symbiodinium* in endosymbiosis within the ciliate *Tiarina*** ». Il s'agit du premier cas de mutualisme décrit entre un protiste planctonique et le genre *Symbiodinium*. Chacun des deux partenaires de l'association est représenté par plusieurs fragments V9 différents ayant chacun une biogéographie distincte. Ces deux cas d'étude, présentés dans le **chapitre II**, montre que des caractéristiques des symbioses tel le cycle de vie particulier des symbiotes et la spécificité d'interaction peuvent être capturés par le metabarcoding.

Enfin, j'ai cherché à développer des méthodes, complémentaires à l'inférence de réseaux de cooccurrences, dédiées à la détection de symbioses et de leur niveau de spécificité. J'ai ainsi développé un filtre basé sur la distribution des lectures des metabarcodes parmi les fractions de taille étudiées et permettant de distinguer les metabarcodes provenant d'organismes symbiotiques de ceux provenant d'organismes non symbiotiques. J'ai également mis au point une méthode permettant de partitionner génétiquement les metabarcodes en groupes génétiques imbriqués définis à différents niveaux de résolution. Ces méthodes ont été utilisées pour la préparation de deux articles, le premier visant à les valider et à identifier de nouveaux cas de photosymbioses dans le plancton, « **Unveiling photosymbiotic associations across phylogenetic gradients in world-wide marine plankton based on massive eukaryotic rDNA metabarcoding** ». Dans le second article, les abondances des metabarcodes assignés à des groupes taxinomiques parasitiques sont comparées à celle d'hôtes potentiels afin de mettre en avant la diversité des interactions parasitiques dans le plancton, « **Parasites diversity and abundance in the Tara Oceans metabarcoding dataset challenge classic views on marine plankton ecology** ». Ces deux articles en préparation sont présentés dans le **chapitre III** de ce manuscrit.

Chapitre I

Diversité et structure des communautés planctoniques eucaryotes de la zone photique des océans



N. Le Bescot & C. de Vargas

Dans ce chapitre, un état des lieux de la diversité et de la structure des communautés du *pico-nano-micro-meso-plancton* (0,8-2000 µm) eucaryote de la zone photique des océans tempérés à tropicaux a été réalisé. Ensuite une méthode de détection des interactions biotiques à large échelle est appliquée, nous permettant ainsi de valider le concept de détection de symbioses par metabarcoding. Afin de mieux estimer la place des interactions symbiotiques au sein de communautés planctoniques des océans, j'ai mené un important travail bibliographique aboutissant à la constitution d'une liste des associations symbiotiques décrites dans le plancton impliquant des protistes comme symbiotes (non hôtes) et l'assignation fonctionnelle de la base de références taxinomiques V9_PR2 utilisée pour l'assignation des metabarcodes de *Tara Oceans*. Cette base de références découle de l'extraction des fragments V9 de la base de références de gènes 18S PR2 (Guillou *et al.*, 2013) à laquelle des modifications concernant la taxinomie associée aux séquences ont été apportées. La liste d'interactions provenant de la littérature regroupe 574 symbioses dont 408 (71 %) sont parasitaires. Chaque association est répertoriée au maximum de résolution taxinomique et ou génétique possible. Pour certaines interactions, la résolution taxinomique maximale retrouvée de l'un des deux partenaires est la classe (par exemple Dinophyceae ou Pelagophyceae) alors que dans d'autres cas la résolution atteinte est intraspécifique et la séquence 18S correspondant au partenaire est reportée. Il y a 168 interactions différentes lorsque l'on considère les deux partenaires au niveau du genre et dans ce cas, les interactions pour lesquelles le genre de l'un des deux partenaires n'est pas connu ne sont pas prises en compte. Lorsque l'on représente cette liste d'interactions sous la forme d'un réseau où chaque nœud correspond à une espèce et chaque arrête à une association symbiotique, on peut observer la présence de deux grandes communautés (Figure 1).

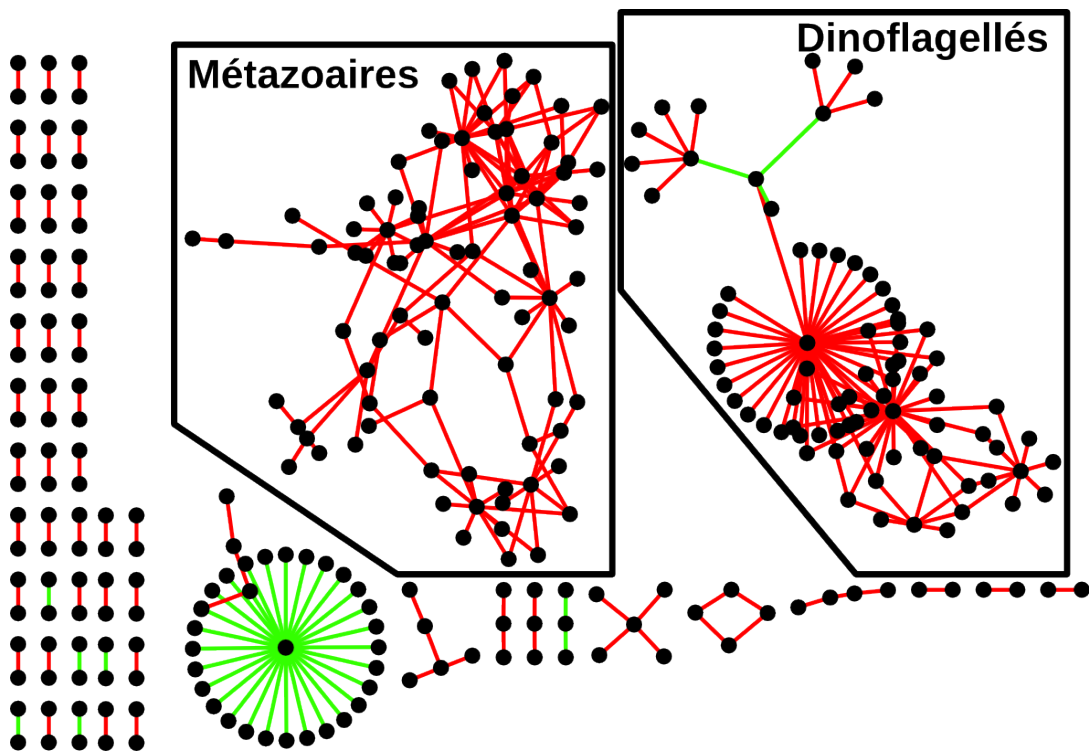


Figure 1: Réseau des associations symbiotiques entre eucaryotes du plancton marin décrites dans la littérature. Pour chaque association, au moins un des deux partenaires est un protiste. Chaque nœud en noir correspond à une espèce et chaque arrête correspond à une association symbiotique, parasitaire en rouge ou mutualiste en vert. Les deux encarts sont les deux plus grandes communautés de ce réseau. Dans la première, les hôtes sont exclusivement des métazoaires et dans la seconde les hôtes sont, à l'exception de deux noeuds, des dinoflagellés.

L'une regroupe des métazoaires et leurs parasites eucaryotes et l'autre des dinoflagellés et leurs parasitoïdes. Il semblerait que les précédents travaux concernant les symbioses se sont principalement concentrés sur l'étude de ces groupes et que les autres cas ont été répertoriés plus anecdotiquement. L'assignation fonctionnelle de la base de références taxinomiques a été réalisée de la façon suivante. Chaque séquence de référence hérite de trois caractères fonctionnels au regard de l'organisme qui lui est associé. Ces caractères sont la présence ou non chez l'organisme de chloroplastes permanents, la capacité de celui-ci à former des symbioses en tant que parasite, mutualiste ou commensal et la capacité de l'organisme à héberger à l'intérieur de ses cellules des organismes photosynthétiques dont il exploite les produits de la photosynthèse. L'assignation de ces deux dernières catégories a été grandement facilitée par la liste d'interactions symbiotiques présentée précédemment. La combinaison de ces trois caractères a permis de définir des fonctions trophiques pour chacune des séquences de référence.

Le premier article de ce chapitre, « **Eukaryotic plankton diversity in the sunlit ocean** » illustre à partir des données de metabarcoding de l'expédition *Tara* Oceans les patrons de diversité des eucaryotes du *pico-nano-micro-mesoplancton* à l'échelle des océans tempérés à tropicaux. Il décrit également le processus expérimental et informatique ayant abouti à la production de ces données. Les échantillons étudiés ici proviennent de 47 stations de la zone photique des océans, et ont été collectés à deux profondeurs différentes, la surface et la Deep Chlorophyll Maximum (DCM) c'est à dire la profondeur à laquelle la concentration de chlorophylle est maximale. Ces échantillons ont été fractionnés en 4 gammes de taille d'organismes, 0,8-5, 5-20, 20-180 et 180-2000 µm. Des courbes de raréfaction représentant la détection de nouvelles OTUs en fonction du nombre de lectures générées ont été calculées par échantillon, par fraction ainsi que pour l'ensemble des échantillons. Leur analyse montre que globalement un séquençage plus profond ne nous aurait pas permis de découvrir beaucoup d'OTUs supplémentaires. Considérant notre effort de séquençage, le séquençage de 100,000 lectures supplémentaires ne produit plus qu'une OTU supplémentaire pour l'ensemble du jeu de données. Le constat est similaire lorsque l'on considère les courbes construites pour chaque fraction de taille, même si l'on constate qu'il resterait un nombre plus important d'OTUs à découvrir dans le *piconano*-plancton où la diversité est la plus importante. Moins de 1 % des OTUs détectées sont identiques à une séquence de référence et la majorité (85 %) est assignée à des lignées de protistes. Ceci suggère qu'un nombre très important d'espèces de protiste reste à décrire formellement et que le nombre d'espèces de protiste du plancton serait très loin des ~11 200 espèces décrites jusque là. Il faut garder à l'esprit que toutes les espèces décrites ne disposent pas nécessairement de séquences de référence et que certaines de ces dernières correspondent à des lignées environnementales, il est donc délicat de faire le lien entre le nombre d'OTUs détectées et un nombre d'espèces. Parmi les 85 lignées eucaryotes identifiées dans les données de metabarcoding, onze ont été caractérisées de « hyperdiversifiées », c'est à dire qu'elles contiennent plus de 1000 OTUs. Sept de ces lignées contiennent des espèces parasites et deux d'entre elles seraient exclusivement composées d'espèces parasites, il s'agit des Marine Alveolates I et II (MALV I et MALV II) toutes deux appartenant aux syndiniales. L'assignation fonctionnelle des OTUs nous permet d'explorer les modes trophiques de l'océan, et de montrer que les protistes hétérotrophes, dont les parasites, tiennent une place importante dans les écosystèmes planctoniques tant en terme de diversité que d'abondance.

Dans le second article de ce chapitre, « **Determinants of community structure in the global plankton interactome** », la structure globale des communautés planctoniques des

océans est étudiée à partir d'un réseau de cooccurrences global (interactome). Cet interactome a été produit à partir des abondances provenant de différents types de données suivant le type d'organisme considéré (virus, procaryotes ou eucaryotes) mais aussi des mesures physico-chimiques réalisées lors de l'expédition *Tara Oceans*. Les données concernant les virus sont obtenues par partitionnement de contigs metagénomiques, les données bactériennes par extraction des séquences d'ARN 16S présentes à l'intérieur de contigs metagénomiques (mitags), et les données eucaryotes par metabarcoding (V9) correspondent à celles décrites dans le premier article. Différents réseaux de cooccurrences (23) ont été inférés séparément pour deux profondeurs (surface et DCM), quatre fractions de taille (0,8-5, >0,8, 20-180 et 180-2000 µm) et leurs combinaisons, la fraction de taille procaryote (0,2-1,6 et 0,2-3 µm) et ses combinaisons avec chaque fraction de taille eucaryote et de virus (<0,2 µm). Ces réseaux ont été construits comme dans (Faust *et al.*, 2012), les abondances ont été comparées en utilisant deux mesures de dissimilarité, le rho de Spearman (ρ) et la divergence de Kullback-Leibler, les p-values ont été calculées par permutation, renormalisation et bootstrapping, unifiées grâce à la méthode de Brown (Brown, 1975) et corrigées pour des tests multiples par la méthode de Benjamini-Hochberg (Benjamini & Hochberg, 1995). Ces réseaux ont été ensuite assemblés en un réseau global, appelé interactome. L'étude de l'interactome montre que la structure des communautés planctoniques est peu influencée par l'environnement abiotique et qu'elles seraient donc expliquées par les associations entretenues entre les organismes les constituant. Les associations entre eucaryotes dominent l'interactome (67 % de l'ensemble des associations) et parmi celles-ci, 35 % impliquent des parasites. La liste d'interactions symbiotiques constituée à partir de la littérature et présentée précédemment a été utilisée comme étalon pour estimer la propension de ce type de réseau à détecter des associations symbiotiques. Au niveau du genre, 42% des interactions présentes dans cette liste ont été retrouvées. Parmi les interactions prédites par ce réseau, une association entre un metabarcode assigné au genre *Tetraselmis* (microalgue chlorophyte) et un metabarcode assigné au genre *Symsagittifera* (acoel), a particulièrement retenu notre attention car elle rappelle la symbiose mutualiste entre cette microalgue et *Symsagittifera roscoffensis*, observée en milieu benthique. Cette association a été validée expérimentalement par microscopie confocale et séquençage de la région V9 à partir d'individus isolés des échantillons biologiques de l'expédition *Tara Oceans* où les metabarcodes correspondants étaient les plus abondants. Cet article met donc en évidence la possibilité, à partir d'un réseau de cooccurrences, de retrouver des interactions symbiotiques malgré leur complexité et, en

retournant aux échantillons biologiques, de les valider grâce à une caractérisation morphogénétique des deux partenaires.

Eukaryotic plankton diversity in the sunlit ocean

Colomban de Vargas^{1,2,†,*}, Stéphane Audic^{1,2,†}, Nicolas Henry^{1,2,†}, Johan Decelle^{1,2,†}, Frédéric Mahé^{3,1,2,†}, Ramiro Logares⁴, Enrique Lara⁵, Cédric Berney^{1,2}, Noan Le Bescot^{1,2}, Ian Probert^{6,7}, Margaux Carmichael^{11,2,8}, Julie Poulain⁹, Sarah Romac^{1,2}, Sébastien Colin^{1,2,8}, Jean-Marc Aury⁹, Lucie Bittner^{10,11,8,1,2}, Samuel Chaffron^{12,13,14}, Micah Dunthorn³, Stefan Engelen⁹, Olga Flegontova^{15,16}, Lionel Guidi^{17,18}, Aleš Horák^{15,16}, Olivier Jaillon^{9,19,20}, Gipsi Lima-Mendez^{12,13,14}, Julius Lukes^{15,16,21}, Shruti Malviya⁸, Raphael Morard^{22,1,2}, Matthieu Mulot⁵, Eleonora Scalco²³, Raffaele Siano²⁴, Flora Vincent^{13,8}, Adriana Zingone²³, Céline Dimier^{1,2,8}, Marc Picheral^{17,18}, Sarah Searson^{17,18}, Stefanie Kandels-Lewis^{25,26}, *Tara Oceans Coordinators*[†], Silvia G. Acinas⁴, Peer Bork^{25,27}, Chris Bowler⁸, Gabriel Gorsky^{17,18}, Nigel Grimsley^{28,29}, Pascal Hingamp³⁰, Daniele Iudicone²³, Fabrice Not^{1,2}, Hiroyuki Ogata³¹, Stephane Pesant^{32,22}, Jeroen Raes^{12,13,14}, Michael E. Sieracki^{33,34}, Sabrina Speich^{35,36}, Lars Stemmann^{17,18}, Shinichi Sunagawa²⁵, Jean Weissenbach^{9,19,20}, Patrick Wincker^{9,19,20,*}, Eric Karsenti^{26,8,*}

¹ CNRS, UMR 7144, Station Biologique de Roscoff, Place Georges Teissier, 29680 Roscoff, France. ² Sorbonne Universités, UPMC Univ Paris 06, UMR 7144, Station Biologique de Roscoff, Place Georges Teissier, 29680 Roscoff, France.

³ Department of Ecology, University of Kaiserslautern, Erwin-Schroedinger Street, 67663 Kaiserslautern, Germany.

⁴ Department of Marine Biology and Oceanography, Institute of Marine Science (ICM)-CSIC, Pg. Marítim de la Barceloneta 37-49, Barcelona E08003, Spain. ⁵ Laboratory of Soil Biology, University of Neuchâtel, Rue Emile-Argand 11, 2000 Neuchâtel, Switzerland.

⁶ CNRS, FR2424, Roscoff Culture Collection, Station Biologique de Roscoff, Place Georges Teissier, 29680 Roscoff, France. ⁷ Sorbonne Universités, UPMC Univ Paris 06, FR 2424, Roscoff Culture Collection, Station Biologique de Roscoff, Place Georges Teissier, 29680 Roscoff, France. ⁸ Ecole Normale Supérieure, Institut de Biologie de l'ENS (IBENS), and Inserm U1024, and CNRS UMR 8197, Paris, F-75005 France ⁹ CEA, Institut de Génomique, GENOSCOPE, 2 rue Gaston Crémieux, 91000 Evry, France. ¹⁰ CNRS FR3631, Institut de Biologie Paris-Seine, F-75005, Paris, France. ¹¹ Sorbonne Universités, UPMC Univ Paris 06, Institut de Biologie Paris-Seine (IBPS), F-75005, Paris, France.

¹² Department of Microbiology and Immunology, Rega Institute, KU Leuven, Herestraat 49, 3000 Leuven, Belgium. ¹³ Center for the Biology of Disease, VIB, Herestraat 49, 3000 Leuven, Belgium. ¹⁴ Department of Applied Biological Sciences, Vrije Universiteit Brussel, Pleinlaan 2, 1050 Brussels, Belgium. ¹⁵ Institute of Parasitology, Biology Centre, Czech Academy of Sciences, Branišovská 31, 37005 České Budějovice, Czech Republic. ¹⁶ Faculty of Science, University of South Bohemia, Branišovská 31, 37005 České Budějovice, Czech Republic. ¹⁷ CNRS, UMR 7093, LOV, Observatoire océanologique, F-06230, Villefranche-sur-mer, France. ¹⁸ Sorbonne Universités, UPMC Univ Paris 06, UMR 7093, LOV, Observatoire Océanologique, F-06230, Villefranche-sur-mer, France. ¹⁹ CNRS, UMR 8030, CP5706, Evry, France. ²⁰ Université d'Evry, UMR 8030, CP5706, Evry, France. ²¹ Canadian Institute for Advanced Research, 180 Dundas Street West, Suite 1400, Toronto ON M5G 1Z8, Canada. ²² MARUM, Center for Marine Environmental Sciences, University of Bremen, 28359 Bremen, Germany. ²³ Stazione Zoologica Anton Dohrn, Villa Comunale, 80121 Naples, Italy. ²⁴ Ifremer, Centre de Brest, DYNECO/Pelagos CS 10070, 29280 Plouzané, France. ²⁵ Structural and Computational Biology, European Molecular Biology Laboratory, Meyerhofstr. 1, 69117 Heidelberg, Germany. ²⁶ Directors' Research, European Molecular Biology Laboratory, Meyerhofstr. 1, 69117 Heidelberg, Germany. ²⁷ Max-Delbrück-Centre for Molecular Medicine, 13092 Berlin, Germany. ²⁸ CNRS UMR 7232, BIOM, Avenue du Fontaulé, 66650 Banyuls-sur-Mer, France. ²⁹ Sorbonne Universités Paris 06, OOB UPMC, Avenue du Fontaulé, 66650 Banyuls-sur-Mer, France. ³⁰ Aix Marseille Université, CNRS IGS UMR 7256, 13288 Marseille, France. ³¹ Institute for Chemical Research, Kyoto University, Gokasho, Uji, Kyoto, 611-0011, Japan. ³² PANGAEA, Data Publisher for Earth and Environmental Science, University of Bremen, Bremen, Germany. ³³ Bigelow Laboratory for Ocean Sciences, East Boothbay, ME, USA. ³⁴ National Science Foundation, Arlington, VA, USA. ³⁵ Department of Geosciences, Laboratoire de Météorologie Dynamique (LMD), Ecole Normale Supérieure, 24 rue Lhomond, 75231 Paris Cedex 05, France. ³⁶ Laboratoire de Physique des Océans, UBO-IUEM, Place Copernic, 29820 Plouzané, France.

[†]Tara Oceans coordinators and affiliations are listed at the end of this manuscript.

^{*}These authors contributed equally to this work.

^{*}Correspondence to: vargas@sb-roscott.fr; pwincker@genoscope.cns.fr; karsenti@embl.de

Published in *Science*, 2015, vol. 348, no 6237, p. 1261605.

Abstract

Marine plankton support global biological and geochemical processes. Surveys of their biodiversity have hitherto been geographically restricted and have not accounted for the

full range of plankton size. We assessed eukaryotic diversity from 334 size-fractionated photic-zone plankton communities collected across tropical and temperate oceans during the circum-global *Tara* Oceans expedition. We analysed 18S rDNA sequences across the intermediate plankton size spectrum from the smallest unicellular eukaryotes (protists, $>0.8\mu\text{m}$) to small animals of a few millimeters. Eukaryotic ribosomal diversity saturated at $\sim 150,000$ Operational Taxonomic Units (OTUs), about one third of which could not be assigned to known eukaryotic groups. Diversity emerged at all taxonomic levels, both within the groups comprising the $\sim 11,200$ catalogued morphospecies of eukaryotic plankton, and amongst twice as many other deep-branching lineages of unappreciated importance in plankton ecology studies. Most eukaryotic plankton biodiversity belonged to heterotrophic protistan groups, particularly those known to be parasites or symbiotic hosts.

Introduction

The sunlit surface layer of the world's oceans functions as a giant biogeochemical membrane between the atmosphere and the ocean interior (1). This biome includes plankton communities that fix CO₂ and other elements into biological matter, which then enters the food web. This biological matter can be remineralized or exported to the deeper ocean, where it may be sequestered over ecological to geological time scales. Study of this biome has typically focused on either conspicuous phyto- or zoo-plankton at the larger end of the organismal size spectrum, or "microbes" (prokaryotes and viruses) at the smaller end. Here, we studied the taxonomic and ecological diversity of the intermediate size spectrum (from 0.8μm to a few mm), which includes all unicellular eukaryotes (protists) and ranges from the smallest protistan cells to small animals (2). The ecological biodiversity of marine planktonic protists has been analyzed using Sanger (e.g. (3-5)) and high-throughput (e.g. (6-7)) sequencing of mainly ribosomal DNA (rDNA) gene markers, on relatively small taxonomic and/or geographical scales, unveiling key new groups of phagotrophs (8), parasites (9), and phototrophs (10). We sequenced 18S rDNA metabarcodes up to local and global saturations from size-fractionated plankton communities sampled systematically across the world tropical and temperate sunlit oceans.

A global metabarcoding approach

To explore patterns of photic-zone eukaryotic plankton biodiversity, we generated ~ 766 million raw rDNA sequence reads from 334 plankton samples collected during the

circum-global *Tara* Oceans expedition (11). At each of 47 stations, plankton communities were sampled at two water-column depths corresponding to the main hydrographic structures of the photic zone: subsurface mixed-layer waters and the Deep Chlorophyll Maximum (DCM) at the top of the thermocline. A low-shear, non-intrusive peristaltic pump and plankton nets of various mesh-sizes were used on board *Tara* to sample and concentrate appropriate volumes of seawater to theoretically recover complete local eukaryotic biodiversity from four major organismal size fractions: *piconano*-plankton (0.8-5 μ m), *nano*-plankton (5-20 μ m), *micro*-plankton (20-180 μ m), and *meso*-plankton (180-2000 μ m) (see (12) for detailed *Tara* Oceans field sampling strategy and protocols).

We extracted total DNA from all samples, PCR amplified the hyper-variable V9 region of the nuclear gene that encodes 18S rRNA (13), and generated an average of 1.73 ± 0.65 million sequence reads (paired-end Illumina) per sample (11). Strict bioinformatic quality control led to a final dataset of 580 million reads, of which ~ 2.3 million were distinct, hereafter denoted *metabarcodes*. We then clustered metabarcodes into biologically meaningful OTUs (14), and assigned a eukaryotic taxonomic path to all metabarcodes and OTUs by global similarity analysis with 77,449 reference, Sanger-sequenced V9 rDNA barcodes covering the known diversity of eukaryotes and assembled into an in-house database called *V9_PR2* (15). Beyond taxonomic assignation, we inferred basic trophic and symbiotic ecological modes (photo- versus hetero-trophy; parasitism, commensalism, mutualism for both hosts and symbionts) to *Tara* Oceans reads and OTUs, based on their genetic affiliation to large, monophyletic and monofunctional groups of reference barcodes. We finally inferred large-scale ecological patterns of eukaryotic biodiversity across geography, taxonomy, and organismal size-fractions based on rDNA abundance data and community similarity analyses, and compared them to current knowledge extracted from the literature.

The extent of eukaryotic plankton diversity in the photic-zone of the world ocean

Sequencing of ~ 1.7 million V9 rDNA reads from each of the 334 size-fractionated plankton samples was sufficient to approach saturation of eukaryotic richness at both local and global scales (Fig. 1A,B). Local richness represented on average $9.7 \pm 4\%$ of global richness, the latter approaching saturation at ~ 2 million eukaryotic metabarcodes or $\sim 110,000$ OTUs (16). The global pool of OTUs displayed a good fit to the truncated Preston log-normal distribution (17), which, by extrapolation, suggests a total photic-zone eukaryotic plankton

richness of ~150,000 OTUs, of which ~40,000 were not found in our survey (Fig. 1C). Thus we estimate that our survey unveiled ~75% of eukaryotic ribosomal diversity in the globally distributed water masses analyzed. The extrapolated ~150,000 total OTUs is much higher than the ~11,200 formally described species of marine eukaryotic plankton (see below), and likely represents a highly conservative, lower boundary estimate of the true number of eukaryotic species in this biome given the relatively limited taxonomic resolution power of the 18S rDNA gene. Our data indicate that eukaryotic taxonomic diversity is higher in smaller organismal size fractions, with a peak in the *piconano*-plankton (Fig. 1A), highlighting the richness of tiny organisms that are poorly characterized in terms of morpho-taxonomy and physiology (18). A first-order, super-group level classification of all *Tara* Oceans OTUs demonstrated the prevalence, at the biome scale and across the >4 orders of size-magnitude sampled, of protist rDNA biodiversity with respect to that of classical multicellular eukaryotes, i.e., animals, plants, and fungi (Fig. 2A). Protists accounted for >85% of total eukaryotic ribosomal diversity, a ratio that may well hold true for other marine, freshwater, and terrestrial oxygenic ecosystems (19). The latest estimates of total marine eukaryotic biodiversity based on statistical extrapolations from classical taxonomic knowledge predict the existence of 0.5 to 2.2 million species (including all benthic and planktonic systems from reefs to deep-sea vents (20, 21), but do not take into account the protistan knowledge gap highlighted here. Simple application of our ‘animal to other eukaryotes’ ratio of ~13% to the robust prediction of the total number of metazoan species from (20) would imply that 16.5 million and 60 million eukaryotic species potentially inhabit the oceans and the Earth, respectively.

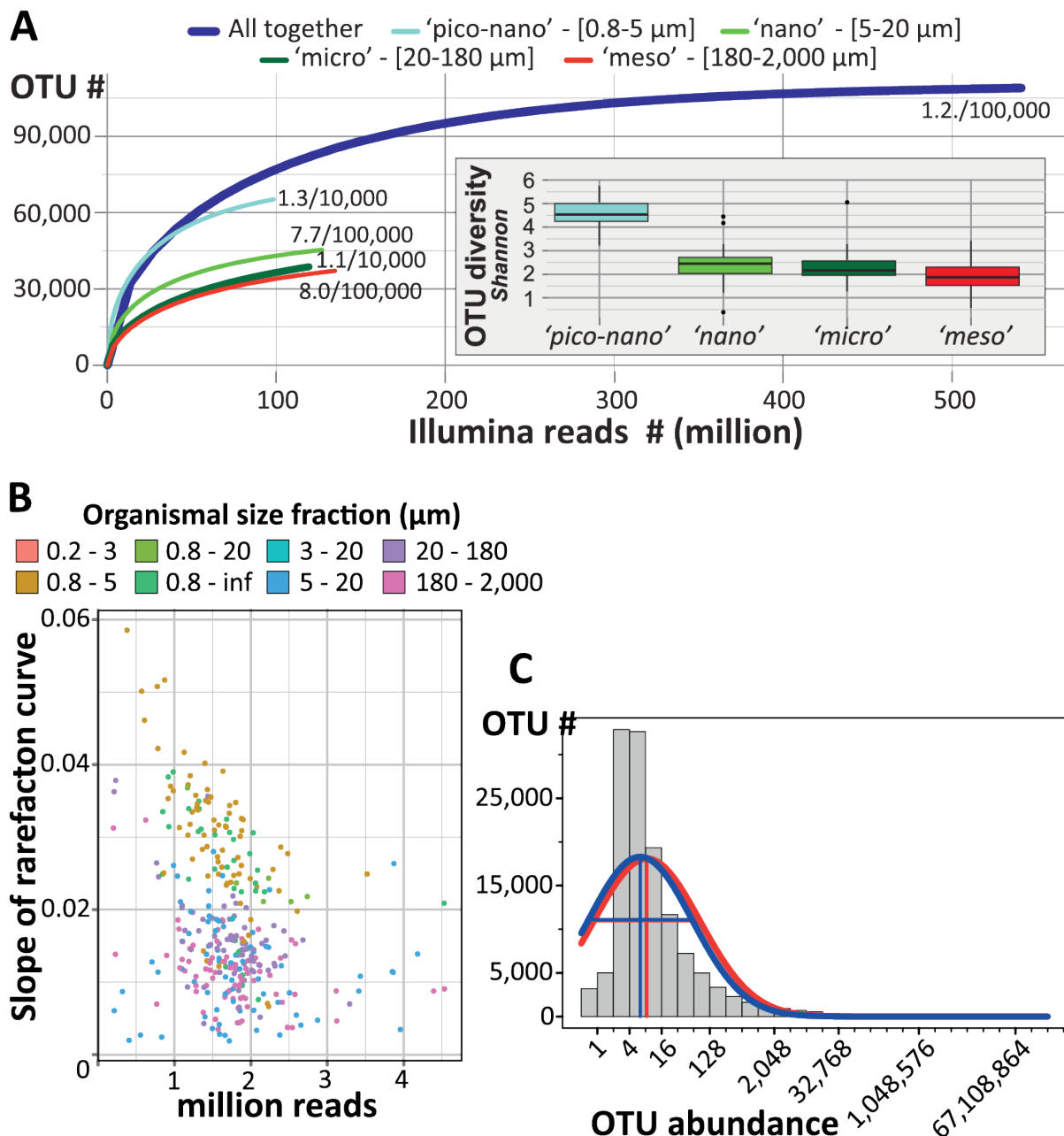


Fig. 1: Photic-zone eukaryotic plankton ribosomal diversity. (A) V9 rDNA OTUs rarefaction curves and overall diversity (*Shannon* index, inset) for each plankton organismal size fraction. Proximity to saturation is indicated by weak slopes at the end of each rarefaction curve (e.g. 1.2/100,000 means 1.2 novel metabarcodes obtained every 100,000 rDNA reads sequenced). (B) Saturation slope *versus* number of V9 rDNA reads for all of the 334 samples (dots) analyzed herein; a slope of 0.02 indicates that 2 novel barcodes can be recovered if 100 new reads are sequenced. Samples are colored according to size-fraction. (C) Global OTU-abundance distribution and fit to the Preston log-normal model. Most OTUs in our dataset were represented by 3 to 16 reads, while fewer OTUs presented less or more abundances. Quasi-Poisson fit to octaves (red curve) and maximized likelihood to log₂ abundances (blue curve) approximations were used to fit the OTU-abundance distribution to the Preston log-normal model. Overall, the global (A) and local (B) saturation values indicate that our extensive sampling effort -in terms of spatio-temporal coverage and sequencing depth- uncovered the majority of eukaryotic ribosomal diversity within the photic layer of the world tropical to temperate oceans. Calculation of the Preston Veil, which infers the number of OTUs that we missed (or were veiled) during our sampling (~40,000), confirmed that we captured most of protistan richness, thus allowing extraction of holistic and general patterns of eukaryotic plankton biodiversity from our dataset.

Phylogenetic breakdown of photic-zone eukaryotic biodiversity

About one third of eukaryotic ribosomal diversity in our dataset did not match any reference barcode in the extensive *V9_PR2* database ('*unassigned*' category in Fig. 2A). This unassignable diversity represented only a small proportion (2.6%) of total reads, and increased in both richness and abundance in smaller organismal size fractions, suggesting that it may correspond in part to rare and minute taxa that have escaped previous characterization. Some may also correspond to divergent rDNA pseudogenes, known to exist in eukaryotes (22, 23), or sequencing artefacts (24), although both of these would be expected to be present in equal proportion in all size-fractions (details in (16)). The remaining ~87,000 assignable OTUs were classified into 97 deep-branching lineages covering the full spectrum of catalogued eukaryotic diversity amongst the 7 recognized super-groups and multiple *incertae sedis* lineages (15) whose origins go back to the primary radiation of eukaryotic life in the Neo-Proterozoic. Although highly represented in the *V9_PR2* reference database, several well-known lineages adapted to terrestrial, marine benthic, or anaerobic habitats (e.g. Embryophyta, apicomplexan and trypanosome parasites of land plants and animals, amoeboflagellate Breviatea, several lineages of Amoebozoa, Excavata and Cercozoa) were not detected in our metabarcoding dataset, suggesting the absence of contamination during the PCR and sequencing steps on land, and reducing the number of deep branches of eukaryotic plankton to 85 (Fig. 3).

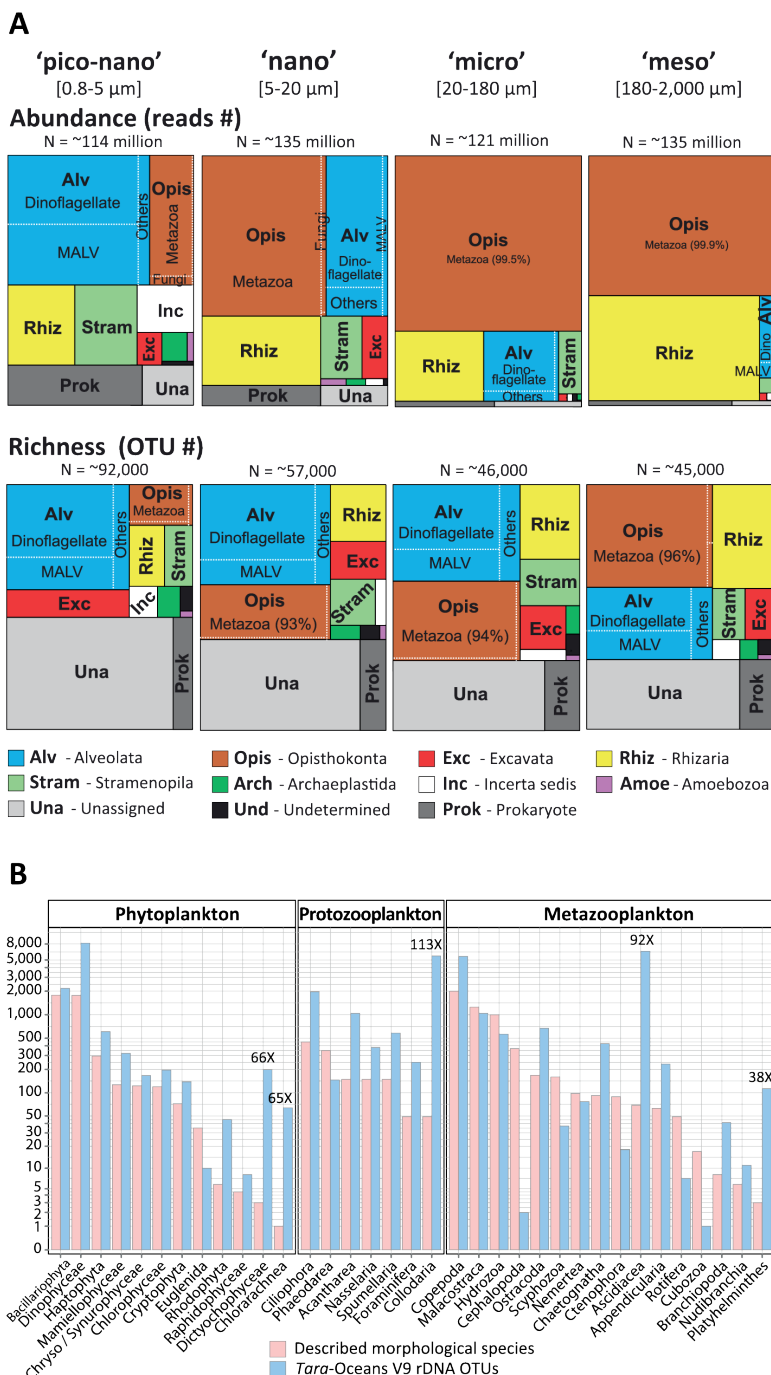


Fig. 2: Unknown and known components of eukaryotic plankton biodiversity. (A) Phylogenetic breakdown of the entire metabarcoding dataset at the eukaryotic supergroup level. All Tara Oceans V9 rDNA reads and OTUs were classified amongst the 7 recognized eukaryotic supergroups plus the known but unclassified deep-branching lineages (incertae sedis). The treemaps display the relative abundance (upper part) and richness (lower part) of the different eukaryotic supergroups in each organismal size fraction. Note that ~5% of barcodes were assigned to prokaryotes, essentially in the pico-nano fraction, witnessing the universality of the eukaryotic primers used. Barcodes are "unassigned" when sequence similarity to a reference sequence is <80%, and "undetermined" when eukaryotic supergroups could not be discriminated (at similarity >80%). (B) Ribosomal DNA diversity associated with the morphologically known and catalogued part of eukaryotic plankton. The total number of morphologically described species in the literature (red bars, based on (25–27)) and the corresponding total number of Tara Oceans V9 rDNA OTUs (blue bars) are indicated for each of the 35 classical lineages of eukaryotic phyto-, protozoo-, and metazoo- plankton. The 5 classical groups that were found to be significantly more diverse than previously thought (from 38 to 113-fold more OTUs than morphospecies) are highlighted. Note that in the classical, morphological view, phyto- and metazoo-plankton comprise ~88% of total eukaryotic plankton diversity.

We then extracted the metabarcodes assigned to morphologically well-known planktonic eukaryotic taxa from our dataset, and compared them with the conventional, 150 year-old morphological view of marine eukaryotic plankton that includes ~11,200 catalogued species divided into three broad categories: ~4,350 species of phytoplankton (microalgae), ~1,350 species of protozooplankton (relatively large, often biomineralized, heterotrophic protists) and ~5,500 species of metazooplankton (holoplanktonic animals) (25-27). A congruent picture of the distribution of morpho-genetic diversity amongst and within these organismal categories emerged from our dataset (Fig. 2B), but typically 3 to 8 times more rDNA OTUs were found than described morphospecies in the best-known lineages within these categories. This is within the range of the number of cryptic species typically detected in globally-distributed pelagic taxa using molecular data (28, 29). The general congruency between genetic and morphological data in the catalogued compartment of eukaryotic plankton suggests that the protocols used, from plankton sampling to DNA sequencing, recovered the known eukaryotic biodiversity without significant qualitative or quantitative biases. However, OTUs related to morphologically described taxa represented only a minor part of the total eukaryotic plankton ribosomal and phylogenetic diversity. Overall, <1% of OTUs were strictly identical to reference sequences, and OTUs were on average only ~86% similar to any V9 reference sequence (Fig. 3F and (16)). This shows that most photic-zone eukaryotic plankton V9 rDNA diversity had not been previously sequenced from cultured strains, single-cell isolates, or even environmental clone library surveys. The *Tara Oceans* metabarcode dataset added considerable phylogenetic information to previous protistan rDNA knowledge, with an estimated mean tree length increase of 453%, reaching >100% in 43 lineages (16). Even in the best-referenced groups such as the diatoms (1,232 reference sequences, Fig. 3B), we identified many new rDNA sequences both within known groups and forming new clades (16).

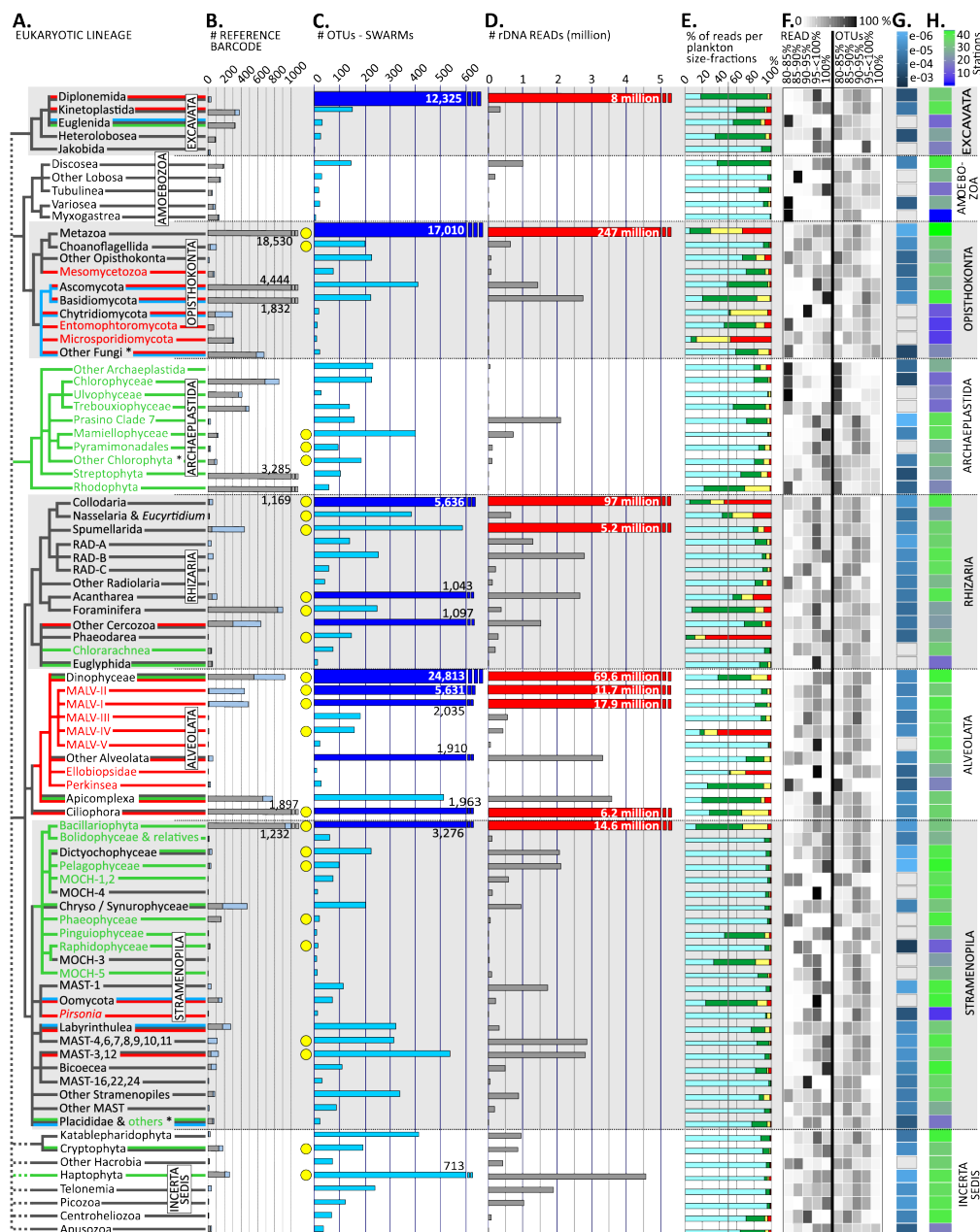


Fig. 3: Phylogenetic distribution of the assignable component of eukaryotic plankton ribosomal diversity. (A) Schematic phylogeny of the 85 deep-branching eukaryotic lineages represented in our global-oceans metabarcoding dataset, with broad ecological traits based on current knowledge: red = parasitic; green = photoautotrophic; blue = osmo/saprotrophic; black = mostly hetero/phagotrophic lineages. Lineages known only from environmental sequence data were colored in black by default. For simplicity, 3 branches (*) artificially group a few distinct lineages (details in (15)). (B) Number of reference V9 rDNA barcodes used to annotate the metabarcoding dataset (grey = with known taxonomy at the genus and/or species level; light blue = from previous 18S rDNA environmental clone libraries). (C) Tara Oceans V9 rDNA OTU richness; the dark-blue thicker bars indicate the 11 hyper-diverse lineages containing >1,000 OTUs. Yellow circles highlight the 25 lineages that have been recognized as significant in previous marine plankton biodiversity and ecology studies using morphological and/or molecular data (see also (15)). (D) Eukaryotic plankton abundance expressed as numbers of rDNA reads (the red bars indicate the 9 most abundant lineages with >5 million reads). (E) Proportion of rDNA reads per organismal size fraction, with light blue = *piconano*-; green = *nano*-; yellow = *micro*-; red = *meso*-plankton. (F) Percentage of reads and OTUs with [80-85%], [85-90%], [90-95%], [95-<100%], [100%] sequence similarity to a reference sequence. (G) Slope of OTU rarefaction curves. (H) Mean geographic occupancy (average number of stations in which OTUs were observed, weighted by OTU abundance).

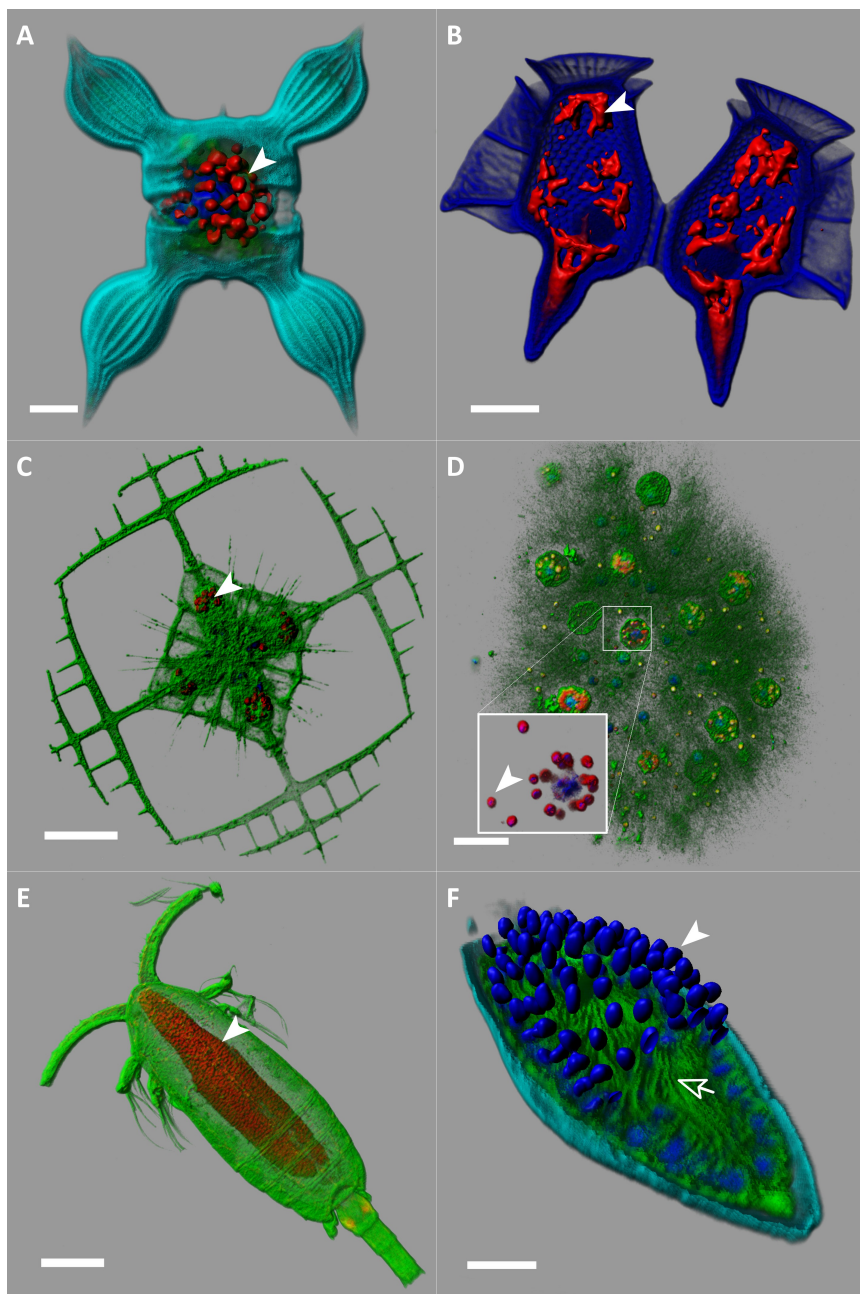


Fig. 4: Illustration of key eukaryotic plankton lineages. (A) Stramenopila; a phototrophic diatom *Chaetoceros bulbosus*, with its chloroplasts in red (scale bar 10µm). (B) Alveolata; a heterotrophic dinoflagellate *Dinophysis caudata* harboring kleptoplasts (in red, arrow head, scale bar 20µm (75)). (C) Rhizaria; an acantharian *Lithoptera* sp. with endosymbiotic haptophyte cells from the genus *Phaeocystis* (in red, arrow head, scale bar 50µm (41)). (D) Rhizaria; inside a colonial network of Collodaria, a cell surrounded by several captive dinoflagellate symbionts of the genus *Brandtiodinium* (arrow head, scale bar 50µm (33)). (E) Opisthokonta; a copepod whose gut is colonized by the parasitic dinoflagellate *Blastodinium* (red area are nuclei, arrow head, scale bar 100µm (51)). (F) Alveolata; a cross-sectioned, dinoflagellate cell infected by the parasitoid alveolate *Amoebophrya* (MALV II). Each blue spot (arrow head) is the nucleus of future free-living dinospores; their flagella are visible in green inside the mastigocoel cavity (arrow) (scale bar 5µm). The cellular membranes were stained with DiOC6 (green), DNA and nuclei with Hoechst (blue) (the dinoflagellate theca in B was also stained by this dye), chlorophyll autofluorescence is shown in red (excepted for E), an unspecific fluorescent painting of the cell surface (cyan) was used to reveal cell shape for A and F. All specimens come from *Tara Oceans* samples preserved for confocal laser scanning fluorescent microscopy. Images were 3D reconstructed with Imaris (Bitplane).

Eleven ‘hyper-diverse’ lineages each contained >1,000 OTUs, together representing ~88% and ~90% of all OTUs and reads, respectively (Fig. 3C). Amongst these, the only permanently phototrophic taxa were diatoms (Fig. 4A) and about a third of dinoflagellates (Fig. 4B-F), together comprising ~15% and ~13% of hyper-diverse OTUs and reads, respectively (30). Most hyper-diverse photic-zone plankton belonged to three super-groups, the Alveolata, Rhizaria, and Excavata, about which we have limited biological or ecological information. The Alveolata, which consist mostly of parasitic (MALVs, Fig. 4F) and phagotrophic (ciliates and most dinoflagellates) taxa, were by far the most diverse super-group, comprising ~42% of all assignable OTUs. The Rhizaria are a group of amoeboid heterotrophic protists with active pseudopods displaying a broad spectrum of ecological behavior from phagotrophy to parasitism and mutualism (symbioses) (31). Rhizarian diversity peaked in the Retaria (Fig. 4C, D), a subgroup including giant protists that build complex skeletons of silicate (Polycystinea), strontium sulfate (Acantharia, Fig. 4C), or calcium carbonate (Foraminifera), and thus comprise key microfossils for paleoceanography. Unsuspected rDNA diversity was recorded within the Collodaria (5,636 OTUs), polycystines which are mostly colonial, poorly silicified or naked, and live in obligatory symbiosis with photosynthetic dinoflagellates (Fig. 4D) (32, 33). Arguably the most surprising component of novel biodiversity was the >12,300 OTUs related to reference sequences of diplomonemids, an excavate lineage that has only two described genera of flagellate grazers, one of which parasitizes diatoms and crustaceans (34, 35). Their ribosomal diversity was not only much higher than that observed in classical plankton groups such as foraminifers, ciliates, or diatoms (50-fold, 6-fold, and 3.8-fold higher, respectively), but was also far from richness saturation (Fig. 3E). Eukaryotic rDNA diversity peaked especially in the few lineages that extend across larger size fractions (i.e. metazoans, rhizarians, dinoflagellates, ciliates, diatoms; Fig. 3E). Larger cells or colonies not only provide protection against predation via size-mediated avoidance and/or construction of composite skeletons, but also support for complex and coevolving relationships with often specialized parasites or mutualistic symbionts.

Beyond this hyper-diverse, largely heterotrophic eukaryotic majority, our dataset also highlighted phylogenetic diversity of poorly known phagotrophic (e.g., 413 OTUs of Katablepharidophyta, 240 OTUs of Telonemia), osmotrophic (e.g., 410 OTUs of Ascomycota, 322 OTUs of Labyrinthulea), and parasitic (e.g., 384 OTUs of gregarine apicomplexans, 160 OTUs of Ascetosporea, 68 OTUs of Ichthyosporea) protist groups. Amongst the 85 major

lineages presented in the phylogenetic framework of Fig. 3, less than a third (~25) have been recognized as significant in previous marine plankton biodiversity and ecology studies using morphological and/or molecular data (Fig. 3C and (15)). The remaining ~60 branches had either never been observed in marine plankton, or were detected through morphological description of one or a few species and/or the presence of environmental sequences in geographically restricted clone library surveys (15). This understudied diversity represents ~25% of all taxonomically assignable OTUs (>21,500) and covers broad taxonomic and geographic scales, thus representing a wealth of new actors to integrate into future plankton systems biology studies.

Insights into photic-zone eukaryotic plankton ecology

Functional annotation of taxonomically-assigned V9 rDNA metabarcodes was used as a first attempt to explore ecological patterns of eukaryotic diversity across broad spatial scales and organismal size-fractions, focusing on fundamental trophic modes (photo- vs. heterotrophy) and symbiotic interactions (parasitism to mutualism). Heterotroph (protists and metazoans) V9 rDNA metabarcodes were significantly more diverse (63%) and abundant (62%) than phototroph metabarcodes that represented <20% of OTUs and reads across all size-fractions and geographic sites, with an increasing heterotroph to phototroph ratio in the *micro-* and *meso*-plankton (Fig. 5A, confirmed in 17 non-size-fractionated samples (30)). These results challenge the classical, morphological view of plankton diversity, biased by a terrestrial ecology approach, whereby phyto- and metazoo-plankton (the plant/animal paradigm) are thought to comprise ~88% of eukaryotic plankton diversity (Fig. 2B) and heterotrophic protists are typically reduced in food web modeling to a single entity, often idealized as ciliate grazers.

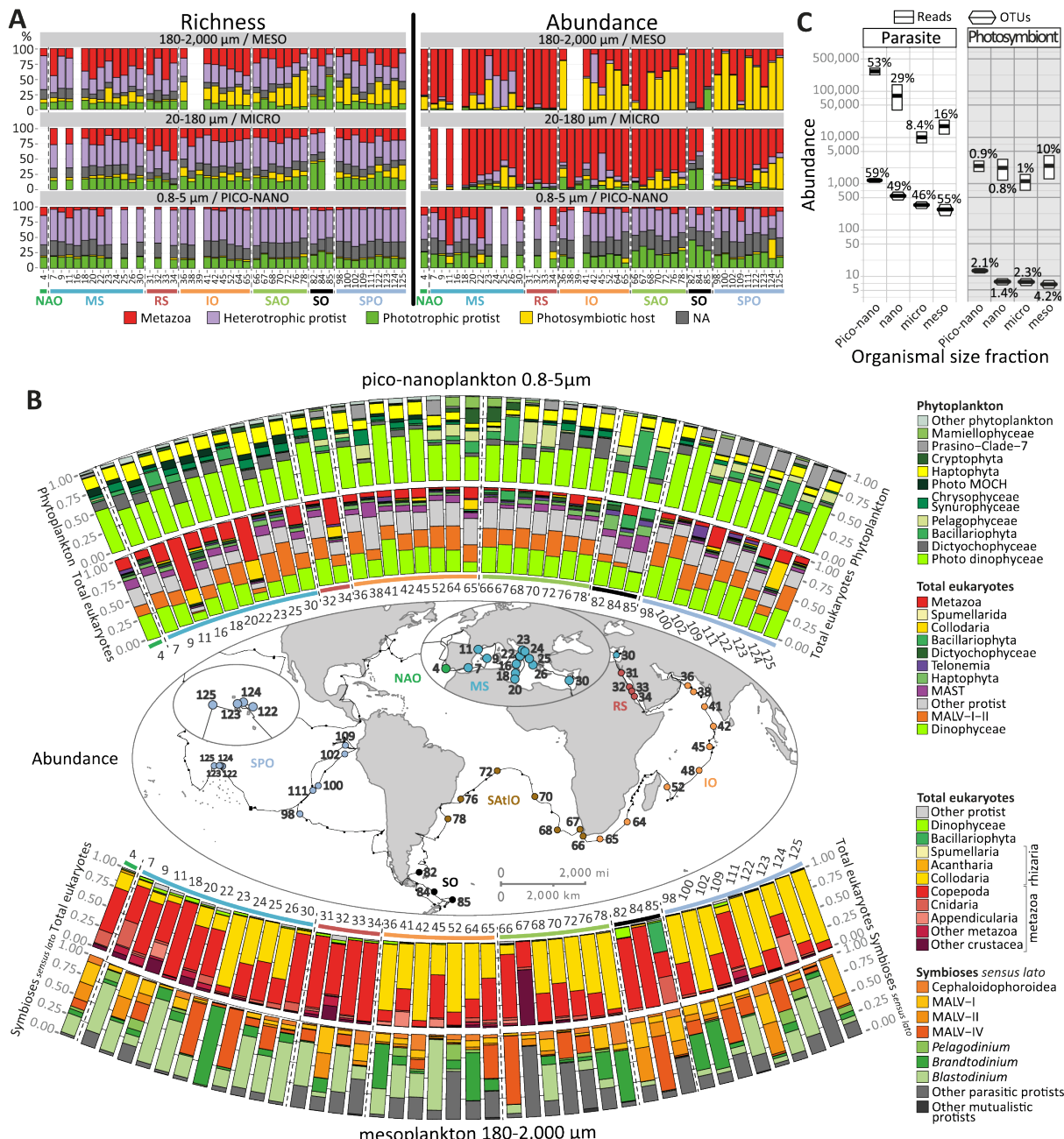


Fig. 5: Metabarcoding inference of trophic and symbiotic ecological diversity of photic-zone eukaryotic plankton. (A) Richness (OTU number) and abundance (read number) of rDNA metabarcodes assigned to various trophic taxo-groups across plankton organismal size fractions and stations. Note that the nano- size fraction contained too scarce data to be used in this biogeographical analysis (for all size-fractions data, see (30)). (B) Relative abundance of major eukaryotic taxa across *Tara Oceans* stations for: (i) phytoplankton and all eukaryotes in piconano-plankton (above the map); (ii) all eukaryotes and symbiotic, *sensu lato*, protists in meso-plankton (below the map). Note the pattern of inverted relative abundance between between collodarian colonies (Fig. 4) and copepods in respectively the oligotrophic and eu/meso-trophic systems. The dinoflagellates *Brandtодинум* and *Pelagodinium* are endophotosymbionts in Collodaria (33) and Foraminifera (40, 42), respectively. (C) Richness and abundance of parasitic and photosymbiotic (microalgae) protists across organismal size fractions. The relative contribution (%) of parasites to total heterotrophic protists, and photosymbionts to total phytoplankton, are indicated above each symbol.

An unsuspected richness and abundance of metabarcodes assigned to monophyletic groups of heterotrophic protists that cannot survive without endosymbiotic microalgae was found in larger size fractions ('photosymbiotic hosts' in Fig. 5A). Their abundance and even diversity were sometimes greater than those of all metazoan metabarcodes, including those from copepods. Most of these cosmopolitan photosymbiotic hosts were found within the hyper-diverse radiolarians Acantharia (1,043 OTUs) and Collodaria (5,636 OTUs, Figs. 3, 4B and 5D), which have often been overlooked in traditional morphological surveys of plankton-net collected material because of their delicate gelatinous and/or easily dissolved structures, but are known to be very abundant from microscope-based and *in situ* imaging studies(36-38). All 95 known colonial collodarian species described since the 19th century (39) harbour intracellular symbiotic microalgae and these key players for plankton ecology are protistan analogues of photosymbiotic corals in tropical coastal reef ecosystems with no equivalent in terrestrial ecology. In addition to their contribution to total primary production (36, 38), these diverse, biologically complex, often biomineralized, and relatively long-lived giant mixotrophic protists stabilize carbon in larger size fractions and likely increase its flux to the ocean interior (38). Conversely, the microalgae that are known obligate intracellular partners in open-ocean photosymbioses (33, 40-42) (Fig. 5B) were neither very diverse nor highly abundant, and occurred evenly across organismal size fractions (Fig. 5C). However, their relative contribution was greatest in the *meso*-plankton category (10%) (Fig. 5C), where the known photosymbionts of pelagic rhizarians were found (together with their hosts Fig. 5B). The stable and systematic abundance of photosymbiotic microalgae across size fractions (a pattern not shown by non-photosymbiotic microalgae, see (30)) suggests that pelagic photosymbionts maintain free-living and potentially actively growing populations in the *piconano*- and *nano*-plankton, representing an accessible pool for recruitment by their heterotrophic hosts. This appears to contrast with photosymbioses in coral reefs and terrestrial systems where symbiotic microalgal populations mainly occur within their multicellular hosts (43).

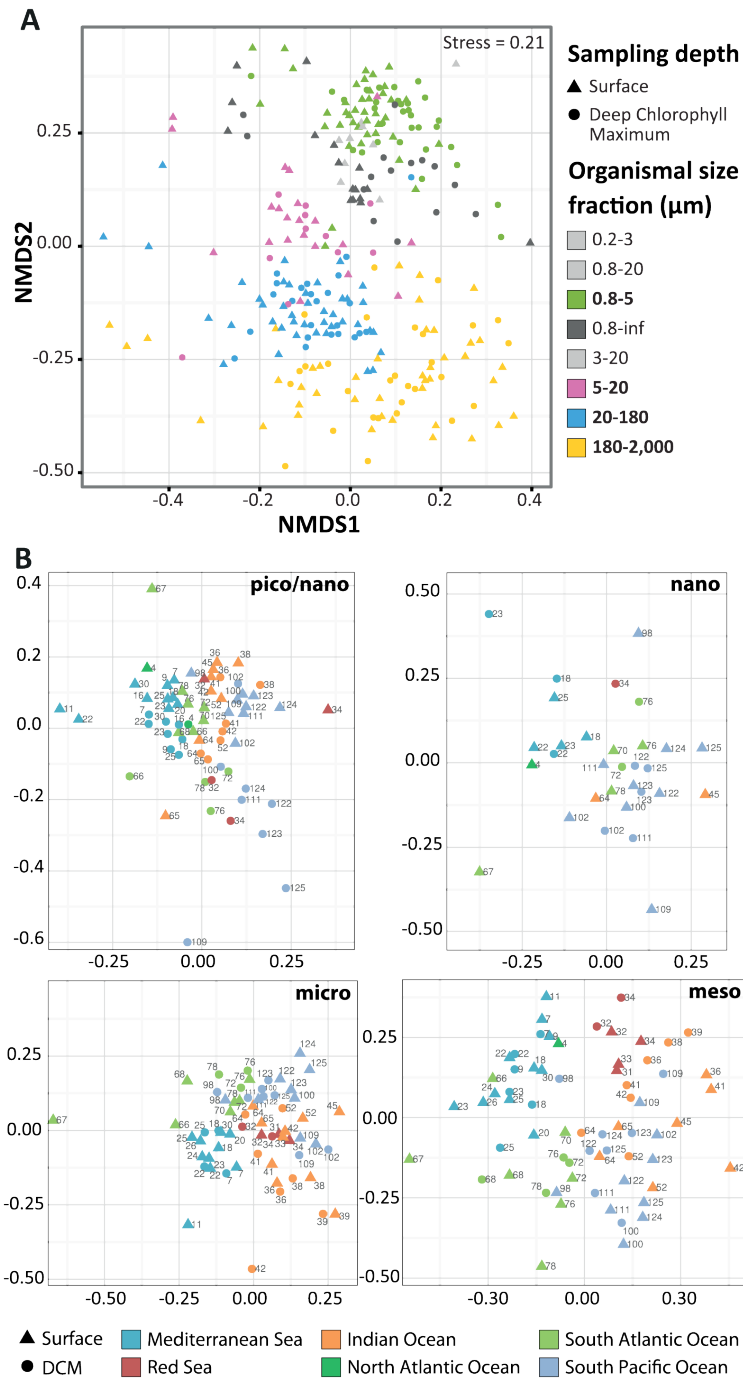


Fig. 6: Community structuring of eukaryotic plankton across temperate and tropical sunlit oceans. (A) Grouping of local communities according to taxonomic compositional similarity (Bray-Curtis distances) using Non-linear Multi-Dimensional Scaling. Each symbol represents one sample or eukaryotic community, corresponding to a particular depth (shape) and organismal size fraction (color). (B) Same as in A., but the different plankton organismal size-fractions were analyzed independently and communities are distinguished by depth (shape) and ocean basins' origin (color). An increasing geographic community differentiation along increasing organismal size-fractions is visible and confirmed by Mantel test (p -value = 10-3, $R_m=0.36, 0.49, 0.50, 0.51$ for the highest, piconano- to meso-plankton correlations in Mantel correlograms; see also (54)). In addition, samples from the piconano-plankton only were discriminated by depth (Surface vs. DCM; p -value=0.001, $r^2 =0.2$). The higher diversity and abundance of eukaryotic phototrophs in this fraction (Fig. 5A) may explain overall community structuring by light, and thus depth.

On the other end of the spectrum of biological interactions, rDNA metabarcodes affiliated to groups of known parasites were ~90 times more diverse than photosymbionts in the *piconano*-plankton, where they represented ~59% of total heterotrophic protistan ribosomal richness, and ~53% of abundance (Fig. 4; Fig. 5C), although this latter value may be inflated by a hypothetically higher rDNA copy number in some marine alveolate lineages (18). Parasites in this size fraction were mostly (89% of diversity and 88% of abundance, across all stations) within the MALV-I and II Syndiniales (30), which are known exclusively as parasitoid species that kill their host and release hundreds of small (2 to 10 μm), non-phagotrophic, dinospores (44, 9) that survive for only a few days in the water column (45). Abundant parasite-assigned metabarcodes in small size fractions (Fig. 5B, C) suggest the existence of a large and diverse pool of free-living parasites in photic-zone *piconano*-plankton, mirroring phage ecology (46), and reflecting the extreme diversity and abundance of their known hosts, essentially radiolarians, ciliates, and dinoflagellates (Fig. 3) (9, 47-49). Contrasting with the pattern observed for metabarcodes affiliated to purely phagotrophic taxa, the relative abundance and richness of putative parasite metabarcodes decreased in the *nano*- and *micro*-planktonic size fractions, but increased again in the *meso*-plankton (Fig. 5C), where parasites are most likely in their infectious stage within larger-sized host organisms. This putative *in hospite* parasites richness, equivalent to only 23% of that in the *piconano*-plankton, consisted mostly of a variety of alveolate taxa known to infect crustaceans: MALV-IV such as *Haematodinium* and *Syndinium*, dinoflagellates such as *Blastodinium* (Fig. 4E), and apicomplexan gregarines, mainly *Cephaliodophoroidea* (Fig. 5B) (9, 50, 51). This pattern contrasts with terrestrial systems where most parasites live within their hosts, and are typically transmitted either vertically or through vectors since they generally do not survive outside their hosts (52). In the pelagic realm, free-living parasitic spores, like phages, are protected from dessication, dispersed by water diffusion, and are apparently massively produced, which likely increases horizontal transmission rate.

Community structuring of photic-zone eukaryotic plankton

Clustering of communities by their compositional similarity revealed the primary influence of organism size ($p\text{-value} = 10^{-3}$, $r^2 = 0.73$) on community structuring, with *piconano*-plankton displaying stronger cohesiveness than larger organismal size fractions (Fig. 6A). Filtered size fraction-specific communities separated by thousands of kilometers were more similar in composition than they were to communities from other size fractions at

the same location. This was emphasized by the fact that ~36% of all OTUs were restricted to a single size category (53). Further analyses within each organismal size fraction indicated that geography plays a role in community structuring, with samples being partially structured according to basin of origin, a pattern that was stronger in larger organismal size fractions (p-value=0.001 in all cases, $r^2 = 0.255$ for *piconano*-plankton, 0.371 for *nano*-plankton, 0.473 for *micro*-plankton and 0.570 for *meso*-plankton) (Fig. 6B). Mantel correlograms comparing Bray-Curtis community similarity to geographic distances between all samples indicated significant positive correlations in all organismal size-fractions over the first ~6,000 km, the correlation breaking down at larger geographic distances (54). This positive correlation between community dissimilarity and geographic distance, expected under neutral biodiversity dynamics (55), challenges the classical niche model for photic-zone eukaryotic plankton biogeography (56). The significantly stronger community differentiation by ocean basin in larger organismal size fractions (Fig. 6B) suggests increasing dispersal limitation from *piconano*- to *nano*-, *micro*-, and *meso*-plankton. Thus, larger-sized eukaryotic plankton communities, containing the highest abundance and diversity of metazoans (Fig. 2A and Fig. 5B), were spatially more heterogeneous in terms of both taxonomic (Fig. 6) and functional (Fig. 5A) composition and abundance. The complex life-cycle and behaviors of metazooplankton, including temporal reproductive and growth cycles and vertical migrations, together with putative rapid adaptive evolution processes to mesoscale oceanographic features (57), may explain the stronger geographic differentiation of *meso*-planktonic communities. By contrast, eukaryotic communities in the *piconano*-plankton were richer (Fig. 1A) and more homogeneous in taxonomic composition (Fig. 6), representing a stable compartment across the world's oceans (58).

Even though protistan communities were diverse, the proportions of abundant (>1%) and rare (<0.01%) OTUs were more or less constant across communities, as has been observed in coastal waters (6). Only 2 to 17 OTUs (i.e. 0.2 to 8% of total OTUs per and across sample) dominated each community (54), suggesting that a small proportion of eukaryotic taxa are key for local plankton ecosystem function. On a worldwide scale, an occurrence vs. abundance analysis of all ~110,000 *Tara Oceans* OTUs revealed the hyper-dominance of cosmopolitan taxa (Fig. 7A). The 381 (0.35% of the total) cosmopolitan OTUs represented ~68% of the total number of reads in the dataset. Of these, 269 (71%) OTUs had >100,000 reads and accounted for nearly half (48%) of all rDNA reads (Fig. 7A), a pattern reminiscent of hyper-dominance in the largest forest ecosystem on Earth, where only 227 tree

species out of an estimated total of 16,000 account for half of all trees in Amazonia (59). The cosmopolitan OTUs belonged mainly (314 of 381) to the 11 hyper-diverse eukaryotic planktonic lineages (Fig. 3C), and were essentially phagotrophic (40%) or parasitic (21%), with relatively few (15%) phytoplanktonic taxa (54), 25% of the cosmopolitan OTUs, which represent organisms that are likely amongst the most abundant eukaryotes on Earth, had poor identity (<95%) to reference taxa, and 11 of these OTUs could not even be affiliated to any available reference sequence (Fig. 7B and (54)).

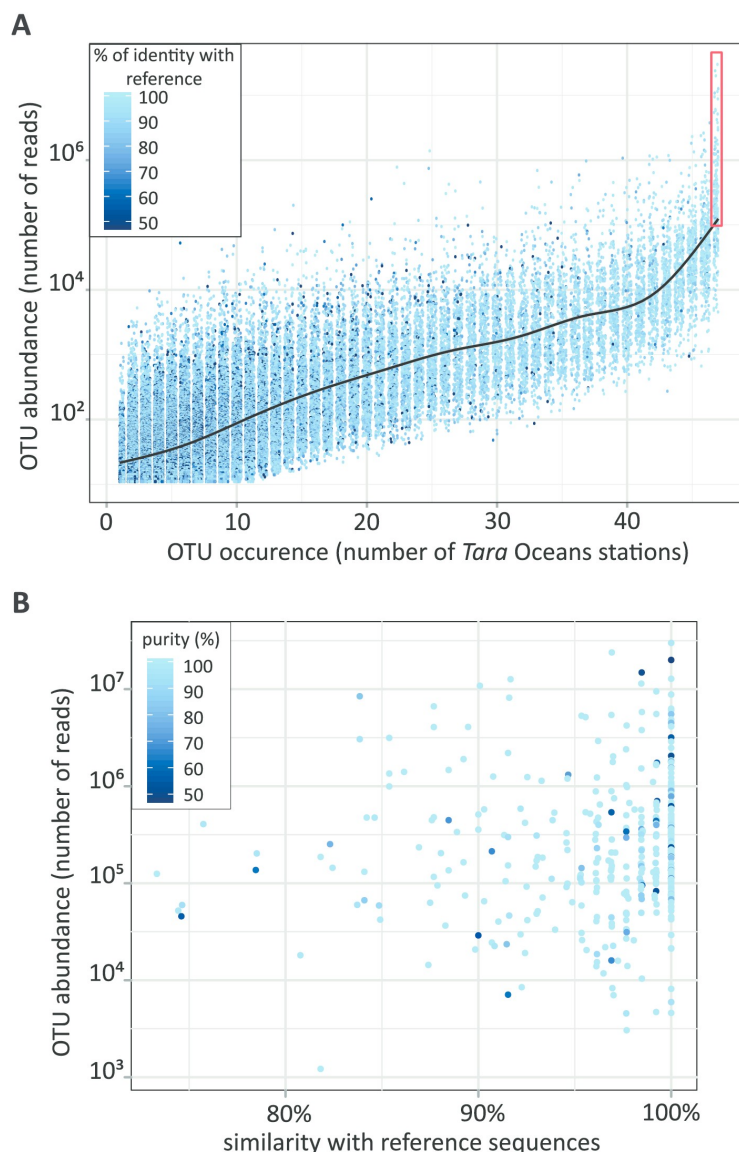


Fig. 7: Cosmopolitanism and abundance of eukaryotic marine plankton. (A) Occurrence/Abundance (x/y axis) plot including the ~110,000 Tara Oceans V9 rDNA OTUs. OTUs are colored according to their identity with reference sequence, and a fitted curve indicates the median OTU size value for each OTU geographic occurrence value. The red rectangle encloses the cosmopolitan and hyper-dominant (>105 reads) OTUs. (B) Similarity to reference barcode and taxonomic purity (a measure of taxonomic assignment consistency defined as the % of reads within an OTU assigned to the same taxon; see (13)) of the 381 cosmopolitan OTUs, along their abundance (y axis).

Conclusions and perspectives

We used rDNA sequence data to explore the taxonomic and ecological structure of total eukaryotic plankton from the photic oceanic biome, and integrated these data with existing morphological knowledge. We found that eukaryotic plankton are more diverse than previously thought, especially heterotrophic protists which may display a wide range of trophic modes (60) and include an unsuspected diversity of parasites and photosymbiotic taxa. Dominance of unicellular heterotrophs in plankton ecosystems likely emerged at the dawn of the radiation of eukaryotic cells, together with arguably their most important innovation: phagocytosis. The onset of eukaryophagy in the Neoproterozoic (61) likely led to adaptive radiation in heterotrophic eukaryotes through specialization of trophic modes and symbioses, opening novel serial biotic ecological niches. The extensive co-diversification of relatively large heterotrophic eukaryotes and their associated parasites supports the idea that biotic interactions, rather than competition for resources and space (62), are the primary forces driving organismal diversification in marine plankton systems. Based on rDNA, heterotrophic protists may be even more diverse than prokaryotes in the planktonic ecosystem (63). Given that organisms in highly diverse and abundant groups such as the alveolates and rhizarians can have genomes more complex than those of humans (64), eukaryotic plankton may contain a vast reservoir unknown marine planktonic genes (65). Insights are developing into how heterotrophic protists contribute to a multi-layered and integrated ecosystem. The protistan parasites and mutualistic symbionts increase connectivity and complexity of pelagic food webs (66, 67) while contributing to the carbon quota of their larger, longer-lived, often biomimeticized, symbiotic hosts, which themselves contribute to carbon export when they die. Decoding the ecological and evolutionary rules governing plankton diversity remains essential for understanding how the critical ocean biomes contribute to the functioning of the Earth system.

Materials & Methods

V9-18S rDNA for eukaryotic metabarcoding

We used universal eukaryotic primers (68) to PCR amplify (25 cycles in triplicate) the V9-18S rDNA genes from all *Tara Oceans* samples. This barcode presents a combination of advantages for addressing general questions of eukaryotic biodiversity over extensive taxonomic and ecological scales: (*i*) it is universally conserved in length (130±4bp) and

simple in secondary structure, thus allowing relatively unbiased PCR amplification across eukaryotic lineages followed by *Illumina* sequencing, (ii) it includes both stable and highly-variable nucleotide positions over evolutionary time frames, allowing discrimination of taxa over a significant phylogenetic depth, (iii) it is extensively represented in public reference databases across the eukaryotic tree of life, allowing taxonomic assignment amongst all known eukaryotic lineages (13).

Biodiversity analyses

Our bioinformatic pipeline included quality-check (phred score filtering, elimination of reads without perfect forward and reverse primers, chimera removal) and conservative filtering (removal of metabarcodes present in less than 3 reads and 2 distinct samples). The ~2.3 million metabarcodes (distinct reads) were clustered using an agglomerative, unsupervised single-linkage clustering algorithm, allowing OTUs to reach their natural limits while avoiding arbitrary global clustering thresholds (13, 14). This clustering limited overestimation of biodiversity due to errors in PCR amplification or DNA sequencing as well as intragenomic polymorphism of rDNA gene copies (13). *Tara* Oceans metabarcodes and OTUs were taxonomically assigned by comparison to the 77,449 reference barcodes included in our *V9_PR2* database (15). This database derives from the Protist Ribosomal Reference (PR2) database (69) but focuses on the V9 region of the gene and includes the following re-organizations: (i) extension of the number of ranks for groups with finer taxonomy (e.g. animals), (ii) expert curation of the taxonomy and re-naming in novel environmental groups and dinoflagellates, (iii) resolution of all taxonomic conflicts and inclusion of environmental sequences only if they provide additional phylogenetic information, (iv) annotation of basic trophic/symbiotic modes for all reference barcodes assigned to the genus level (see (53) and (15) for details). The *V9_PR2* reference barcodes represent 24,435 species and 13,432 genera from all known major lineages of the tree of eukaryotic life (15). Metabarcodes with $\geq 80\%$ identity to a reference V9 rDNA barcode were considered assignable. Below this threshold it is not possible to discriminate between eukaryotic supergroups given the short length of V9 rDNA sequences and the relatively fast rate accumulation of substitution mutations in the DNA. In addition to assignment at the finest-possible taxonomic resolution, all assignable metabarcodes were classified into a reference taxonomic framework consisting of 97 major monophyletic groups comprising all known high-rank eukaryotic diversity. This framework, primarily based on a synthesis of protistan biodiversity (19), also included all key, but still unnamed planktonic clades revealed by previous environmental rDNA clone library surveys

(70) (e.g. MALV ‘marine alveolates’, MAST ‘marine stramenopiles’, MOCH ‘marine ochrophytes’, RAD ‘radiolarians’ (15). Details of molecular and bioinformatics methods are available on a companion web site at <http://taraoceans.sb-roscoff.fr/EukDiv/> (53). We compiled our data into two databases including the taxonomy, abundance, and size-fraction/biogeography information associated to each metabarcode and OTU (71).

Ecological inferences

From our *Tara* Oceans metabarcoding dataset, we inferred patterns of eukaryotic plankton functional ecology. Based on a literature survey, all reference barcodes assigned to at least the genus level that recruited *Tara* Oceans metabarcodes were associated to basic trophic and symbiotic modes of the organism they come from (15), and used for a taxo-functional annotation of our entire metabarcoding dataset with the same set of rules used for taxonomic assignation (53). False positive were minimized by (i) assigning ecological modes to all individual reference barcodes in *V9_PR2*, (ii) inferring ecological modes to metabarcodes related to mono-modal reference barcode(s) (otherwise transfer them to a ‘NA - non applicable’ category), and (iii) exploring broad and complex trophic and symbiotic modes that involve fundamental reorganization of the cell structure and metabolism, emerged relatively rarely in the evolutionary history of eukaryotes, and most often concern *all* known species within monophyletic and ancient groups (see (15) for details). In case of photo- versus heterotrophy, >75% of the major, deep-branching eukaryotic lineages considered (Fig. 3) are ‘mono-modal’ and recruit ~87% and ~69% of all *Tara* Oceans V9 rDNA reads and OTUs, respectively. For parasitism, ~91% of *Tara* Oceans metabarcodes are falling within monophyletic and major groups containing exclusively parasitic species (essentially within the major MALVs groups). Although biases could arise in functional annotation of metabarcodes relatively distant from reference barcodes in the few complex poly-modal groups (e.g. the dinoflagellates that can be phototrophic, heterotrophic, parasitic, or photosymbiotic), a conservative analysis of the trophic and symbiotic ecological patterns presented in Fig. 3, using a ≥99% assignation threshold, shows that these are stable across organismal size fractions and space independently of the similarity cutoff (80% or 99%), demonstrating their robustness across evolutionary times (30).

Note that rDNA gene copy number varies from one to thousands in single eukaryotic genomes (72, 73), precluding direct translation of rDNA read number into abundance of individual organisms. However, the number of rDNA copies per genome correlates positively

to the size (73) and particularly to the biovolume (72) of the eukaryotic cell it represents. We compiled published data from the last ca. 20 years, confirming the positive correlation between eukaryotic cell size and rDNA copy number across a wide taxonomic and organismal size range (see (74), note however the ~1 order of magnitude of cell size variation for a given of rDNA copy number. To verify whether our molecular ecology protocol preserved this empirical correlation, light microscopy counts of phytoplankton belonging to different eukaryotic supergroups (coccolithophores, diatoms, dinoflagellates) were performed from 9 *Tara* Oceans stations from the Indian, Atlantic, and Southern Oceans, transformed into biomass and biovolume data and then compared with the relative number of V9 rDNA reads found for the identified taxa in the same samples (74). Results confirmed the correlation between biovolume and V9 rDNA abundance data ($r^2=0.97$, $p\text{-value}=1.\text{e-}16$);, although we cannot rule out the possibility that some eukaryotic taxa may not follow the general trend.

References and notes

1. FIELD, Christopher B., BEHRENFELD, Michael J., RANDERSON, James T., *et al.* Primary production of the biosphere: integrating terrestrial and oceanic components. *Science*, 1998, vol. 281, no 5374, p. 237-240.
2. CARON, David A., COUNTWAY, Peter D., JONES, Adriane C., *et al.* Marine protistan diversity. *Annual review of marine science*, 2012, vol. 4, p. 467-493.
3. LÓPEZ-GARCÍA, Purificación, RODRIGUEZ-VALERA, Francisco, PEDRÓS-ALIÓ, Carlos, *et al.* Unexpected diversity of small eukaryotes in deep-sea Antarctic plankton. *Nature*, 2001, vol. 409, no 6820, p. 603-607.
4. MOON-VAN DER STAAY, Seung Yeo, DE WACHTER, Rupert, et VAULOT, Daniel. Oceanic 18S rDNA sequences from picoplankton reveal unsuspected eukaryotic diversity. *Nature*, 2001, vol. 409, no 6820, p. 607-610.
5. DÍEZ, Beatriz, PEDRÓS-ALIÓ, Carlos, et MASSANA, Ramon. Study of genetic diversity of eukaryotic picoplankton in different oceanic regions by small-subunit rRNA gene cloning and sequencing. *Applied and environmental microbiology*, 2001, vol. 67, no 7, p. 2932-2941.
6. LOGARES, Ramiro, AUDIC, Stéphane, BASS, David, *et al.* Patterns of rare and abundant marine microbial eukaryotes. *Current Biology*, 2014, vol. 24, no 8, p. 813-821.

7. EDGCOMB, Virginia, ORSI, William, BUNGE, John, *et al.* Protistan microbial observatory in the Cariaco Basin, Caribbean. I. Pyrosequencing vs Sanger insights into species richness. *The ISME journal*, 2011, vol. 5, no 8, p. 1344-1356.
8. MASSANA, Ramon, CASTRESANA, Jose, BALAGUÉ, Vanessa, *et al.* Phylogenetic and ecological analysis of novel marine stramenopiles. *Applied and Environmental Microbiology*, 2004, vol. 70, no 6, p. 3528-3534.
9. GUILLOU, Laure, VIPREY, Manon, CHAMBOUVET, A., *et al.* Widespread occurrence and genetic diversity of marine parasitoids belonging to Syndiniales (Alveolata). *Environmental Microbiology*, 2008, vol. 10, no 12, p. 3349-3365.
10. LIU, Hui, PROBERT, Ian, UITZ, Julia, *et al.* Extreme diversity in noncalcifying haptophytes explains a major pigment paradox in open oceans. *Proceedings of the National Academy of Sciences*, 2009, vol. 106, no 31, p. 12803-12808.
11. Companion website: Figure W1 and Database W1 (available at <http://taraoceans.sb-roscoff.fr/EukDiv/>).
12. PESANT, Stéphane, NOT, Fabrice, PICHERAL, Marc, *et al.* Open science resources for the discovery and analysis of Tara Oceans data. *Scientific Data*, 2015, vol. 2.
13. Companion website: Text W1 and Figure W2 (available at <http://taraoceans.sb-roscoff.fr/EukDiv/>).
14. MAHÉ, Frédéric, ROGNES, Torbjørn, QUINCE, Christopher, *et al.* Swarm: robust and fast clustering method for amplicon-based studies. *PeerJ*, 2014, vol. 2, p. e593.
15. Companion website: Database W2, Database W3 and Database W6 (available at <http://taraoceans.sb-roscoff.fr/EukDiv/>).
16. Companion website: Text W3, Text W4, Text W5, Figure W4, Figure W5, Figure W6 and Figure W7 (available at <http://taraoceans.sb-roscoff.fr/EukDiv/>).
17. PRESTON, Frank W. The commonness, and rarity, of species. *Ecology*, 1948, vol. 29, no 3, p. 254-283.
18. MASSANA, Ramon. Eukaryotic picoplankton in surface oceans. *Annual review of microbiology*, 2011, vol. 65, p. 91-110.
19. PAWLOWSKI, Jan, AUDIC, Stéphane, ADL, Sina, *et al.* CBOL protist working group: barcoding eukaryotic richness beyond the animal, plant, and fungal kingdoms. *PLOS Biology*, 2012, vol. 10, p. e1001419.

20. MORA, Camilo, TITTENSOR, Derek P., ADL, Sina, *et al.* How many species are there on Earth and in the ocean? *PLOS Biology*, 2011, vol. 9, p. e1001127.
21. APPELTANS, Ward, AHYONG, Shane T., ANDERSON, Gary, *et al.* The magnitude of global marine species diversity. *Current Biology*, 2012, vol. 22, no 23, p. 2189-2202.
22. MÁRQUEZ, Luis M., MILLER, David J., MACKENZIE, Jason B., *et al.* Pseudogenes contribute to the extreme diversity of nuclear ribosomal DNA in the hard coral *Acropora*. *Molecular Biology and Evolution*, 2003, vol. 20, no 7, p. 1077-1086.
23. SANTOS, SCOTT R., KINZIE, ROBERT A., SAKAI, KAZUHIKO, *et al.* Molecular Characterization of Nuclear Small Subunit (ISS)-rDNA Pseudogenes in a Symbiotic Dinoflagellate (*Symbiodinium*, Dinophyta). *Journal of Eukaryotic Microbiology*, 2003, vol. 50, no 6, p. 417-421.
24. DECELLE, Johan, ROMAC, Sarah, SASAKI, Eriko, *et al.* Intracellular diversity of the V4 and V9 regions of the 18S rRNA in marine protists (Radiolarians) assessed by high-throughput sequencing. *PLOS One*, 2014, vol 9, p. e104297.
25. SOURNIA, Alain, CHRÉTIENNOT-DINET, Marie-Josèphe, et RICARD, Michel. Marine phytoplankton: how many species in the world ocean?. *Journal of Plankton Research*, 1991, vol. 13, no 5, p. 1093-1099.
26. WIEBE, Peter H., BUCKLIN, Ann, MADIN, Laurence, *et al.* Deep-sea sampling on CMarZ cruises in the Atlantic Ocean—an Introduction. *Deep Sea Research Part II: Topical Studies in Oceanography*, 2010, vol. 57, no 24, p. 2157-2166.
27. BOLTOVSKOY, Demetrio, CORREA, Nancy, et BOLTOVSKOY, Andrés. Diversity and endemism in cold waters of the South Atlantic: contrasting patterns in the plankton and the benthos. *Scientia Marina*, 2005, vol. 69, no S2, p. 17-26.
28. DE VARGAS, Colomban, NORRIS, Richard, ZANINETTI, Louise, *et al.* Molecular evidence of cryptic speciation in planktonic foraminifers and their relation to oceanic provinces. *Proceedings of the National Academy of Sciences*, 1999, vol. 96, no 6, p. 2864-2868.
29. HALBERT, Kristin MK, GOETZE, Erica, et CARLON, David B. High cryptic diversity across the global range of the migratory planktonic copepods *Pleuromamma piseki* and *P. gracilis*. *PLOS one*, 2013, vol. 8, no 10, p. e77011.
30. Companion website: Figure W8, Figure W9, Figure W10 and Figure W14 (available at <http://taraoceans.sb-roscoff.fr/EukDiv/>).

31. BURKI, Fabien et KEELING, Patrick J. Rhizaria. *Current Biology*, 2014, vol. 24, no 3, p. R103-R107.
32. SWANBERG, Neil Ralph. *The ecology of colonial radiolarians: their colony morphology, trophic interactions and associations, behavior, distribution, and the photosynthesis of their symbionts*. 1979. Doctoral dissertation. Massachusetts Institute of Technology and Woods Hole Oceanographic Institution.
33. PROBERT, Ian, SIANO, Raffaele, POIRIER, Camille, et al. *Brandtodium* gen. nov. and *B. nutricula* comb. Nov.(Dinophyceae), a dinoflagellate commonly found in symbiosis with polycystine radiolarians. *Journal of Phycology*, 2014, vol. 50, no 2, p. 388-399.
34. HEYDEN, Sophie, CHAO, Ema E., VICKERMAN, Keith, et al. Ribosomal RNA phylogeny of bodonid and diplonemid flagellates and the evolution of Euglenozoa. *Journal of Eukaryotic Microbiology*, 2004, vol. 51, no 4, p. 402-416.
35. SCHNEPF, Eberhard. Light and Electron Microscopical Observations in *Rhynchopus coscinodiscivorus* spec. nov., a Colorless, Phagotrophic Euglenozoan with Concealed Flagella). *Archiv für Protistenkunde*, 1994, vol. 144, no 1, p. 63-74.
36. DENNETT, Mark R., CARON, David A., MICHAELS, Anthony F., et al. Video plankton recorder reveals high abundances of colonial Radiolaria in surface waters of the central North Pacific. *Journal of Plankton Research*, 2002, vol. 24, no 8, p. 797-805.
37. STEMMANN, Lars, YOUNGBLUTH, Marsh, ROBERT, Kevin, et al. Global zoogeography of fragile macrozooplankton in the upper 100–1000 m inferred from the underwater video profiler. *ICES Journal of Marine Science*, 2008, vol. 65, no 3, p. 433-442.
38. MICHAELS, Anthony F., CARON, David A., SWANBERG, Neil R., et al. Planktonic sarcodines (Acantharia, Radiolaria, Foraminifera) in surface waters near Bermuda: abundance, biomass and vertical flux. *Journal of Plankton Research*, 1995, vol. 17, no 1, p. 131-163.
39. HAECKEL, Ernst. Report on the scientific results of the voyage of the HMS Challenger during the years 1873-1876. *Zoology*, 1887, vol. 18.
40. SIANO, Raffaele, MONTRESOR, Marina, PROBERT, Ian, et al. *Pelagodinium* gen. nov. and *P. bérii* comb. nov., a dinoflagellate symbiont of planktonic foraminifera. *Protist*, 2010, vol. 161, no 3, p. 385-399.

41. DECELLE, Johan, PROBERT, Ian, BITTNER, Lucie, *et al.* An original mode of symbiosis in open ocean plankton. *Proceedings of the National Academy of Sciences*, 2012, vol. 109, no 44, p. 18000-18005.
42. SHAKED, Yonathan et DE VARGAS, Colomban. Pelagic photosymbiosis: rDNA assessment of diversity and evolution of dinoflagellate symbionts and planktonic foraminiferal hosts. *Marine Ecology Progress Series*, 2006, vol. 325, p. 59-71.
43. DECELLE, Johan. New perspectives on the functioning and evolution of photosymbiosis in plankton: Mutualism or parasitism?. *Communicative & integrative biology*, 2013, vol. 6, no 4, p. e24560.
44. SIANO, Raffaele, ALVES-DE-SOUZA, C., FOULON, E., *et al.* Distribution and host diversity of Amoebophryidae parasites across oligotrophic waters of the Mediterranean Sea. *Biogeosciences*, 2011, vol. 8, no 2, p. 267-278.
45. COATS, D. Wayne et PARK, Myung Gil. Parasitism of photosynthetic dinoflagellates by three strains of *Amoebophrya* (Dinophyta): Parasite survival, infectivity, generation time, and host specificity. *Journal of Phycology*, 2002, vol. 38, no 3, p. 520-528.
46. WOMMACK, K. Eric et COLWELL, Rita R. Viriplankton: viruses in aquatic ecosystems. *Microbiology and Molecular Biology Reviews*, 2000, vol. 64, no 1, p. 69-114.
47. SKOVGAARD, Alf. Dirty tricks in the plankton: Diversity and Role of Marine Parasitic Protists: diversity and role of marine parasitic protists. *Acta Protozoologica*, 2014, vol. 53, no 1, p. 51-62.
48. BRÅTE, Jon, KRABBERØD, Anders K., DOLVEN, Jane K., *et al.* Radiolaria associated with large diversity of marine alveolates. *Protist*, 2012, vol. 163, no 5, p. 767-777.
49. BACHVAROFF, Tsvetan R., KIM, Sunju, GUILLOU, Laure, *et al.* Molecular diversity of the syndinean genus *Euduboscquella* based on single-cell PCR analysis. *Applied and environmental microbiology*, 2012, vol. 78, no 2, p. 334-345.
50. RUECKERT, Sonja, SIMDYANOV, Timur G., ALEOSHIN, Vladimir V., *et al.* Identification of a divergent environmental DNA sequence clade using the phylogeny of gregarine parasites (Apicomplexa) from crustacean hosts. *PloS one*, 2011, vol. 6, no 3, p. e18163-e18163.
51. SKOVGAARD, Alf, KARPOV, Sergey A., et GUILLOU, Laure. The parasitic dinoflagellates *Blastodinium* spp. inhabiting the gut of marine, planktonic copepods:

- morphology, ecology, and unrecognized species diversity. *Frontiers in microbiology*, 2012, vol. 3.
52. MCCALLUM, Hamish I., KURIS, Armand, HARVELL, C. Drew, *et al.* Does terrestrial epidemiology apply to marine systems?. *Trends in Ecology & Evolution*, 2004, vol. 19, no 11, p. 585-591.
53. Companion website: Detailed Material and Methods, Database W9 and Figure W11 (available at <http://taraoceans.sb-roscoff.fr/EukDiv/>).
54. Companion website: Figure W12, Figure W13, Database W7 and Database W8 (available at <http://taraoceans.sb-roscoff.fr/EukDiv/>).
55. HOLYOAK, Marcel, LEIBOLD, Mathew A., et HOLT, Robert D. *Metacommunities: spatial dynamics and ecological communities*. University of Chicago Press, 2005.
56. BAAS-BECKING, Lourens Gerhard Marinus. *Geobiologie; of inleiding tot de milieukunde*. WP Van Stockum & Zoon NV, 1934.
57. PEIJNENBURG, Katja TCA et GOETZE, Erica. High evolutionary potential of marine zooplankton. *Ecology and evolution*, 2013, vol. 3, no 8, p. 2765-2781.
58. SMETACEK, Victor. Microbial food webs: The ocean's veil. *Nature*, 2002, vol. 419, no 6907, p. 565-565.
59. TER STEEGE, Hans, PITMAN, Nigel CA, SABATIER, Daniel, *et al.* Hyperdominance in the Amazonian tree flora. *Science*, 2013, vol. 342, no 6156, p. 1243092.
60. VAULOT, Daniel, ROMARI, Khadidja, et NOT, Fabrice. Are autotrophs less diverse than heterotrophs in marine picoplankton?. *Trends in microbiology*, 2002, vol. 10, no 6, p. 266.
61. KNOLL, Andrew H. Paleobiological perspectives on early eukaryotic evolution. *Cold Spring Harbor perspectives in biology*, 2014, vol. 6, no 1, p. a016121.
62. SMETACEK, Victor. A watery arms race. *Nature*, 2001, vol. 411, no 6839, p. 745-745.
63. SUNAGAWA, Shinichi, COELHO, Luis Pedro, CHAFFRON, Samuel, *et al.* Structure and function of the global ocean microbiome. *Science*, 2015, vol. 348, no 6237, p. 1261359.
64. OLIVER, Matthew J., PETROV, Dmitri, ACKERLY, David, *et al.* The mode and tempo of genome size evolution in eukaryotes. *Genome research*, 2007, vol. 17, no 5, p. 594-601.
65. ABIDA, Heni, RUCHAUD, Sandrine, RIOS, Laurent, *et al.* Bioprospecting marine plankton. *Marine drugs*, 2013, vol. 11, no 11, p. 4594-4611.

66. LIMA-MENDEZ, Gipsi, FAUST, Karoline, HENRY, Nicolas, *et al.* Determinants of community structure in the global plankton interactome. *Science*, 2015, vol. 348, no 6237, p. 1262073.
67. LAFFERTY, Kevin D., DOBSON, Andrew P., et KURIS, Armand M. Parasites dominate food web links. *Proceedings of the National Academy of Sciences*, 2006, vol. 103, no 30, p. 11211-11216.
68. AMARAL-ZETTLER, Linda A., MCCLIMENT, Elizabeth A., DUCKLOW, Hugh W., *et al.* A method for studying protistan diversity using massively parallel sequencing of V9 hypervariable regions of small-subunit ribosomal RNA genes. *PLoS One*, 2009, vol. 4, no 7, p. e6372.
69. GUILLOU, Laure, BACHAR, Dipankar, AUDIC, Stéphane, *et al.* The Protist Ribosomal Reference database (PR2): a catalog of unicellular eukaryote small sub-unit rRNA sequences with curated taxonomy. *Nucleic acids research*, 2013, p. gks1160.
70. MASSANA, Ramon, DEL CAMPO, Javier, SIERACKI, Michael E., *et al.* Exploring the uncultured microeukaryote majority in the oceans: reevaluation of ribogroups within stramenopiles. *The ISME journal*, 2014, vol. 8, no 4, p. 854-866.
71. Companion website: Database W4 and Database W5 (available at <http://taraoceans.sbroscuff.fr/EukDiv/>).
72. GODHE, Anna, ASPLUND, Maria E., HÄRNSTRÖM, Karolina, *et al.* Quantification of diatom and dinoflagellate biomasses in coastal marine seawater samples by real-time PCR. *Applied and environmental microbiology*, 2008, vol. 74, no 23, p. 7174-7182.
73. ZHU, Fei, MASSANA, Ramon, NOT, Fabrice, *et al.* Mapping of picoeucaryotes in marine ecosystems with quantitative PCR of the 18S rRNA gene. *FEMS microbiology ecology*, 2005, vol. 52, no 1, p. 79-92.
74. Companion website: Text W2 and Figure W3 (available at <http://taraoceans.sbroscuff.fr/EukDiv/>).
75. KIM, Miran, NAM, Seung Won, SHIN, Woongghi, *et al.* *Dinophysis caudata* (dinophyceae) sequesters and retains plastids from the mixotrophic ciliate prey mesodinium rubrum. *Journal of Phycology*, 2012, vol. 48, no 3, p. 569-579.

Acknowledgements

We thank the commitment of the following people and sponsors: CNRS (in particular the GDR3280, EMBL, Genoscope/CEA, UPMC, VIB, Stazione Zoologica Anton Dohrn, UNIMIB, Rega Institute, KU Leuven; Fund for Scientific Research – The French Ministry of Research, the French Government 'Investissements d'Avenir' programmes OCEANOMICS (ANR-11-BTBR-0008), FRANCE GENOMIQUE (ANR-10-INBS-09-08), MEMO LIFE (ANR-10-LABX-54), PSL* Research University (ANR-11-IDEX-0001-02), ANR (projects POSEIDON/ANR-09-BLAN-0348, PROMETHEUS/ANR-09-PCS-GENM-217, PHYTBACk/ANR-2010-1709-01, TARA-GIRUS/ANR-09-PCS-GENM-218, EU FP7 (MicroB3/No.287589, IHMS/HEALTH-F4-2010-261376, ERC Advanced Grant Awards to CB (Diatomite:294823), GBMF grant #3790 to MBS, Spanish Ministry of Science and Innovation grant CGL2011-26848/BOS MicroOcean PANGENOMICS, and TANIT (CONES 2010-0036) grant from the AGAUR to SGA, JSPS KAKENHI Grant #26430184 to HO. We also thank the support and commitment of Agnès b., Etienne Bourgois, and Romain Troublé, Région Bretagne and Gilles Ricono, the Veolia Environment Foundation, Lorient Agglomération, World Courier, Illumina, the EDF Foundation; FRB, the Prince Albert II de Monaco Foundation, the *Tara* schooner and its captains and crew. We thank MERCATOR-CORIOLIS and ACRI-ST for providing daily satellite data during the expedition. We are also grateful to the French Ministry of Foreign Affairs for supporting the expedition and to the countries who graciously granted sampling permissions. *Tara* Oceans would not exist without continuous support from 23 institutes (<http://oceans.taraexpeditions.org>). We also acknowledge excellent assistance from EBI, in particular Guy Cochrane and Petra ten Hoopen, as well as the EMBL Advanced Light Microscopy Facility (ALMF), in particular Rainer Pepperkok. We thank Francoise Gaill, Bernard Kloareg, Francois Lallier, Demetrio Boltovskoy, Andy Knoll, Daniel Richter, and Emilie Médard, for their help and advice on the manuscript. The authors further declare that all data reported herein are fully and freely available from the date of publication, with no restrictions, and that all of the samples, analyses, publications, and ownership of data are free from legal entanglement or restriction of any sort by the various nations whose waters the *Tara* Oceans expedition sampled in. Data described herein is available at <http://taraoceans.sb-roscoff.fr/EukDiv/>, at EBI under the project ID PRJEB402 and PRJEB6610, and at PANGAEA (see Table S1). The data release policy regarding future public release of *Tara* Oceans data is described in Pesant *et al.* (12).

All authors approved the final manuscript. This article is contribution number 24 of *Tara Oceans*. Supplement contains additional data.

***Tara Oceans* Coordinators**

Silvia G. Acinas¹, Peer Bork², Emmanuel Boss³, Chris Bowler⁴, Colombar de Vargas^{5,6}, Michael Follows⁷, Gabriel Gorsky^{8,9}, Nigel Grimsley^{10,11}, Pascal Hingamp¹², Daniele Iudicone¹³, Olivier Jaillon^{14,15,16}, Stefanie Kandels-Lewis^{2,17}, Lee Karp-Boss³, Eric Karsenti^{4,17}, Uros Krzic¹⁸, Fabrice Not^{5,6}, Hiroyuki Ogata¹⁹, Stephane Pesant^{20,21}, Jeroen Raes^{22,23,24}, Emmanuel G. Reynaud²⁵, Christian Sardet^{26,27}, Mike Sieracki²⁸, Sabrina Speich^{29,30}, Lars Stemmann⁸, Matthew B. Sullivan³¹, Shinichi Sunagawa², Didier Velayoudon³², Jean Weissenbach^{14,15,16}, Patrick Wincker^{14,15,16}

¹Department of Marine Biology and Oceanography, Institute of Marine Science (ICM)-CSIC, Pg. Marítim de la Barceloneta, 37-49, Barcelona E08003, Spain. ²Structural and Computational Biology, European Molecular Biology Laboratory, Meyerhofstr. 1, 69117 Heidelberg, Germany. ³School of Marine Sciences, University of Maine, Orono, Maine, USA. ⁴Ecole Normale Supérieure, Institut de Biologie de l'ENS (IBENS), and Inserm U1024, and CNRS UMR 8197, Paris, F-75005 France. ⁵CNRS, UMR 7144, Station Biologique de Roscoff, Place Georges Teissier, 29680 Roscoff, France. ⁶Sorbonne Universités, UPMC Univ Paris 06, UMR 7144, Station Biologique de Roscoff, Place Georges Teissier, 29680 Roscoff, France. ⁷Dept of Earth, Atmospheric and Planetary Sciences, Massachusetts Institute of Technology, Cambridge, USA. ⁸CNRS, UMR 7093, LOV, Observatoire Océanologique, F-06230, Villefranche-sur-mer, France. ⁹Sorbonne Universités, UPMC Univ Paris 06, UMR 7093, LOV, Observatoire Océanologique, F-06230, Villefranche-sur-mer, France. ¹⁰CNRS UMR 7232, BIOM, Avenue du Fontaulé, 66650 Banyuls-sur-Mer, France. ¹¹Sorbonne Universités Paris 06, OOB UPMC, Avenue du Fontaulé, 66650 Banyuls-sur-Mer France. ¹²Aix Marseille Université CNRS IGS UMR 7256 13288 Marseille France. ¹³Stazione Zoologica Anton Dohrn, Villa Comunale, 80121, Naples, Italy. ¹⁴CEA - Institut de Génomique, GENOSCOPE, 2 rue Gaston Crémieux, 91057 Evry, France. ¹⁵CNRS, UMR 8030, CP5706, Evry France. ¹⁶Université d'Evry, UMR 8030, CP5706, Evry France. ¹⁷Directors' Research, European Molecular Biology Laboratory, Meyerhofstr. 1, 69117 Heidelberg, Germany. ¹⁸Cell Biology and Biophysics, European Molecular Biology Laboratory, Meyerhofstr. 1, 69117 Heidelberg, Germany. ¹⁹Institute for Chemical Research, Kyoto University, Gokasho, Uji, Kyoto, 611-0011, Japan. ²⁰PANGAEA, Data Publisher for Earth and Environmental Science, University of Bremen, Bremen, Germany. ²¹MARUM, Center for Marine Environmental Sciences, University of Bremen, Bremen, Germany. ²²Department of Microbiology and Immunology, Rega Institute, KU Leuven, Herestraat 49, 3000 Leuven, Belgium. ²³Center for the Biology of Disease, VIB, Herestraat 49, 3000 Leuven, Belgium. ²⁴Department of Applied Biological Sciences, Vrije Universiteit Brussel, Pleinlaan 2, 1050 Brussels, Belgium. ²⁵Earth Institute, University College Dublin, Dublin, Ireland. ²⁶CNRS, UMR 7009 Biodev, Observatoire Océanologique, F-06230 Villefranche-sur-mer, France. ²⁷Sorbonne Universités, UPMC Univ Paris 06, UMR 7009 Biodev, F-06230 Observatoire Océanologique, Villefranche-sur-mer, France. ²⁸Bigelow Laboratory for Ocean Sciences, East Boothbay, USA. ²⁹Department of Geosciences, Laboratoire de Météorologie Dynamique (LMD), Ecole Normale Supérieure, 24 rue Lhomond 75231 Paris Cedex 05 France. ³⁰Laboratoire de Physique des Océans UBO-IUEM Palce Copernic 29820 Polouzané, France. ³¹Department of Ecology and Evolutionary Biology, University of Arizona, 1007 E Lowell Street, Tucson, AZ, 85721, USA. ³²DVIP Consulting, Sèvres, France.

Determinants of community structure in the global plankton interactome

Gipsi Lima-Mendez^{1,2,3,†}, Karoline Faust^{1,2,3,†}, Nicolas Henry^{4,5,†}, Johan Decelle^{4,5}, Sébastien Colin^{4,5,6}, Fabrizio Carcillo^{2,3,7}, Samuel Chaffron^{1,2,3}, J. Cesar Ignacio-Espinosa⁸, Simon Roux⁸, Flora Vincent^{2,6}, Lucie Bittner^{4,5,6}, Youssef Darzi^{2,3}, Jun Wang^{1,2}, Stéphane Audic^{4,5}, Léo Berline^{9,10}, Gianluca Bontempi⁷, Ana M. Cabello¹¹, Laurent Coppola^{9,10}, Francisco M. Cornejo-Castillo¹¹, Francesco d'Ovidio¹², Luc De Meester¹³, Isabel Ferrera¹¹, Marie-José Garet-Delmas^{4,5}, Lionel Guidi^{9,10}, Elena Lara¹¹, Stéphane Pesant^{14,15}, Marta Royo-Llonch¹¹, Guillem Salazar¹¹, Pablo Sánchez¹¹, Marta Sebastian¹¹, Caroline Souffreau¹³, Céline Dimier^{4,5,6}, Marc Picheral^{9,10}, Sarah Searson^{9,10}, Stefanie Kandels-Lewis¹⁶, *Tara Oceans* coordinators[‡], Gabriel Gorsky^{9,10}, Fabrice Not^{4,5}, Hiroyuki Ogata¹⁷, Sabrina Speich^{18,19}, Lars Stemmann^{9,10}, Jean Weissenbach^{20,21,22}, Patrick Wincker^{20,21,22}, Silvia G. Acinas¹¹, Shinichi Sunagawa¹⁶, Peer Bork¹⁶, Matthew B. Sullivan⁸, Eric Karsenti^{6,16,*}, Chris Bowler^{6,*}, Colomban de Vargas^{4,5,*} and Jeroen Raes^{1,2,3,*}.

¹Department of Microbiology and Immunology, Rega Institute KU Leuven, Herestraat 49, 3000 Leuven, Belgium. ²VIB Center for the Biology of Disease, VIB, Herestraat 49, 3000 Leuven, Belgium. ³Laboratory of Microbiology, Vrije Universiteit Brussel, Pleinlaan 2, 1050 Brussels, Belgium. ⁴CNRS, UMR 7144, Station Biologique de Roscoff, Place Georges Teissier, 29680 Roscoff, France. ⁵Sorbonne Universités, UPMC Univ Paris 06, UMR 7144, Station Biologique de Roscoff, Place Georges Teissier, 29680 Roscoff, France. ⁶Ecole Normale Supérieure, Institut de Biologie de l'ENS (IBENS), and Inserm U1024, and CNRS UMR 8197, Paris, F-75005 France. ⁷Interuniversity Institute of Bioinformatics in Brussels (IB)², ULB Machine Learning Group, Computer Science Department, Université Libre de Bruxelles. ⁸Department of Ecology and Evolutionary Biology, University of Arizona, Tucson, AZ, 85721, USA. ⁹CNRS, UMR 7093, LOV, Observatoire océanologique, 06230, Villefranche/mer, France. ¹⁰Sorbonne Universités, UPMC Univ Paris 06, UMR 7093, LOV, Observatoire océanologique, 06230, Villefranche/mer, France. ¹¹Department of Marine Biology and Oceanography, Institute of Marine Science (ICM)-CSIC, Pg. Marítim de la Barceloneta, 37-49, Barcelona E08003, Spain. ¹²Sorbonne Universités, UPMC, Univ Paris 06, CNRS-IRD-MNHN, LOCEAN Laboratory, 4 Place Jussieu, 75005, Paris, France. ¹³KU Leuven, Laboratory of Aquatic Ecology, Evolution and Conservation, Charles Deberiotstraat 32, 3000 Leuven. ¹⁴PANGAEA, Data Publisher for Earth and Environmental Science, University of Bremen, Hochschulring 18, 28359 Bremen, Germany. ¹⁵MARUM, Center for Marine Environmental Sciences, University of Bremen, Hochschulring 18, 28359 Bremen, Germany. ¹⁶Structural and Computational Biology, European Molecular Biology Laboratory, Meyerhofstr. 1, 69117 Heidelberg, Germany. ¹⁷Institute for Chemical Research, Kyoto University, Gokasho, Uji, 611-0011 Kyoto, Japan. ¹⁸Department of Geosciences, Laboratoire de Météorologie Dynamique (LMD), Ecole Normale Supérieure, 24 rue Lhomond, 75231 Paris Cedex 05, France. ¹⁹Laboratoire de Physique des Océans, UBO-IUEM, Palce Copernic, 29820 Polouzané, France. ²⁰CEA, Genoscope, 2 rue Gaston Crémieux, 91000 Evry France. ²¹CNRS, UMR 8030, 2 rue Gaston Crémieux, 91000 Evry, France. ²²Université d'Evry, UMR 8030, CP5706 Evry, France.

Published in *Science*, 2015, vol. 348, no 6237, p. 1262073.

[‡]*Tara Oceans* coordinators and affiliations are listed below the Acknowledgements section.

[†]These authors contributed equally to this work.

^{*}Correspondence to: jeroen.raes@vib-kuleuven.be, vargas@sb-roscoff.fr, cbowler@biologie.ens.fr, karsenti@embl.de

Abstract

Species interaction networks are shaped by abiotic and biotic factors. Here, as part of the *Tara Oceans* project, we studied the photic zone interactome using environmental factors and organismal abundance profiles. We found associations across plankton functional types and phylogenetic groups to be non-randomly distributed on the network. We identified interactions among grazers, primary producers, viruses and (mainly parasitic) symbionts, and

validated network-generated hypotheses using microscopy to confirm symbiotic relationships. We have thus provided a resource to support further research on ocean food webs and development of ocean models.

Introduction

The structure of oceanic ecosystems results from the complex interplay between resident organisms and their environment. In the world's largest ecosystem, oceanic plankton (composed of viruses, prokaryotes, microbial eukaryotes, phytoplankton and zooplankton) form trophic and symbiotic interaction networks (1-4) that are influenced by environmental conditions. Ecosystem structure and composition are governed by abiotic as well as biotic factors. The former include environmental conditions and nutrient availability (5), while the latter include grazing, pathogenicity and parasitism (6, 7). Historically, abiotic factors have been considered to have a stronger effect, but recently appreciation for biotic factors is growing (8, 9). We sought to develop a quantitative understanding of biotic and abiotic interactions in natural systems where the organisms are taxonomically and trophically diverse (10). We used sequencing technologies to profile communities across trophic levels, organismal sizes, and geographic ranges, and to predict organismal interactions across biomes based on co-occurrence patterns (11). Previous efforts addressing these issues have provided insights on the structure (12, 13) and dynamics of microbial communities (14-16).

Here we analyze data from 313 plankton samples the *Tara Oceans* expedition (17) derived from 7 size-fractions covering collectively 68 stations at 2 depths across 8 oceanic provinces (Table S1). The plankton samples spanned sizes that include organisms from viruses to small metazoans. We derived viral, prokaryotic and eukaryotic abundance profiles from clusters of metagenomic contigs, ^mtags and 18S rDNA V9 sequences, respectively (10, 18, 19) (Table S1) and collected environmental data from on-site and satellite measurements (17, 20, 21). We used network inference methods and machine learning techniques to disentangle biotic and abiotic signals shaping ocean plankton communities, and to construct an interactome that described the network of interactions among photic zone plankton groups. We used the interactome to focus on specific relationships, which we validated by microscopic analysis of symbiont pairs and *in silico* analysis of phage-host pairings.

Evaluating the effect of abiotic and biotic factors on community structure

We first re-assessed the effects of environment and geography on community structure. Using variation partitioning (22) we found that on average, the percentage of variation in community composition explained by environment alone was 18%, by environment combined with geography 13%, and by geography alone only 3% (23, 24). In addition, we built random forest-based models (25) to predict abundance profiles of the Operational Taxonomic Units (OTU) using a) OTUs alone, b) environmental variables alone, c) OTUs and environmental variables combined, and tested for each OTU whether one of the three approaches outcompeted the other (see Methods). These analyses revealed that 95% of the OTU-only models are more accurate in predicting OTU abundances than environmental variable models, while combined models were no better than the OTU-only models (26, 27). This suggests that abiotic factors have a more limited effect on community structure than previously assumed (8).

To study the role of biotic interactions, we developed a method to identify robust species associations in the context of environmental conditions. Twenty-three taxon-taxon and taxon-environment co-occurrence networks were constructed based on 9,292 taxa, representing the combinations of two depths, seven organismal size ranges and four organismal domains (Bacteria, Archaea, Eukarya, viruses) (28). To reduce noise and thus false positive predictions, we restricted our analysis to taxa present in at least 20% of the samples and used conservative statistical cutoffs (see Methods). We merged the individual networks into a global network, which features a total of 127,995 unique edges, of which 92,633 are taxon-taxon edges and 35,362 are taxon-environment edges (Table 1). Node degree does not depend on the abundance of the node (28). As such this network represents a resource to examine species associations in the global oceans (28-31).

Table 1. Properties of the merged taxon network. The positive subset of the network was clustered with the leading eigen vector algorithm (91).

Nodes	Edges	Positive edges (%)	Negative edges	Average clustering coefficient	Average path length	Diameter	Average betweenness	Modularity of positive network	Number of modules in positive network
9169	92633	68856 (74.33)	23777	0.229	3.43	12	11024	0.51	51

Next, we assessed how many of the taxon links represented ‘niche effects’ driven by geography or environment (such as when taxa respond similarly to a common environmental

condition). We examined motifs consisting of two correlated taxa that also correlate with at least one common environmental parameter (“environmental triplets” to identify associations that were driven by environment) using three approaches (interaction information, sign pattern analysis, and network deconvolution (32)). We identified 29,912 taxon-taxon-environment associations (32.3% of total). Among environmental factors, we found that PO₄, temperature, NO₂ and mixed layer depth were frequent drivers of network connections (Fig. 1A). While the three methodologies pinpoint indirect associations; only interaction information directly identifies synergistic effects in these biotic-abiotic triplets. Exploiting this property, we disentangled the 29,912 environment-affected associations into 11,043 edges driven solely by abiotic factors (31, 33) (excluded from the network for the remainder of the study) and 18,869 edges whose dependencies result from biotic-abiotic synergistic effects. Thus, we find that a minority of associations can be explained by an environmental factor.

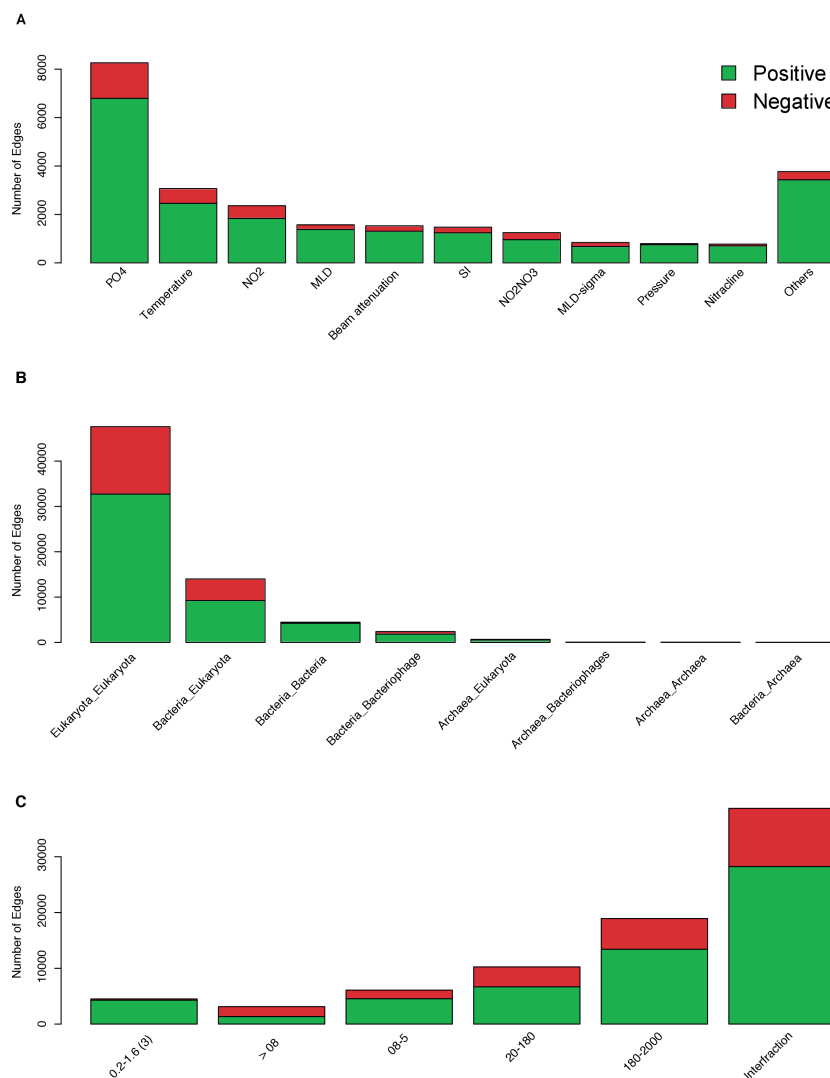


Fig. 1. Global oceanic taxon-environment interaction network properties. (A) Major environmental factors affecting abundance patterns. Phosphate concentration (PO₄), Temperature and Nitrite concentration (NO₂) are the top 3 parameters driving abiotic associations followed by Mixed Layer Depth (MLD, assessed by temperature change), Particulate beam attenuation measured at 660 nm, Silica concentration (Si), Nitrite+Nitrate concentration (NO₂NO₃), MLD-sigma (Mixed Layer Depth, assessed by density change), Pressure, Nitracline, and others corresponds to the agglomerated contribution of the rest of parameters tested. (B) Number of inter-domain and intra-domain copresences and mutual exclusions. (C) Distribution of edges across size fractions: 0.2-1.6(3), prokaryote-enriched fractions 0.2-1.6 µm and 0.2-3 µm; >08 µm, non-size-fractionated samples; 08-5 µm, piconano-plankton; 20-180 µm, micro-plankton; 180-2000 µm, meso-plankton; interfrac, includes interfraction networks 08-5 µm versus 20-180 µm, 08-5 µm versus 180-2000 µm, 20-180 µm versus 180-2000 µm and 0.2-1.6(3) µm versus ≤0.2 µm (virus-enriched fraction).

Evaluation of predicted interactions

Co-occurrence techniques have heretofore been mainly applied to bacteria. We detected eukaryotic interactions based on analysis of sequences at the V9 hypervariable

region of the 18S rRNA gene. We built a literature-curated collection (34) of 573 known symbiotic interactions (including both parasitism and mutualism) in marine eukaryotic plankton (30, 35). From 43 genus level interactions represented by OTUs in the abundance pre-processed input matrices, we found 42% (18 genus pairs; 47 % when limiting to parasitic interactions) represented in our reference list. The probability of having found each of these interactions by chance alone was <0.01 (Fisher exact test, average pval = 4e-3, median pval = 5e-7). Based on this sensitivity and a false discovery rate averaging to 9% (computed from null models; see Methods), we estimate the number of interactions among eukaryotes present in our filtered input matrices to be between 53,000 and 139,000. Most of the false negative interactions were due to the strict filtering rules we used to avoid false positives; this hampers detection when, for example, interactions are facultative or when interaction partners may vary among closely related groups depending on oceanic region (4). False positives could represent indirect interactions between species (bystander effects) or environmental effects caused by factors not captured in this study (36, 37).

Biotic interactions within and across kingdoms

The integrated network contained 81,590 predicted biotic interactions (30) that were non-randomly distributed within and between size fractions (Figure 1B, C) (38). Positive associations outnumbered mutual exclusions (72% versus 28%), and we observed a non-random edge distribution with regard to phylogeny (Fig. 2A), with most associations derived from syndiniales and other dinoflagellates (see Fig. 3A below for examples), and exclusions involving arthropods. Certain combinations of phylogenetic groups are over-represented (39). For instance, we found a clade of syndiniales (the MALV-II Clade 1 belonging to *Amoebophrya* (3)) enriched in positive associations with tintinnids ($P = 2e-4$), amongst the most abundant ciliates in marine plankton (40). The tintinnid *Xystonella lohmani* was described in 1964 to be infected by *Amoebophrya tintinnis* (41) and tintinnids can feed on *Amoebophrya* free-living stages (42). Other found host-parasite associations included the copepod parasites *Blastodinium*, *Ellobiopsis* and *Vampyrophrya* (41, 43-45).

On the other hand, *Maxillopoda*, *Bacillariophyceae* and collodarians, three groups of relatively large sized organisms whose biomass can dominate planktonic ecosystems, are rich in negative associations among them (33). Collodarians and copepods are abundant in, respectively, the oligotrophic tropical and eu/meso-trophic temperate systems (10, 46). The decoupling of phyto- and zooplankton in open oceans by diatoms anti-correlating to copepods

(47, 48) is attributed to growth rate differences and to the diatom production of compounds harmful to their grazers (49). The combination of these effects could lie at the basis of this observation, which contrasts with other free-living autotrophs represented in the network (cyanobacteria and prymnesiophytes), which display primarily positive associations (Fig. 2A).

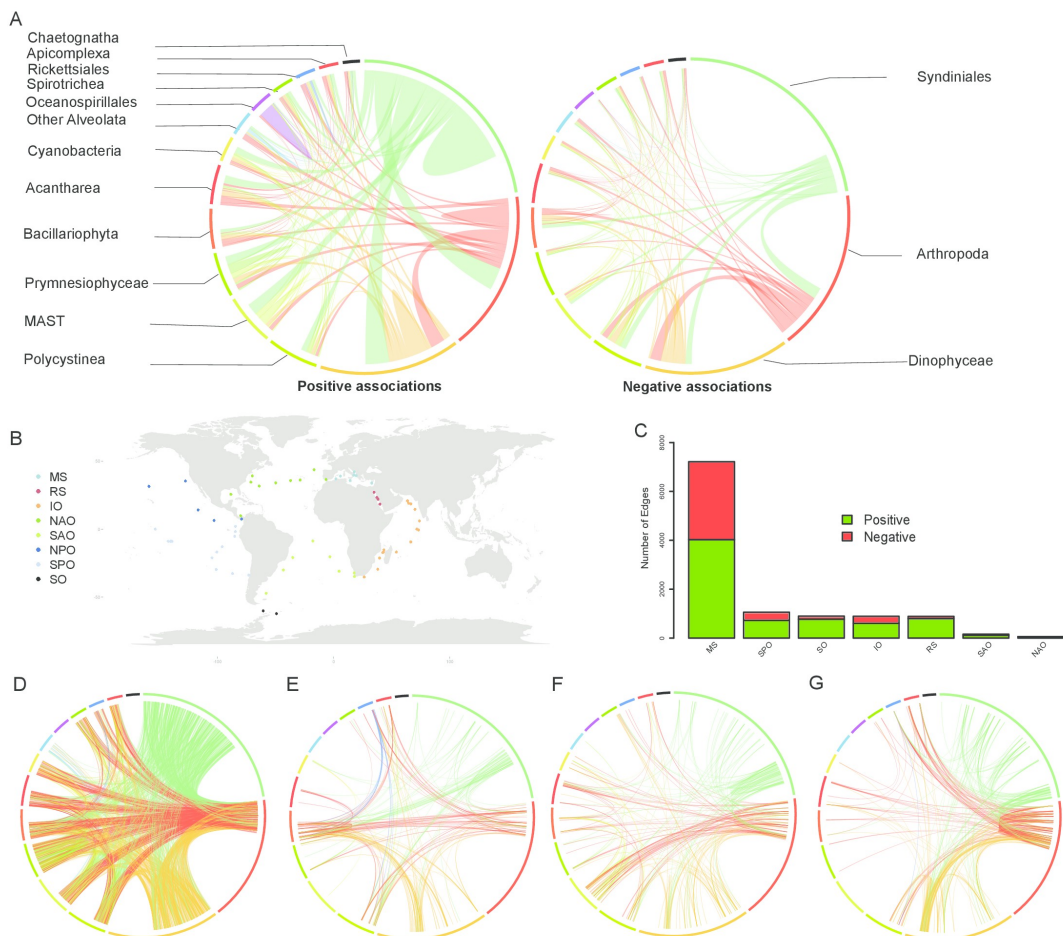


Fig. 2. Taxonomic and geographic patterns within the co-occurrence network. (A) Top 15 interacting taxon groups depicted as colored segments in a CIRCOS plot, where ribbons connecting two segments indicate copresence and exclusion links, on left and right, respectively. Size of the ribbon is proportional to the number of links (copresences and exclusions) between the OTUs assigned to the respective segments, and color is the one of the segment (of the two involved) with more total links. Links are dominated by the obligate parasites syndiniales and by Arthropoda and Dinophyceae. (B) Tara Oceans sampling stations grouped by oceanic provinces. (C) Frequency of local co-occurrence patterns across the oceanic provinces, showing that most local patterns are located in MS. (D to G) Taxonomic patterns of co-occurrences across MS (D), SPO (E), IO (F) and RS (G). Edges are represented as ribbons between barcodes grouped into their taxonomic order as in A. Links sharing the same segment are affiliated to the same taxon (Order), showing that the connectivity patterns across taxa are conserved at high taxonomic ranks. The local specificity of interactions at higher resolution (OTUs) is apparent by thin ribbons (edge resolution) with different starts and end positions (different OTUs) within the shared (taxon) segment, section color and ordering correspond to those in panel A. SO-specific associations are mainly driven by bacterial interactions (53).

Cross-kingdom associations between Bacteria and Archaea were limited to 24 mutual exclusions. Within Archaea, Thermoplasmatales (Marine Group II) co-occur with several phytoplankton clades. Links between Bacteria and protists recovered 5 out of 8 recently discovered interactions from protist single-cell sequencing (50). Associations between Diatoms and Flavobacteria agreed with their described symbioses (51). We also observed co-occurrence of uncultured dinoflagellates with members of Rhodobacterales (*Ruegeria*), in agreement with a symbiosis between *Ruegeria* sp. TM1040 and *Pfiesteria piscicida* around the ability of *Ruegeria* to metabolize dinoflagellate-produced DMSP (52).

Global versus local associations

We further investigated whether our network was driven by global trends or is defined by local signals. To this aim, we divided our set of samples into 7 main regions: Mediterranean Sea (MS), Red Sea (RS), Indian Ocean (IO), South Atlantic (SAO), Southern Ocean (SO), South Pacific Ocean (SPO) and North Atlantic Ocean (NAO), and assessed the ‘locality’ of associations by comparing the score with or without that region (see Methods). We found that association patterns were mostly driven by global trends as only 14% of edges were identified as local (Figure 2B, C). Approximately two thirds of local associations occur in MS (7,215) followed by SPO (1,058), while the rest are contributed by SO (901), IO (894), RS (889), SAO (163) and NAO (60) (Fig. 2C-G). MS was the region with most sampling sites, which allowed us to recover more local patterns. Nevertheless, Figures 2C-G show that although the same major groups (order level) interact in both the global and local networks, each local site has its own specific interaction profile (Pval < 1e-8) (33, 39, 53).

Parasite impact on plankton functional types

Parasitic interactions are the most abundant pattern present in the network, which is also eminent by repeated microscopic observation of parasitic interactions from the Tara samples (Fig. 3A). We focused on predicted parasitic interactions and assessed their potential impact on biogeochemical processes by exploring a functional sub-network (21,572 edges) of known and novel plankton parasites (10) together with classical ‘plankton functional types’ (PFTs (54)). PFTs group taxa by trophic strategy (e.g., autotrophs vs. heterotrophs) and role in ocean biogeochemistry (Figure 3A) (55). The relationship between the different PFTs (network density of 0.65) highlights strong dependencies between phytoplankton and grazers. We find that all PFTs are associated with parasites, but not always to the same extent. Most

links involve syndiniales MALV-I and MALV-II clades associated to zooplankton and, to a lesser extent, to microphytoplankton (excluding diatoms). This emphasizes the role of alveolate parasitoids as top-down effectors of zooplankton and microphytoplankton population structure and functioning (3) - although the latter group is also affected by grazing (1). The meso-planktonic networks contain known syndiniales targets (Dinophyceae, Ciliophora, Acantharia and Metazoa; Figure 3B) (56). In large size fractions, we found interactions between known parasites and groups of organisms that in theory are too small to be their hosts (57); 32% of these associations involved the abundant and diverse marine stramenopiles (MAST) and diplonemids (other Discoba and Diplonema) (10). Eco-physiology studies (58, 59) suggest a parasitic role for these lineages. The association of these groups with other parasites would be explained by putative co-infection of the same hosts. Contrasting with the above observations, we find phytoplankton silicifiers (diatoms) displaying a variety of mutual exclusions. One possible interpretation of this is that diatom silicate exoskeletons (60) and toxic compound production (49) could act as efficient barriers against top-down pressures (61).

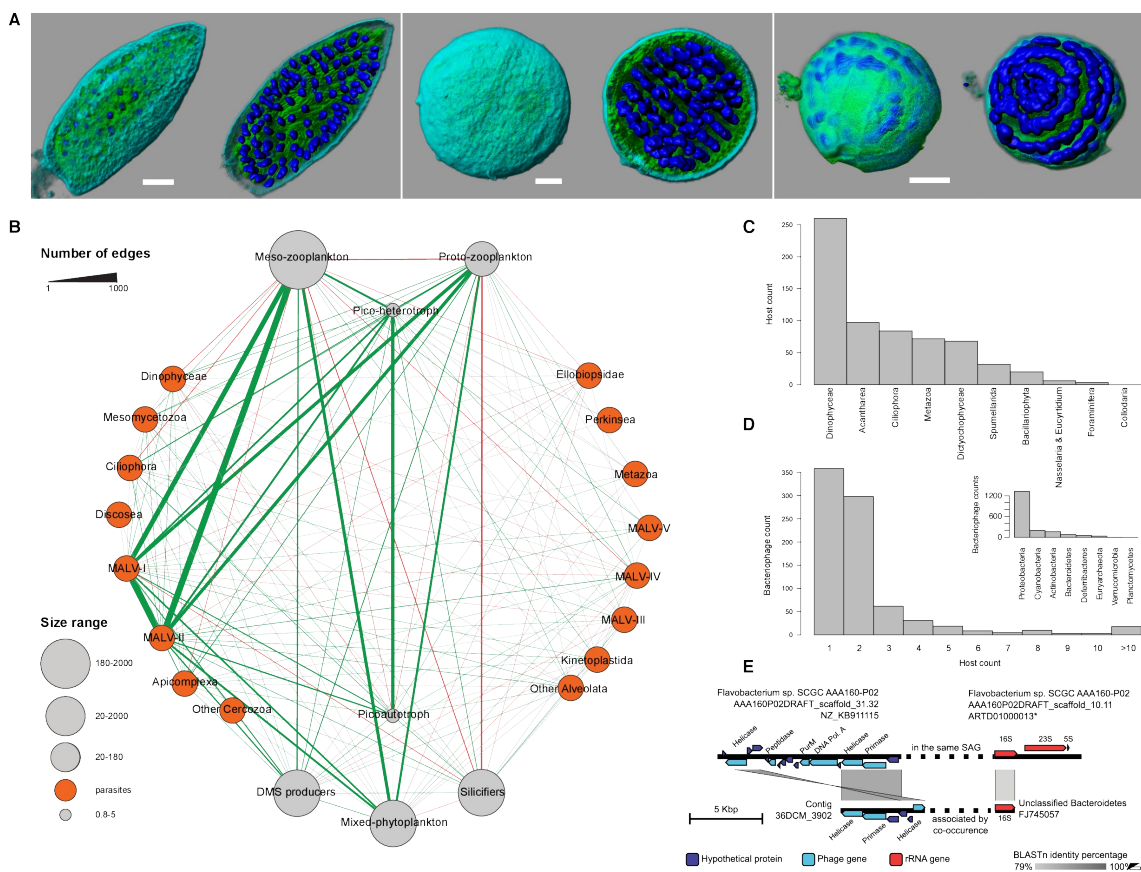


Figure 3. Top-down interactions in plankton. (A) Three different dinoflagellate specimens from TARA samples display an advanced infectious stage by syndiniales parasites. The cross-section of the cell shows the typical folded structure of the parasitoid chain, which fills the entire host cell. Each nucleus (blue) of the coiled ribbon corresponds to a future free-living parasite. (DNA is stained with Hoechst (blue), membranes are stained with DiOC6 (green) and specimen surface is cyan; scale bar is 5 μ m) (B) Subnetwork of metanodes that encapsulate barcodes affiliated to parasites or Plankton Functional Types (PFTs). The PFTs mapped onto the network are: phytoplankton dimethyl sulfide (DMS) producers, mixed phytoplankton, phytoplankton silicifiers, pico-eukaryotic heterotrophs, proto-zooplankton and meso-zooplankton. Edge width reflects the number of edges in the taxon graph between the corresponding metanodes. Over-represented links (multiple-test corrected $P_{\text{val}} < 0.05$) are colored in green if they represent copresences and in red if they represent exclusions; grey means non over-represented combinations. When both copresences and exclusions were significant, the edge is shown as copresence. (C) Parasite connections within micro- and zooplankton groups. (D) Number of hosts per phage (inset: phage associations to bacterial (target) phyla). (E) Putative Bacteroidetes viruses detected by co-occurrence and detection in a single-cell genome (SAG). On the left, viral sequences from a Flavobacterium SAG (top) and *Tara Oceans* virome (bottom), displaying an average of 89% nucleotide identity. On the right is the correspondence between the ribosomal genes detected in the same SAG (top) and the 16S sequence associated to the *Tara Oceans* contig based on co-occurrence (79% nucleotide identity). For clarity, a subset of contig ARTD0100013 only (from 10,000 to 16,000 nucleotides) is displayed. This sequence was also reverse-complemented. PurM: Phosphoribosylaminoimidazole synthetase, DNA Pol. A: DNA polymerase A.

Phage-microbe associations

We investigated phage-microbe interactions, another major top-down process affecting global bacterial/archaeal community structure (7). Here, surface (SRF) and deep chlorophyll

maximum (DCM) virus-bacteria networks revealed 1,869 positive associations between viral populations and 7 of the 54 known bacterial phyla (specifically – Proteobacteria, Cyanobacteria, Actinobacteria, Bacteroidetes, Deferribacteres, Verrucomicrobia and Planctomycetes), and one archaeal phylum (Euryarchaeota). These 8 phyla represent most of abundant bacterial/archaeal groups across 37 investigated samples (Fig. 3D), suggesting that the networks are detecting abundant virus-host interactions. Additionally, these interactions include phyla of microbes lacking viral genomes in RefSeq databases including Verrucomicrobia, and non-extremophile Euryarchaeota, hinting at genomic sequences for understudied viral taxa (Fig. 3E) (39, 62, 63). Among the phage populations in the network, we found 8 corresponding to phage sequences available in GenBank (>50% of genes with a >50% amino acid identity match). In all 8 cases, the predicted host from the network corresponded to the annotated host family in the GenBank record, which is significantly higher than expected by chance ($P=0.001$; see methods) (62).

Next, we evaluated viral host range, fundamental for predictive modeling and thus far largely limited to observations of cultured virus-host systems that insufficiently map complex community interactions (64). Our virus-host interaction data suggest that viruses are very host specific: ~43% of the phage populations interact with only a single host OTU, and the remaining 57% interact with only a few, often closely related OTUs (Fig. 3D). These networks are modular at large scales (65), suggesting that viruses are host-range-limited across large sections of host space. Nestedness analysis showed inconsistent results across algorithms (see methods).

Microscopic validation of predicted interactions

Our data predicted a photosymbiotic interaction between an acoel flatworm (*Symsagittifera* sp.) and a green microalga (*Tetraselmis* sp.). We validated this by Laser Scanning Confocal Microscopy (LSCM), 3D reconstruction, and reverse molecular identification on flatworm specimens isolated from *Tara Oceans* preserved morphological samples (see Methods). We observed microalgal cells (5 to 10 μm diameter) within each of the 15 isolated acoel specimens (Fig. 4) (66). The 18S sequence from several sorted holobionts matched the metabarcodes pair identified in the co-occurrence global network. Thus, molecular ecology, bioinformatics and microscopic analysis can enable the discovery of marine symbioses.

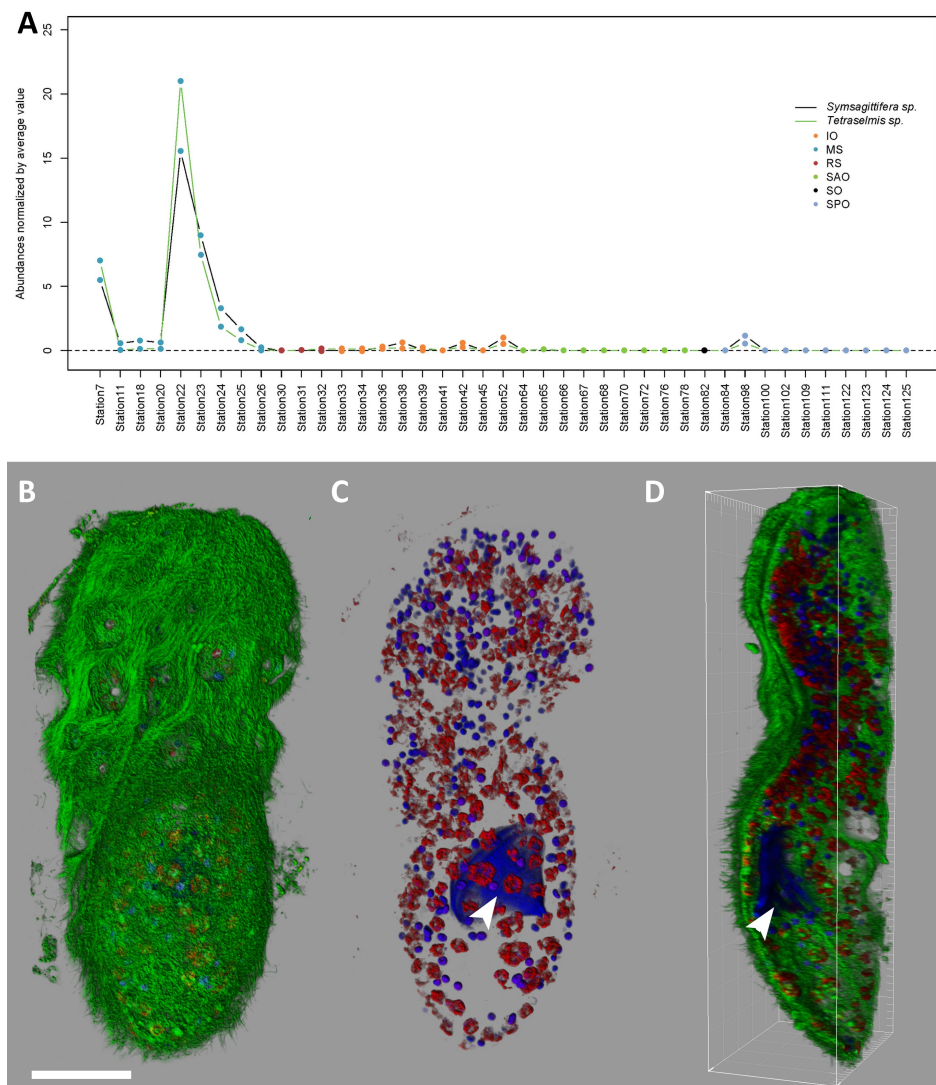


Figure 4. Experimental validation of network-predicted interaction (photosymbiosis). Guided by the predictions from the co-occurrence network and abundance patterns, acoel flatworms (*Symsagittifera* sp.) together with their photosynthetic green microalgal endosymbionts (*Tetraselmis* sp.) were collected in microplankton samples from *Tara Oceans* Station 22 in the Mediterranean Sea. Pictures show a 3D reconstructed specimen from LSCM images (Green channel: cellular membranes (DiOC6); Blue channel: DNA and the nuclei (Hoechst33342); Red channel: chlorophyll autofluorescence). **(A)** Co-occurrence plot of *Symsagittifera* and *Tetraselmis* related OTUs along *Tara Oceans* stations, showing the relatively high abundance of the holobiont at Station 22. **(B)** Dorsal view of the entire acoel flatworm specimen (~300 µm). The epidermis (green) is completely covered with cilia and displays some pore holes. **(C)** The removal of the green channel reveals the widespread distribution of small unicellular algae (red areas) inside the acoel body. The worm's nuclei display a clear signal (compact round blue shapes) while the algal nuclei are dimmer. A dinoflagellate theca (arrow head) is located in the central syncytium likely indicating predation. **(D)** Cross-section along a ZY plane allows localization of the algae, beneath the epidermis in the parenchyma. Only the external cell layer (green signal) from the dorsal view is visible, due to the thickness and opacity of the worm. Scale bar: 50 µm.

Conclusion

The global ocean interactome can be used to predict the dynamics and structure of ocean ecosystems. The interactome reported here spans all three organismal domains and viruses. The analyses presented emphasize the role of top-down biotic interactions in the epipelagic zone. This data will inform future research to understand how symbionts, pathogens, predators and parasites interact with their target organisms, and ultimately help elucidate the structure of the global food webs that drive nutrient and energy flow in the ocean.

Methods

Sampling

The sampling strategy used in the *Tara Oceans* expedition is described in (67) and samples used in the present study are listed in Table S1 and <http://doi.pangaea.de/10.1594/PANGAEA.840721>. The *Tara Oceans* nucleotide sequences are available at the European Nucleotide Archive (ENA) under projects PRJEB402 and PRJEB6610.

Physical and environmental measurements

Physical and environmental measurements were carried out with a vertical profile sampling system (CTD-Rosette) and data collected from Niskin bottles. We measured temperature, salinity, chlorophyll, CDOM fluorescence (fluorescence of the colored dissolved organic matter), particles abundance, nitrate concentration and particle size distribution (using an Underwater Vision Profiler). In addition, mean mixed layer depth (MLD), maximum fluorescence, vertical maximum of the Brünt-Väisälä Frequency N (s⁻¹), vertical range of dissolved oxygen, and of change of nitrates were determined. Satellite altimetry provided the Okubo-Weiss parameter, Lyapunov exponent, mesoscale eddie retention and sea surface temperature (SST) gradients at eddie fronts (19). Data are available at <http://www.pangaea.de> (<http://doi.pangaea.de/10.1594/PANGAEA.840718>).

Abundance table construction

Prokaryotic 16S rDNA metagenomic reads were identified, annotated and quantified from Illumina sequenced metagenomes (hereafter *mi*tags) as described in (68) using the SILVA v.115 database (19, 69, 70). The abundance table was normalized using the summed read count per sample (19, 71). Quality-checked V9 rDNA metabarcodes were clustered into swarms as in (10, 72), and annotated using the V9 PR2 database (73). PR2 barcodes were associated to fundamental trophic modes (auto- or hetero-trophy) and symbiotic interactions (parasitism and mutualism) based on literature (Taxonomic and trophic mode annotations are available at <http://doi.pangaea.de/10.1594/PANGAEA.840718> and <http://doi.pangaea.de/10.1594/PANGAEA.840722>). Swarm abundance and normalization was performed as in (10, 72). Bacteriophage metagenomes were obtained from the < 0.2 μ m fractions for 48 samples and contigs were annotated and quantified as in (18). The abundance matrix was normalized by total sample read count and contig length.

In all cases, only OTUs with relative abundance $> 1^{-8}$ and detected in at least 20 % of samples were retained. Because sample number in the input tables ranged from 17 to 63, prevalence thresholds varied (from 22% to 40%). The sum of all filtered OTU relative abundances was kept in the tables to preserve proportions. Abundance tables are available at <http://www.raeslab.org/companion/ocean-interactome.html>.

Random forest-based models

Eukaryotic, prokaryotic and environmental matrices were merged into two matrices (Deep Chlorophyll Maximum layer (DCM) and surface water layer (SRF)). For each of the three models (OTU versus other OTUs (MOTU), environmental factors (MENV) or combined (MOTU+ENV)), regressions were performed with OTU abundance as dependent and the abundances of other OTUs or environmental factors as independent variables. For each regression, up to 20 independent variables were selected using the minimum Redundancy Maximum Relevance (mRMR) filter-ranking algorithm. Random forest regression (25) was followed by a leave-one-out cross-validation. The variable subset with the minimum leave-one-out NMSE (Normalized Mean Square Error) was selected. To identify the best model for a given target OTU, the significance of the NMSE difference was tested on the absolute error values (paired Wilcoxon test adjusted by Benjamini-Hochberg FDR

estimation (74)). NMSE computed on random data are larger than those from original data. In addition, MENV outperformed MOTU when OTU abundances were randomized.

Variance partitioning

Environmental variables were z-score-transformed; spatial variables (MEM eigenvectors) were calculated based on latitude and longitude (75). Forward selection (76) was carried out with function forward.sel in R-package packfor. Significance of the selected variables was assessed with 1000 permutations using functions rda and anova.cca in vegan. Variance partitioning (77) was performed using function varpart in vegan on Hellinger-transformed abundance data, the forward-selected environmental variables, and the forward-selected spatial variables and tested for significance with 1000 permutations.

Network inference

Taxon-taxon co-occurrence networks were constructed as in (78), selecting Spearman and Kullback-Leibler dissimilarity measures. To compute p-values, we first generated permutation and bootstrap distributions, with 1,000 iterations each, by shuffling taxon abundances and resampling from samples with replacement, respectively. The measure-specific p-value was then obtained as the probability of the null value (represented by the mean of the permutation distribution) under a Gauss curve fitted to the mean and standard deviation of the bootstrap distribution. Permutations computed for Spearman included a renormalization step, which mitigates compositionality bias (ReBoot). Measure-specific p-values were merged using Brown's method (79) and multiple-testing-corrected with Benjamini-Hochberg (74). Finally, edges with an adjusted p-value above 0.05, with a score below the thresholds (30) or not supported by both measures after assessment of significance were discarded.

Taxon-environment networks were computed with the same procedure, starting with 8,000 initial positive and negative edges, each supported by both methods. For computational efficiency, we computed 23 taxon-taxon and taxon-environment networks separately, for two depths (DCM and SRF), four eukaryotic size fractions ($0.8\text{-}5 \mu\text{m}$, $>0.8 \mu\text{m}$, $20\text{-}180 \mu\text{m}$ and $180\text{-}2000 \mu\text{m}$) and their combinations, the prokaryotic size fraction ($0.2\text{-}1.6\mu\text{m}$ and $0.2\text{-}3.0\mu\text{m}$) and its combination with each of the eukaryotic and virus ($< 0.2 \mu\text{m}$) size fractions. We then generated 23 taxon-environment union networks for environmental triplet detection and merged the taxon-taxon networks into a global network with 92,633 edges.

Estimation of false discovery rate

We estimated the false discovery rate (FDR) of network construction with two null models. The first shuffles counts while preserving overall taxon proportions and total sample count sums, but removing any dependencies between taxa. For the second, we fitted a Dirichlet-Multinomial distribution to the input matrix using the dirmult package in R (80) and generated a null matrix by sampling from this distribution, preserving total sample count sums. Null matrices were generated from count matrices (0.8-5 μ m, 20-180 μ m and 180-2000 μ m eukaryotic and prokaryotic size fraction as well as bacteriophage-prokaryotic composite, SRF and DCM). Network construction was performed with the 20 null matrices and thresholds applied to the original matrices (28). From edge numbers in the original and the null networks, we estimated an average FDR of 9% (28).

Indirect taxon edge detection

For each taxon-environment union network, node triplets consisting of two taxa and one environmental parameter were identified. For each triplet, interaction information II was computed as: $II = CI(X, Y | Z) - I(X, Y)$, where CI is the conditional mutual information between taxa X and Y given environmental parameter Z and I the mutual information between X and Y . CI and I were estimated using minet (81). Taxon edges in environmental triplets were considered indirect when $II < 0$ and within the 0.05 quantile of the random II distribution obtained by shuffling environmental vectors (500 iterations). If a taxon was part of more than one environmental triplet, the triplet with minimum interaction information was selected.

For each environmental triplet, we also checked whether its sign pattern (the combination of positive and/or negative correlations) was consistent with an indirect interaction. From 8 possible patterns, 4 indicate indirect relationships (e.g. two negatively correlated taxa correlated with opposite signs to an environmental factor).

Network deconvolution (32) was carried out with beta=0.9. We considered an environmental triplet as indirect according to network deconvolution if any of its edges were removed.

All (11,043) negative interaction information triplets were consistent with an indirect relationship according to their sign patterns and a majority (8,209) was also supported by network deconvolution.

Influence of ocean regions on co-occurrence patterns

Samples were divided into groups according to region membership. The impact of each sample group on the Spearman correlation of each edge in the network was assessed by dividing the (absolute) omission score (OS; Spearman correlation without these samples) by the absolute original Spearman score. To account for group size, the OS was computed repeatedly for random, same-sized sample sets. Nonparametric p-values were calculated as the number of times random OSs were smaller than the sample group OS, divided by number of random OS (500 for each taxon pair). Edges were classified as region-specific when the ratio of OS and absolute original score was below 1 and multiple-testing-corrected p-values (Benjamini-Hochberg) were below 0.05.

Over-representation analysis

Significance of taxon–taxon counts at high taxonomic ranks was assessed with the hypergeometric distribution implemented in the R function `phyper`. Mutual exclusion vs copresence analysis was performed using the binomial distribution implemented in the R function `pbinom`, with the background probability estimated by the frequency of edges in the network.

Oceanic region analysis was also assessed using R's `pbinom` function, with the background probability estimated by dividing total ocean-specific edge number by total edge number. The p-value was computed as the probability of obtaining the observed number of ocean-specific edges among the edges of a taxon pair. The same procedure was repeated for each oceanic region separately, with region-specific success probabilities. Edges classified as indirect were discarded before the analysis.

In all tests, P-values were adjusted for multiple testing according to Benjamini, Hochberg and Yekutieli (BY), implemented in the R function `p.adjust`.

Extracting functional groups from the global plankton interactome

Functional groups consist of a mix of major monophyletic lineages of parasites, together with classical polyphyletic Plankton Functional Types (PFT), as defined in (10, 54, 55). Metabarcodes in the network were sorted into 15 parasite groups and 7 PFTs (55) based on their (*i*) taxonomical classification, (*ii*) membership in a given size fraction, (*iii*) trophic

mode, and (iv) biogeochemical role in DMS production or silicification. After mapping the metabarcodes and their edges onto PFTs and parasites, edges are weighted by the number of links they represent. Over-representation of the number of links included in each edge was assessed with the hypergeometric distribution.

Parasite links in large fractions may point to parasite-host connections. We extracted all edges in the large fractions (20-180 μm and 180-2000 μm) between barcodes annotated as parasites and non-parasitic barcodes. Partners of parasites comprised potential hosts (Fig 3B) but also organisms that are either too small or without size information. The former may represent unknown parasites (e.g. co-infecting a host with known parasites) while the latter may represent novel hosts.

Nestedness and modularity analysis

The analysis was carried out for 1,869 positively correlated phage-prokaryotic pairs. Modularity was computed with the LP (Label propagation) BRIM algorithm (82) in BiMAT (83) with 100 permutations. Nestedness of the host-phage network as quantified with the NODF (nestedness with overlap and decreasing fill) algorithm (84) in BiMAT with 100 permutations (preserving edge number and degree distribution) was significant, but not with the NTC algorithm (85). We also tested the impact of random removal or addition of 5%, 10%, 15% and 20% edges. After random addition/deletion of edges modularity and nestedness (according to NODF) remained significant.

Confirmation of predicted viruses-host associations

Two different approaches were used to confirm virus-host associations predicted by the co-occurrence network. First, the network host prediction was compared to the “known” host for viral populations closely related to an isolated virus, i.e. populations with more than 50% of predicted genes affiliated to the same phage reference genome (based on a BLASTp against RefseqVirus, threshold of 10^{-03} on e-value and 50 on bit score (18)). Known phages corresponded to viruses infecting SAR11, SAR116 and Cyanobacteria, so that a predicted host was considered correct if affiliated to Alphaproteobacteria, Alphaproteobacteria and Cyanobacteria, respectively (the lowest rank for which there was taxonomic assignment for those bacterial OTUs (69)). This procedure was repeated on 1000 randomized networks (with same degree distribution) to calculate the significance of the results. Second, contigs of

putative hosts predicted by co-occurrence analysis were compared with BLAST to a set of viral sequences detected in draft and single-cell genomes with VirSorter (<https://pods.iplantcollaborative.org/wiki/display/DEapps/VIRSorter+1.0.1>). One contig (36DCM_3902, Figure 3E) displayed significant similarity to one contig detected in a single-cell genome (AA160P02DRAFT_scaffold_31.32). In order to compare the putative host associated to each contig, rRNA genes were predicted in the single-cell amplified genome (SAG) contigs with meta-rRNA (86). Sequences were annotated based on BLAST against the non-redundant (nr) database, and the comparison plot was generated with Easyfig (87).

Literature-based evaluation of predicted protist interactions

A panel of 4 experts, 2 specialized in the study of planktonic mutualistic protists (Dr C. de Vargas and Dr J. Decelle) and 2 specialized in the study of planktonic parasitic protists (Dr C. Berney and N. Henry), screened literature looking for symbiotic interactions occurring among eukaryotic plankton. From this search, they built a list of 573 known symbiotic interactions sensu lato (i.e., parasitism and mutualism, at least 1 protist partner) in marine eukaryotic plankton, covering 197 eukaryotic genera, described in 76 publications since 1971. The experts extracted only symbiotic interaction cases described either from direct observation of both interacting partners through microscope (45%), sequence from symbiont isolated from the observed host (14%) or both (41%). Direct observation of partners interacting (86%) provides high confidence for the interaction, while the symbiont sequence allows its taxonomic identification. The protocol to build the list was the following: 1) the experts manually screened 3170 publications associated to each PR2 db sequence (http://ssu-rRNA.org/doc_bibliography.html); 2) the experts screened 293 publications retrieved from Web of Science with the following query: 'TOPIC:(plankton* AND (marin* OR ocean*)) AND (parasit* OR symbios* OR mutualis*)'; 3) the experts screened GenBank 18S rDNA sequences of symbionts for which the 'host' field was known. They labeled these interactions as 'Unpublished'. Finally, the experts discussed any observed discordance until agreement was reached. The final table of literature-curated interactions includes a column indicating the type of evidence gathered about the interaction: 1 for only getting symbiont sequence, 2 for direct observation, and 3 for both. Symbiont GenBank host field belongs to category 1.

Experimental validation of a predicted interaction

V9 pairs were searched for organisms of suitable size to allow its isolation from morphological samples. This way, we targeted a predicted photosymbiosis between an acoel flatworm (V9 rDNA metabarcode 83% similar to *Symsagittifera psammophila* (88) and a photosynthetic microalga (*Tara* Oceans V9 metabarcode 100% similar to a *Tetraselmis* sp) (89).

Fifteen acoel specimens (hosts) were isolated from formaldehyde-4% microplankton samples of station 22 (A100000458), where both partner OTUs displayed high abundances. Prior to imaging, specimens were rinsed with artificial seawater, then DNA and membrane structures were stained for 60 minutes with 10µM Hoechst 33342 and 1.4µM DiOC6(3) (Life Technologies). Microscopy was conducted using a Leica TCS SP8 (Leica Microsystems) confocal laser scanning microscope and a HC PL APO 40x/1.10 W motCORR CS2 objective. The DiOC6 signal (ex488nm/em500-520nm) was collected simultaneously with the chlorophyll signal (ex488nm/em670-710nm), followed by the Hoechst signal (ex405 nm/em420-470nm). Images were processed with Fiji (90), and 3D specimens were reconstructed with Imaris (Bitplane).

To obtain the sequences of the metabarcodes of each partner, seven acoels were isolated from ethanol-preserved samples from station 22 (TARA_A100000451), individually rinsed in filtered seawater, and stored at -20°C in absolute ethanol. DNA was extracted with MasterPure™ DNA/RNA purification kit (Epicenter) and PCR amplified using the universal-eukaryote primers (forward 1389F and reverse 1510R) from (10). Chlorophyte-specific primers (Chloro2F: 5'- CGTATATTAAAGTTGTYTGCAG-3' and Tetra2-rev 5'- CAGCAATGGCGGTGGC GAAC-3') were designed to amplify the microalgae V9 rDNA as in (4). Purified amplicons were subjected to poly-A reaction and ligated in pCR®4-TOPO TA Cloning vector (Invitrogen), cloned using chemically competent *E. coli* cells and Sanger-sequenced with the ABI-PRISM Big Dye Terminator Sequencing kit (Applied Biosystems) using the 3130xl Genetic Analyzer, Applied Biosystems.

References

1. AZAM, Farooq, FENCHEL, Tom, FIELD, John G, *et al.* The ecological role of water-column microbes in the sea. *Estuaries*, 1983, vol. 50, no 2.

2. THOMPSON, Anne W., FOSTER, Rachel A., KRUPKE, Andreas, *et al.* Unicellular cyanobacterium symbiotic with a single-celled eukaryotic alga. *Science*, 2012, vol. 337, no 6101, p. 1546-1550.
3. CHAMBOUVET, Aurelie, MORIN, Pascal, MARIE, Dominique, *et al.* Control of toxic marine dinoflagellate blooms by serial parasitic killers. *Science*, 2008, vol. 322, no 5905, p. 1254-1257.
4. DECELLE, Johan, PROBERT, Ian, BITTNER, Lucie, *et al.* An original mode of symbiosis in open ocean plankton. *Proceedings of the National Academy of Sciences*, 2012, vol. 109, no 44, p. 18000-18005.
5. SMETACEK, Victor. Making sense of ocean biota: How evolution and biodiversity of land organisms differ from that of the plankton. *Journal of biosciences*, 2012, vol. 37, no 4, p. 589-607.
6. SABO, John L. et GERBER, Leah R., "Trophic ecology," *AccessScience* (McGraw-Hill Education, 2014); available at www.accessscience.com/content/trophic-ecology/711650.
7. ROHWER, Forest et THURBER, Rebecca Vega. Viruses manipulate the marine environment. *Nature*, 2009, vol. 459, no 7244, p. 207-212.
8. VERITY, Peter G., SMETACEK, Victor, *et al.* Organism life cycles, predation, and the structure of marine pelagic ecosystems. *Marine Ecology Progress Series*, 1996, vol. 130.
9. WORDEN, Alexandra Z., FOLLOWS, Michael J., GIOVANNONI, Stephen J., *et al.* Rethinking the marine carbon cycle: Factoring in the multifarious lifestyles of microbes. *Science*, 2015, vol. 347, no 6223, p. 1257594.
10. DE VARGAS, Colombe, AUDIC, Stéphane, HENRY, Nicolas, *et al.* Eukaryotic plankton diversity in the sunlit ocean. *Science*, 2015, vol. 348, no 6237, p. 1261605.
11. FAUST, Karoline et RAES, Jeroen. Microbial interactions: from networks to models. *Nature Reviews Microbiology*, 2012, vol. 10, no 8, p. 538-550.
12. CHAFFRON, Samuel, REHRAUER, Hubert, PERNTHALER, Jakob, *et al.* A global network of coexisting microbes from environmental and whole-genome sequence data. *Genome research*, 2010, vol. 20, no 7, p. 947-959.
13. RAES, Jeroen, LETUNIC, Ivica, YAMADA, Takuji, *et al.* Toward molecular trait-based ecology through integration of biogeochemical, geographical and metagenomic data. *Molecular systems biology*, 2011, vol. 7, no 1, p. 473.

14. GILBERT, Jack A., STEELE, Joshua A., CAPORASO, J. Gregory, *et al.* Defining seasonal marine microbial community dynamics. *The ISME journal*, 2012, vol. 6, no 2, p. 298-308.
15. BEMAN, J. Michael, STEELE, Joshua A., et FUHRMAN, Jed A. Co-occurrence patterns for abundant marine archaeal and bacterial lineages in the deep chlorophyll maximum of coastal California. *The ISME journal*, 2011, vol. 5, no 7, p. 1077-1085.
16. CHOW, Cheryl-Emiliane T., KIM, Diane Y., SACHDEVA, Rohan, *et al.* Top-down controls on bacterial community structure: microbial network analysis of bacteria, T4-like viruses and protists. *The ISME journal*, 2014, vol. 8, no 4, p. 816-829.
17. KARSENTI, Eric, ACINAS, Silvia G., BORK, Peer, *et al.* A holistic approach to marine eco-systems biology. *PLoS biol*, 2011, vol. 9, no 10, p. e1001177.
18. BRUM, Jennifer R., IGNACIO-ESPINOSA, J. Cesar, ROUX, Simon, *et al.* Patterns and ecological drivers of ocean viral communities. *Science*, 2015, vol. 348, no 6237, p. 1261498.
19. SUNAGAWA, Shinichi, COELHO, Luis Pedro, CHAFFRON, Samuel, *et al.* Structure and function of the global ocean microbiome. *Science*, 2015, vol. 348, no 6237, p. 1261359.
20. VILLAR, Emilie, FARRANT, Gregory K., FOLLOWS, Michael, *et al.* Environmental characteristics of Agulhas rings affect interocean plankton transport. *Science*, 2015, vol. 348, no 6237, p. 1261447.
21. Companion web site table w2 available at <http://www.raeslab.org/companion/ocean-interactome/tables/W2.xlsx>
22. MEOT, Alain, LEGENDRE, Pierre, et BORCARD, Daniel. Partialling out the spatial component of ecological variation: questions and propositions in the linear modelling framework. *Environmental and Ecological Statistics*, 1998, vol. 5, no 1, p. 1-27.
23. Companion web site table w3 available at <http://www.raeslab.org/companion/ocean-interactome/tables/W3.xlsx>
24. Companion web site figure w1 available at <http://www.raeslab.org/companion/ocean-interactome/figures//W1.pdf>
25. BREIMAN, Leo. Random forests. *Machine learning*, 2001, vol. 45, no 1, p. 5-32.
26. Companion web site table w4 available at <http://www.raeslab.org/companion/ocean-interactome/tables/W4.xlsx>

27. Companion web site figure w2 available at <http://www.raeslab.org/companion/ocean-interactome/figures/W2.pdf>
28. Companion web site table w5 available at <http://www.raeslab.org/companion/ocean-interactome/tables/W5.xlsx>
29. Companion web site table w6 available at <http://www.raeslab.org/companion/ocean-interactome/tables/W6.xlsx>
30. Companion web site table w7 available at <http://www.raeslab.org/companion/ocean-interactome/tables/W7.xlsx>
31. Companion web site figure w3 available at <http://www.raeslab.org/companion/ocean-interactome/figures/W3.pdf>
32. FEIZI, Soheil, MARBACH, Daniel, MÉDARD, Muriel, *et al.* Network deconvolution as a general method to distinguish direct dependencies in networks. *Nature biotechnology*, 2013, vol. 31, no 8, p. 726-733.
33. Companion web site table w8 available at <http://www.raeslab.org/companion/ocean-interactome/tables/W8.xlsx>
34. CUSICK, Michael E., YU, Haiyuan, SMOLYAR, Alex, *et al.* Literature-curated protein interaction datasets. *Nature methods*, 2009, vol. 6, no 1, p. 39-46.
35. Companion web site table w9 available at <http://www.raeslab.org/companion/ocean-interactome/tables/W9.xlsx>
36. FUHRMAN, Jed A., CRAM, Jacob A., et NEEDHAM, David M. Marine microbial community dynamics and their ecological interpretation. *Nature Reviews Microbiology*, 2015.
37. Companion web site additional material available at http://www.raeslab.org/companion/ocean-interactome/Accompanying_Material.docx
38. Companion web site figure w4 available at <http://www.raeslab.org/companion/ocean-interactome/figures/W4.pdf>
39. Companion web site table w10 available at <http://www.raeslab.org/companion/ocean-interactome/tables/W10.xlsx>
40. MCMANUS, George B. et SANTOFERRARA, Luciana F. Tintinnids in microzooplankton communities. *The Biology and Ecology of Tintinnid Ciliates: Models for Marine Plankton*, 2012, p. 198-213.

41. CACHON, Jean. Contribution à l'étude des péridiniens parasites. Cytologie, cycles évolutifs. *Annales des Sciences Naturelles - Zoologie et Biologie Animale*, 1964, vol. 6, p. 1-158.
42. SALOMON, Paulo S., GRANÉLI, Edna, NEVES, Maria HCB, et al. Infection by *Amoebophrya* spp. parasitoids of dinoflagellates in a tropical marine coastal area. *Aquatic microbial ecology*, 2009, vol. 55, no 2, p. 143-153.
43. GÓMEZ, Fernando, LÓPEZ-GARCÍA, Purificación, NOWACZYK, Antoine, et al. The crustacean parasites *Ellobiopsis* Caullery, 1910 and *Thalassomyces* Niezabitowski, 1913 form a monophyletic divergent clade within the Alveolata. *Systematic parasitology*, 2009, vol. 74, no 1, p. 65-74.
44. OHTSUKA, Susumu, HORA, Mariko, SUZAKI, Toshinobu, et al. Morphology and host-specificity of the apostome ciliate *Vampyrophrya pelagica* infecting pelagic copepods in the Seto Inland Sea, Japan. *Marine Ecology Progress Series*, 2004, vol. 282, p. 129-142.
45. SKOVGAARD, Alf, KARPOV, Sergey A., et GUILLOU, Laure. The parasitic dinoflagellates *Blastodinium* spp. inhabiting the gut of marine, planktonic copepods: morphology, ecology, and unrecognized species diversity. *Frontiers in microbiology*, 2012, vol. 3.
46. STEMMANN, Lars, YOUNGBLUTH, Marsh, ROBERT, Kevin, et al. Global zoogeography of fragile macrozooplankton in the upper 100-1000 m inferred from the underwater video profiler. *ICES journal of marine science*, 2008, vol. 65, no 3, p. 433-442.
47. GASOL, Josep M., DEL GIORGIO, Paul A., et DUARTE, Carlos M. Biomass distribution in marine planktonic communities. *Limnology and Oceanography*, 1997, vol. 42, no 6, p. 1353-1363.
48. WARD, Ben A., DUTKIEWICZ, Stephanie, et FOLLOW, Michael J. Modelling spatial and temporal patterns in size-structured marine plankton communities: top-down and bottom-up controls. *Journal of Plankton Research*, 2014, vol. 36, no 1, p. 31-47.
49. IANORA, Adrianna, MIRALTO, Antonio, POULET, Serge A., et al. Aldehyde suppression of copepod recruitment in blooms of a ubiquitous planktonic diatom. *Nature*, 2004, vol. 429, no 6990, p. 403-407.
50. MARTINEZ-GARCIA, Manuel, BRAZEL, David, POULTON, Nicole J., et al. Unveiling in situ interactions between marine protists and bacteria through single cell sequencing. *The ISME journal*, 2012, vol. 6, no 3, p. 703-707.

51. JOLLEY, Elizabeth T. et JONES, Alvin K. The interaction between *Navicula muralis* Grunow and an associated species of *Flavobacterium*. *British Phycological Journal*, 1977, vol. 12, no 4, p. 315-328.
52. MILLER, Todd R. et BELAS, Robert. Dimethylsulfoniopropionate metabolism by *Pfiesteria*-associated *Roseobacter* spp. *Applied and environmental microbiology*, 2004, vol. 70, no 6, p. 3383-3391.
53. Companion web site figure w5 available at <http://www.raeslab.org/companion/ocean-interactome/figures/W5.pdf>
54. QUERE, Corinne Le, HARRISON, Sandy P., COLIN PRENTICE, I., *et al.* Ecosystem dynamics based on plankton functional types for global ocean biogeochemistry models. *Global Change Biology*, 2005, vol. 11, no 11, p. 2016-2040.
55. Companion web site table w11 available at <http://www.raeslab.org/companion/ocean-interactome/tables/W11.xlsx>
56. SKOVGAARD, Alf. Dirty tricks in the plankton: Diversity and Role of Marine Parasitic Protists: diversity and role of marine parasitic protists. *Acta Protozoologica*, 2014, vol. 53, no 1, p. 51-62.
57. Companion web site figure w6 available at <http://www.raeslab.org/companion/ocean-interactome/figures/W6.pdf>
58. HEYDEN, Sophie, CHAO, Ema E., VICKERMAN, Keith, *et al.* Ribosomal RNA phylogeny of bodonid and diplomirimid flagellates and the evolution of Euglenozoa. *Journal of Eukaryotic Microbiology*, 2004, vol. 51, no 4, p. 402-416.
59. GÓMEZ, Fernando, MOREIRA, David, BENZERARA, Karim, *et al.* *Solenicola setigera* is the first characterized member of the abundant and cosmopolitan uncultured marine stramenopile group MAST-3. *Environmental microbiology*, 2011, vol. 13, no 1, p. 193-202.
60. HAMM, Christian E., MERKEL, Rudolf, SPRINGER, Olaf, *et al.* Architecture and material properties of diatom shells provide effective mechanical protection. *Nature*, 2003, vol. 421, no 6925, p. 841-843.
61. ASSMY, Philipp et SMETACEK, Victor. Algal blooms. *Encyclopedia of Microbiology/Moselio Schaechter, Editor. Oxford: Elsevier (Academic Pr.)*, 2009, p. 27-41.
62. Companion web site table w12 available at <http://www.raeslab.org/companion/ocean-interactome/tables/W12.xlsx>

63. Companion web site figure w7 available at <http://www.raeslab.org/companion/ocean-interactome/figures/W7.pdf>
64. WEITZ, Joshua S., POISOT, Timothée, MEYER, Justin R., et al. Phage–bacteria infection networks. *Trends in microbiology*, 2013, vol. 21, no 2, p. 82-91.
65. Companion web site table w13 available at <http://www.raeslab.org/companion/ocean-interactome/tablesW13.xlsx>
66. Companion web site figure w9 available at http://www.raeslab.org/companion/ocean-interactome/companion_figures/W9.pdf
67. PESANT, Stéphane, NOT, Fabrice, PICHERAL, Marc, et al. Open science resources for the discovery and analysis of Tara Oceans data. *Scientific Data*, 2015, vol. 2.
68. LOGARES, Ramiro, SUNAGAWA, Shinichi, SALAZAR, Guillem, et al. Metagenomic 16S rDNA Illumina tags are a powerful alternative to amplicon sequencing to explore diversity and structure of microbial communities. *Environmental microbiology*, 2014, vol. 16, no 9, p. 2659-2671.
69. PRUESSE, Elmar, QUAST, Christian, KNITTEL, Katrin, et al. SILVA: a comprehensive online resource for quality checked and aligned ribosomal RNA sequence data compatible with ARB. *Nucleic acids research*, 2007, vol. 35, no 21, p. 7188-7196.
70. EDGAR, Robert C. Search and clustering orders of magnitude faster than BLAST. *Bioinformatics*, 2010, vol. 26, no 19, p. 2460-2461.
71. WANG, Qiong, GARRITY, George M., TIEDJE, James M., et al. Naive Bayesian classifier for rapid assignment of rRNA sequences into the new bacterial taxonomy. *Applied and environmental microbiology*, 2007, vol. 73, no 16, p. 5261-5267.
72. MAHÉ, Frédéric, ROGNES, Torbjørn, QUINCE, Christopher, et al. Swarm: robust and fast clustering method for amplicon-based studies. *PeerJ*, 2014, vol. 2, p. e593.
73. GUILLOU, Laure, BACHAR, Dipankar, AUDIC, Stéphane, et al. The Protist Ribosomal Reference database (PR2): a catalog of unicellular eukaryote small sub-unit rRNA sequences with curated taxonomy. *Nucleic acids research*, 2013, p. gks1160.
74. BENJAMINI, Yoav et HOCHBERG, Yosef. Controlling the false discovery rate: a practical and powerful approach to multiple testing. *Journal of the Royal Statistical Society. Series B (Methodological)*, 1995, p. 289-300.

75. BORCARD, Daniel, LEGENDRE, Pierre, AVOIS-JACQUET, Carol, *et al.* Dissecting the spatial structure of ecological data at multiple scales. *Ecology*, 2004, vol. 85, no 7, p. 1826-1832.
76. BLANCHET, F. Guillaume, LEGENDRE, Pierre, et BORCARD, Daniel. Forward selection of explanatory variables. *Ecology*, 2008, vol. 89, no 9, p. 2623-2632.
77. BORCARD, Daniel, LEGENDRE, Pierre, et DRAPEAU, Pierre. Partialling out the spatial component of ecological variation. *Ecology*, 1992, vol. 73, no 3, p. 1045-1055.
78. FAUST, Karoline, SATHIRAPONGSASUTI, J. Fah, IZARD, Jacques, *et al.* Microbial co-occurrence relationships in the human microbiome. *PLoS computational biology*, 2012, vol. 8, no 7, p. e1002606-e1002606.
79. BROWN, Morton B. 400: A method for combining non-independent, one-sided tests of significance. *Biometrics*, 1975, p. 987-992.
80. TVEDEBRINK, Torben. Overdispersion in allelic counts and θ -correction in forensic genetics. *Theoretical population biology*, 2010, vol. 78, no 3, p. 200-210.
81. MEYER, Patrick E., LAFITTE, Frederic, et BONTEMPI, Gianluca. minet: A R/Bioconductor package for inferring large transcriptional networks using mutual information. *BMC bioinformatics*, 2008, vol. 9, no 1, p. 461.
82. LIU, Xin et MURATA, Tsuyoshi. Community detection in large-scale bipartite networks. In : *Web Intelligence and Intelligent Agent Technologies, 2009. WI-IAT'09. IEEE/WIC/ACM International Joint Conferences on*. IET, 2009. p. 50-57.
83. FLORES, Cesar O., POISOT, Timothée, et WEITZ, Joshua S. BiMAT: a MATLAB (R) package to facilitate the analysis and visualization of bipartite networks. *arXiv preprint arXiv:1406.6732*, 2014.
84. BARBER, Michael J. Modularity and community detection in bipartite networks. *Physical Review E*, 2007, vol. 76, no 6, p. 066102.
85. ATMAR, Wirt et PATTERSON, Bruce D. The measure of order and disorder in the distribution of species in fragmented habitat. *Oecologia*, 1993, vol. 96, no 3, p. 373-382.
86. HUANG, Ying, GILNA, Paul, et LI, Weizhong. Identification of ribosomal RNA genes in metagenomic fragments. *Bioinformatics*, 2009, vol. 25, no 10, p. 1338-1340.
87. SULLIVAN, Mitchell J., PETTY, Nicola K., et BEATSON, Scott A. Easyfig: a genome comparison visualizer. *Bioinformatics*, 2011, vol. 27, no 7, p. 1009-1010.

88. RUIZ-TRILLO, Iñaki, RIUTORT, Marta, LITTLEWOOD, D. Timothy J., *et al.* Acoel flatworms: earliest extant bilaterian metazoans, not members of Platyhelminthes. *Science*, 1999, vol. 283, no 5409, p. 1919-1923.
89. GAST, Rebecca J., MCDONNELL, Tracey A., et CARON, David A. srDna-based taxonomic affinities of algal symbionts from a planktonic foraminifer and a solitary radiolarian. *Journal of Phycology*, 2000, vol. 36, no 1, p. 172-177.
90. SCHINDELIN, Johannes, ARGANDA-CARRERAS, Ignacio, FRISE, Erwin, *et al.* Fiji: an open-source platform for biological-image analysis. *Nature methods*, 2012, vol. 9, no 7, p. 676-682.
91. NEWMAN, Mark EJ. Finding community structure in networks using the eigenvectors of matrices. *Physical review E*, 2006, vol. 74, no 3, p. 036104.

Acknowledgements

We thank the commitment of the following people and sponsors: CNRS (in particular Groupement de Recherche GDR3280), European Molecular Biology Laboratory (EMBL), Genoscope/CEA, VIB, Stazione Zoologica Anton Dohrn, UNIMIB, Fund for Scientific Research – Flanders (GLM, KF, SC, JR), Rega Institute (JR), KU Leuven (JR), The French Ministry of Research, the French Government 'Investissements d'Avenir' programmes OCEANOMICS (ANR-11-BTBR-0008), FRANCE GENOMIQUE (ANR-10-INBS-09-08), MEMO LIFE (ANR-10-LABX-54), PSL* Research University (ANR-11-IDEX-0001-02), ANR (projects POSEIDON/ANR-09-BLAN-0348, PHYTBACK/ANR-2010-1709-01, PROMETHEUS/ANR-09-PCS-GENM-217, TARA GIRUS/ANR-09-PCS-GENM-218, European Union FP7 (MicroB3/No.287589, IHMS/HEALTH-F4-2010-261376, ERC Advanced Grant Awards to CB (Diatomite: 294823), Gordon and Betty Moore Foundation grant (#3790) to MBS, Spanish Ministry of Science and Innovation grant CGL2011-26848/BOS MicroOcean PANGENOMICS to SGA, TANIT (CONES 2010-0036) from the Agència de Gestió d'Ajusts Universitaris i Reserca funded to SGA, JSPS KAKENHI Grant Number 26430184 to HO, FWO, BIO5, Biosphere 2, Agnès b., the Veolia Environment Foundation, Region Bretagne, Lorient Agglomeration, World Courier, Illumina, the EDF Foundation, FRB, the Prince Albert II de Monaco Foundation, Etienne Bourgois, the *Tara* schooner and its captain and crew. We are also grateful to the French Ministry of Foreign Affairs for supporting the expedition and to the countries that graciously granted sampling permissions. *Tara* Oceans would not exist without continuous support from 23 institutes

(<http://oceans.taraexpeditions.org>). We also acknowledge the EMBL Advanced Light Microscopy Facility (ALMF), and in particular Rainer Pepperkok. The authors further declare that all data reported herein are fully and freely available from the date of publication, with no restrictions, and that all of the samples, analyses, publications, and ownership of data are free from legal entanglement or restriction of any sort by the various nations whose waters the Tara Oceans expedition sampled in. Data described herein is available at www.raeslab.org/companion/ocean-interactome.html, at the EBI under the projects PRJEB402 and PRJEB6610, and at Pangaea <http://doi.pangaea.de/10.1594/PANGAEA.840721>, <http://doi.pangaea.de/10.1594/PANGAEA.840718>, <http://doi.pangaea.de/10.1594/PANGAEA.843018> and <http://doi.pangaea.de/10.1594/PANGAEA.843022> and on table S1. The data release policy regarding future public release of Tara Oceans data are described in Pesant et al. (67). All authors approved the final manuscript. This article is contribution number 25 of Tara Oceans. The supplementary materials contain additional data.

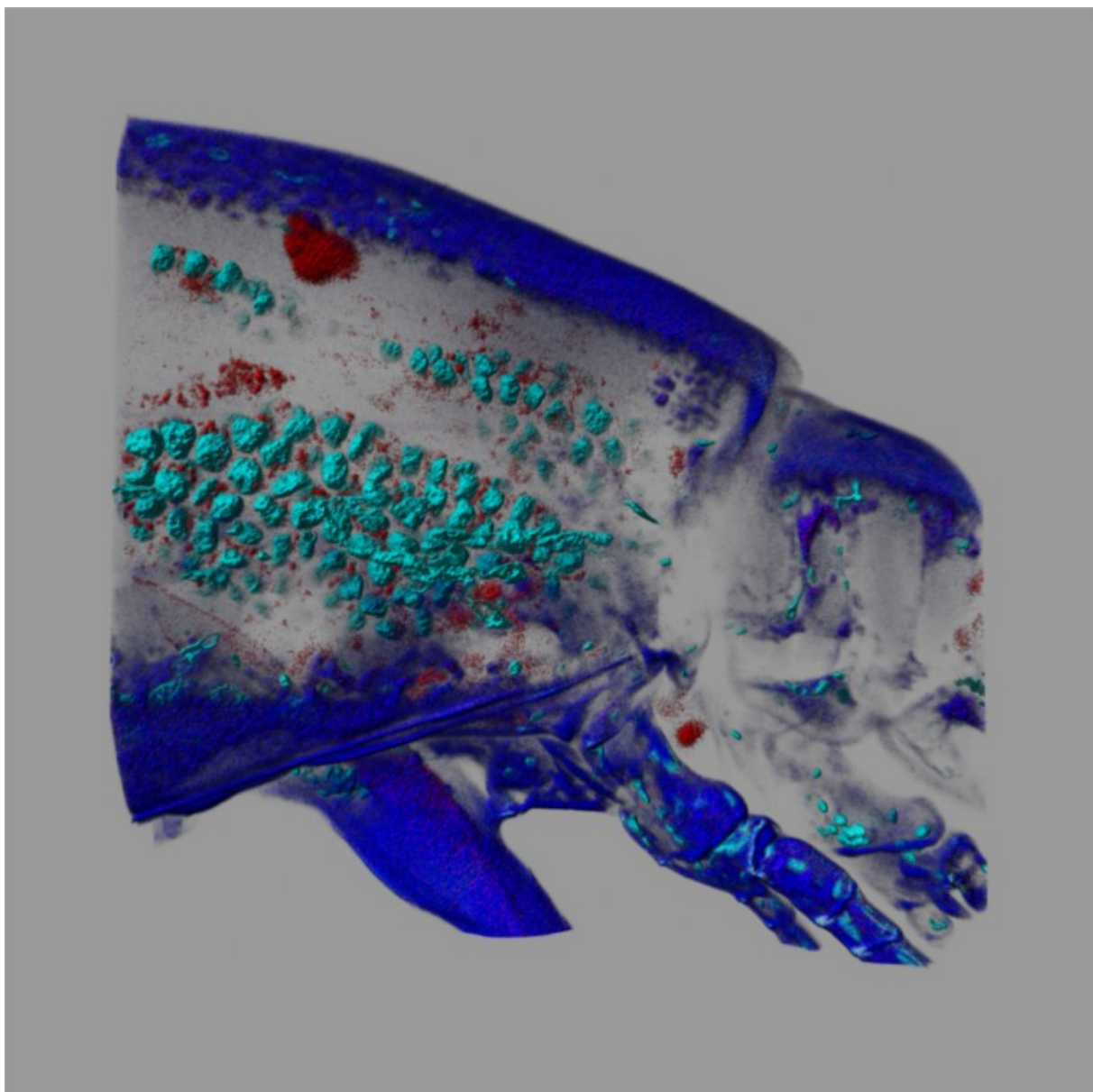
Tara Oceans Coordinators

Silvia G. Acinas¹, Peer Bork², Emmanuel Boss³, Chris Bowler⁴, Colomban De Vargas^{5,6}, Michael Follows⁷, Gabriel Gorsky^{8,9}, Nigel Grimsley^{10,11}, Pascal Hingamp¹², Daniele Iudicone¹³, Olivier Jaillon^{14,15,16}, Stefanie Kandels-Lewis², Lee Karp-Boss³, Eric Karsenti^{17,18}, Uros Krzic¹⁹, Fabrice Not^{5,6}, Hiroyuki Ogata²⁰, Stephane Pesant^{21,22}, Jeroen Raes^{23,24,25}, Emmanuel G. Reynaud²⁶, Christian Sardet⁸, Mike Sieracki²⁷, Sabrina Speich^{28,29}, Lars Stemmann⁸, Matthew B. Sullivan³⁰, Shinichi Sunagawa², Didier Velayoudon³¹, Jean Weissenbach^{14,15,16}, Patrick Wincker^{14,15,16}

¹Department of Marine Biology and Oceanography, Institute of Marine Science (ICM)-CSIC, Barcelona, Spain. ²Structural and Computational Biology, European Molecular Biology Laboratory, Heidelberg, Germany. ³School of Marine Sciences, University of Maine, Orono, USA. ⁴Environmental and Evolutionary Genomics Section, Institut de Biologie de l'Ecole Normale Supérieure, Centre National de la Recherche Scientifique, Unité Mixte de Recherche 8197, Institut National de la Santé et de la Recherche Médicale U1024, Ecole Normale Supérieure, Paris, France. ⁵CNRS, UMR 7144, Station Biologique de Roscoff, Roscoff, France. ⁶Sorbonne Universités, UPMC Univ Paris 06, UMR 7144, Station Biologique de Roscoff, Roscoff, France. ⁷Dept of Earth, Atmospheric and Planetary Sciences, Massachusetts Institute of Technology, Cambridge, USA. ⁸CNRS/UPMC, UMR 7009, BioDev, Observatoire océanologique, Villefranche/mer, France. ⁹Sorbonne Universités, UPMC Univ Paris 06, UMR 7093, LOV, Observatoire océanologique, Villefranche/mer, France. ¹⁰CNRS UMR 7232, BIOM, Banyuls-sur-Mer, France. ¹¹Sorbonne Universités, OOB, UPMC Paris 06, Banyuls-sur-Mer, France. ¹²Aix Marseille Université, CNRS, IGS UMR 7256, Marseille, France. ¹³Laboratory of Ecology and Evolution of Plankton, Stazione Zoologica Anton Dohrn, Naples, Italy. ¹⁴CEA, Genoscope, Evry France. ¹⁵CNRS, UMR 8030, Evry, France. ¹⁶Université d'Evry, UMR 8030, Evry, France. ¹⁷Environmental and Evolutionary Genomics Section, Institut de Biologie de l'Ecole Normale Supérieure, CNRS, UMR 8197, Institut National de la Santé et de la Recherche Médicale U1024, Ecole Normale Supérieure, Paris, France. ¹⁸Directors' Research, European Molecular Biology Laboratory, Heidelberg, Germany. ¹⁹Cell Biology and Biophysics, European Molecular Biology Laboratory, Heidelberg, Germany. ²⁰Institute for Chemical Research, Kyoto University, Kyoto, Japan. ²¹PANGAEA, Data Publisher for Earth and Environmental Science, University of Bremen, Bremen, Germany. ²²MARUM, Center for Marine Environmental Sciences, University of Bremen, Bremen, Germany. ²³Department of Microbiology and Immunology, Rega Institute KU Leuven, Leuven, Belgium. ²⁴VIB Center for the Biology of Disease, VIB, Leuven, Belgium. ²⁵Laboratory of Microbiology, Vrije Universiteit Brussel, Brussels, Belgium. ²⁶School of Biology and Environmental Science, University College Dublin, Dublin, Ireland. ²⁷Bigelow Laboratory for Ocean Sciences, East Boothbay, USA. ²⁸Department of Geosciences, Laboratoire de Météorologie Dynamique (LMD), Ecole Normale Supérieure, Paris, France. ²⁹Laboratoire de Physique des Océans, UBO-IUEM, Polouzané, France. ³⁰Department of Ecology and Evolutionary Biology, University of Arizona, Tucson, USA. ³¹DVIP Consulting, Sèvres, France.

Chapitre II

Cas spécifiques de symbioses eucaryotes planctoniques



Copépode infecté par *Blastodinium* spp. S. Colin

Les articles présentés dans le chapitre précédent montrent que les symbiotes représentent une part importante de la diversité et de l'abondance des eucaryotes des écosystèmes marins planctoniques (premier article) et que les symbioses, comme les autres interactions biotiques, seraient les forces majeures expliquant la structure des communautés de ces écosystèmes (second article). Dans ce chapitre deux cas de symbiose eucaryote planctonique : un cas de parasitisme entre le dinoflagellé parasite *Blastodinium* et des copépodes et un cas de mutualisme (photosymbiose) entre le dinoflagellé photosynthétique *Symbiodinium* et le cilié *Tiarina*. L'étude de cas spécifiques de symbioses m'est apparu indispensable afin d'identifier de quelle manière se répercute les spécificités des interactions symbiotiques dans des données de metabarcoding. Quelques unes de ces spécificités sont identifiées dans ce chapitre et seront prises en compte dans le troisième et dernier chapitre de ce manuscrit.

Le premier article « ***Symbiodinium* in endosymbiosis within the ciliate *Tiarina*** » met en évidence une nouvelle photosymbiose impliquant le dinoflagellé *Symbiodinium* et une nouvelle espèce de cilié calcifiant du genre *Tiarina*. Il s'agit de la première observation dans le plancton d'une interaction symbiotique entre un protiste et le genre *Symbiodinium* qui, jusque là, n'avait été observé qu'en association avec des hôtes ayant au moins une phase de leur vie benthique, principalement des cnidaires et des mollusques. L'observation d'une division active des symbiotes à l'intérieur des ciliés suggère que l'association est durable. De plus, à l'instar de la plupart des photosymbioses planctoniques, cette association est principalement observée dans les environnements oligotrophes, ce qui laisse à penser qu'il s'agit d'une association mutualiste permettant à l'hôte cilié d'obtenir une partie de son énergie grâce à son symbiose dans un environnement où la disponibilité en proies est limitée. Des études moléculaires réalisées à partir de séquences d'ADN ribosomique 18S, ITS2 et 28S sur les symbiotes de *Tiarina* ont permis de mettre en évidence une toute nouvelle diversité à l'intérieur du genre *Symbiodinium*. Chacun de ces nouveaux génotypes a une distribution particulière à travers les différentes stations *Tara Oceans* et plusieurs de ces génotypes ont été décrits avec le même génotype hôte (Figure 2).

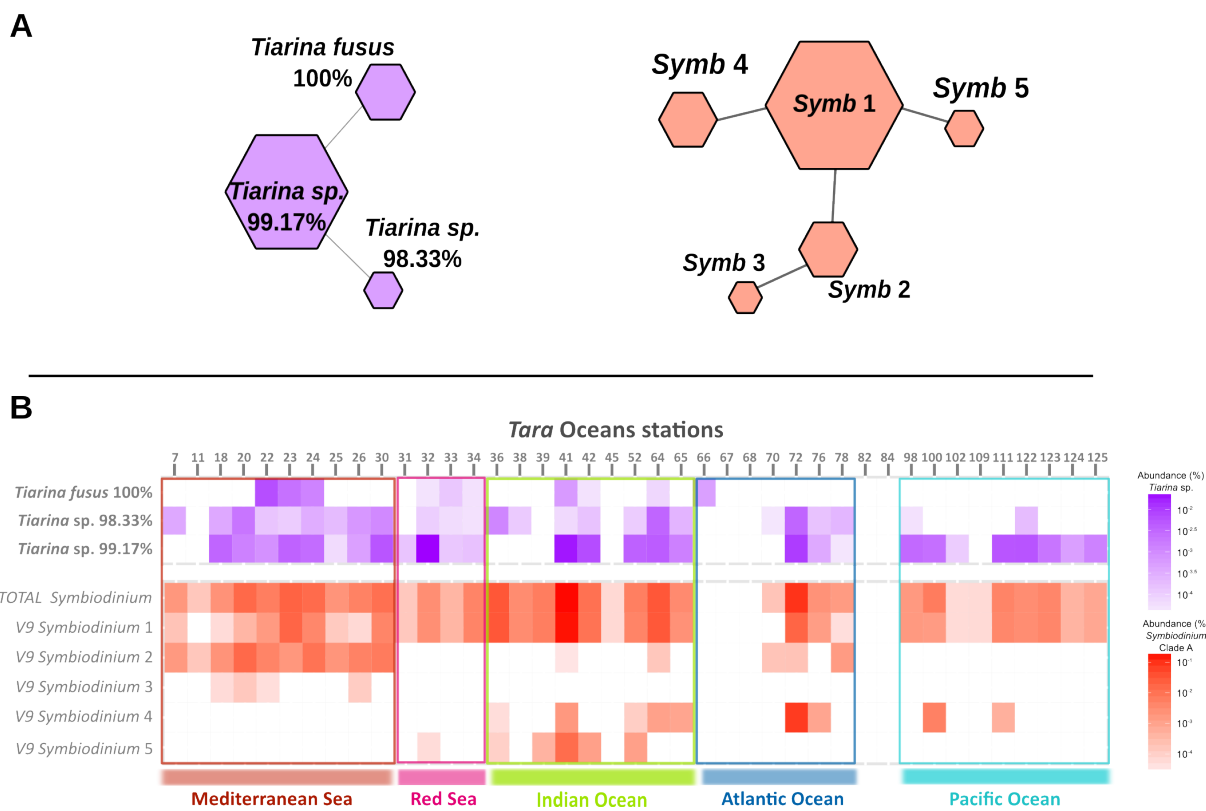


Figure 2: Diversité génétique (A) et biogéographie (B) des metabarcodes séquencés à partir des individus de *Tiarina* et de *Symbiodinium* en symbiose. Les réseaux d'haplotypes (A) sont constitués de nœuds correspondant aux metabarcodes et dont la taille est proportionnelle à leur nombre de lecture dans la gamme de taille 20-180 µm. Les arrêtes correspondent à une mutation génétique. Le réseau d'haplotypes de *Tiarina*, en violet, comprend le metabbarcode associé à l'espèce non symbiotique, *Tiarina fusus*. Les abondances de ces metabarcodes parmi les stations Tara Oceans, dans la gamme de taille 20-180 µm, sont représentées par un gradient de couleur, les couleurs claires étant pour des faibles abondances. Le blanc indique l'absence du metabbarcode dans la station correspondante.

Ces résultats montrent que le niveau de spécificité de cette interaction est relativement lâche tout comme d'autres cas précédemment décrits de photosymbiose (Decelle et al., 2012; Probert et al., 2014). Ceci renforce la nécessité de prendre en compte la présence, dans le plancton, de symbioses peu spécifiques lors de tentatives de détections statistiques de ces dernières, sujet qui sera abordé dans le dernier chapitre.

Le second article « **Size-fractionated global DNA metabarcoding reveals ecological significance of the planktonic dinoflagellate parasite *Blastodinium* in sunlit oceans.** » décrit la diversité, l'écologie et la biogéographie du dinoflagellé *Blastodinium*, parasite de copépodes, à l'échelle des océans tempérés à tropicaux, à partir des données de metabarcoding Tara Oceans. La distribution du nombre de lectures des metabarcodes assignés à *Blastodinium* parmi les fractions de taille est comparée à celles d'*Azadinium* et d'*Alexandrium* (deux genres de dinoflagellés a priori non parasites). Tandis qu'*Azadinium*, de petite taille

(~10-20 µm), est abondant dans les fractions de taille 0.8-5µm et 5-20µm et décline dans la fraction 20-180µm jusqu'à presque disparaître dans la fraction 180-2000µm, *Alexandrium*, plus gros (~100 µm), est peu abondant dans la fraction 0.8-5µm, abondant dans les fractions 5-20µm et 20-180µm, et de nouveau peu abondant dans la fraction 180-2000µm. *Blastodinium*, quant à lui, est abondant dans les fractions 0.8-5µm et 5-20µm, relativement moins dans la fraction 20-180µm et de nouveau abondant en 180-2000µm. Il y a là une signature du style de vie parasitaire de *Blastodinium*, abondant dans sa forme libre (0.8-5µm et 5-20µm), mais que l'on retrouve également dans la plus grande fraction de taille, probablement associé à son hôte. Toutefois, cette distribution varie légèrement entre les différents groupes de *Blastodinium* ce qui suggère une légère variabilité de leurs cycles de vie. Lorsque les abondances des metabarcodes assignés à *Blastodinium* sont comparées à celles des copépodes pour la fraction de taille correspondant à la phase parasitaire du dinoflagellé (180-2000 µm), la spécificité d'interaction décrite dans la littérature est globalement respectée. Cet article suggère que l'étude de la distribution des lectures associées à un organisme parmi différentes fractions de taille adjacentes peut nous renseigner sur son style de vie. De plus il semble pertinent, dans l'optique de détecter des associations symbiotiques, de comparer les abondances (nombre de lectures) des metabarcodes dans les fractions de taille où sont présents les hôtes en symbiose. Dans le cas de *Blastodinium*, il s'agit de la gamme de taille 180-2000 µm.

The symbiotic life of *Symbiodinium* in the open ocean within a new species of calcifying ciliate (*Tiarina* sp.)

Solenn Mordret^{1,2*}, Sarah Romac^{1,2}, Nicolas Henry^{1,2}, Sébastien Colin^{1,2}, Margaux Carmichael^{1,2}, Cédric Berney^{1,2}, Stéphane Audic^{1,2}, Daniel J. Richter^{1,2}, Xavier Pochon^{3,4}, Colomban de Vargas^{1,2}, Johan Decelle^{1,2}

¹- EPEP - *Evolution des Protistes et des Ecosystèmes Pélagiques* - team, Sorbonne Universités, UPMC Univ Paris 06, UMR 7144, Station Biologique de Roscoff, 29680 Roscoff, France

²- CNRS, UMR 7144, Station Biologique de Roscoff, 29680 Roscoff, France

³- Coastal and Freshwater Group, Cawthron Institute, 7010 Nelson, New Zealand

⁴- Institute of Marine Science, University of Auckland, 1142 Auckland, New Zealand

Correspondence: J Decelle (johandecelle@yahoo.fr) and C de Vargas (vargas@sb-roscocff.fr)

* Current address: Stazione Zoologica Anton Dohrn, Villa Comunale, 80121 Naples, Italy

In press, *The ISME Journal*

Abstract

Symbiotic partnerships between heterotrophic hosts and intracellular microalgae are common in tropical and subtropical oligotrophic waters of benthic and pelagic marine habitats. The iconic example is the photosynthetic dinoflagellate genus *Symbiodinium* that establishes mutualistic symbioses with a wide diversity of benthic hosts, sustaining highly biodiverse reef ecosystems worldwide. Paradoxically, while various species of photosynthetic dinoflagellates are prevalent eukaryotic symbionts in pelagic waters, *Symbiodinium* has not yet been reported in symbiosis within oceanic plankton, despite its high propensity for the symbiotic lifestyle. Here we report a new pelagic photosymbiosis between a calcifying ciliate host and the microalga *Symbiodinium* in surface ocean waters. Confocal and scanning electron microscopy, together with an 18S rDNA-based phylogeny, showed that the host is a new ciliate species closely related to *Tiarina fusus* (Colepidae). Phylogenetic analyses of the endosymbionts based on the 28S rDNA gene revealed multiple novel closely-related *Symbiodinium* clade A genotypes. A haplotype network using the high-resolution ITS2 marker showed that these genotypes form eight divergent, biogeographically structured, sub-clade types, which do not seem to associate with any benthic hosts. Ecological analyses using the *Tara Oceans* metabarcoding dataset (V9 region of the 18S rDNA) and contextual oceanographic parameters showed a global distribution of the symbiotic partnership in nutrient-poor surface waters. The discovery of the symbiotic life of *Symbiodinium* in the open

ocean provides new insights into the ecology and evolution of this pivotal microalga and raises new hypotheses about coastal-pelagic connectivity.

Introduction

Symbiosis is central to the evolution and ecology of ecosystems, and is present in virtually all living organisms (Maynard Smith, 1989; Margulis and Fester, 1991). This intimate and long-term association between organisms of different species can range from parasitism, where one partner benefits at the expense of the other, to mutualism, where both partners benefit (de Bary, 1879). Photosymbiosis, defined as a close symbiotic relationship with a photosynthetic partner (generally the symbiont), has led to the acquisition of transient and even permanent photosynthesis in different eukaryotic lineages (Keeling, 2010). In marine and freshwater ecosystems, this type of symbiosis is common (Stoecker *et al.*, 2009) and is considered mutualistic: the symbiont transfers photosynthetic products to its host, which in turn provides a nutrient-rich micro-environment and protection from parasites and predators (Muscatine *et al.*, 1984; Yellowlees *et al.*, 2008; Davy *et al.*, 2012). One of the best-known examples of marine photosymbiosis involves the photosynthetic dinoflagellate *Symbiodinium* that lives within a wide diversity of benthic hosts, including metazoans (e.g. corals, jellyfishes, anemones, sponges, mollusks) and protists (e.g. ciliates and foraminiferans; LaJeunesse, 2001) in tropical reef ecosystems. Symbioses involving *Symbiodinium* are ecologically and economically important as on the one hand they sustain the very productive and biologically diverse reef ecosystems worldwide (Stanley, 2006), and on the other hand provide close to \$375 billion in goods and services each year (Costanza *et al.*, 1997). The genus *Symbiodinium* is genetically diverse, having evolved throughout the Cenozoic into nine divergent lineages or clades (A to I), each containing several sub-clade genotypes that can have distinct physiological capacities, spatial distribution and host spectra (Rowan, 2004; Coffroth and Santos, 2005; Pochon and Gates, 2010).

Photosymbioses are also pervasive in planktonic ecosystems, especially in tropical and sub-tropical oligotrophic waters (Taylor, 1982; Stoecker *et al.*, 2009; Decelle *et al.*, 2015), but remain poorly studied compared to benthic ecosystems. Due to their mixotrophic capacity, photosymbiotic protists play a significant dual role as primary producers and predators in pelagic ecosystems (Michaels *et al.*, 1995; Swanberg and Caron 1991). Many hosts build mineral skeletons of calcium carbonate, silica, or strontium sulfate, hence contributing to the biogeochemical cycles of these elements (Bernstein *et al.*, 1987). For instance, the rhizarian

Radiolaria and Foraminifera are known to develop obligate photosymbioses in surface waters with diverse eukaryotic microalgae, such as photosynthetic dinoflagellates (e.g. *Brandtodium*, *Pelagodinium*) and haptophytes (e.g. *Phaeocystis*) (Gast and Caron, 2001; Shaked and de Vargas, 2006; Decelle *et al.*, 2012; Probert *et al.*, 2014). Some heterotrophic dinoflagellates have also been found to host prasinophyte (Sweeney, 1976) or pelagophyte (Daugbjerg *et al.*, 2013) microalgae. Paradoxically, while several photosynthetic dinoflagellate taxa have been described to be common symbionts in the oceanic plankton, to date the ubiquitous coastal symbiont *Symbiodinium* has never been found in symbiosis in the pelagic realm.

Ciliates are also known to acquire phototrophy through photosymbiosis with eukaryotic or prokaryotic microalgal cells (Stoecker *et al.*, 2009; Esteban *et al.*, 2010; Dziallas *et al.*, 2012). In freshwater habitats, many ciliate species (e.g. *Paramecium bursaria*, *Coleps hirtus viridis*) are found in symbiosis with the green alga *Chlorella*, while in marine ecosystems rare examples of photosymbiosis with eukaryotic microalgae have been reported (Stabell *et al.*, 2002; Stoecker *et al.*, 2009; Johnson, 2011). The benthic ciliates *Maristentor dinoferus* and *Euplates uncinatus* host *Symbiodinium* endosymbionts in coral reefs (Lobban *et al.*, 2002, 2005) and some Oligotrichida ciliates associate with green algae (prasinophytes) in estuarine environments (Stoecker *et al.*, 1988-1989). These photosymbiotic ciliates almost exclusively dwell in coastal waters or benthic habitats, whereas there are virtually no examples of symbiotic partnerships involving eukaryotic microalgae in the surface open ocean. In this study, we used a combination of microscopy and molecular tools to characterize a novel pelagic photosymbiosis between a calcifying ciliate host and *Symbiodinium* endosymbionts. Exploration of this symbiosis in the samples and metabarcoding dataset of the worldwide *Tara* Oceans expedition (Karsenti *et al.*, 2011; de Vargas *et al.*, 2015) allowed us to study the global specificity, biogeography and ecology of this novel interaction.

Materials and Methods

Morphological identification of the host

Plankton samples and metadata used in this study originated from the *Tara* Oceans expedition (2009-2012) (Karsenti *et al.*, 2011; de Vargas *et al.*, 2015). From ethanol-preserved plankton samples, 20 ciliate cells were isolated and cleaned under microscopy, and individually placed on a polycarbonate filter without any chemical fixatives for scanning

electron microscopy observations (Table 1). Additional cells ($n = 11$) from formaldehyde-preserved samples were also imaged with Confocal Laser Scanning Microscope (CLSM, Leica TCS SP8), equipped with an HC PL APO 40x/1.10 W motCORR CS2 objective. Multiple fluorescent dyes were used sequentially to observe the cellular components of the ciliate (host) and the intracellular microalgae (symbionts), such as the nuclei (blue) and the cellular membranes (green) with Hoechst (Ex405/Em420-470) and DiOC6 (Ex488/Em500-520), respectively. Red autofluorescence of the chlorophyll (Ex638/Em680-700) was also visualized to highlight the chloroplasts of the symbiotic microalgae. Image processing and 3D reconstructions were conducted with Fiji (Schindelin *et al.*, 2012) and IMARIS ® (Bitplane) software. Live observations in brightfield microscopy of several ciliate cells (> 50) from the Mediterranean Sea (Villefranche-sur-Mer, France, and Naples, Italy) were also conducted and two individual cells were specifically sampled for molecular investigation (Med 2 and Med 3).

Table 1 Information about the ciliate cells (*Tiarina* sp.) isolated in this study for morphological investigation using different transmitted light and electron microscopy techniques and molecular analyses.

Sampling location	Date	Bright field microscopy	Scanning electron microscopy	Confocal laser scanning microscopy	Molecular analyses
Mediterranean Sea -Villefranche-sur-Mer (France)	Nov. 2011	> 50 live cells			2 cells
Mediterranean Sea - Naples MareChiara (LTER-MC)	From Nov. to Jan. 2014-2015	10-20 live cells			
Red Sea - station Tara_32	Jan. 2010				2 cells
North Indian Ocean - station Tara_41	Mar. 2010		8 cells	7 cells	7 cells
South Indian Ocean -station Tara_52	May 2010				1 cell
South Indian Ocean - station Tara_64	Jul. 2010			1 cells	
South Atlantic Ocean - station Tara_72	Oct. 2010		12 cells	2 cells	5 cells
South Pacific Ocean - station Tara_122	Jul. 2011				2 cells

Phylogenetic identification of the symbiotic partners

a) Sampling and PCR amplifications

Ciliate cells were isolated from ethanol-preserved surface samples collected by a plankton net (20 μm mesh-size) at five *Tara* Oceans stations in the Red Sea and Indian, Pacific and Atlantic Oceans (Table 2, and see Pesant *et al.*, 2015 and de Vargas *et al.*, 2015 for

more details). In addition, two individual ciliates (Med 2 and Med 3) were also collected from live samples in 2011 in the bay of Villefranche-sur-Mer (Mediterranean Sea, France). Cells observed with scanning electron and confocal laser scanning microscopy were not subjected to molecular studies. Ciliate cells were individually isolated using a glass micropipette, carefully washed in three successive baths of 0.22 μ m-filtered and sterile seawater, transferred into a sterile microtube, and preserved in lysis buffer (Tissue and Cell Lysis Solution from MasterPure™ DNA and RNA Purification Kit, Epicenter) at -20°C. DNA extraction was then performed following the protocol of the MasterPure™ DNA and RNA purification kit (Epicenter). In order to obtain different phylogenetic ribosomal markers, single cell PCR amplifications were conducted with the Phusion® High-Fidelity DNA Polymerase (Finnzymes). The PCR mixture (25 μ L final volume) contained 0.5 ng (1 μ L) of DNA, 0.35 μ M (final concentration) of each primer, 3% of DMSO and 2X of GC buffer Phusion MasterMix (Finnzymes). Amplifications were conducted in a PCR thermocycler (Applied Biosystems™) with the following PCR program: initial denaturation step at 98°C for 30 sec, followed by 36-38 cycles of 10 sec at 98°C, 30 sec at the annealing temperature of the primer sets (Supplementary Table S1), 30 sec at 72°C and final elongation step at 72°C for 10 min. For the nested PCR approach, the amplicons obtained in the first PCR (with 25 cycles) were re-amplified with 40 cycles using internal primers. PCR amplicons were visualized on agarose gels, purified with the ExoStar purification kit (Illustra™ Exostar™ 1_Step, GE Healthcare Bio-Sciences Corp.), and Sanger sequenced using the ABI-PRISM Big Dye Terminator Sequencing kit (Applied Biosystems). Amplicon sequences were visualized and assembled using Chromas Pro (version 1.7.5). In addition to washing and rinsing ciliate cells to remove any contaminants, different negative controls were used during the single cell DNA extraction (a sample with no cell) and the PCR amplifications (a sample without DNA template) to confirm that the PCR products were only from the DNA of the ciliate and the intracellular microalgae. DNA from different phytoplankton cultures, including *Symbiodinium*, was used to control the primer specificity

For the ciliate (host), a 640 bp-long fragment of the 18S rRNA gene was PCR-amplified using the ciliate-specific primers Cil_384F and Cil_1147R (Dopheide *et al.*, 2008). A second 2000 bp-long fragment, that includes the hypervariable V9 region of the 18S rRNA gene, was obtained with a nested PCR using newly designed specific primers: TiaV4-F1 and Cil28S-R1 (PCR 1) and the internal primers TiaV4-F2 and Cil28S-R2 (PCR 2) (see Supplementary Table S1 and Figure S1 for more information about the primers used in this

study). Contigs of the different amplicons were obtained and a matrix of 18S rDNA sequences was built with these new sequences and public sequences from GenBank (release 203.0, supplementary Table S2).

In order to identify the lineage of the endosymbiotic microalgae, a cloning approach was first adopted on the 18S and 28S rRNA genes using the TOPO TA Cloning kit (Invitrogen) and universal eukaryotic primers: 63F and 1818R (Lepèvre *et al.*, 2011) and D1R and D2C (Scholin *et al.*, 1994) for 18S and 28S rDNA, respectively (Figure S1). Specific primers and direct sequencing were subsequently employed for the rest of the isolated ciliates to obtain the 28S rRNA gene (D1-D3 domains; with primers ITS-Dino and LO from Pochon *et al.*, 2001) and the rDNA Internal Transcribed Spacer (ITS; with primers Din464F and ITS-DinoRev from Gómez *et al.*, 2001 and this study, respectively) of the microalgal symbionts (Figure S1). For the ciliates, a matrix of 18S rDNA sequences was built with the new sequences obtained and public sequences from GenBank (release 203.0, supplementary Table S2). Matrices of 28S rDNA and ITS2 sequences were then constructed with reference sequences from previous studies (Supplementary Tables S3 and S4, LaJeunesse *et al.*, 2009, Pochon *et al.*, 2014). Sequences obtained in this study have been deposited in GenBank (accession numbers are given in Table 2 and in the supplementary Tables S2 (18S rDNA), S3 (28S rDNA), S4 (ITS2), S5 (V9 rDNA)).

b) Phylogenetic analyses based on ribosomal gene markers

The three matrices of 18S rDNA (host ciliate), and the 28S rDNA and ITS2 (intracellular microalgae) were aligned with MUSCLE from the Seaview software (Edgar, 2004; Gouy *et al.*, 2010), and phylogenetic analyses were conducted with the TOPALI software (Topali V2, Milne *et al.*, 2009). According to Modeltest v0.1.1 (Posada, 2008), the general time-reversible (GTR) and the Tamura-Nei (TrN) models of nucleotide substitution were selected for the symbiont 28S rDNA (56 taxa; 795 nucleotide positions) and the ciliate 18S rDNA (34 taxa; 1419 nucleotide positions) alignments, respectively. Phylogenetic inference by Maximum Likelihood (ML) was then performed with PhyML v3.0 (Guindon and Gascuel, 2003), and robustness of inferred topologies was assessed by performing 100 non-parametric bootstraps. Final trees were rooted with outgroups and visualized with FigTree (v. 1.4; <http://tree.bio.ed.ac.uk/software/figtree/>). For the ITS2 sequences of the symbiont (239-bp long fragment), a statistical parsimony network was constructed with the TCS software (95

% connection limit, 10 or less connection steps, gaps considered as fifth state) (Clement *et al.*, 2000), and visualized and edited with Cytoscape software (Shannon *et al.*, 2003).

Ecological significance of the symbiosis

For both the host ciliate and endosymbiotic microalgae, the hypervariable V9 region of the 18S rRNA gene was specifically extracted from multiple sequence alignments using the primers 1389F and 1510R (Amaral-Zettler *et al.*, 2009) in order to interrogate the V9 metabarcoding dataset obtained dataset from 47 stations of the *Tara* Oceans expedition (Karsenti *et al.*, 2011; de Vargas *et al.*, 2015). This publicly available metabarcoding dataset includes millions of V9 rDNA sequences of eukaryotic planktonic organisms obtained by PCR with universal eukaryotic primers and sequenced with Illumina technology. In this study, samples corresponding to the micro-plankton size fraction (20-180 µm) collected at subsurface mixed-layer waters, where the ciliates were found and isolated, were specifically analyzed. Only V9 reads that were 100% identical to the V9 sequence of the ciliates and the symbiont were retrieved in the *Tara* Oceans barcode table (doi: 10.1594/PANGAEA.843018). Contextual oceanographic parameters, such as temperature, salinity, nitrite and nitrate concentrations, silica and chlorophyll *a* concentrations, oxygen minimum and Deep Chlorophyll Maximum (DCM) depths, and Photosynthetically Active Radiation (PAR), were also used for statistical analyses (Supplementary Table S6). In order to assess co-occurrence patterns between host and symbiont, and the effect of abiotic parameters, multiple pairwise comparisons were performed using Spearman's rank correlation tests based on environmental physico-chemical parameters, and the distribution and abundance of V9 reads of both partners. P-values were adjusted using the False Discovery Rate (FDR) approach (Benjamini and Hochberg, 1995). Correlation between pairs of variables were considered significant when p-values were lower than 0.05. Statistical analyses were performed in the R environment (R Development Core Team 2008), and correlations between variables were visualized as a network using the Cytoscape software (Shannon *et al.*, 2003).

Results and Discussion

Morphological identity of the host ciliate

Live observations in light microscopy showed that the ciliates were actively swimming with the help of numerous cilia around the cell (Supplementary Figure S2). From

20 cells, various morphological characters were observed with scanning electron microscopy, notably an armored skeleton composed of calcium carbonate plates (Figure 1A-B), indicating that the ciliate belongs to the family Colepidae Ehrenberg, 1838 (class Prostomatea, order Prorodontida; Lynn, 2008; Chen et al., 2012). A morphological comparison with six previously described ciliate species from the family Colepidae (*Coleps hirtus*, *Nolandia nolandi*, *Apocoleps magnus*, *Levicoleps biwae*, *Tiarina meunieri* and *Tiarina fusus*) indicated that *T. fusus* is the species that most closely resembles the ciliate isolated in this study (Supplementary Table S7). Both taxa live in marine waters and display a fusiform and elongated body with large longitudinal rows of calcium carbonate plates arranged in six different regions (called "tiers"), as well as a wing-like structure that is absent in other Colepidae species (Figure 1A-B; Chen et al., 2012). These morphological commonalities, which are typically used for genus recognition within the Colepidae (Foissner et al., 2008), lead us to argue that the newly isolated ciliate belongs to the genus *Tiarina*, Berg 1881. In addition to *T. fusus*, the genus *Tiarina* is composed of several species including *T. meunieri*, *T. borealis*, *T. antarctica* and *T. levigata*, but these have very old, incomplete morphological descriptions without reference microscopy images or molecular data. Only *T. fusus* (Chen et al., 2012) and *T. meunieri* (previously named *Stapperisa fusus*, observed in the Arctic and the North Sea; Meunier, 1910; Kahl, 1930) are taxonomically recognized species. Compared to *T. fusus*, the newly isolated ciliate has a larger length-to-width ratio (1.5 times more), lacks armor spines, and possesses long somatic cilia arranged in 18 or more ciliary rows (*T. fusus* has 15-17 longitudinal rows; Supplementary Table S7). As shown by brightfield (on more than 50 cells) and confocal (on 11 cells) microscopy images (Figure 1D-E; Supplementary Figure S2), another distinct morphological character of the isolated ciliate is the presence of 10 to 25 intracellular microalgal cells, which has never been reported in *T. fusus* (Foissner, 2008; Lynn, 2008; Chen et al., 2012). Kahl (1930) observed "ingested dinoflagellates" ("Nahrung kleine Peredineen") in the arctic species *T. meunieri* but this old and succinct description has not been confirmed in the literature. In the newly isolated ciliate, the ovoid microalgae of about 10 µm in diameter tend to be located next to the macronucleus and the micronucleus of the host (both highlighted in cyan), and seem to be intact as shown by the presence of non-degraded nuclei and plastids, in blue and red respectively (Figure 1D-E). Based on these confocal images, it is not possible to distinguish whether there is a single reticulated or several chloroplasts in each microalgal cell. A very small fraction of cells seemed to be degraded, possibly as a consequence of preservation biases and/or host digestion. Several observations indicate cell division for some of the microalgae (Figure 1E;

Supplementary Figure S2). The cellular features observed in CLSM on several host individuals ($n=11$), collected in the Mediterranean Sea and Indian and Atlantic Oceans (*Tara* Oceans stations 22, 41, 64, 72), suggest that the relationship between *Tiarina* sp. and its symbionts of eukaryotic origin is a putative mutualistic endosymbiosis, rather than predation or kleptoplastidy.

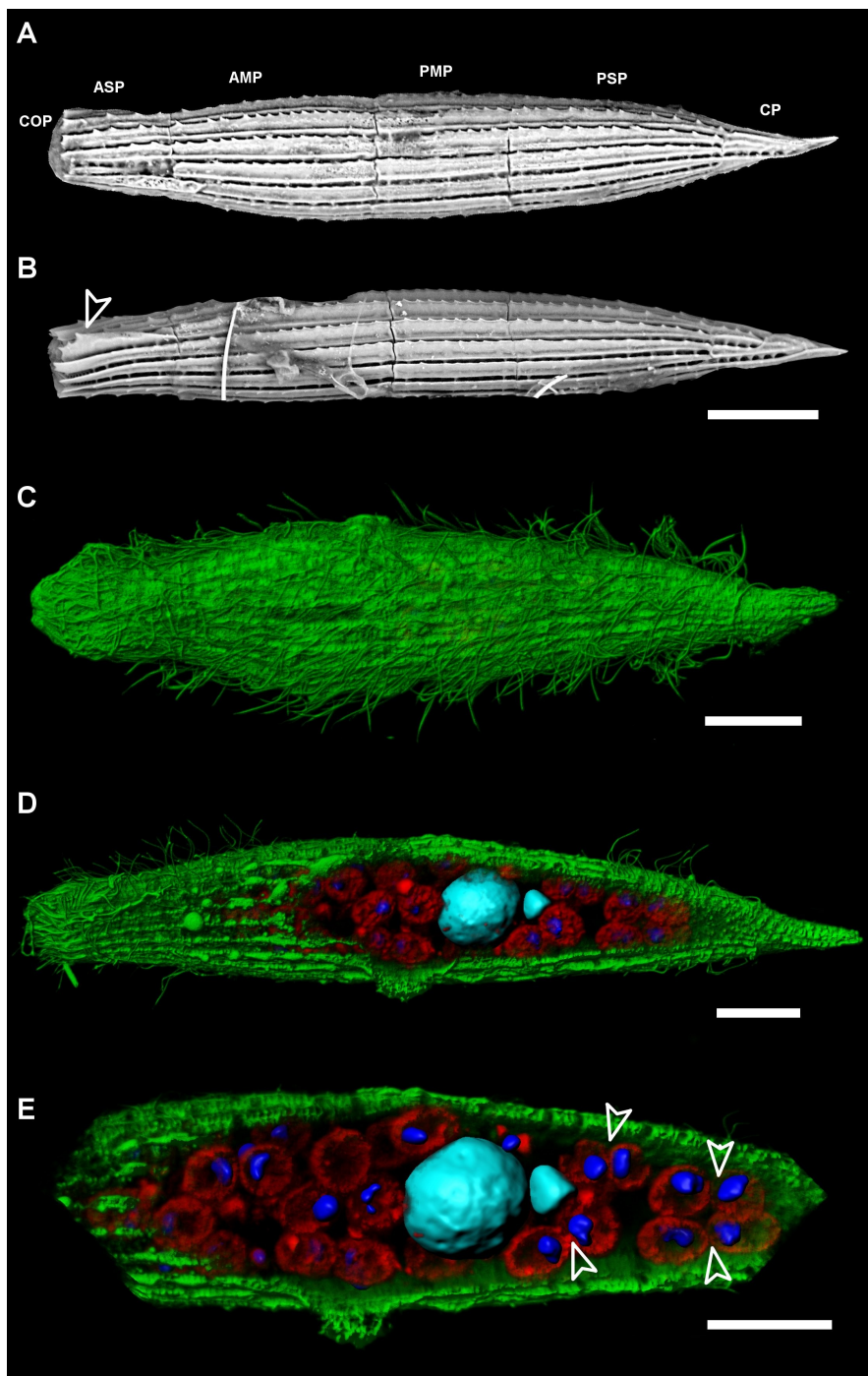


Figure 1 Microscopy images of the photosymbiosis between the ciliate *Tiarina* sp. (the host) and its intracellular symbiotic microalgae collected in surface oceanic waters. (A, B) Scanning electron microscopy images reveal the calcified skeleton of the ciliate composed of six different tiers: circumoral (COT), anterior secondary (AST), anterior main (AMT), posterior main (PMT), posterior secondary (PST) and caudal (CT). (B) The arrow indicates the wing-like structure that is a morphological feature of the genus *Tiarina* within the Colepidae family. (C–E) The three-dimensional (3D) reconstructions of symbiotic specimens imaged with confocal laser scanning microscopy (CLSM). (C) The ciliate exhibits numerous cilia, highlighted in green (DiOC₆). (D, E) The nuclei of the ciliate (cyan) and the symbiotic microalgae (blue) were reconstructed from the Hoechst fluorescence signal, and the chloroplasts of the microalgae are highlighted by the red chlorophyll autofluorescence. (E) The arrows indicate putative cell division events. Scale bar=20 µm.

Phylogenetic identification of the host ciliate

Partial 18S rDNA sequences (i.e. a 1419 bp-long fragment from the V3 to the V9 regions) were obtained from 15 individual ciliates collected in six oceanic regions: the Mediterranean Sea (n=2), and the Indian (n=6), Atlantic (n=5) and Pacific (n=2) Oceans (Table 2). The majority of the 18S rDNA sequences were identical irrespective of their geographic location (which we subsequently call genotype 1), except for four sequences (Med_2, Med_3, TI_381 and TI_382) that have one nucleotide difference in the V9 region (which we call genotype 2). While *Tiarina* sp. genotype 1 was found in most plankton samples, genotype 2 was specifically observed in the Mediterranean Sea and the South Atlantic Ocean. In the latter region (e.g. station 72), both genotypes were found. Based on BLAST analyses, we found no environmental Sanger sequences identical to the newly isolated *Tiarina* sp. (both genotypes) in GenBank (release 207.0; April 2015); the closest sequence corresponded to the ciliate *Tiarina fusus* (FJ858217).

Table 2 Information about the geographic origin and sequence data obtained for each symbiotic ciliate (*Tiarina* sp., named hereafter TI_XX) and their associated endosymbiotic microalgae (the dinoflagellate genus *Symbiodinium*)

Holobiont ID	Sampling station	Oceanic region	Coordinates	Host (the ciliate <i>Tiarina</i> sp.) 18S rDNA	Symbiont (<i>Symbiodinium</i>)	
					ITS2	28S rRNA
TI_355	Tara_41	North Indian Ocean	14°36'N; 69°54'E	KR022062	KR022044	
TI_356	Tara_41	North Indian Ocean	14°36'N; 69°54'E	KR022031	KR022063	KR022045
TI_357	Tara_41	North Indian Ocean	14°36'N; 69°54'E	KR022032	KR022064	KR022046
TI_358	Tara_41	North Indian Ocean	14°36'N; 69°54'E		KR022065	KR022047
TI_363	Tara_41	North Indian Ocean	14°36'N; 69°54'E	KR022033	KR022066	KR022048
TI_365	Tara_41	North Indian Ocean	14°36'N; 69°54'E	KR022034		
TI_366	Tara_41	North Indian Ocean	14°36'N; 69°54'E	KR022035	KR022067	KR022049
TI_371	Tara_52	South Indian Ocean	16°53'S; 54°00'E	KR022036	KR022068	KR022050
TI_376	Tara_72	South Atlantic Ocean	8°35'S; 17°54'W	KR022037	KR022069	KR022051
TI_377	Tara_122	South Pacific Ocean	8°58'S; 139°11'W	KR022038	KR022070	KR022052
TI_378	Tara_122	South Pacific Ocean	8°58'S; 139°11'W	KR022039	KR022071	KR022053
TI_379	Tara_72	South Atlantic Ocean	8°35'S; 17°54'W	KR022040	KR022072	KR022054
TI_380	Tara_72	South Atlantic Ocean	8°35'S; 17°54'W	KR022041	KR022073	KR022055
TI_381	Tara_72	South Atlantic Ocean	8°35'S; 17°54'W	KR022042	KR022074	KR022056
TI_382	Tara_72	South Atlantic Ocean	8°35'S; 17°54'W	KR022043	KR022075	KR022057
TI_392	Tara_32	Red Sea	23°24'N; 37°12'E		KR022078	KR022060
TI_393	Tara_32	Red Sea	23°24'N; 37°12'E		KR022079	KR022061
Med_2	Villefranche-sur-Mer (France)	Mediterranean Sea	43°42'N; 7°18'E	KR022029	KR022076	KR022058
Med_3	Villefranche-sur-Mer (France)	Mediterranean Sea	43°42'N; 7°18'E	KR022030	KR022077	KR022059

In the 18S rDNA phylogenetic tree (Figure 2), sequences of genotypes 1 and 2 grouped together and were placed within a highly supported monophyletic clade (Bootstrap values (BV) = 100%), which corresponds to the family Colepidae, confirming the

morphological identification. The monophyly of the Colepidae was also recovered in a previous study (Yi et al., 2010). Within this family, phylogenetic analyses showed that sequences of our new ciliate grouped with *T. fusus* and an environmental clone (EF526888) in a highly supported monophyletic sub-clade (BV= 100%) that likely corresponds to the genus *Tiarina*. However, the isolated *Tiarina* sp. is genetically clearly different from *Tiarina fusus*, as it is distinguished by 10 and 11 nucleotide differences in the 18S rDNA for genotypes 1 and 2, respectively. These molecular results corroborate the morphological dissimilarities highlighted above and provide further evidence that the new ciliate is a novel *Tiarina* species that requires formal description.

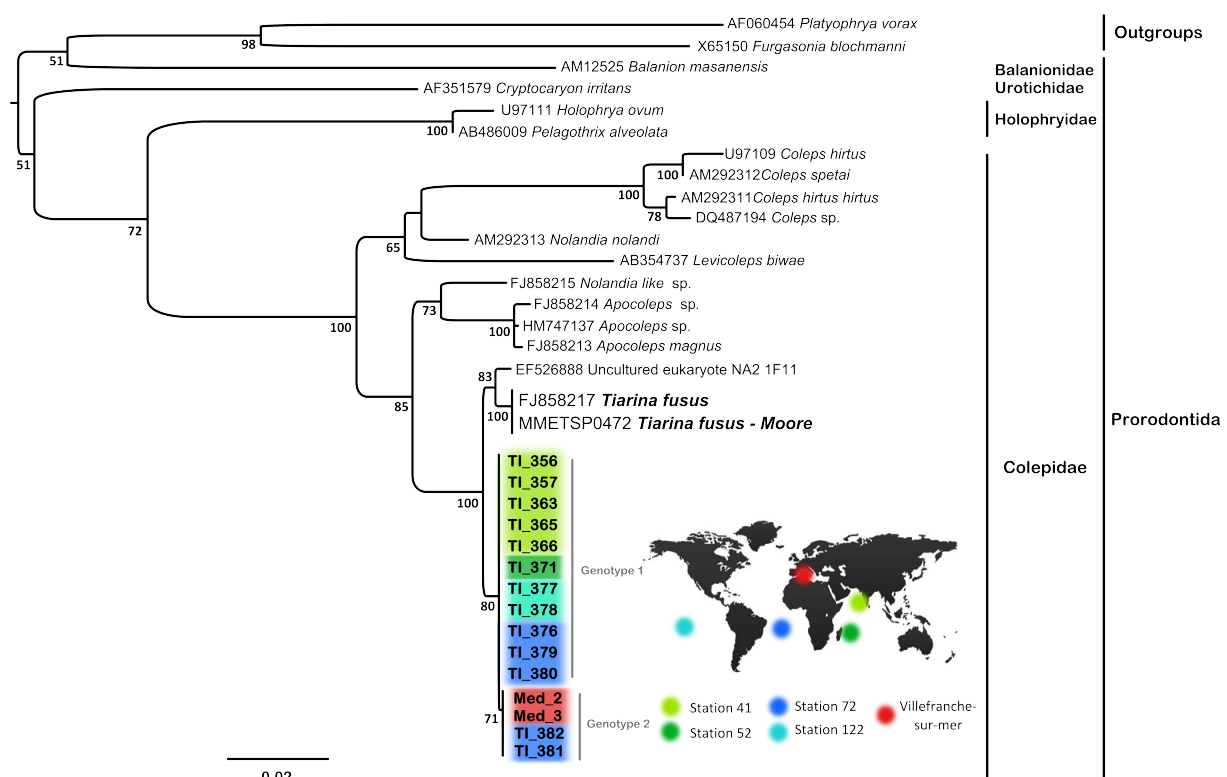


Figure 2 Maximum likelihood phylogeny inferred from partial 18S rDNA sequences of the ciliate order Prorodontida (1419 aligned nucleotide positions) and the Tamura–Nei (TrN) model of nucleotide substitution. Sequences of individual cells of *Tiarina* sp. obtained in this study are colored according to their geographic origin. Bootstrap percentages based on 100 pseudoreplicates are indicated at each node when support values are >50%.

Phylogenetic identification of the microalgal symbiont

Ribosomal gene sequencing was also performed to reveal the identity and diversity of the intracellular eukaryotic microalgae observed in the ciliate *Tiarina* sp.. Amplification of the 18S and 28S rRNA genes with universal eukaryotic primers followed by a cloning procedure

showed that the microalgae of different isolated host cells systematically belonged to the dinoflagellate genus *Symbiodinium*. Twenty partial sequences of the 28S rRNA gene (a 795 bp-long fragment covering the D1-D3 regions) were subsequently obtained with *Symbiodinium*-specific primers (Figure 3). The phylogenetic tree, which has the same topology as in previous studies (Pochon *et al.*, 2012, 2014), demonstrated that *Symbiodinium* isolated from all ciliates (genotypes 1 and 2) collected in different oceanic regions belong to clade A (maximum support: BV=100%), the earliest branching *Symbiodinium* lineage. Within this clade, the new sequences of *Symbiodinium* are different from any known reference sequences, and separate analyses with shorter 28S rDNA sequences showed that they also do not belong to the "Temperate A" sub-clade (Savage *et al.*, 2002; Casado-Amezúa *et al.*, 2014; Supplementary Figure S3). These new 28S rDNA sequences of *Symbiodinium* display genetic dissimilarities (five to nine polymorphic sites) according to their sampling location. This means that the host ciliate *Tiarina* sp. is systematically found in symbiosis with *Symbiodinium* clade A worldwide, but can associate with different types or sub-clades depending on the oceanic region (e.g. Mediterranean Sea and South Pacific Ocean; Figure 3). However, up to three different *Symbiodinium* types can also be found at the same location (e.g. station 72 in the south Atlantic Ocean and station 41 in the North Indian Ocean). From station 72, we note that host genotypes 1 and 2 are associated with different but genetically close *Symbiodinium* types (3 nucleotide differences out of 795 bp of the 28S rDNA sequence), indicating a symbiont specificity within the same location.

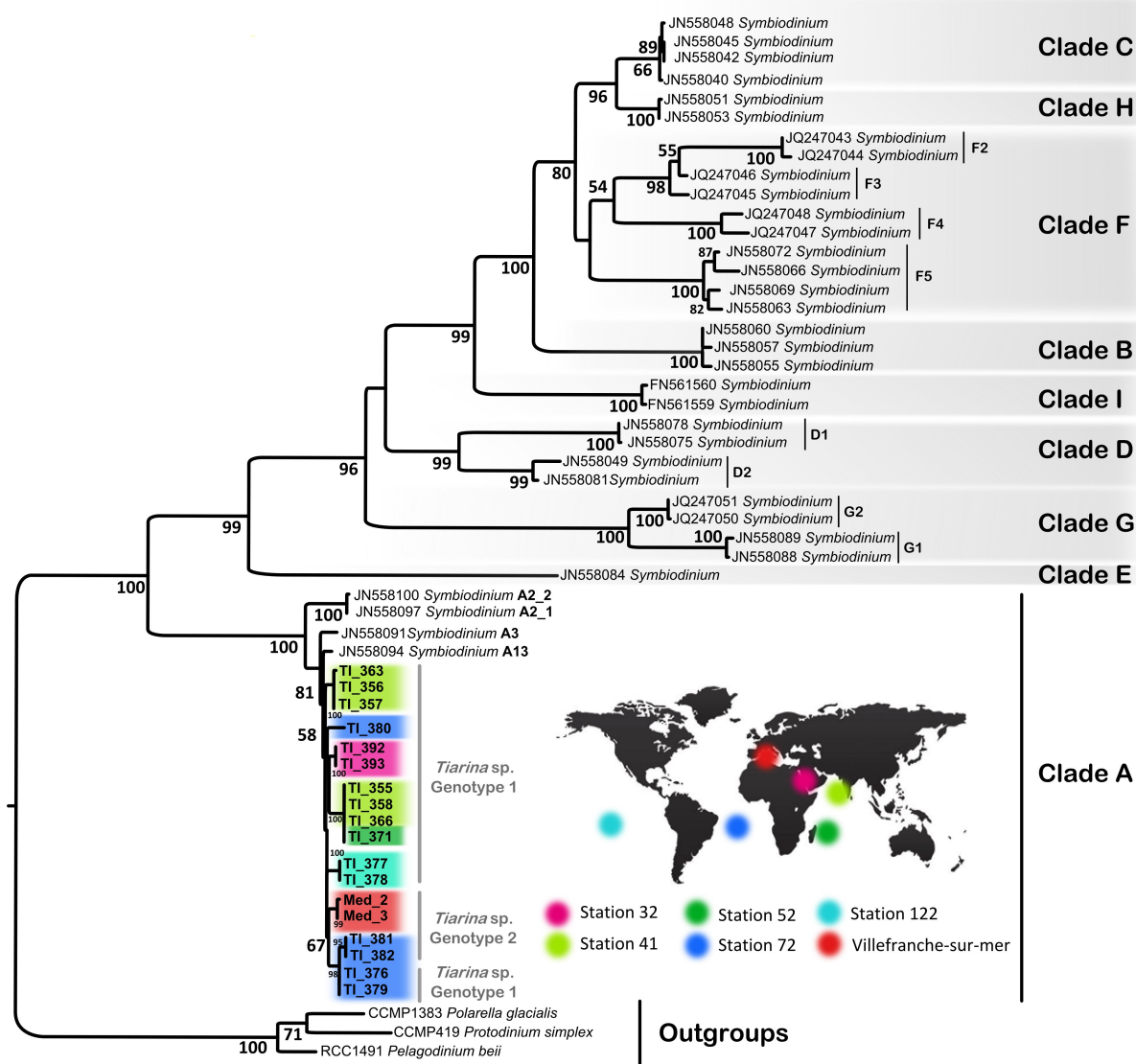


Figure 3 Maximum likelihood phylogeny of the genus *Symbiodinium* inferred from 28S rDNA sequences (D1–D3 regions) and the general time-reversible (GTR) model of nucleotide substitutions. Novel *Symbiodinium* sequences obtained in this study are colored according to their geographic origin, and the name of their corresponding host is given (for example, TI_363). Bootstrap percentages based on 100 pseudoreplicates are indicated at each node when support values are >50%.

The earliest diverging clade A is found within several benthic hosts (e.g. mollusks, corals, anemones and jellyfish) in temperate and tropical waters of the Atlantic, Pacific, Indian Oceans, and Red Sea (Franklin *et al.*, 2012; Goulet *et al.*, 2008). Our results raise the question of whether the novel diversity of *Symbiodinium* associated with a planktonic ciliate in the open ocean can also live within benthic hosts from coastal waters. A complex genetic diversity composed of 15 common sub-clade types has been recognized in clade A with the highly resolute ITS2 marker (LaJeunesse *et al.*, 2001; 2009; Franklin *et al.*, 2012; Lee *et al.*, 2015). This marker was therefore used in this study to assign the new *Symbiodinium*

sequences at the sub-clade level, and thus to provide a better understanding of the identity of the *Tiarina* symbiont and the specificity of the symbiotic partnership (LaJeunesse, 2001). A statistical parsimony network using the ITS2 sequences (239 bp-long) was constructed including *Symbiodinium* sequences obtained from *Tiarina* sp. and those of 14 described sub-clade types from different hosts and oceanic regions (Figure 4, Supplementary Table S3). Sub-clade A2 was not included in the network because it was too divergent (over 10 polymorphic sites). Confirming the 28S rDNA phylogeny, ITS2 sequences of *Symbiodinium* found in *Tiarina* sp. did not match any previously described clade A sequence types, and instead represented 8 novel divergent sub-clade types (7 of which have ≥ 2 nucleotide differences). Remarkably, this *Symbiodinium* diversity from a single host taxon is relatively high, and equivalent to the diversity described so far from about 50 benthic host taxa in reef ecosystems worldwide (Franklin *et al.*, 2012). The ITS2 diversity of *Symbiodinium* from *Tiarina* sp., like that of the 28S rRNA gene, is partly structured by geography, whereby sequences from the same oceanic region tend to be similar (South Pacific Ocean, and Mediterranean and Red Seas). However, the converse also occurs in the Indian and South Atlantic oceans, where up to three highly divergent *Symbiodinium* sub-clade types (over 10 polymorphic sites) can co-exist at the same location. Overall, the ITS2 haplotype network showed a clear genetic separation between *Symbiodinium* from benthic hosts and *Symbiodinium* from the pelagic *Tiarina* sp.. For instance, in the Pacific Ocean, *Symbiodinium* from benthic hosts (sub-clades A5, A6, A7, A8, and A12, in light blue) are very distinct from *Symbiodinium* found in *Tiarina* sp. (TI_377 and TI_378). With two nucleotide differences in the ITS2 sequence, the closest sub-clade type to the ciliate *Symbiodinium* is A4. In corals, this sub-clade type is known for its high photosynthetic efficiency and resistance to photodamage when exposed to temperature stress (Warner *et al.*, 2006). *Symbiodinium* A4 has also been found in the jellyfish *Linuche unguiculata*, which alternates between the benthic (polyp stage) and planktonic compartments during its life history (Trench and Thinh, 1995; Montgomery and Kremer, 1995; LaJeunesse, 2001). Therefore, sub-clade A4 could represent an evolutionary and ecological transition between the benthic and pelagic environments, where different selective pressures have caused evolutionary changes within *Symbiodinium*.

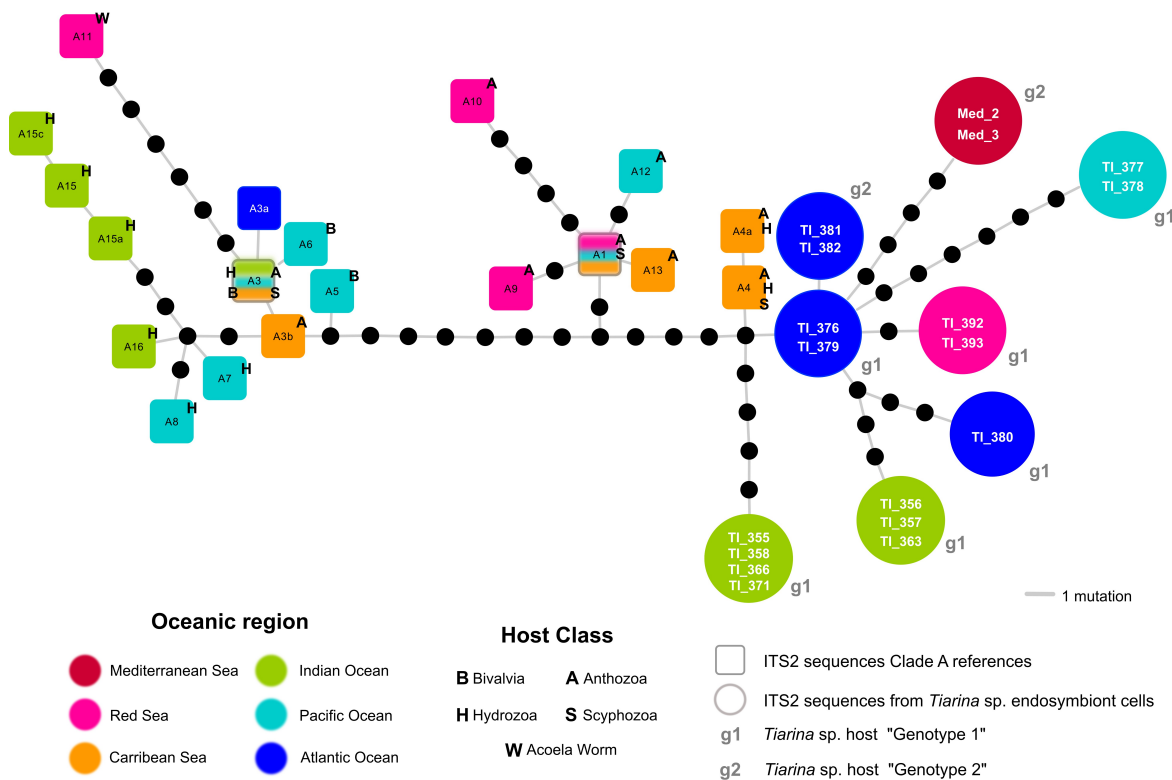


Figure 4 Statistical parsimony network with ITS2 sequences of the different subclades of *Symbiodinium* clade A. Published sequences and those obtained in this study from the planktonic ciliate *Tiarina* sp. are represented by a square and a circle, respectively (see Supplementary Table S4 for the GenBank accession numbers). Based on the GeoSymbio database (Franklin *et al.*, 2012), the geographic origin and host spectrum for each *Symbiodinium* subclade are indicated by a color and a letter, respectively. All of the previously described subclade types (A1–A16 in squares) were found in benthic coastal hosts (~50 host species).

Ecological significance of the symbiosis between the ciliate *Tiarina* and *Symbiodinium*

To explore the geographical distribution of the symbiotic relationship over large spatial scales, the two V9 sequences of the host ciliate (genotypes 1 and 2, differentiated by a single nucleotide) were used to interrogate the V9 rDNA Tara Oceans metabarcoding dataset (de Vargas *et al.*, 2015). V9 metabarcodes that were 100% identical to the V9 of genotypes 1 and 2 were detected in 32 stations across the oceans, mainly at equatorial, tropical and subtropical latitudes (Figure 5A-B). The highest abundances of V9 reads occurred in the Red Sea (station 32), and the Indian (station 41) and South Atlantic (station 72) Oceans, and they were not detected in the Southern Ocean. Both genotypes co-existed in 21 stations in the Mediterranean and Red Seas, and the Indian, Atlantic and Pacific Oceans. Genotype 1 was more cosmopolitan and abundant (10 to 100 times more, in terms of the relative proportion of

reads in a given sample), compared to genotype 2, which was detected in fewer stations (Figure 5A-B).

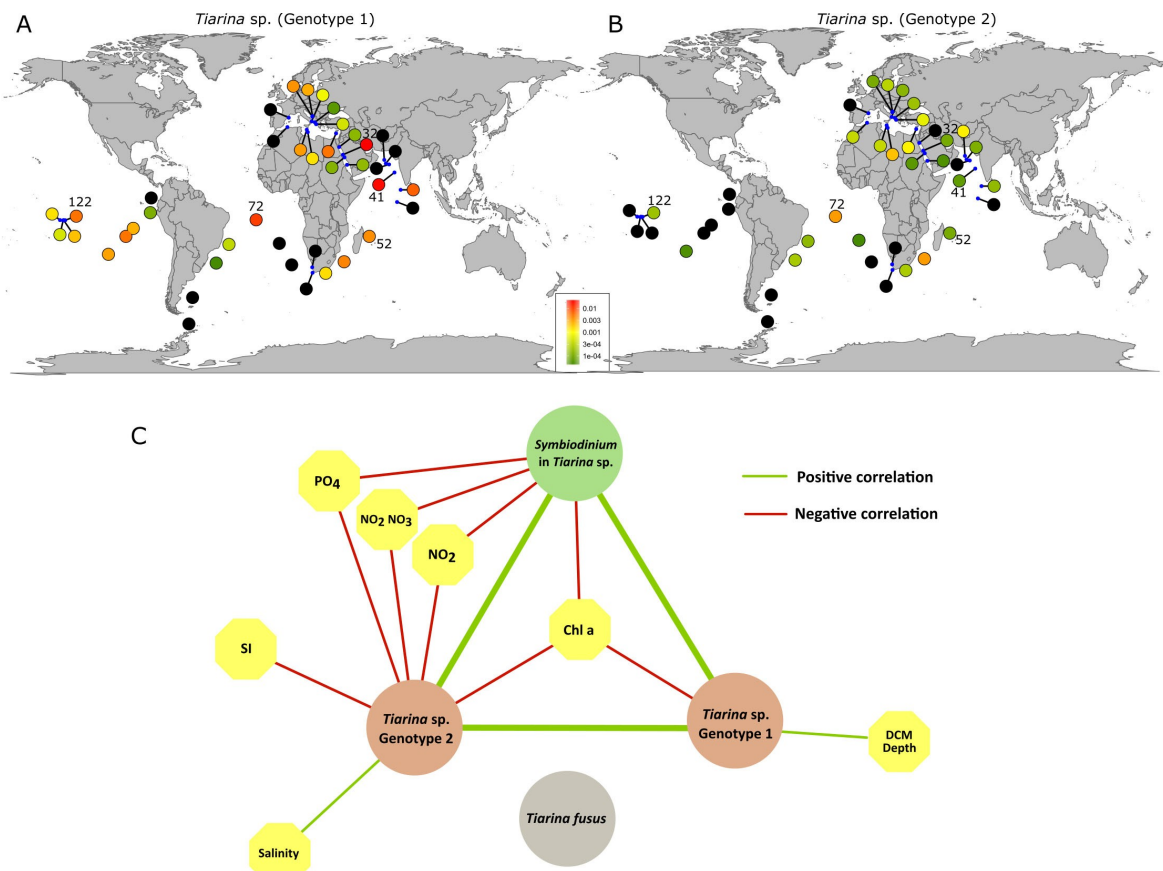


Figure 5 Geographic distribution and ecology of the photosymbiosis between the host ciliate *Tiarina* and the microalga *Symbiodinium*. **(a, b)** Mapping of the relative abundance of rDNA V9 reads identical to the V9 sequences of *Tiarina* genotype 1 **(a)** and *Tiarina* genotype 2 **(b)** in Tara Oceans stations (surface samples in the 20–180 µm size fraction). The color gradient indicates the relative abundance of V9 reads from green to red for low to high values, respectively. Black dots indicate that no V9 reads were detected at the given station. **(c)** Network showing the different correlations (statistically significant; $P < 0.05$) between the V9 read abundances of *Symbiodinium* (represented by five distinct V9 sequences), *Tiarina* genotypes 1 and 2, *T. fusus* and several physicochemical parameters (see Supplementary Tables S6 and S8 for the data used and the P -values of the different correlations, respectively).

The ecological preferences of the symbiosis between *Tiarina* sp. and *Symbiodinium* were investigated through correlation network analyses including different contextual oceanographic parameters and the relative abundance of V9 reads of *Symbiodinium* (representing five distinct V9 sequences), *Tiarina* sp. (genotypes 1 and 2), and *Tiarina fusus* (Figure 5C, Supplementary Tables S6 and S8). This analysis revealed a positive correlation between *Symbiodinium* and both genotypes of *Tiarina* sp., demonstrating that there is an intimate ecological interaction between these taxa in surface ocean waters. In addition,

Symbiodinium V9 reads correlated negatively to the concentration of some nutrients (NO_2 , PO_4) and chlorophyll *a*. Reads of genotypes 1 and 2 of the ciliate *Tiarina* sp. significantly co-occurred and displayed negative correlation with chlorophyll *a*. Reads of genotype 2 also displayed negative correlations with some nutrients (NO_2 , PO_4 , Si), while those of genotype 1 had positive correlations with the depth of the DCM. Thus, the correlation patterns between the host, its symbiont and their abiotic environment clearly indicate that the symbiotic partnership predominantly occurs in oligotrophic conditions (typically characterized by a deep DCM and low chlorophyll and nutrient concentrations), mirroring the ecology of other known planktonic photosymbioses (Stoecker *et al.*, 2009; Decelle *et al.*, 2012; de Vargas and Shackett, 2006). More specifically, we note that genotype 2 positively correlated with salinity, very likely because of its prevalence in the Mediterranean Sea. No significant correlations were detected between *T. fusus* and *Symbiodinium*, nor between *T. fusus* and different oceanographic parameters, showing that the life mode and the ecology of *T. fusus* and the novel *Tiarina* sp. are distinct. To date, *T. fusus* has been reported essentially from coastal and productive marine waters, such as European fjords (Smetacek, 1981; Dale and Dahl, 1987; Lynn, 2008; Chen *et al.*, 2012), where it can dominate ciliate abundance and/or biomass (maximum density reported: 34 000 cells. m^{-3}). *T. fusus* is particularly known for its significant grazing activity on a variety of toxic and/or red-tide microalgae (Jeong *et al.*, 2002). In this study, V9 reads assigned to *T. fusus* (100% identical to the reference sequence) were only detected in low abundance in coastal stations in the Adriatic and Red Seas, and in the Indian and Atlantic Oceans (Supplementary Figure S4). According to the ecological species concept (Boenigk *et al.*, 2012), these results therefore provide additional evidence that the symbiotic *Tiarina* sp. is a novel species distinct from *T. fusus*.

Conclusion and Perspectives

Our study identified and characterized a novel and widespread pelagic photosymbiosis between an undescribed calcifying ciliate (*Tiarina* sp.) and the dinoflagellate *Symbiodinium*. Consistent microscopy observations on multiple specimens, systematic PCR detection of *Symbiodinium* within the ciliate, and the geographic distribution in surface oceans together provide evidence in favor of a long-term mutualistic symbiosis rather than predation or kleptoplastidy. This newly described partnership is relevant not only because the host is a previously unknown planktonic protistan species, but also because the occurrence of *Symbiodinium* as a symbiont in the open ocean was previously unknown, despite the fact that

Symbiodinium is one of the most extensively studied microalgal genera. We revealed a novel and highly diverse assemblage within *Symbiodinium* clade A composed of 8 sub-clade types, which appear to be endemic to pelagic waters as they have not been reported from hosts in benthic-coastal habitats so far (e.g. tropical reefs, temperate coastal areas). Selective pressures inherent to the pelagic realm and host specialization might have created a distinct ecological niche and driven the tempo and mode of *Symbiodinium* diversification in the open ocean. Given that clade A is the earliest branching lineage and coelapid fossils date back to the Triassic (220 million year ago, Schmidt *et al.*, 2006), it is possible that the *Tiarina-Symbiodinium* symbiosis occurred relatively early in the evolution of the two lineages.

This cosmopolitan symbiosis likely plays multi-faceted biogeochemical roles in pelagic ecosystems by contributing to primary production and calcium cycling through the *Symbiodinium* photosynthesis and host calcification, respectively. Automatic and *in situ* imaging techniques could be used in the future to properly quantify this interaction, and thus to determine its ecological impact in the environment. The active motility of the cilia-bearing host, which is absent in the "passive" photosymbiotic rhizarian Radiolaria and Foraminifera, makes the partnership highly original and may indicate a chemotactic behavior for finding symbiotic partners, suitable light conditions, and food or nutrient patches, as hypothesized in the photosymbiotic ciliate *Mesodinium rubrum* (Wilkerson and Grunseich, 1990; Fenchel and Blackburn, 1999). Given the metabolic capacities of *Symbiodinium* in reef ecosystems (Yellowlees *et al.*, 2008; Godinot *et al.*, 2009; Pernice *et al.*, 2012), *Tiarina* sp. very likely benefits from a significant source of carbon, nitrogen, phosphate and other key nutrients for growth and reproduction that are otherwise limiting in the open ocean. In addition to its nutritional role, *Symbiodinium* could also play a critical role not only in the calcification of the ciliate's skeleton, as shown in scleractinian corals (Allemand *et al.*, 2011; Davy *et al.*, 2012), but also in UV protection in transparent open ocean waters, since clade A is known to produce a significant amount of UV-absorbing mycosporine-like amino acids (MAAs) in comparison with other clades (Banaszak *et al.*, 2000). Clade A is also known for its tolerance for high irradiance and high temperatures, likely explaining why it is commonly found in shallow-water benthic hosts (Warner *et al.*, 2006; Kemp *et al.*, 2014, 2015) or in the free-living environment (Pochon *et al.*, 2014). Thus, the physiological features of clade A would seem to make this *Symbiodinium* lineage particularly well suited to be a symbiont within single-celled hosts in oligotrophic transparent waters. Future studies should aim to better

understand the nature, ecological role and life cycle of this new photosymbiosis, and explore whether other *Symbiodinium* clades can be found in the open ocean.

Acknowledgements

This work was supported by the project OCEANOMICS, that has received funding from the French government, managed by the Agence Nationale de la Recherche, under the grant agreement “Investissement d’Avenir” ANR-11-BTBR-0008. We thank the European Molecular Biology Laboratory (EMBL, Heidelberg) and more specifically Rainer Pepperkok for providing access to the Advanced Light Microscopy Facility (ALMF). We also thank the coordinators and members of the *Tara* Oceans expedition, Diana Sarno from the Stazione Zoologica Anton Dohrn of Naples for providing brightfield images, and the marine station LOV from Villefranche-sur-Mer for field sampling. We are grateful to Ian Probert and Jan Slapeta for valuable comments on the manuscript. This article is contribution number ## of *Tara* Oceans.

Conflict of interest

The authors declare no conflict of interest.

Supplementary Information accompanies this paper on The ISME Journal website

References

- ALLEMAND, Denis, TAMBUTTÉ, Éric, ZOCCOLA, Didier, *et al.* Coral calcification, cells to reefs. In : *Coral reefs: an ecosystem in transition*. Springer Netherlands, 2011. p. 119-150.
- AMARAL-ZETTLER, Linda A., MCCLIMENT, Elizabeth A., DUCKLOW, Hugh W., *et al.* A method for studying protistan diversity using massively parallel sequencing of V9 hypervariable regions of small-subunit ribosomal RNA genes. *PLoS One*, 2009, vol. 4, no 7, p. e6372.
- BANASZAK, Anastazia T., LAJEUNESSE, Todd C., et TRENCH, Robert K. The synthesis of mycosporine-like amino acids (MAAs) by cultured, symbiotic dinoflagellates. *Journal of Experimental Marine Biology and Ecology*, 2000, vol. 249, no 2, p. 219-233.
- BARY, Anton de. Vortrag: Uber Symbiose. Tagblatt der 51. Versammlung Deutscher Naturforscher und Aerzte in Cassel. Baier & Lewalter, Kassel, 1878, pp. 121-126.

- BENJAMINI, Yoav et HOCHBERG, Yosef. Controlling the false discovery rate: a practical and powerful approach to multiple testing. *Journal of the Royal Statistical Society. Series B (Methodological)*, 1995, p. 289-300.
- BERNSTEIN, R. E., BETZER, P. R., FEELY, R. A., et al. Acantharian fluxes and strontium to chlorinity ratios in the North Pacific Ocean. *Science*, 1987, vol. 237, no 4821, p. 1490-1494.
- BOENIGK, Jens, ERESHEFSKY, Marc, HOEF-EMDEN, Kerstin, et al. Concepts in protistology: species definitions and boundaries. *European journal of protistology*, 2012, vol. 48, no 2, p. 96-102.
- CASADO-AMEZÚA, Pilar, MACHORDOM, Annie, BERNARDO, João, et al. New insights into the genetic diversity of zooxanthellae in Mediterranean anthozoans. *Symbiosis*, 2014, vol. 63, no 1, p. 41-46.
- CHEN, Xiangrui, GAO, Shan, LIU, Weiwei, et al. Taxonomic descriptions of three marine colepid ciliates, *Nolandia sinica* spec. nov., *Apocoleps caoi* spec. nov. and *Tiarina fusa* (Claparède & Lachmann, 1858) Bergh, 1881 (Ciliophora, Prorodontida). *International journal of systematic and evolutionary microbiology*, 2012, vol. 62, no Pt 3, p. 735-744.
- CLEMENT, Mark, POSADA, David., et CRANDALL, Keith A. TCS: a computer program to estimate gene genealogies. *Molecular ecology*, 2000, vol. 9, no 10, p. 1657-1659.
- COFFROTH, Mary Alice et SANTOS, Scott R. Genetic diversity of symbiotic dinoflagellates in the genus *Symbiodinium*. *Protist*, 2005, vol. 156, no 1, p. 19-34.
- COSTANZA Robert, D'ARGE Ralph, DE GROOT Rudolf, et al. The value of the world's ecosystem services and natural capital. *Nature*, 1997, vol. 387, p. 253-260.
- DALE, Torbjørn et DAHL, Einar. Mass occurrence of planktonic oligotrichous ciliates in a bay in southern Norway. *Journal of plankton research*, 1987, vol. 9, no 5, p. 871-879.
- DAUGBJERG, Niels, JENSEN, Maria Hastrup, et HANSEN, Per Juel. Using nuclear-encoded LSU and SSU rDNA sequences to identify the Eukaryotic Endosymbiont in *Amphisolenia bidentata* (Dinophyceae). *Protist*, 2013, vol. 164, no 3, p. 411-422.
- DAVY, Simon K., ALLEMAND, Denis, et WEIS, Virginia M. Cell biology of cnidarian-dinoflagellate symbiosis. *Microbiology and Molecular Biology Reviews*, 2012, vol. 76, no 2, p. 229-261.
- DECELLE, Johan, COLIN, Sébastien, et FOSTER, Rachel A. Photosymbiosis in marine planktonic protists. In : *Marine Protists*. Springer Japan, 2015. p. 465-500.

- DECELLE, Johan, PROBERT, Ian, BITTNER, Lucie, *et al.* An original mode of symbiosis in open ocean plankton. *Proceedings of the National Academy of Sciences*, 2012, vol. 109, no 44, p. 18000-18005.
- DE VARGAS, Colomban, AUDIC, Stéphane, HENRY, Nicolas, *et al.* Eukaryotic plankton diversity in the sunlit ocean. *Science*, 2015, vol. 348, no 6237, p. 1261605.
- DOPHEIDE, Andrew, LEAR, Gavin, STOTT, Rebecca, *et al.* Molecular characterization of ciliate diversity in stream biofilms. *Applied and environmental microbiology*, 2008, vol. 74, no 6, p. 1740-1747.
- DZIALLAS, Claudia, ALLGAIER, Martin, MONAGHAN, Michael T., *et al.* Act together—implications of symbioses in aquatic ciliates. *Frontiers in microbiology*, 2012, vol. 3.
- EDGAR, Robert C. MUSCLE: multiple sequence alignment with high accuracy and high throughput. *Nucleic acids research*, 2004, vol. 32, no 5, p. 1792-1797.
- ESTEBAN, Genoveva F., FENCHEL, Tom, et FINLAY, Bland J. Mixotrophy in ciliates. *Protist*, 2010, vol. 161, no 5, p. 621-641.
- FENCHEL, Tom et BLACKBURN, Nicholas. Motile chemosensory behaviour of phagotrophic protists: mechanisms for and efficiency in congregating at food patches. *Protist*, 1999, vol. 150, no 3, p. 325-336.
- FOISSNER, Wilhelm, KUSUOKA, Yasushi, et SHIMANO, Satoshi. Morphology and gene sequence of *Levicoleps biwae* n. gen., n. sp.(Ciliophora, Prostomatida), a proposed endemic from the ancient Lake Biwa, Japan. *Journal of Eukaryotic Microbiology*, 2008, vol. 55, no 3, p. 185-200.
- FRANKLIN, Erik C., STAT, Michael, POCHON, Xavier, *et al.* GeoSymbio: a hybrid, cloud-based web application of global geospatial bioinformatics and ecoinformatics for *Symbiodinium*–host symbioses. *Molecular Ecology Resources*, 2012, vol. 12, no 2, p. 369-373.
- GAST, Rebecca J. et CARON, David A. Photosymbiotic associations in planktonic foraminifera and radiolaria. *Hydrobiologia*, 2001, vol. 461, no 1-3, p. 1-7.
- GODINOT, C., FERRIER-PAGÈS, C., et GROVER, R. Control of phosphate uptake by zooxanthellae and host cells in the scleractinian coral *Stylophora pistillata*. *Limnology and Oceanography*, 2009, vol. 54, no 5, p. 1627-1633.
- GOMEZ, Fernando, LÓPEZ-GARCÍA, Purificación, et MOREIRA, David. Molecular phylogeny of dinophysoid dinoflagellates: the systematic position of *Oxyphysis oxytoxoides*

and the *Dinophysis hastata* group (Dinophysales, Dinophyceae) 1. *Journal of phycology*, 2011, vol. 47, no 2, p. 393-406.

GOULET, Tamar L., SIMMONS, Christopher, et GOULET, Denis. Worldwide biogeography of Symbiodinium in tropical octocorals. *Marine ecology progress series*, 2008, vol. 355, p. 45.

GOUY, Manolo, GUINDON, Stephane, et GASCUEL, Olivier. SeaView version 4: a multiplatform graphical user interface for sequence alignment and phylogenetic tree building. *Molecular biology and evolution*, 2010, vol. 27, no 2, p. 221-224.

GUINDON, Stéphane et GASCUEL, Olivier. A simple, fast, and accurate algorithm to estimate large phylogenies by maximum likelihood. *Systematic biology*, 2003, vol. 52, no 5, p. 696-704.

JEONG, Hae Jin, YOON, Joo Yih, KIM, Jae Seong, et al. Growth and grazing rates of the prostomatiid ciliate *Tiarina fusus* on red-tide and toxic algae. *Aquatic microbial ecology*, 2002, vol. 28, no 3, p. 289-297.

JOHNSON, Matthew D. Acquired phototrophy in ciliates: a review of cellular interactions and structural adaptations1. *Journal of Eukaryotic Microbiology*, 2011, vol. 58, no 3, p. 185-195.

KAHL Alfred. Urtiere oder Protozoa I: Wimpertiere oder Ciliata (Infusoria) 1. Allgemeiner Teil und Prostomata. *Tierwelt Dtl*, 1930, vol. 18, p. 1-180.

KARSENTI, Eric, ACINAS, Silvia G., BORK, Peer, et al. A holistic approach to marine ecosystems biology. *PLOS biology*, 2011, vol. 9, no 10, p. e1001177.

KEELING, Patrick J. The endosymbiotic origin, diversification and fate of plastids. *Philosophical Transactions of the Royal Society of London B: Biological Sciences*, 2010, vol. 365, no 1541, p. 729-748.

KEMP, Dustin W., HERNANDEZ-PECH, Xavier, IGLESIAS-PRIETO, Roberto, et al. Community dynamics and physiology of *Symbiodinium* spp. before, during, and after a coral bleaching event. *Limnology and Oceanography*, 2014, vol. 59, no 3, p. 788-797.

KEMP, Dustin W., THORNHILL, Daniel J., ROTJAN, Randi D., et al. Spatially distinct and regionally endemic *Symbiodinium* assemblages in the threatened Caribbean reef-building coral *Orbicella faveolata*. *Coral Reefs*, 2015, vol. 34, no 2, p. 535-547.

- LAJEUNESSE, Todd C. Investigating the biodiversity, ecology, and phylogeny of endosymbiotic dinoflagellates in the genus *Symbiodinium* using the ITS region: in search of a “species” level marker. *Journal of Phycology*, 2001, vol. 37, no 5, p. 866-880.
- LAJEUNESSE, Todd C., LOH, William, et TRENCH, Robert K. Do introduced endosymbiotic dinoflagellates ‘take’ to new hosts?. *Biological invasions*, 2009, vol. 11, no 4, p. 995-1003.
- LEE, Sung Yeon, JEONG, Hae Jin, KANG, Nam Seon, et al. *Symbiodinium tridacnidorum* sp. nov., a dinoflagellate common to Indo-Pacific giant clams, and a revised morphological description of *Symbiodinium microadriaticum* Freudenthal, emended Trench & Blank. *European Journal of Phycology*, 2015, vol. 50, no 2, p. 155-172.
- LEPERE, Cécile, DEMURA, Mikihide, KAWACHI, Masanobu, et al. Whole-genome amplification (WGA) of marine photosynthetic eukaryote populations. *FEMS Microbiology Ecology*, 2011, vol. 76, no 3, p. 513-523.
- LOBBAN, C., SCHEFTER, M., SIMPSON, A., et al. *Maristentor dinoferus* n. gen., n. sp., a giant heterotrich ciliate (Spirotrichea: Heterotrichida) with zooxanthellae, from coral reefs on Guam, Mariana Islands. *Marine Biology*, 2002, vol. 140, no 2, p. 411-423.
- LOBBAN, C. S., MODEO, L., VERNI, F., et al. *Euplotes uncinatus* (Ciliophora, Hypotrichia), a new species with zooxanthellae. *Marine Biology*, 2005, vol. 147, no 5, p. 1055-1061.
- LYNN, Denis H. (ed.). *The ciliated protozoa: characterization, classification, and guide to the literature*. Springer Science & Business Media, 2008.
- MARGULIS, Lynn et FESTER, René. *Symbiosis as a source of evolutionary innovation: speciation and morphogenesis*. MIT Press, 1991.
- MAYNARD SMITH John. Generating novelty by symbiosis. *Nature*, 1989, vol. 341, p. 284-285.
- MEUNIER, A. Microplankton des Mers de Barents et de Kara [Microplankton from the Barents and Kara Seas]. Duc d'Orléans, Campagne Arctique de 1907. 1910.
- MICHAELS, Anthony F., CARON, David A., SWANBERG, Neil R., et al. Planktonic sarcodines (Acantharia, Radiolaria, Foraminifera) in surface waters near Bermuda: abundance, biomass and vertical flux. *Journal of Plankton Research*, 1995, vol. 17, no 1, p. 131-163.

- MILNE, Iain, LINDNER, Dominik, BAYER, Micha, et al. TOPALi v2: a rich graphical interface for evolutionary analyses of multiple alignments on HPC clusters and multi-core desktops. *Bioinformatics*, 2009, vol. 25, no 1, p. 126-127.
- MONTGOMERY, M. K. et KREMER, P. M. Transmission of symbiotic dinoflagellates through the sexual cycle of the host scyphozoan *Linuche unguiculata*. *Marine Biology*, 1995, vol. 124, no 1, p. 147-155.
- MUSCATINE, L., FALKOWSKI, P. G., PORTER, J. W., et al. Fate of Photosynthetic Fixed Carbon in Light-and Shade-Adapted Colonies of the Symbiotic Coral *Stylophora pistillata*. *Royal Society of London Proceedings Series B*, 1984, vol. 222, p. 181-202.
- PERNICE, Mathieu, MEIBOM, Anders, VAN DEN HEUVEL, Annemieke, et al. A single-cell view of ammonium assimilation in coral–dinoflagellate symbiosis. *The ISME journal*, 2012, vol. 6, no 7, p. 1314-1324.
- PESANT, Stéphane, NOT, Fabrice, PICHERAL, Marc, et al. Open science resources for the discovery and analysis of Tara Oceans data. *Scientific Data*, 2015, vol. 2.
- POCHON, Xavier, PUTNAM, Hollie M., et GATES, Ruth D. Multi-gene analysis of *Symbiodinium* dinoflagellates: a perspective on rarity, symbiosis, and evolution. *PeerJ*, 2014, vol. 2, p. e394.
- POCHON, Xavier, PUTNAM, Hollie M., BURKI, Fabien, et al. Identifying and characterizing alternative molecular markers for the symbiotic and free-living dinoflagellate genus *Symbiodinium*. *PLOS One*, 2012, vol. 7, no 1, p. e29816.
- POCHON, Xavier et GATES, Ruth D. A new *Symbiodinium* clade (Dinophyceae) from soritid foraminifera in Hawai'i. *Molecular phylogenetics and evolution*, 2010, vol. 56, no 1, p. 492-497.
- POCHON, Xavier, PAWLOWSKI, J., ZANINETTI, Louisette, et al. High genetic diversity and relative specificity among *Symbiodinium*-like endosymbiotic dinoflagellates in soritid foraminiferans. *Marine Biology*, 2001, vol. 139, no 6, p. 1069-1078.
- POSADA, David. jModelTest: phylogenetic model averaging. *Molecular biology and evolution*, 2008, vol. 25, no 7, p. 1253-1256.
- PROBERT, Ian, SIANO, Raffaele, POIRIER, Camille, et al. *Brandtodinium* gen. nov. and *B. nutricula* comb. Nov.(Dinophyceae), a dinoflagellate commonly found in symbiosis with polycystine radiolarians. *Journal of Phycology*, 2014, vol. 50, no 2, p. 388-399.

- ROWAN, Rob. Coral bleaching: thermal adaptation in reef coral symbionts. *Nature*, 2004, vol. 430, no 7001, p. 742-742.
- SAVAGE, A. M., GOODSON, M. S., VISRAM, S., et al. Molecular diversity of symbiotic algae at the latitudinal margins of their distribution: dinoflagellates of the genus *Symbiodinium* in corals and sea anemones. *Marine ecology. Progress series*, 2002, vol. 244, p. 17-26.
- SCHINDELIN, Johannes, ARGANDA-CARRERAS, Ignacio, FRISE, Erwin, et al. Fiji: an open-source platform for biological-image analysis. *Nature methods*, 2012, vol. 9, no 7, p. 676-682.
- SCHMIDT, Alexander R., RAGAZZI, Eugenio, COPPELLOTTI, Olimpia, et al. A microworld in Triassic amber. *Nature*, 2006, vol. 444, no 7121, p. 835-835.
- SCHOLIN, Christopher A., HERZOG, Michel, SOGIN, Mitchell, et al. Identification of group-and strain-specific genetic markers for globally distributed *Alexandrium* (Dinophyceae). II. Sequence analysis of a fragment of the LSU rRNA gene1. *Journal of phycology*, 1994, vol. 30, no 6, p. 999-1011.
- SHAKED, Yonathan et DE VARGAS, Colomban. Pelagic photosymbiosis: rDNA assessment of diversity and evolution of dinoflagellate symbionts and planktonic foraminiferal hosts. *Marine Ecology Progress Series*, 2006, vol. 325, p. 59-71.
- SHANNON, Paul, MARKIEL, Andrew, OZIER, Owen, et al. Cytoscape: a software environment for integrated models of biomolecular interaction networks. *Genome research*, 2003, vol. 13, no 11, p. 2498-2504.
- SMETACEK, Victor The Annual Cycle of Protozooplankton in the Kiel Bight. *Marine Biology*, 1981, vol. 63, p. 1-11.
- STABELL, Trond, ANDERSEN, Tom, et KLAVENESS, Dag. Ecological significance of endosymbionts in a mixotrophic ciliate-an experimental test of a simple model of growth coordination between host and symbiont. *Journal of plankton research*, 2002, vol. 24, no 9, p. 889-899.
- STANLEY, George D. Photosymbiosis and the evolution of modern coral reefs. *Science*, 2006, vol. 312, no 5775, p. 857-858.
- STOECKER, Diane K., JOHNSON, Matthew D., DE VARGAS, Colomban, et al. Acquired phototrophy in aquatic protists. *Aquatic Microbial Ecology*, 2009, vol. 57, p. 279-310.

- STOECKER, Diane K., SILVER, M. W., MICHAELS, A. E., *et al.* Enslavement of algal chloroplasts by four *Strombidium* spp.(Ciliophora, Oligotrichida). *Marine microbial food webs*, 1988, vol. 3, no 2, p. 79-100.
- SWANBERG, Neil R. et CARON, David A. Patterns of sarcodine feeding in epipelagic oceanic plankton. *Journal of Plankton Research*, 1991, vol. 13, no 2, p. 287-312.
- SWEENEY, Beatrice M. *Pedinomonas noctilucae* (Prasinophyceae), the flagellate symbiotic in *Noctiluca* (Dinophyceae) in Southeast Asia. *Journal of phycology*, 1976, vol. 12, no 4, p. 460-464.
- TAYLOR, F. J. R. Symbioses in marine microplankton. *Ann. Inst. Oceanogr.(Paris)*, 1982, vol. 58, p. 61-91.
- TRENCH, R. K. et THINH, Luong-van. *Gymnodinium linucheae* sp. nov.: The dinoflagellate symbiont of the jellyfish *Linuche unguiculata*. *European Journal of Phycology*, 1995, vol. 30, no 2, p. 149-154.
- WARNER, Mark E., LAJEUNESSE, Todd C., ROBISON, Jennifer D., *et al.* The ecological distribution and comparative photobiology of symbiotic dinoflagellates from reef corals in Belize: potential implications for coral bleaching. *Limnology and Oceanography*, 2006, vol. 51, no 4, p. 1887-1897.
- WILKERSON, Frances P. et GRUNSEICH, Gary. Formation of blooms by the symbiotic ciliate *Mesodinium rubrum*: the significance of nitrogen uptake. *Journal of Plankton Research*, 1990, vol. 12, no 5, p. 973-989.
- YI, Zhenzhen, DUNTHORN, Micah, SONG, Weibo, *et al.* Increasing taxon sampling using both unidentified environmental sequences and identified cultures improves phylogenetic inference in the Prorodontida (Ciliophora, Prostomatea). *Molecular phylogenetics and evolution*, 2010, vol. 57, no 2, p. 937-941.
- YELLOWLEES, David, REES, T. Alwyn V., et LEGGAT, William. Metabolic interactions between algal symbionts and invertebrate hosts. *Plant, cell & environment*, 2008, vol. 31, no 5, p. 679-694.

Supplementary information

Table S1. Information about the primer sets used in this study for PCR amplification of ribosomal genes of the host *Tiarina* sp. and the symbiotic microalga *Symbiodinium*.

Target and Primers	Sens	Sequence (5'-3')	Tm (°C)	Source
Ciliophora 18S rRNA gene				
Cil-384F	F	YTB GAT GGT AGT GTA TTG GA	56	Dopheide et al, 2008
Cil_1147R	R	GAC GGT ATC TRA TCG TCT TT	60	Dopheide et al, 2008
<i>Tiarina</i> sp. 18S rRNA gene (external primers)				
TiaV4-F1	F	CTT CTG AAT GTT GCG ACA GTG	47.3	This study
Cil28S_R1	R	ACG ATT TCA AGT CTT TTA ACC	41.4	This study
<i>Tiarina</i> 18S rRNA gene (internal primers)				
TiaV4-F2	F	CGG TCG TTG TAA TGG CAT TCA	47.3	This study
Cil28S_R2	R	GCT TTA GAA GAA GTT TAT CTC	41.3	This study
Dinophyceae 18S rRNA gene + ITS				
Din_464F	F	TAA CAA TAC AGG GCA TCC AT	51	Gómez et al. 2011
ITS_dinoRev	R	GTG AAT TGC CAG AAC TCC GTG	49	Pochon et al., 2001
Dinophyceae 28S rRNA gene				
ITS_dinoF	F	GTG AAT TGC AGA ACT CCG TG	60	Pochon et al., 2001
LO	R	GCT ATC CTG AGR GAA ACT TCG	49.2	Shaked & de Vargas, 2006
Eukaryotic 18S rRNA gene				
63F	F	ACG CTT GTC TCA AAG ATT	67	Lepere et al., 2011
1818R	R	ACG GAA ACC TTG TTA CGA	65	Lepere et al., 2011
Eukaryotic 28S rRNA gene				
D1R	F	ACC CGC TGA ATT TAA GCA TA	59	Scholin et al., 1994
D2C	R	CCT TGG TCC GTG TTT CAA GA	56	Scholin et al., 1994

Table S2. 18S rDNA sequences of ciliates (order Prorodontida) used for phylogenetic analyses. GenBank accession numbers in bold indicate the sequences of *Tiarina* sp. produced in this study.

Gene	Taxon	GenBank Accession number
18S rRNA	<i>Platyphyra vorax</i>	AF060454
18S rRNA	<i>Furgaosonia blachmanni</i>	X65150
18S rRNA	<i>Balanion masanensis</i>	AM12525
18S rRNA	<i>Cryptocaryon irritans</i>	AF351579
18S rRNA	<i>Holophrya ovum</i>	U97111
18S rRNA	<i>Pelagothrix alveolata</i>	AB486009
18S rRNA	<i>Levicoleps biwae</i>	AB354737
18S rRNA	<i>Nolandia nolandii</i>	AM292313
18S rRNA	<i>Coleps hirtus</i>	U97109
18S rRNA	<i>Coleps spetai</i>	AM292312
18S rRNA	<i>Coleps hirtus hirtus</i>	AM292311
18S rRNA	<i>Coleps</i> sp.	DQ487194
18S rRNA	<i>Nolandia</i> like sp.	FJ858215
18S rRNA	<i>Apocooleps</i> sp.	FJ858214
18S rRNA	<i>Apocooleps</i> sp.	HM747137
18S rRNA	<i>Apocooleps magnus</i>	FJ858213
18S rRNA	Uncultured eukaryote NA21F11	EF526888
18S rRNA	<i>Tiarina fusus</i>	FJ858217
18S rRNA	<i>Tiarina fusus</i> - Moore transcriptome	MMETSP0472
18S rRNA	<i>Tiarina</i> sp. Cilie 2	KR022029
18S rRNA	<i>Tiarina</i> sp. Cilie 3	KR022030
18S rRNA	<i>Tiarina</i> sp. TI_356	KR022031
18S rRNA	<i>Tiarina</i> sp. TI_357	KR022032
18S rRNA	<i>Tiarina</i> sp. TI_363	KR022033
18S rRNA	<i>Tiarina</i> sp. TI_365	KR022034
18S rRNA	<i>Tiarina</i> sp. TI_366	KR022035
18S rRNA	<i>Tiarina</i> sp. TI_371	KR022036
18S rRNA	<i>Tiarina</i> sp. TI_376	KR022037
18S rRNA	<i>Tiarina</i> sp. TI_377	KR022038
18S rRNA	<i>Tiarina</i> sp. TI_378	KR022039
18S rRNA	<i>Tiarina</i> sp. TI_379	KR022040
18S rRNA	<i>Tiarina</i> sp. TI_380	KR022041
18S rRNA	<i>Tiarina</i> sp. TI_381	KR022042
18S rRNA	<i>Tiarina</i> sp. TI_382	KR022043

Table S3. 28S rDNA sequences of *Symbiodinium* (clades A-H) used for phylogenetic analyses. GenBank accession numbers in bold indicate the sequences of *Symbiodinium* clade A produced in this study.

Gene marker	Clade	ITS2 subclade type	Host taxon	GenBank Accession number
28S rRNA	C	C91	<i>Sorites</i> sp.	JN558048
28S rRNA	C	C90	<i>Sorites</i> sp.	JN558045
28S rRNA	C	C15	<i>Amphisorus hemprichii</i>	JN558042
28S rRNA	C	C1	<i>Amphisorus hemprichii</i>	JN558040
28S rRNA	H	H1	<i>Sorites</i> sp.	JN558051
28S rRNA	H	H1a	<i>Sorites</i> sp.	JN558053
28S rRNA	F2	F2	<i>Sorites</i> sp.	JQ247043
28S rRNA	F2	F2a	<i>Sorites</i> sp.	JQ247044
28S rRNA	F3	F3.2	<i>Amphisorus hemprichii</i>	JQ247046
28S rRNA	F3	F3.1a	<i>Amphisorus hemprichii</i>	JQ247045
28S rRNA	F4	F4.8	<i>Sorites</i> sp.	JQ247048
28S rRNA	F4	F4.1	<i>Sorites</i> sp.	JQ247047
28S rRNA	F5	F5.2g	<i>Montastraea faveolata</i>	JN558072
28S rRNA	F5	F1	<i>Montipora verrucosa</i>	JN558066
28S rRNA	F5	F5.1d	<i>Sinularia</i> sp.	JN558069
28S rRNA	F5	F5.1	<i>Meandrina meandrites</i>	JN558063
28S rRNA	B	B2	<i>Eunicea flexuosa</i>	JN558060
28S rRNA	B	B1	<i>Plexaura kuna</i>	JN558057
28S rRNA	B	B19a	<i>Plexaura kuna</i>	JN558055
28S rRNA	I	I2	<i>Sorites</i> sp.	FN561560
28S rRNA	I	I1	<i>Sorites</i> sp.	FN561559
28S rRNA	D1	D1a	unknown anemone	JN558078
28S rRNA	D1	D1	<i>Acropora</i> sp.	JN558075
28S rRNA	D2	D1.1	<i>Marginopora vertebralis</i>	JQ247049
28S rRNA	D2	D1.2	<i>Haliclona koremella</i>	JN558081
28S rRNA	G2	G2.2*	<i>Cliona orientalis</i>	JQ247051
28S rRNA	G2	G2.1*	<i>Cliona orientalis</i>	JQ247050
28S rRNA	G1	G2	<i>Marginopora vertebralis</i>	JN558089
28S rRNA	G1	G2b	<i>Marginopora vertebralis</i>	JN558088
28S rRNA	E	E1	<i>Anthopleura elegantissima</i>	JN558084
28S rRNA	A	A2_2	<i>Gorgonia ventallina</i>	JN558100
28S rRNA	A	A2_1	<i>Bartholomea annulata</i>	JN558097
28S rRNA	A	A3	<i>Pseudoplexaura porosa</i>	JN558091
28S rRNA	A	A13	<i>Plexaura kuna</i>	JN558094
28S rRNA	A	A17	<i>Tiarina</i> Genotype 1- TI_376	KR022051
28S rRNA	A	A17	<i>Tiarina</i> Genotype 1- TI_379	KR022054
28S rRNA	A	A18	<i>Tiarina</i> Genotype 2- TI_381	KR022056
28S rRNA	A	A18	<i>Tiarina</i> Genotype 2- TI_382	KR022057
28S rRNA	A	A19	<i>Tiarina</i> Genotype 1- TI_380	KR022055
28S rRNA	A	A20	<i>Tiarina</i> Genotype 1- TI_392	KR022060
28S rRNA	A	A20	<i>Tiarina</i> Genotype 1- TI_393	KR022061
28S rRNA	A	A21	<i>Tiarina</i> Genotype 1- TI_356	KR022045
28S rRNA	A	A21	<i>Tiarina</i> Genotype 1- TI_357	KR022046
28S rRNA	A	A21	<i>Tiarina</i> Genotype 1- TI_363	KR022048
28S rRNA	A	A22	<i>Tiarina</i> Genotype 1- TI_355	KR022044
28S rRNA	A	A22	<i>Tiarina</i> Genotype 1- TI_358	KR022047
28S rRNA	A	A22	<i>Tiarina</i> Genotype 1- TI_366	KR022049
28S rRNA	A	A22	<i>Tiarina</i> Genotype 1- TI_371	KR022050
28S rRNA	A	A23	<i>Tiarina</i> Genotype 2- Med_2	KR022058
28S rRNA	A	A23	<i>Tiarina</i> Genotype 2- Med_3	KR022059
28S rRNA	A	A24	<i>Tiarina</i> Genotype 1- TI_377	KR022052
28S rRNA	A	A24	<i>Tiarina</i> Genotype 1- TI_378	KR022053
28S rRNA	Outgroup	<i>Polarella glacialis</i>	-	JN558108
28S rRNA	Outgroup	<i>Protodinium simplex</i>	-	JN558103
28S rRNA	Outgroup	<i>Pelagodinium bei</i>	-	JN558106

Table S4. ITS2 sequences of different *Symbiodinium* sub-clade types within clade A used for haplotype network reconstruction. GenBank accession numbers in bold indicate the sequences produced in this study.

Sub-clade type	Host origin	GenBank Accession number
A1	-	AF333505
A3	-	EU074857
A3a	-	EU449035
A3b	-	EU449043
A4	-	AF333508
A4a	-	AF499778
A5	-	AF333508
A6	-	AF186058
A7	-	AY239360
A8	-	EU449038
A9	-	EU449028
A10	-	EU792882
A11	-	EU449041
A12	-	EU792883
A13	-	AF333504
A15	-	EU792884
A15a	-	EU792885
A15b	-	EU792886
A15c	-	EU792887
A16	-	EU792888
A17	<i>Tiarina</i> TI_376	KR022069
A17	<i>Tiarina</i> TI_379	KR022072
A18	<i>Tiarina</i> TI_381	KR022074
A18	<i>Tiarina</i> TI_382	KR022075
A19	<i>Tiarina</i> TI_380	KR022073
A20	<i>Tiarina</i> TI_392	KR022078
A20	<i>Tiarina</i> TI_393	KR022079
A21	<i>Tiarina</i> TI_356	KR022063
A21	<i>Tiarina</i> TI_357	KR022064
A21	<i>Tiarina</i> TI_363	KR022066
A22	<i>Tiarina</i> TI_355	KR022062
A22	<i>Tiarina</i> TI_358	KR022065
A22	<i>Tiarina</i> TI_366	KR022067
A22	<i>Tiarina</i> TI_371	KR022068
A23	<i>Tiarina</i> Med_2	KR022076
A23	<i>Tiarina</i> Med_3	KR022077
A24	<i>Tiarina</i> TI_377	KR022070
A24	<i>Tiarina</i> TI_378	KR022071

Table S5. V9 rDNA sequences of *Tiarina* sp. (host) and the corresponding symbiont *Symbiodinium* used to interrogate the Tara Oceans metabarcoding dataset.

Holobiont ID	Host (the ciliate <i>Tiarina</i> sp.)	Symbiont (<i>Symbiodinium</i>)
TI_355	-	KR817711
TI_356	KR817696	KR817712
TI_357	KR817697	KR817713
TI_358	-	KR817714
TI_361	-	KR817715
TI_363	KR817698	KR817716
TI_365	KR817699	KR817717
TI_366	KR817700	-
TI_371	KR817701	KR817718
TI_376	KR817702	KR817719
TI_377	KR817703	KR817720
TI_378	KR817704	-
TI_379	KR817705	-
TI_380	KR817706	KR817721
TI_381	KR817709	-
TI_382	KR817710	-
TI_392	-	-
TI_393	-	-
Med_2	KR817707	KR817722
Med_3	KR817708	KR817723

Table S6. Contextual oceanographic parameters and the relative abundance of V9 reads of *Symbiodinium* (representing five distinct V9 sequences), *Tiarina* sp. (genotypes 1 and 2), and *Tiarina fusus* at each Tara Oceans station to perform correlation network analyses.

Station	Total <i>Symbiodinium</i>	<i>Tiarina</i> 98.33% genotype2	<i>Tiarina</i> 99.17% genotype1	<i>Tiarina fusus</i> 100%	Mean Latitude	Mean Depth Max Fluo m	Mixed Layer depth	Mean Depth MLD Sigma m	Euphotic zone depth	Day duration	Oxygen Depth min O ₂	Oxygen Depth max O ₂	Salinity Depth 10m	AMODIS PAR8d Einstein.s.m ⁻² .d ⁻¹	AMODIS PARm Einstein.s.m ⁻² .d ⁻¹	Mean Depth Max N2 m	NO2	PO4	NO2NO3	SI
100	6.68E-03	0.00E+00	2.47E-03	0.00E+00	1.30E+01	6.09E+01	2.53E+01	3.46E+01	2.19E+01	7.09E+02	1.80E+00	2.16E+02	3.58E+01	4.18E+01	4.24E+01	5.14E+01	1.40E-01	6.80E-01	6.20E+00	1.20E+00
102	5.73E-05	0.00E+00	1.15E-04	0.00E+00	5.25E+00	3.66E+01	2.48E+01	1.77E+01	2.35E+01	7.18E+02	8.36E-01	2.07E+02	3.47E+01	4.21E+01	4.47E+01	3.61E+01	3.20E-01	1.00E+00	1.26E+01	5.00E+00
109	6.03E-05	0.00E+00	0.00E+00	0.00E+00	1.99E+00	2.84E+01	2.75E+01	9.29E+00	2.49E+01	7.32E+02	1.59E+00	2.04E+02	3.34E+01	5.16E+01	4.24E+01	4.24E+01	4.00E-02	2.70E-01	9.00E-01	1.70E+00
11	1.61E-04	0.00E+00	0.00E+00	0.00E+00	4.17E+01	NA	NA	NA	NA	7.08E+02	NA	NA	NA	NA	NA	NA	NA	NA	NA	NA
111	4.51E-03	0.00E+00	5.29E-03	0.00E+00	1.70E+01	8.25E+01	2.27E+01	6.70E+01	1.84E+01	6.71E+02	4.61E+00	2.09E+02	3.60E+01	3.44E+01	3.76E+01	7.99E+01	4.00E-02	5.00E-01	2.68E+00	1.00E+00
122	3.00E-03	1.97E-04	5.51E-03	0.00E+00	9.92E+00	2.84E+01	2.66E+01	7.14E+01	NA	7.01E+02	2.27E+01	1.88E+02	3.54E+01	4.02E+01	4.16E+01	1.07E+02	1.20E-01	5.70E-01	5.46E+00	2.19E+00
123	4.09E-03	0.00E+00	2.05E-03	0.00E+00	8.91E+00	3.50E+01	2.66E+01	8.79E+01	2.25E+01	7.03E+02	3.42E+01	1.89E+02	3.54E+01	4.52E+01	4.32E+01	1.22E+02	1.40E-01	5.30E-01	4.90E+00	2.22E+00
124	4.35E-04	0.00E+00	5.22E-04	0.00E+00	9.15E+00	3.30E+01	2.65E+01	9.17E+01	NA	7.04E+02	4.31E+01	1.90E+02	3.54E+01	NA	4.33E+01	1.15E+02	1.60E-01	6.30E-01	6.18E+00	2.52E+00
125	8.25E-04	0.00E+00	1.36E-03	0.00E+00	8.88E+00	4.36E+01	2.68E+01	9.50E+01	2.09E+01	7.06E+02	4.18E+01	1.88E+02	3.54E+01	4.02E+01	4.16E+01	1.07E+02	1.20E-01	5.60E-01	3.73E+00	1.80E+00
18	2.34E-03	3.90E-04	3.34E-03	0.00E+00	3.58E+01	8.35E+01	2.14E+01	3.85E+01	1.15E+01	6.41E+02	1.74E+02	2.35E+02	3.79E+01	2.20E+01	1.95E+01	5.70E+01	1.83E-02	2.60E-02	1.20E-01	5.60E-01
20	1.56E-02	2.05E-03	1.39E-03	0.00E+00	3.45E+01	9.25E+01	2.14E+01	6.05E+01	1.97E+01	6.27E+02	2.37E+02	2.73E+02	3.84E+01	2.36E+01	2.04E+01	7.00E+01	6.30E-03	1.31E-02	2.00E-02	5.40E-01
22	6.19E-03	1.47E-04	8.35E-04	6.34E-03	3.98E+01	1.77E+01	1.70E+01	9.00E+00	1.35E+01	5.98E+02	1.77E+02	2.22E+02	3.77E+01	1.61E+01	1.32E+01	5.63E+01	7.00E-02	2.00E-02	2.10E-01	2.03E+00
23	1.98E-02	1.14E-04	3.63E-03	2.33E-03	4.22E+01	5.43E+01	1.69E+01	9.33E+00	1.66E+01	5.82E+02	1.92E+02	2.26E+02	3.82E+01	7.74E+00	1.03E+01	5.47E+01	1.00E-02	6.00E-03	4.00E-02	1.38E+00
24	1.41E-02	3.25E-04	2.68E-03	1.30E-03	4.25E+01	4.35E+01	1.82E+01	4.00E+00	1.10E+01	5.75E+02	1.90E+02	2.25E+02	3.81E+01	6.42E+00	1.04E+01	4.70E+01	1.40E-02	6.00E-03	9.00E-02	2.18E+00
25	2.19E-03	2.05E-04	6.83E-05	0.00E+00	3.94E+01	5.40E+01	1.83E+01	2.87E+01	1.30E+01	5.87E+02	1.73E+02	2.30E+02	3.82E+01	1.36E+01	1.37E+01	3.77E+01	4.50E-03	6.50E-03	3.00E-02	1.05E+00
26	5.12E-03	6.87E-04	5.00E-04	0.00E+00	3.85E+01	5.60E+01	1.90E+01	4.55E+01	1.26E+01	5.90E+02	1.83E+02	2.29E+02	3.84E+01	1.76E+01	1.47E+01	5.65E+01	6.00E-03	8.50E-03	6.50E-03	1.03E+00
30	1.14E-02	1.10E-03	5.27E-03	0.00E+00	3.39E+01	7.07E+01	2.03E+01	4.13E+01	1.23E+01	5.95E+02	1.66E+02	2.16E+02	3.94E+01	1.39E+01	1.53E+01	6.57E+01	0.00E+00	5.00E+02	8.20E-01	1.80E+00
31	1.51E-04	0.00E+00	1.51E-04	0.00E+00	2.72E+01	8.40E+01	2.50E+01	4.50E+01	1.23E+01	6.32E+02	4.91E+02	1.91E+02	4.00E+01	2.82E+01	2.79E+01	8.95E+01	1.35E-02	2.40E-02	3.00E-02	8.20E-01
32	2.81E-03	1.06E-04	2.23E-02	5.30E-05	2.34E+01	8.03E+01	2.58E+01	3.53E+01	1.13E+01	6.49E+02	2.42E+02	1.88E+02	3.97E+01	2.47E+01	1.42E+02	1.40E-02	1.75E-02	0.00E+00	8.70E-01	1.56E+00
33	4.02E-04	6.69E-05	1.34E-04	1.34E-04	2.20E+01	5.25E+01	2.72E+01	2.65E+01	1.57E+01	6.54E+02	2.22E+01	1.85E+02	3.90E+01	3.18E+01	3.40E+01	7.90E+01	2.00E-03	5.30E-02	4.50E-03	1.51E+00
34	4.54E-03	5.54E-05	1.66E-04	5.54E-05	1.84E+01	4.25E+01	2.76E+01	2.55E+01	1.59E+01	6.72E+02	2.15E+01	1.86E+02	3.86E+01	3.54E+01	3.52E+01	7.80E+01	2.00E-02	1.90E-01	3.00E-02	3.91E+00
36	3.17E-02	1.19E-03	0.00E+00	0.00E+00	2.08E+01	2.10E+01	2.54E+01	6.67E+00	1.79E+01	7.17E+02	4.27E+00	1.89E+02	3.65E+01	4.25E+01	4.65E+01	2.30E+01	5.00E-02	3.70E-01	1.30E-01	1.20E+00
38	3.16E-03	1.24E-04	0.00E+00	0.00E+00	1.90E+01	3.15E+01	2.61E+01	1.06E+01	1.79E+01	7.21E+02	2.71E+02	1.89E+02	3.66E+01	4.77E+01	4.47E+01	1.08E+02	1.40E-02	3.20E-01	6.00E-02	1.18E+00
39	6.51E-03	0.00E+00	0.00E+00	1.86E+01	3.49E+01	2.71E+01	8.50E+00	1.85E+01	7.24E+02	2.62E+02	1.92E+02	3.63E+01	4.69E+01	4.67E+01	8.29E+01	5.00E-03	2.30E-01	3.00E-02	1.44E+00	
41	1.89E-01	7.26E-05	1.90E-02	6.17E-04	1.46E+01	6.52E+01	2.91E+01	5.00E+00	1.09E+01	7.35E+02	2.65E+00	1.94E+02	3.60E+01	4.76E+01	4.85E+01	5.68E+01	3.00E-03	1.40E-01	9.00E-02	1.47E+00
42	1.11E-02	1.63E-04	6.75E-03	5.44E-05	6.03E+00	7.57E+01	3.00E+01	2.13E+01	1.17E+01	7.31E+02	5.95E+00	1.91E+02	3.46E+01	5.17E+01	4.68E+01	1.03E+02	0.00E+00	8.00E-02	3.00E-02	2.21E+00
45	6.44E-05	0.00E+00	4.57E-03	4.80E-04	3.05E+00	1.40E+01	1.31E+01	7.27E+02	4.59E+01	1.85E+02	3.52E+01	3.39E+01	4.84E+01	4.70E+01	2.00E-02	1.94E+00	2.86E+01	1.51E+01	1.51E+00	
52	5.80E-03	1.13E-04	3.83E-03	0.00E+00	1.70E+01	7.10E+01	2.79E+01	4.70E+01	1.75E+01	6.78E+02	1.17E+02	2.23E+02	3.46E+01	3.39E+01	3.79E+01	6.90E+01	0.00E+00	1.20E-01	0.00E+00	2.67E+00
64	3.14E-02	3.35E-03	4.38E-03	7.97E-05	2.95E+01	5.22E+01	2.22E+01	7.12E+01	1.50E+01	6.20E+02	1.51E+02	2.19E+02	3.53E+01	1.50E+01	1.86E+01	1.61E+02	4.00E-03	8.00E-02	0.00E+00	1.77E+00
65	3.38E-03	2.57E-04	1.46E-03	0.00E+00	3.52E+01	2.62E+01	2.16E+01	4.70E+01	1.59E+01	5.97E+02	1.52E+02	2.11E+02	3.54E+01	9.21E+00	1.54E+01	8.92E+01	NA	NA	NA	NA
66	0.00E+00	0.00E+00	5.14E-04	3.49E+01	2.20E+01	1.49E+01	9.00E+01	2.27E+01	6.01E+02	2.02E+02	2.39E+02	3.53E+01	1.43E+01	1.65E+01	1.04E+02	3.00E-01	3.40E-01	3.34E+00	2.74E+00	
67	0.00E+00	0.00E+00	0.00E+00	3.21E+01	9.75E+00	1.28E+01	1.22E+01	2.54E+01	6.97E+02	2.90E+01	1.69E+02	3.48E+01	3.77E+01	3.41E+01	2.52E+01	1.71E-01	1.02E+00	7.09E+00	1.39E+01	1.39E+00
68	0.00E+00	0.00E+00	0.00E+00	3.11E+01	3.71E+01	1.66E+01	1.87E+02	2.35E+01	7.10E+02	1.70E+02	2.34E+02	3.57E+01	3.41E+01	3.61E+01	2.00E+02	2.50E-01	2.29E-01	1.30E+00	2.60E+00	
7	1.88E-03	3.86E-04	0.00E+00	0.00E+00	3.70E+01	4.43E+01	1.80E+01	NA	NA	7.27E+02	NA	NA	3.75E+01	2.99E+01	3.52E+01	4.05E+01	0.00E+00	6.00E-02	3.00E-02	5.20E-01
70	1.84E-04	4.61E-05	0.00E+00	0.00E+00	2.04E+01	5.44E+01	1.97E+01	1.47E+02	2.22E+01	7.25E+02	1.42E+02	2.15E+02	3.64E+01	4.82E+01	4.59E+01	1.54E+02	5.40E-02	3.64E-01	9.86E-01	1.36E+00
72	9.66E-02	3.32E-03	9.95E-03	0.00E+00	8.78E+00	9.71E+01	2.50E+01	7.47E+01	1.23E+01	7.33E+02	8.36E+01	1.99E+02	3.64E+01	3.75E+01	4.60E+01	9.83E+01	3.00E-03	1.04E-01	1.80E-02	8.68E-01
76	2.31E-03	1.61E-04	3.76E-04	0.00E+00	2.09E+01	1.29E+02	2.32E+01	3.43E+01	8.13E+00	7.55E+02	1.67E+02	2.08E+02	3.71E+01	NA	NA	1.54E+02	1.00E-03	5.60E-02	NA	8.14E-01
78	1.55E-03	2.42E-04	4.84E-05	0.00E+00	3.01E+01	1.13E+02	1.99E+01	3.35E+01	1.12E+01	8.02E+02	1.98E+02	2.22E+02	3.63E+01	NA	NA	4.07E+01	0.00E+00	0.00E+00	1.70E-02	4.81E-01
82	0.00E+00	0.00E+00	0.00E+00	0.00E+00	4.72E+01	4.53E+01	7.24E+00	2.93E+01	3.20E+01	9.45E+02	1.66E+02	3.08E+02	3.40E+01	2.75E+01	3.57E+01	6.23E+01	1.51E-01	1.30E+00	1.	

Table S7. Comparison of different morphological characters of seven ciliates within the Colepidae family, including the newly isolated ciliate *Tiarina* sp.

	<i>Coleps hirtus</i>	<i>Nolandia nolandii</i>	<i>Levicoles biwae</i>	<i>Apocoles magnus</i>	<i>Tiarina meunieri</i>	<i>Tiarina fusus</i>	Novel ciliate
Body Shape	Oval	Cylindrical	Oval	Fusiform	Fusiform	Twisted Fusiform	Fusiform
Body Length (μm)	40-60	40-65	65-81	80-120	~ 80	60-135	140.2 ± 18.1
Body Width (μm)	-	-	42-60	30-45	no data	28-36	23.1 ± 3.8
Length-Width Ratio	~ 1.9	~ 2.5	~ 1.5	~ 2.5	~ 4- 4.5	~ 4	~ 6
Tiers (n)	6	6	6	8	6	6	6
Ciliary rows	15-16	12-14	20-27	22-24	no data	15-17	~ 18
Macronucleus length (μm)	-	-	12.4	14.4	no data	14.6	20
Wing-like structure	absent	absent	absent	absent	no data	present	present
Armor spines	present	present	absent	present	absent	present	absent
Symbionts	<i>Chlorella</i> sp.	no	no	no	-	no	<i>Symbiodinium</i> clade A
Habitat	Freshwater	Marine	Freshwater	Marine	Marine	Marine	Marine
Molecular data available	yes	yes	yes	yes	no	yes	yes
References for morphology	Foissner, 1999, 1984; Lemloh et al., 2013	Chen et al., 2010; 2012, Foissner, 2008	Foissner et al., 2008	Chen et al., 2009	Kahl, 1930; Chen et al., 2012	Chen et al., 2012	This study
References for molecular data	Yi et al., 2010	Barth et al., 2008	Foissner et al., 2008	Foissner et al., 2008		Yi et al., 2010	This study

Table S8. Significant P-values of the different correlations between environmental physico-chemical parameters and the distribution and relative abundance of V9 rDNA reads of ciliates and *Symbiodinium*.

	Total Symbiodinium	Tiarina 98.33% genotype2	Tiarina 99.17% genotype1	Tiarina fusus 100%	Mean Latitude	Mean Depth Max Fluo m	Mixed Layer mean temperature °C	Mean Depth Sigma m	Euphotic zone depth MLD	Day integrated Chla g.m⁻²
Total Symbiodinium	1.1E-299	3.5E-05	3.5E-05	7.8E-02	6.9E-01	3.4E-01	2.3E-01	2.8E-01	2.7E-02	1.5E-01
<i>Tiarina</i> 98.33% genotype2	3.5E-05	0.0E+00	2.9E-02	4.3E-01	1.9E-01	1.1E-01	6.3E-01	6.9E-01	6.7E-04	1.2E-01
<i>Tiarina</i> 99.17% genotype1	3.5E-05	2.9E-02	1.1E-299	9.2E-02	3.0E-01	2.4E-03	1.9E-01	3.3E-01	1.5E-03	7.8E-02
<i>Tiarina</i> fusus 100%	7.8E-02	4.3E-01	9.2E-02	0.0E+00	3.4E-01	4.3E-01	9.9E-01	8.8E-02	1.8E-01	6.3E-02
	Oxygen Depth min O ₂	Oxygen Depth max O ₂	Salinity 10m	AMODIS PAR8d Einstein.s.m⁻².d⁻¹	AMODIS PARm Einstein N2 m.m⁻².d⁻¹	Mean Depth Max	NO2	PO4	NO2NO3	SI
Total Symbiodinium	8.6E-01	9.9E-01	7.1E-02	7.2E-01	9.9E-01	8.2E-01	6.9E-03	1.7E-02	7.6E-03	1.4E-01
<i>Tiarina</i> 98.33% genotype2	5.9E-02	3.1E-01	1.2E-02	6.3E-02	9.9E-02	6.0E-01	1.5E-04	3.1E-05	1.2E-04	3.6E-03
<i>Tiarina</i> 99.17% genotype1	9.7E-01	9.1E-01	3.2E-01	5.1E-01	6.6E-01	2.8E-01	6.3E-02	7.0E-02	7.7E-02	2.6E-01
<i>Tiarina</i> fusus 100%	5.4E-01	9.9E-01	2.8E-01	1.3E-01	1.0E-01	9.2E-01	6.2E-01	6.3E-02	1.8E-01	3.2E-01

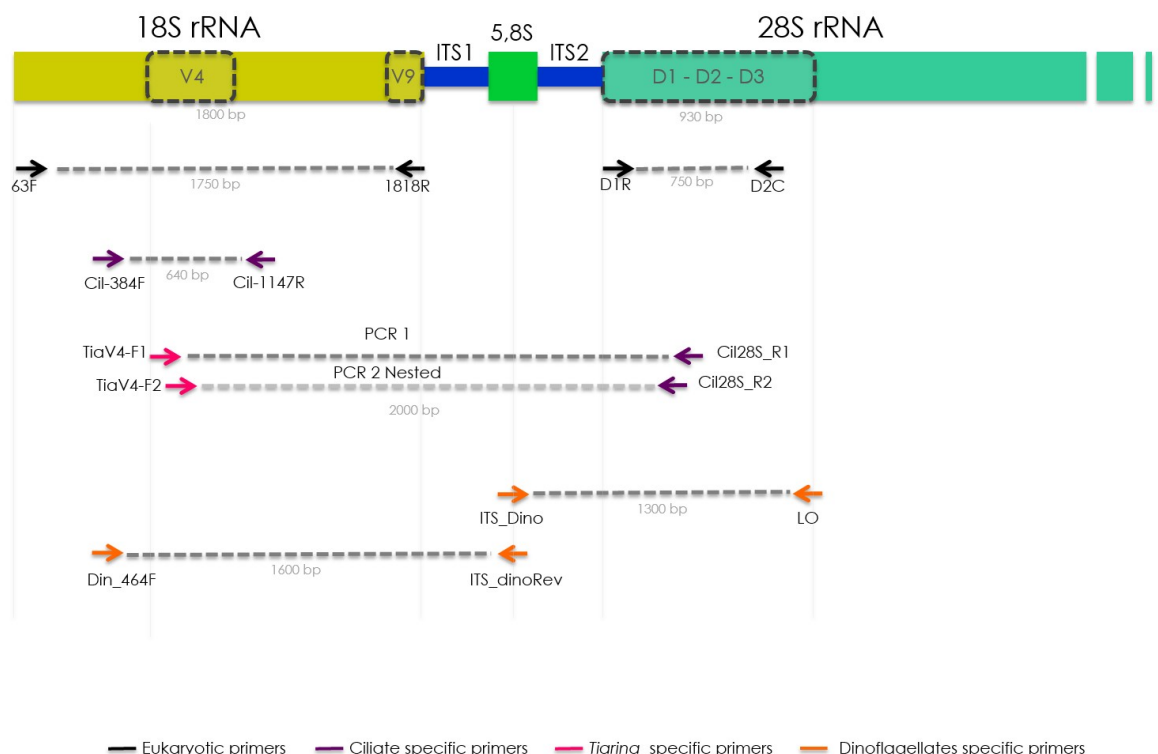


Figure S1. Schematic diagram of the ribosomal operon (18S and 28S rRNA genes, and ITS) showing the position of the different primers used in this study to PCR amplify sequences of the ciliate *Tiarina* and the symbiotic microalgae *Symbiodinium*.

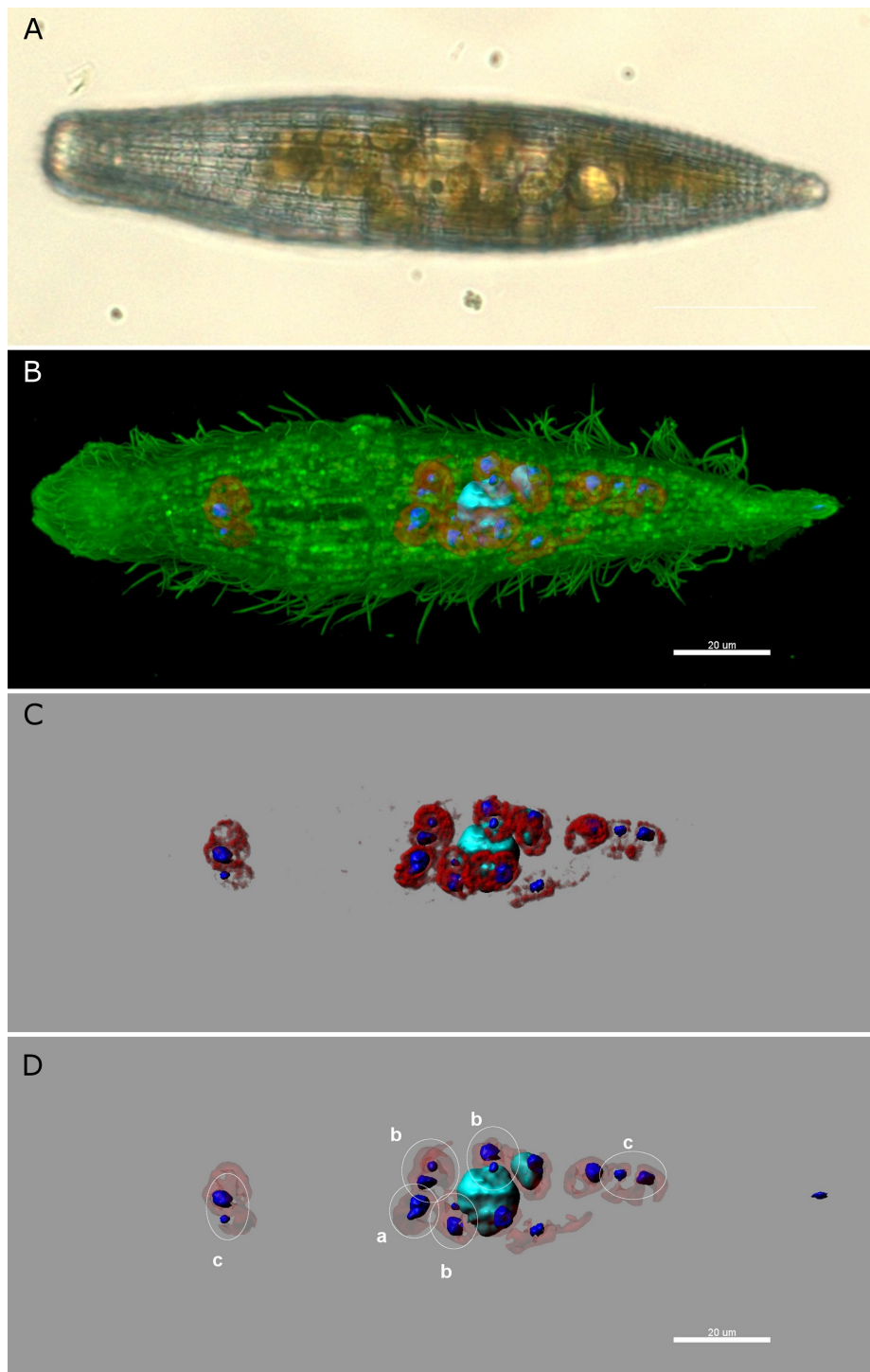


Figure S2. Microscopy images of the photosymbiosis between the ciliate *Tiarina* sp. (the host) and its intracellular symbiotic microalgae collected in surface oceanic waters. A: One live cell of *Tiarina* sp. collected in the Mediterranean Sea (Naples, Italy) in brightfield microscopy (Image courtesy of Diana Sarno). The ciliate is swimming with the help of numerous cilia at the surface of the cell, and harbours microalgal cells in the cytoplasm (golden cells). B-D: 3D reconstructions of symbiotic specimens imaged with Confocal Laser Scanning Microscopy (CLSM). B: Cilia of the ciliate are highlighted in green (DiOC6). C: The nuclei of the ciliate (cyan) and the symbiotic microalgae (blue) have been reconstructed from the Hoechst fluorescence signal, and the chloroplasts of the microalgae are highlighted by the red auto-fluorescence of the chlorophyll. D: Putative cell division events of *Symbiodinium* cells are surrounded and could have occurred at the early (a), middle (b) and late (c) stage of the cycle.

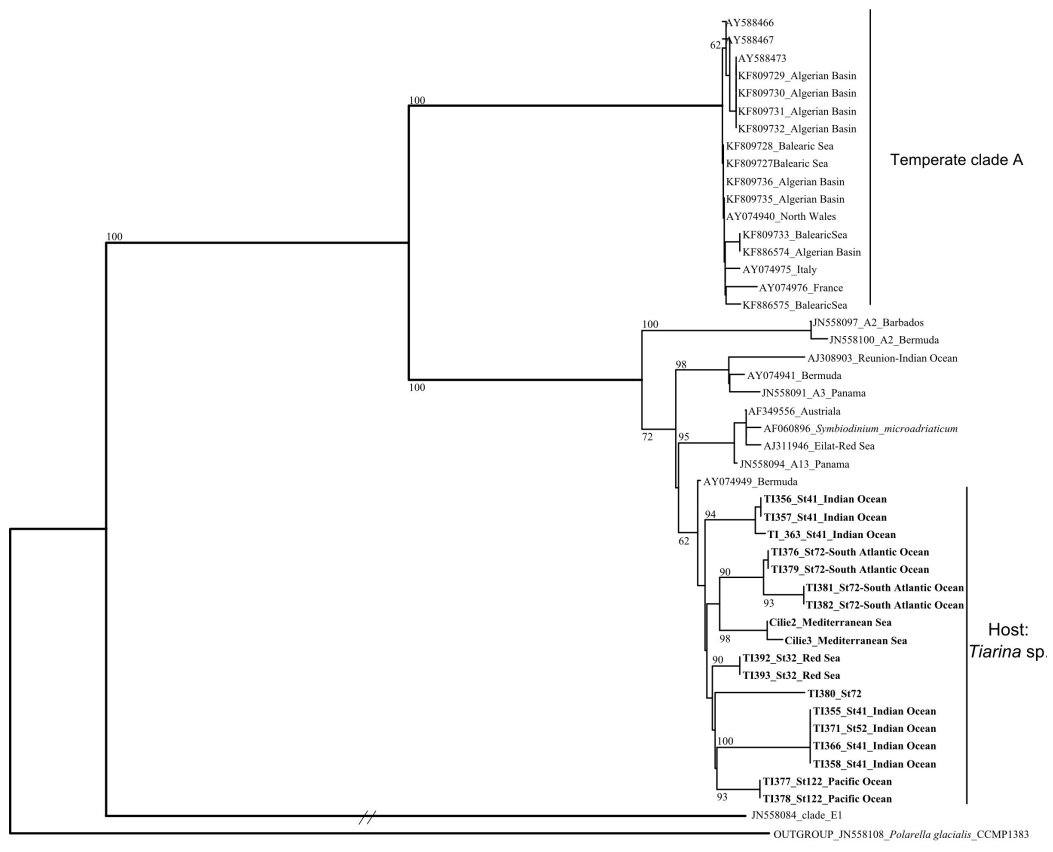


Figure S3. Phylogenetic tree (BioNJ) inferred from partial 28S rDNA sequences of *Symbiodinium* clade A (477 aligned nucleotide positions) with 100 pseudo-replicates. Compared to the 28S rDNA phylogenetic tree in Figure 3, the "temperate clade", only represented by relatively short sequences, was specifically included here to investigate whether *Symbiodinium* associated to the ciliate *Tiarina* (sequences in bold) belongs to this clade.

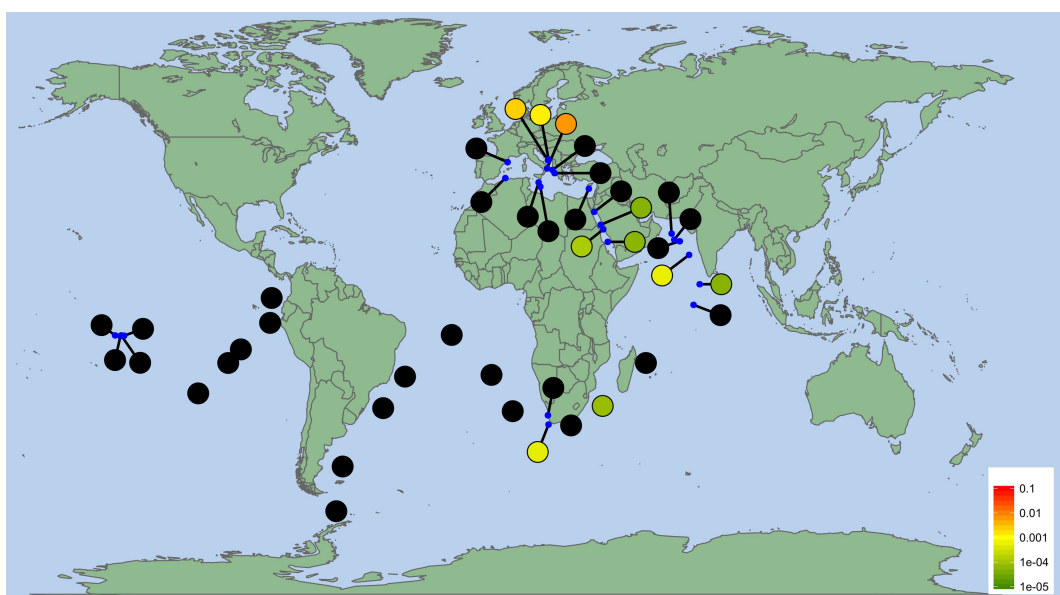


Figure S4. Mapping of the relative abundance of rDNA V9 reads strictly identical to the V9 sequence of the ciliate *Tiarina fusus* in Tara Oceans stations (surface samples and 20-180 µm size fraction). The color gradient indicates the relative abundance of V9 reads from green to red for low to high values, respectively. Black dots indicate that no V9 reads have been detected in the station.

Bibliography from the Supplementary information

- BARTH, Dana, TISCHER, Karolin, BERGER, Helmut, *et al.* High mitochondrial haplotype diversity of Coleps sp.(Ciliophora: Prostomatida). *Environmental microbiology*, 2008, vol. 10, no 3, p. 626-634.
- CHEN, Xiangrui, GAO, Shan, LIU, Weiwei, *et al.* Taxonomic descriptions of three marine colepid ciliates, Nolandia sinica spec. nov., Apocoleps caoi spec. nov. and Tiarina fusa (Claparède & Lachmann, 1858) Bergh, 1881 (Ciliophora, Prorodontida). *International journal of systematic and evolutionary microbiology*, 2012, vol. 62, no Pt 3, p. 735-744.
- CHEN, Xiangrui, WANG, Yangang, LONG, Hongan, *et al.* Morphological studies on two marine colepid ciliates from Qingdao, China, Nolandia orientalis spec. nov. and Pinacocoleps similis (Kahl, 1933) comb. nov.(Ciliophora, Colepidae). *European journal of protistology*, 2010, vol. 46, no 4, p. 254-262.
- CHEN, Xiangrui, WARREN, Alan, et SONG, Weibo. Taxonomic studies on a new marine ciliate, Apocoleps magnus gen. nov., spec. nov.(Ciliophora, Colepidae), isolated from Qingdao, China. *Journal of Ocean University of China*, 2009, vol. 8, no 4, p. 317-321.
- DOPHEIDE, Andrew, LEAR, Gavin, STOTT, Rebecca, *et al.* Molecular characterization of ciliate diversity in stream biofilms. *Applied and environmental microbiology*, 2008, vol. 74, no 6, p. 1740-1747.
- FOISSNER, Wilhelm, KUSUOKA, Yasushi, et SHIMANO, Satoshi. Morphology and gene sequence of Leviscoleps biwae n. gen., n. sp.(Ciliophora, Prostomatida), a proposed endemic from the ancient Lake Biwa, Japan. *Journal of Eukaryotic Microbiology*, 2008, vol. 55, no 3, p. 185-200.
- FOISSNER, Wilhelm., BERGER, Helmut and SCHÄUMBURG, Jochen., *Identification and ecology of limnetic plankton ciliates*. Munich : Informationberichte des Bayerischen Landesamtes für Wasserwirtschaft, 1999
- FOISSNER, Wilhelm., *Infraciliatur, Silberliniensystem und Biometrie einiger neuer und wenig bekannter terrestrischer, limnischer und mariner Ciliaten : (Protozoa: Ciliophora) aus den Klassen Kinetofragminophora, Colpodea und Polyhymenophora*. Linz, Austria : Botanischer Arbeitsgemeinschaft am O.Ö. Landesmuseum Linz, 1984
- GOMEZ, Fernando, LÓPEZ-GARCÍA, Purificación, et MOREIRA, David. Molecular phylogeny of dinophysoid dinoflagellates: the systematic position of *Oxyphysis oxytoxoides*

and the *Dinophysis hastata* group (Dinophysales, Dinophyceae) 1. *Journal of phycology*, 2011, vol. 47, no 2, p. 393-406.

KAHL Alfred. Urtiere oder Protozoa I: Wimpertiere oder Ciliata (Infusoria) 1. Allgemeiner Teil und Prostomata. Tierwelt Dtl, 1930, vol. 18, p. 1-180.

LEMLOH, Marie-Louise, MARIN, Frédéric, HERBST, Frédéric, et al. Genesis of amorphous calcium carbonate containing alveolar plates in the ciliate Coleps hirtus (Ciliophora, Prostomatea). *Journal of structural biology*, 2013, vol. 181, no 2, p. 155-161.

LEPERE, Cécile, DEMURA, Mikihide, KAWACHI, Masanobu, et al. Whole-genome amplification (WGA) of marine photosynthetic eukaryote populations. *FEMS Microbiology Ecology*, 2011, vol. 76, no 3, p. 513-523.

POCHON, Xavier, PAWLowski, J., ZANINETTI, Louisette, et al. High genetic diversity and relative specificity among *Symbiodinium*-like endosymbiotic dinoflagellates in sorid foraminiferans. *Marine Biology*, 2001, vol. 139, no 6, p. 1069-1078.

SHAKED, Yonathan et DE VARGAS, Colomban. Pelagic photosymbiosis: rDNA assessment of diversity and evolution of dinoflagellate symbionts and planktonic foraminiferal hosts. *Marine Ecology Progress Series*, 2006, vol. 325, p. 59-71.

SCHOLIN, Christopher A., HERZOG, Michel, SOGIN, Mitchell, et al. Identification of group-and strain-specific genetic markers for globally distributed *Alexandrium* (Dinophyceae). II. Sequence analysis of a fragment of the LSU rRNA gene1. *Journal of phycology*, 1994, vol. 30, no 6, p. 999-1011.

YI, Zhenzhen, DUNTHORN, Micah, SONG, Weibo, et al. Increasing taxon sampling using both unidentified environmental sequences and identified cultures improves phylogenetic inference in the Prorodontida (Ciliophora, Prostomatea). *Molecular phylogenetics and evolution*, 2010, vol. 57, no 2, p. 937-941.

Size-fractionated global DNA metabarcoding reveals ecological significance of the planktonic dinoflagellate parasite *Blastodinium* in sunlit oceans.

Nicolas Henry^{1,2}, Daniel J. Richter^{1,2}, Sébastien Colin^{1,2}, Sarah Romac^{1,2}, Cédric Berney^{1,2}, Patrick Wincker^{3,4,5}, Colomban de Vargas^{1,2}, Stéphane Audic^{1,2}

¹ EPEP - *Evolution des Protistes et des Ecosystèmes Pélagiques* - team, Sorbonne Universités, UPMC Univ Paris 06, UMR 7144, Station Biologique de Roscoff, 29680 Roscoff, France

² CNRS, UMR 7144, Station Biologique de Roscoff, 29680 Roscoff, France

³ CEA, Institut de Génomique, GENOSCOPE, 2 rue Gaston Crémieux, 91000 Evry, France.

⁴ CNRS, UMR 8030, CP5706, Evry, France.

⁵ Université d'Evry, UMR 8030, CP5706, Evry, France

In preparation

Abstract

The recent advent of massive DNA metabarcoding surveys of environmental samples across large spatio-temporal and taxonomic scales offers a new tool to study ecological patterns of microbial organisms. Here we use a dataset of ~766 million raw rDNA sequence reads generated from 47 open ocean stations from the *Tara Oceans* circum-global expedition to explore the diversity and ecology of the dinoflagellate genus *Blastodinium* across four organismal size fractions, from piconano- to mesoplankton, and to test patterns of co-occurrence with their hosts (copepods). Little is known about the diversity and the host specificity of *Blastodinium* in open oceans, in part because most of the limited observations have been conducted in coastal waters, largely in the Mediterranean Sea. We describe the biogeography of *Blastodinium* across oceanic basins and we produce the first world-wide *Blastodinium*/copepod interactome. Our analysis reveals that the *Blastodinium* genus is highly diverse, in terms of both ecology and phylogeny. The most abundant *Blastodinium* metabarcodes in mesoplankton display high association scores with copepods with respect to previously observed specificities. Overall, our analysis suggests that rDNA metabarcoding data can be used to explore symbiont life style, diversity and host specificity amongst the wealth of microorganisms in the world plankton.

Introduction

The biodiversity of marine pelagic ecosystems appear to be dominated by protistan lineages, characterized by highly diverse interaction and symbiotic patterns (Smetacek, 2012; de Vargas *et al.*, 2015; Lima-Mendez *et al.*, 2015). In particular, protistan parasites have been observed in morphological studies of plankton communities dating back over a century (Apstein, 1911; Chatton, 1920; Cachon and Cachon, 1987), with a renewed interest associated with the use of DNA-based, molecular ecology protocols (Kühn *et al.*, 2004; Figueroa *et al.*, 2008; Alves-de-Souza *et al.*, 2012; Guo *et al.*, 2012; Skovgaard *et al.*, 2012). However, despite significant efforts invested in detection and identification of symbionts *-sensu lato-* in marine plankton, the diversity and host specificity of parasites are often poorly known, as the discovery of new symbioses often begins with direct observations under a microscope, a time-consuming and not easily scalable process.

The marine photosynthetic dinoflagellate genus *Blastodinium* was described infecting copepods in the early 20th century by the French protozoologist Édouard Chatton (Chatton, 1906). Based on morphological characters, and later confirmed by molecular studies, the *Blastodinium* genus, which is not always monophyletic in phylogenetic analysis (Skovgaard *et al.*, 2007; Alves-de-Souza *et al.*, 2011), was separated into three morphologically and genetically coherent entities: the *contortum*, *spinulosum* and *mangini* groups (Chatton, 1920; Skovgaard *et al.*, 2012). After being ingested by a copepod, the *Blastodinium* free-living cell stage, called the dinospore and measuring between 5 and 30 µm, develops inside the gut lumen host to form the parasitic stage (trophont). The trophont stage consists of an arrangement of several hundreds of cells surrounded by a common cuticle, the whole package reaching a length of more than 1 mm (Chatton, 1920). Since copepods are a key trophic link in pelagic food webs (Schminke, 2007), *Blastodinium* infections should exert a strong impact on plankton ecosystems (Fields *et al.*, 2015). Only 78 copepod/*Blastodinium* pairs (at the species level) have been described (Skovgaard *et al.*, 2012) whereas there are 13 accepted species of *Blastodinium* and more than 2500 marine planktonic copepod species (Razouls and de Bovée, 2005). Previous work based on morpho-genetic observations has shown a broad pattern of specificity, in which the *contortum* and *spinulosum* groups infect Calanoida copepods whereas the *mangini* group mainly infects Cyclopoida copepods (including Poecilostomatoida (Boxshall and Halsey, 2004)) and to a lesser extent Calanoida copepods. Little is known about its diversity and host specificity in the open ocean, in part

because most observations of *Blastodinium* have been conducted in coastal waters, especially in the Mediterranean sea (Skovgaard *et al.*, 2012). Nevertheless, this symbiotic interaction which occurs worldwide is one of the better described in the marine planktonic realm, in terms of both morphology and genetics.

Nowadays, the use of environmental DNA metabarcoding is transforming the field of microbial ecology. This approach, based on High Throughput Sequencing methods, allows rapid and massive sequencing of a DNA fragment used as a proxy for assessing organismal diversity in an entire community, and has been used for the study of viral, prokaryotic and eukaryotic populations (de Vargas *et al.*, 2015; Sunagawa *et al.*, 2015). In addition to being used for biodiversity studies, metabarcoding data have been increasingly used in the field of systems ecology, especially for bacteria (Faust *et al.*, 2012) but also for eukaryotes (Lima-Mendez *et al.*, 2015). In this context, a worldwide metabarcoding dataset of V9 sequences (a region towards the 3' end of the eukaryotic 18S ribosomal DNA gene sequence) from size-fractionated marine plankton communities has been generated as one of the outcomes of the *Tara*-Oceans expedition (Karsenti *et al.*, 2011; de Vargas *et al.*, 2015). Here, we used this large scale *Tara*-Oceans metabarcoding dataset to explore the diversity and ecology of *Blastodinium* across four organismal size fractions from *piconano*- to *meso*- plankton (0.8 µm to 2mm) *piconano*- to *meso*-plankton. We describe the phylogenetic diversity and biogeography of *Blastodinium* at a worldwide scale, and show that comparing abundances of metabarcoding data among organismal size fractions generates insights into the parasites' life cycles. We produce the first global *Blastodinium*/copepod interactome and provide directions for future studies to detect symbiotic interactions in plankton from large scale and size-fractionated environmental metabarcoding datasets.

Materials and methods

Data

Data used in this study is part of the primary *Tara*-Oceans V9 rDNA metabarcoding dataset (de Vargas *et al.*, 2015), which consists of ~766 million raw rDNA sequence reads from 334 size-fractionated plankton samples collected at 47 open ocean stations and 2 depths during the circum-global *Tara* Oceans expedition (Karsenti *et al.*, 2011). Material and methods used for plankton sampling, DNA extraction, V9 rDNA amplification and sequencing, as well as the bioinformatic pipeline used for metabarcodes quality check

filtering, clustering, and taxonomic assignation are described in (Pesant *et al.*, 2015) and (de Vargas *et al.*, 2015). All V9 rDNA metabarcodes assigned to *Blastodinium*, *Azadinium*, *Alexandrium*, Copepoda, and MALVs (Marine Alveolata) reference sequences with a percentage identity >90% were extracted from the global dataset. Their diversity and abundance were then studied across oceanic sites, two water-column depths (subsurface -SUR- and Deep Chlorophyll Maximum -DCM) and the four targeted organismal size fractions that contain most eukaryotic plankton biodiversity: *piconano*-plankton (0.8-5µm), *nano*-plankton (5-20µm), *micro*-plankton (20-180µm), and *meso*-plankton (180-2000µm). For a given sample (one site, depth, and size-fraction) and a given metabarcode, the number of reads assigned to the metabarcode divided by the total read number within the sample was used as a proxy for abundance in further statistical analysis. In order to assess whether the distribution pattern of abundance data amongst plankton size fractions may reflect parasitic life cycles, we compared the patterns of *Blastodinium* metabarcodes abundance in *piconano*-, *nano*-, *micro*- and *meso*-plankton to abundance data of metabarcodes assigned to copepods (the host) and two other dinoflagellate genera, *Azadinium* and *Alexandrium*, for which there are no known cases of parasitism. *Azadinium* cells and *Blastodinium* dinospores have similar size (Tillmann *et al.*, 2009, 2010), while *Alexandrium* cells are slightly larger (Balech, 1995).

***Blastodinium* phylogeny**

V9 rDNA metabarcodes and reference sequences used for phylogenetic analysis were aligned using MUSCLE v3.8.31 with default settings (Edgar, 2004). Neighbor-joining phylogenetic trees were then constructed using the BioNJ algorithm (Gascuel, 1997) implemented in Seaview (Gouy *et al.*, 2010). Observed divergences (percentage residues differing between two sequences) were used as genetic distances and bootstrap supports were obtained from 1000 replicates. For each metabarcode, mean relative abundance and distribution across organismal size fractions were displayed using iTOL (Letunic and Bork, 2011). *Blastodinium* metabarcodes were used in the phylogeny if they were represented by at least 300 reads across the entire dataset. Copepod metabarcodes were used in the phylogeny if at least one significant association was found with any *Blastodinium* metabarcode in our analyses (see below).

Interactome inference

We focused on relatively frequent copepod and *Blastodinium* metabarcodes from the largest, meso-planktonic size fraction (180-2000 μm , where *Blastodinium* should be in its trophont, *in hospite* stage) to reconstruct co-abundance host/parasites ecological networks. Only metabarcodes present in more than 30% of meso-plankton samples were used for abundance comparisons. Since only associations between hosts and parasites were targeted, bipartite multiple pairwise comparisons (Poulin, 2010) were performed. As such, metabarcodes of one set (either *Blastodinium* or Copepoda metabarcodes) were compared with metabarcodes of the other set, and not all against all. Comparisons were conducted using Spearman's rho (ρ) tests, removing couples of zero because they are uninformative (Legendre and Legendre, 2012). The p-values were adjusted using the False Discovery Rate (FDR) approach (Benjamini and Hochberg, 1995). *Blastodinium* and copepod metabarcodes were considered as associated when they were positively ($\rho>0$) and significantly ($p<0.001$) correlated.

Results

Blastodinium rDNA abundance, richness, and phylogeny across plankton size fractions

Although Marine Alveolates (MALV), arguably the major group of eukaryotic parasites in marine plankton (de Vargas *et al.*, 2015; Lima-Mendez *et al.*, 2015), are at least as abundant as all dinophyceae (including *Blastodinium*) in the piconano-plankton (0.8-5 μm) metabarcoding dataset, the *Blastodinium* genus is typically more abundant than MALV in the nano- (5-20 μm) and meso- (180-2000 μm) plankton (Figure 1). In this latter and larger organismal size fraction, meso-plankton, the abundance of *Blastodinium* represents 36% of the entire dinoflagellate diversity and exceeds even that of all other dinophyceae in some stations (e.g. stations 7, 18, 109, Figure 1).



Figure 1: Relative abundances of dinophyceae (*Blastodinium* and the other dinophyceae) and Marine Alveolates (MALV) V9 rDNA reads across 4 organismal size fractions (piconano-plankton: 0.8–5 µm, nano-plankton: 5–20 µm, micro-plankton: 20–180 µm, meso-plankton: 180–2000 µm) and 45 Tara Oceans stations (subsurface waters). The relative abundance is the number of rDNA reads of the metabarcode divided by the total number of rDNA reads of the sample. NAs indicate samples for which no data are available.

Overall *Blastodinium* rDNA reads are particularly abundant in *nano-* and *meso-*plankton samples (Figure 2A) with a characteristic drop in the intermediate, *micro*-planktonic size fraction, expected from its parasitic lifestyle. This pattern of relative abundance across size fractions is different from that of non-parasitic dinoflagellates such as the *Alexandrium* and *Azadinium* genera. *Alexandrium* rDNA reads, coming from cell sizes of roughly 100 µm, are more abundant in *micro*-plankton (20–180 µm) samples, whereas *Azadinium* reads, from cell sizes roughly between 10–20 µm (similar to the *Blastodinium* free-living dinospores), are more abundant in *piconano-* and *nano*-plankton samples (0.8–20 µm).

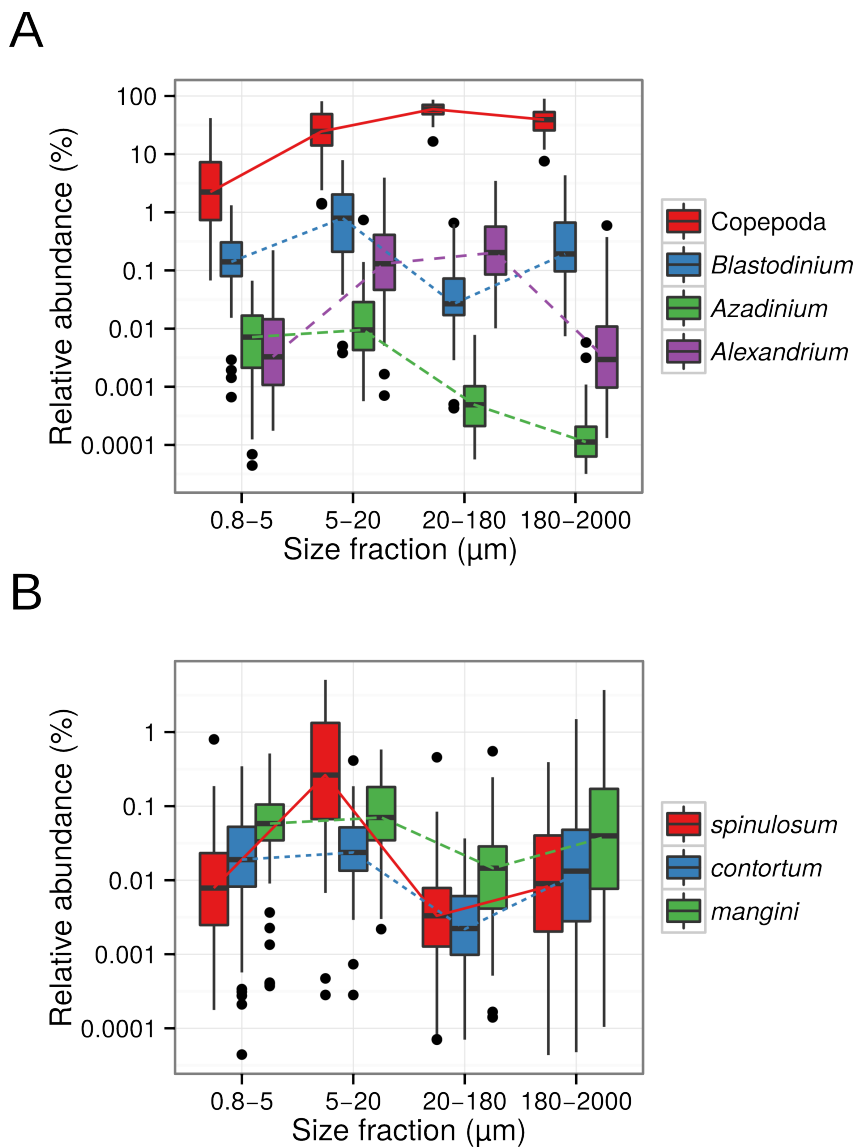


Figure 2: V9 rDNA reads' relative abundances across four organismal size fractions (*piconano*-plankton: 0.8-5 µm, *nano*-plankton: 5-20 µm, *micro*-plankton: 20-180 µm, *meso*-plankton: 180-2000 µm; samples from surface waters). (A) Metabarcodes from the genus *Blastodinium* compared to metabarcodes affiliated to copepods and two other non-symbiotic, free-living dinophyceae genera, *Azadinium* and *Alexandrium*. *Azadinium* cells and *Blastodinium* dinospores have similar size, while *Alexandrium* cells are slightly larger. (B) Metabarcodes assigned to the three known groups of *Blastodinium*: *spinulosum*, *contortum* and *mangini*.

232 of the 234 most abundant *Blastodinium* metabarcodes, (i.e. the metabarcodes which appear more than 300 times in our dataset) are distributed across the three major *Blastodinium* groups (104 from *mangini*, 110 from *spinulosum* and 18 from *contortum*; Figure 3). *Blastodinium* reads are generally relatively scarce in the *micro*-plankton, however, the distribution across size fractions is different amongst *Blastodinium* groups. Ribosomal DNA reads from the *spinulosum* group are mainly found in the *nano*-plankton, whereas reads from the *contortum* and *mangini* groups are generally more abundant in the *meso*-plankton, and

also in one or both of the two smallest size fractions (*piconano* and *nano-plankton*) (Figures 2B and 3). Two metabarcodes, represented by only a few rDNA reads, could not be assigned to a specific group.

***Blastodinium* biogeography**

Blastodinium metabarcodes have been detected in all samples, except in one *meso-planktonic* sample from the Southern Ocean (Figure 4A). Mediterranean sea, Red sea, North Indian Ocean and one station from Pacific Ocean are particularly rich in *Blastodinium* rDNA reads, mainly from the *mangini* group, which can reach up to 8% of the sample total rDNA read abundance. In the *nano-plankton* (5-20 µm), *Blastodinium* rDNA reads are also abundant in subtropical and equatorial part of the Atlantic and Pacific Oceans, and dominated by the *spinulosum* group. With few exceptions (and except for the *nano-plankton*), the proportions of *Blastodinium* groups are relatively stable across stations but vary depending on the considered size fraction (Figure 4B).

Associations with copepods

Among the ~2.3 million metabarcodes generated in the *Tara-Oceans* V9 rDNA metabarcoding dataset, 324,903 and 16,295 are assigned respectively to copepod and *Blastodinium* reference sequences with a percentage identity above 90%. 5,580 copepod and 40 *Blastodinium* metabarcodes appear in more than 30% of *meso-plankton* samples (71 samples).

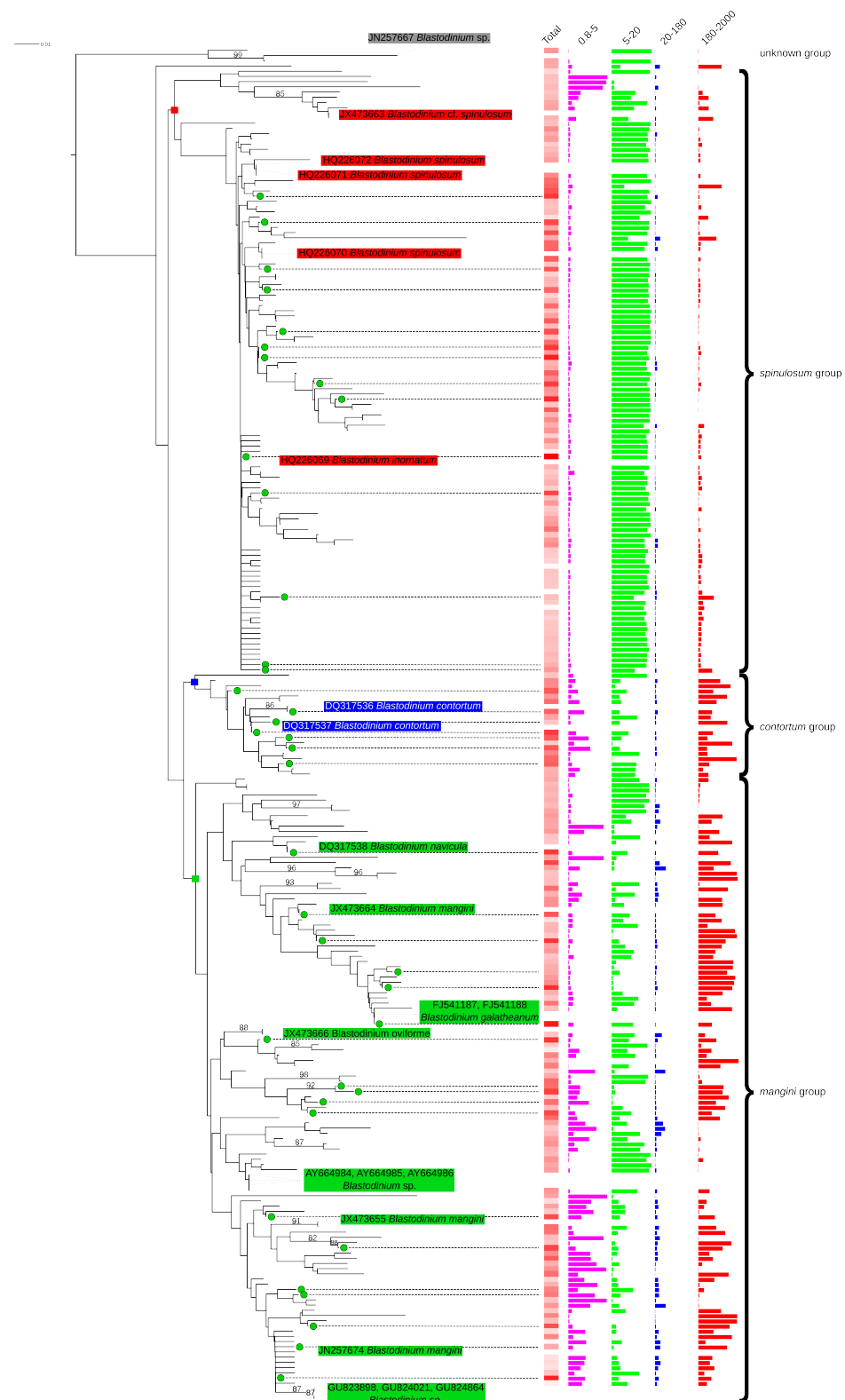


Figure 3: Phylogenetic tree (Neighbor-joining) of the most abundant *Blastodinium* metabarcodes (>300 copies in the Tara-Oceans V9 rDNA metabarcoding dataset), together with their affiliated reference sequences. Numbers are bootstrap values; only values above 80% are shown. Labels at branches indicate GenBank accession numbers with species names for the reference sequences. Green dots indicate metabarcodes used for interactions study (Figures 5 and 6). The color gradient from white to red (Total) is proportional to the abundance of each metabarcode. Bars indicate proportion of total abundance of each metabarcode amongst the four targeted organismal size fractions of this study (purple: piconano-plankton, green: nano-plankton, blue: micro-plankton, red: meso-plankton).

23 of the *Blastodinium* metabarcodes (55%) are significantly correlated ($p<0.001$) with 325 (6% of 5,580) copepod metabarcodes (Figure 5). Calanoida copepods tend to have higher association scores (ρ) with the *contortum* group (mean=0.52) whereas Cyclopoida copepods (including Poecilostomatoida (Boxshall and Halsey, 2004)) tend to have better association scores with the *mangini* group (mean=0.56) (Figure 5). The *spinulosum* group has relatively low scores with either Cyclopoida (mean=0.50) or Calanoida (mean=0.49). Several groups of genetically highly similar metabarcodes from copepods co-occur with the same *Blastodinium* metabarcodes (Figure 6). For instance, 136 metabarcodes closely related (99 to 100% of identity) to *Oncaeа* sp. (Cyclopoida) are mainly associated with one *Blastodinium* metabarcode from the *mangini* group, and, with lower scores, with one metabarcode from the *spinulosum* group (Figure 6). 11 metabarcodes related (~92% identity) to *Corycaeus* sp. (Cyclopoida) are associated with one *Blastodinium* metabarcode from the *mangini* group. On the other hand, a group of 168 metabarcodes closely related (~98% identity) to *Pseudocalanus* sp. (Calanoida), are associated with several *Blastodinium* metabarcodes from the *contortum* group, as well as one metabarcode from the *mangini* group, but with lower *contortum* group are characterized by higher scores. Other copepod metabarcodes from the order Calanoida form associations with both the *spinulosum* and *contortum* groups, whereas metabarcodes from the order Cyclopoida form associations with both the *spinulosum* and *mangini* groups.

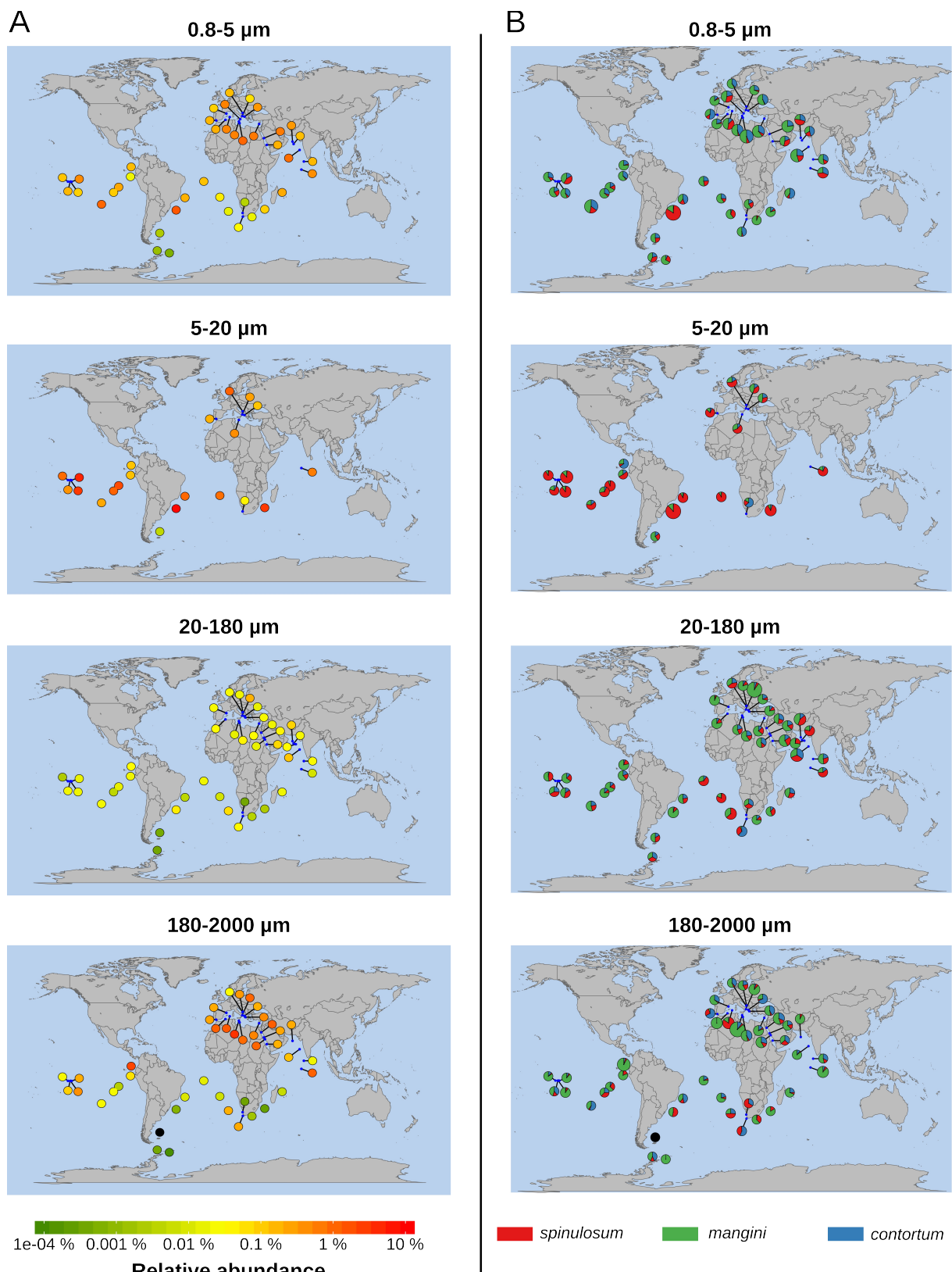


Figure 4: Large-scale biogeography of *Blastodinium* across the four organismal size fractions at the surface from 45 stations. (A) Relative abundances of the genus *Blastodinium*. (B) Proportions of the different *Blastodinium* groups. Sizes of the pie charts are proportional to the relative abundance of *Blastodinium*.

Discussion

Dinoflagellates of the genus *Blastodinium* are highly abundant and diverse in global photic open oceans

The Marine Alveolates (MALV) have been recognized as one of the major groups of parasites playing a key ecological role in marine planktonic ecosystems (Guillou *et al.*, 2008; de Vargas *et al.*, 2015; Lima-Mendez *et al.*, 2015). Indeed, MALVs dominate the dinophyceae metabarcodes (including *Blastodinium* and all other dinoflagellates) in the *piconano*-plankton, which likely reflects their parasitoid life style where infections lead to the death of the host associated with massive production of dispersive stages (de Vargas *et al.*, 2015). However the genus *Blastodinium* represents up to 20% of all dinophyceae metabarcodes in the *nano*-plankton, and up to 80% in the *meso*-plankton. It is typically much more abundant than MALVs in this latter, larger size fraction (Figure 1). Thus, our data suggest that *Blastodinium* play an important role both as a food source for predators in the *nano*-plankton and as one of the main parasites of copepods, the dominant free-living organisms, in the *meso*-plankton. The dinophyceae constitute an important share of the copepod diet in the oligotrophic systems (Saiz and Calbet, 2011) and, according to (Chatton, 1920), the infection cycle of *Blastodinium* begins with the ingestion of a dinospore by a copepod. Thus, relatively high proportions of *Blastodinium* amongst nanoplanktonic dinophyceae would enhance their ability to infect copepods *Blastodinium*. Phylogenetic reconstructions based on V9 rDNA sequences are limited by the small size of the fragment (around 130 base pairs), yet the *spinulosum*, *contortum* and *mangini* groups tend to be well separated in the *Blastodinium* tree (Figure 3), and each contains *Blastodinium*, many sub-clades *spinulosum*, *contortum* and *mangini* groups contain abundant rDNA sequences which are not closely related to reference sequences and most likely correspond to novel species yet to be described.

Blastodinium parasitic lifestyles unveiled by size-fractionated plankton metabarcoding

The distribution of *Blastodinium* reads amongst size fractions is consistent with the parasitic life cycle of this genus (Figure 2). Metabarcodes detected in the *piconano*- and *nano*-plankton correspond to the free-living stage, as the size of dinospores (the dispersive stage) is usually between 5 and 20 µm (Skovgaard *et al.*, 2007). This is confirmed by the fact that rDNA reads belonging to *Azadinium* genus, which are non-parasitic dinoflagellate cells with the same size as *Blastodinium* dinospores (Tillmann *et al.*, 2010), are mainly present in the

piconano- and *nano*-plankton samples. The *micro*-plankton samples are particularly rich in copepod reads, yet the number of *Blastodinium* reads found in these samples is relatively low. A significant fraction of copepod rDNA reads in this size fraction may thus correspond to eggs and nauplii, life stages that precede the copepodite, which is the stage hypothesized to be infected by *Blastodinium* (Alves-de-Souza *et al.*, 2011). The copepodites and adults of small Cyclopoida copepods like *Oithona spp.* and *Oncaeae spp.*, which could be found in the *micro*-plankton (Gallienne and Robins, 2001), should represent only a small proportion of total copepod life cycle stages smaller than 200 µm.

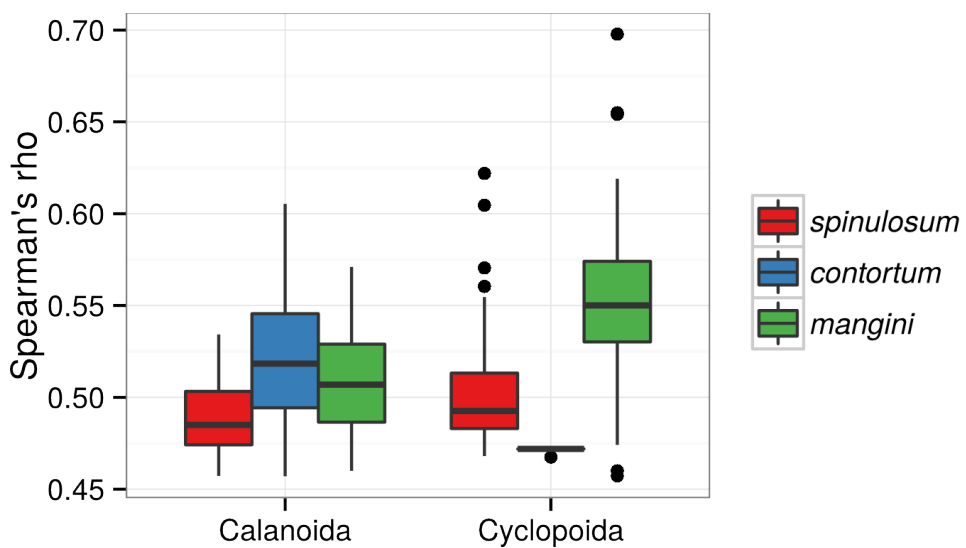


Figure 5: Boxplots of Spearman's rho resulting from comparisons between copepod and *Blastodinium* metabarcode abundance data. Values are aggregated by copepod orders, i.e. Cyclopoida (including Poecilostomatoida), Calanoida, and *Blastodinium* groups, i.e. *spinulosum*, *contortum* and *mangini*.

In contrast to the drop in abundance of *Azadinium* and *Alexandrium* dinoflagellates in the *meso*-plankton (180 - 200 µm; Figure 2), the relatively abundant and re-increasing number of *Blastodinium* rDNA observed in this size fraction should correspond to well-developed trophonts composed by several hundred cells infecting adult copepods. Strikingly, different patterns of size fraction distribution emerge between the three *Blastodinium* groups. Most metabarcodes belonging to the *spinulosum* group are relatively more abundant in the *nano*-plankton (Figures 2B and 3), suggesting that the life cycle of these group members might differ from the other *Blastodinium* groups, with putatively longer free living stages and/or trophonts constituted by fewer cells. Alternatively, the *spinulosum* trophonts may infect hosts from larger plankton size fractions not analysed herein. *Spinulosum* dinospores appear to be larger compared to other *Blastodinium* dinospores, as they are almost exclusively found in the *nano*-plankton, whereas other *contortum* and *mangini* dinospores have similar abundances in *piconano* and *nano*-plankton (Figure 2B).

First insights into the complexity of *Blastodinium*-copepod interactions using metabarcodes co-occurrence analysis

Overall, a relatively low proportion of copepod metabarcodes (6%) are associated with *Blastodinium* metabarcodes, and potential hosts were found for only the half of the tested *Blastodinium* metabarcodes. Several *Blastodinium* species are known to be able to infect more than one species of copepod, and one species of copepod can be infected by several species of *Blastodinium* (Chatton, 1920). In this context, the abundance of one partner may not be explicable only by the abundance of the other. In our study, the relatively limited number of samples across time and space allow detection of only the strongest and more permanent interactions, between the most widespread copepods and *Blastodinium* taxa.

The *Blastodinium* species from the *mangini* group have been mainly described infecting copepods from the Cyclopoida order (with the exception of *B. galatheanum* infecting *Acartia spp.* (Skovgaard and Salomonsen, 2009)) whereas the *Blastodinium* species from the *spinulosum* and *contortum* groups have been exclusively described infecting copepods belonging to the Calanoida order. Comparisons between *Blastodinium* and copepod metabarcode abundances lead to the same broad picture for the *contortum* and *mangini* groups, especially when considering scores of association (Spearman's rho) (Figure 6). However, metabarcodes from the *spinulosum* group are weakly associated with both Calanoida and Cyclopoida, which is not consistent with previous observations (Chatton, 1920; Skovgaard *et al.*, 2012). Distribution among size fractions suggests that *Blastodinium* from the *spinulosum* group could live longer as dinospore and/or live in the host for less time compared to other *Blastodinium* species. This is consistent with the lower association scores of the *spinulosum* group with both the Calanoida and Cyclopoida copepods, as we would expect a lower probability to find both partners (*Blastodinium*/copepod) at the same time.

A

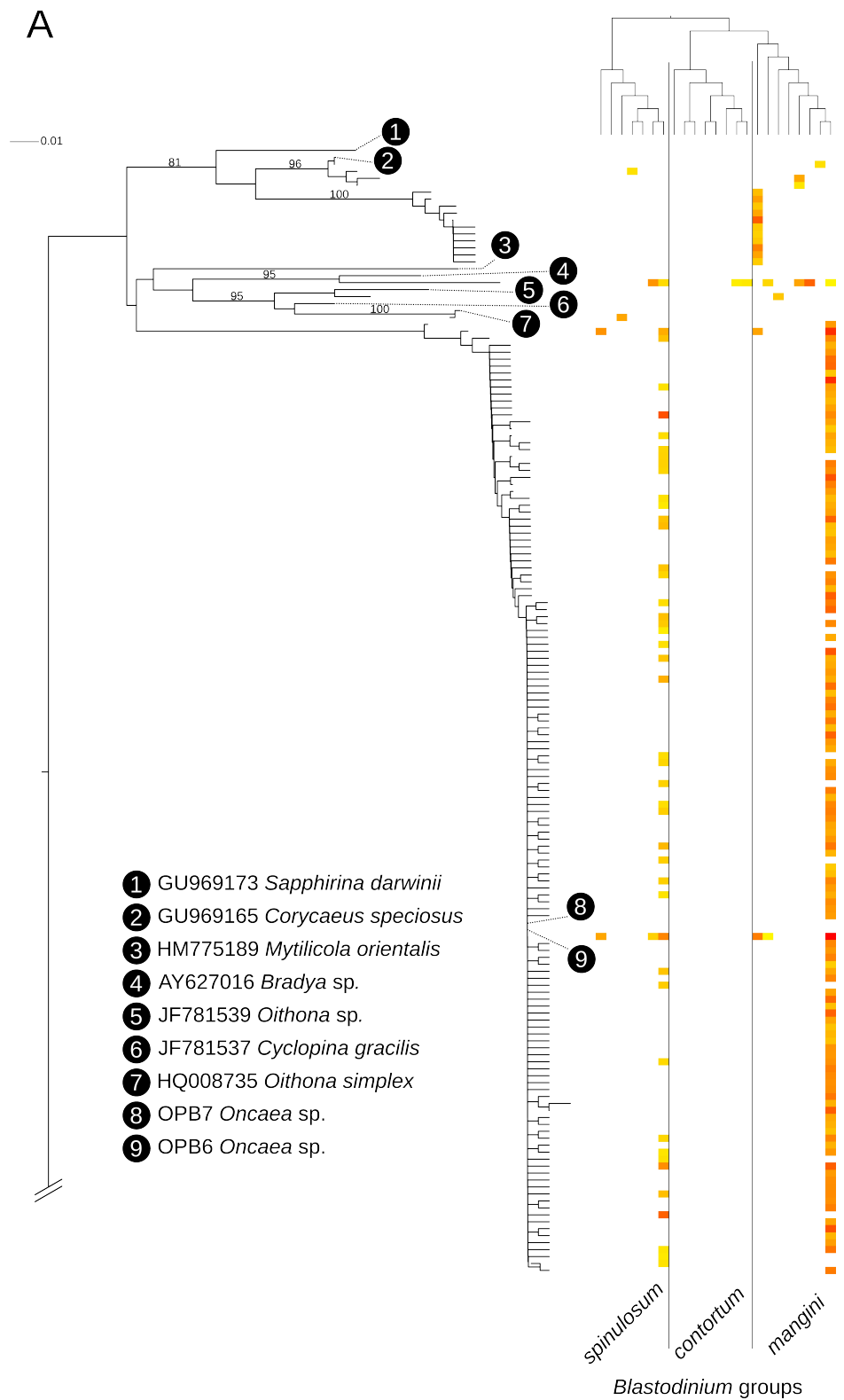
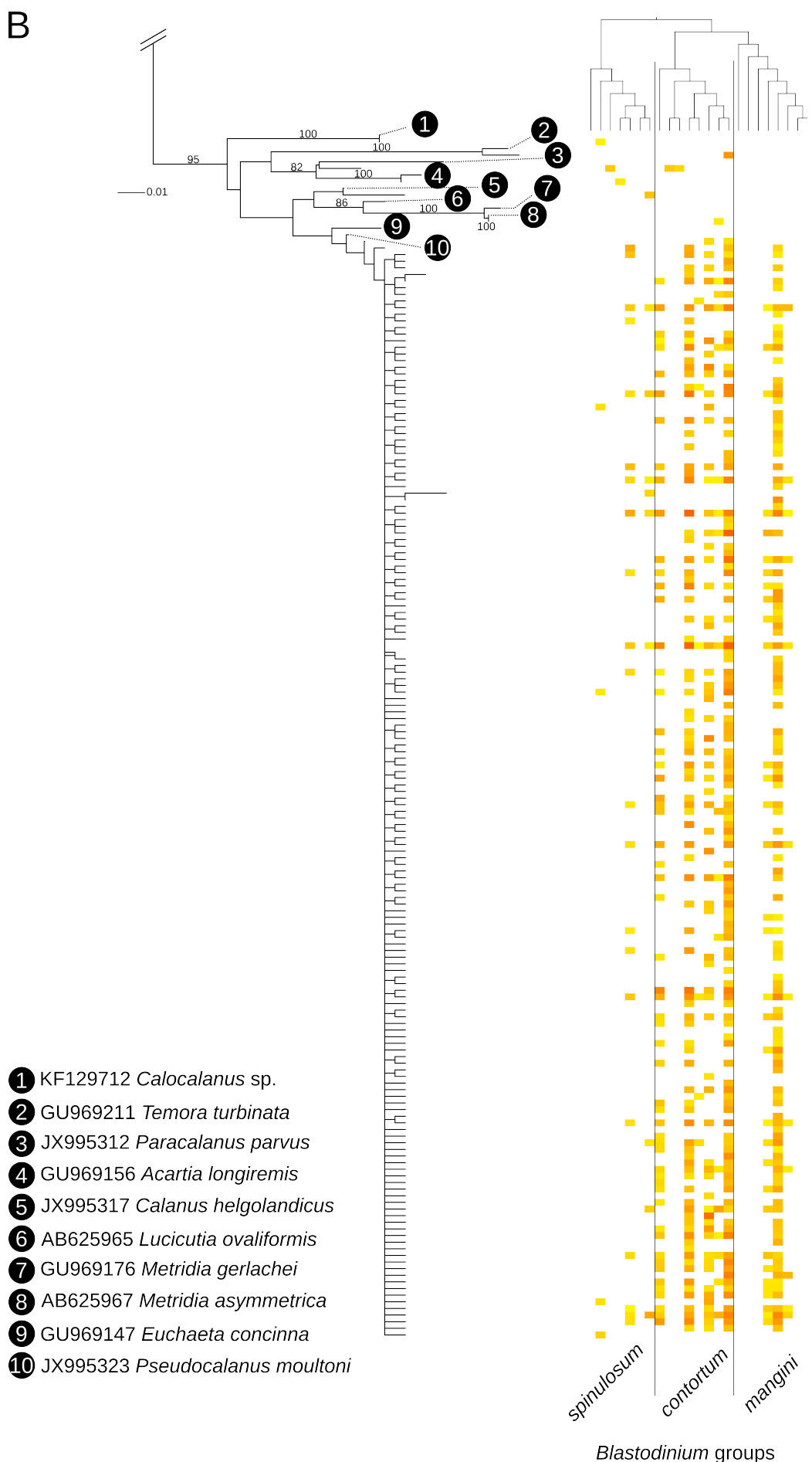


Figure 6: Phylogenetic tree (Neighbor-joining) of copepod metabarcodes for which at least one significant association has been found with one of the *Blastodinium* metabarcodes (represented by the small neighbor-joining phylogenetic tree on the top right corner). Numbers are bootstrap values; only values above 80% are shown. Labels at branches indicate GenBank accession numbers (except OPB6 (Figure S1) and OPB7 (Figure S2), see *supplementary information*) with species names for the reference sequences. The color gradient from yellow (0.45) to red (0.7) indicates Spearman's rho values for associations between copepod and *Blastodinium* metabarcodes. (A) The part of the phylogenetic tree containing copepod metabarcodes assigned to the orders Cyclopoida (including Poecilostomatoida) and Harpacticoida (*Bradya* sp.). (B) The part of the phylogenetic tree containing copepod metabarcodes assigned to the order Calanoida.



Conclusion

We show the power of extensive metabarcoding to explore symbiotic interactions in the plankton. In the plankton, symbiotic protists are generally 10 to 100 times smaller than their hosts (Decelle *et al.*, 2012; Siano *et al.*, 2010; Chambouvet *et al.*, 2008). Metabarcoding on carefully fractionated seawater samples can therefore distinguish free-living stages from symbiotic ones. In the context of time series, the study of parasites in several size fractions would permit a better understanding of infection dynamics. More generally, the distribution of metabarcodes across size fractions provides clues about the life-style and could help to investigate ecological role of organisms only known from environmental sequences. The increase of spatio-temporal sampling and the development of methods to compare abundances of hosts and symbionts, *sensu lato*, across their phylogenetic specificity ranges, will dramatically increase the power of rDNA metabarcoding to unveil new interactions and to assess their ecology.

Acknowledgments

This work was supported by the project OCEANOMICS, that has received funding from the French government, managed by the Agence Nationale de la Recherche, under the grant agreement “Investissement d’Avenir” ANR-11-BTBR-0008. We also thank the coordinators and members of the *Tara* Oceans expedition and Jean-Louis Jamet for the identification of the copepods.

References

- ALVES-DE-SOUZA, Catharina, CORNET, Cindy, NOWACZYK, Antoine, *et al.* *Blastodinium* spp. infect copepods in the ultra-oligotrophic marine waters of the Mediterranean Sea. *Biogeosciences*, 2011, vol. 8, no 8, p. 2125-2136.
- ALVES-DE-SOUZA, Catharina, VARELA, Daniel, IRIARTE, José Luis, *et al.* Infection dynamics of Amoebophryidae parasitoids on harmful dinoflagellates in a southern Chilean fjord dominated by diatoms. *Aquatic Microbial Ecology*, 2012, vol. 66, no 2, p. 183.
- APSTEIN, Carl, Parasiten von *Calanus finmarchicus*. Wissenschaftliche Meeresuntersuchungen. Abt. Kiel., 1911, vol. 13, p. 205-223.
- BALECH, Enrique. *The genus Alexandrium Halim (Dinoflagellata)*. Sherkin Island marine station, 1995.

- BENJAMINI, Yoav et HOCHBERG, Yosef. Controlling the false discovery rate: a practical and powerful approach to multiple testing. *Journal of the Royal Statistical Society. Series B (Methodological)*, 1995, p. 289-300.
- BOXSHALL, Geoffrey Allan, HALSEY, Sheila H., et al. *An introduction to copepod diversity*. Ray Society, 2004.
- CACHON, Jean et CACHON, Monique. Parasitic dinoflagellates. *The biology of dinoflagellates*, 1987, vol. 21, p. 571-610.
- CHAMBOUVET, Aurelie, MORIN, Pascal, MARIE, Dominique, et al. Control of toxic marine dinoflagellate blooms by serial parasitic killers. *Science*, 2008, vol. 322, no 5905, p. 1254-1257.
- CHATTON, Édouard. Les Péridiniens parasites: Morphologie, reproduction, éthologie. *Archives de zoologie expérimentale et générale*, 1920, vol 59, p. 1–475.
- CHATTON, Édouard. Les Blastodinides, ordre nouveaux de Dinoflagellés parasites. *Comptes Rendus de l'Académie des Sciences*, 1906, vol 144, p. 981–983.
- DE VARGAS, Colomban, AUDIC, Stéphane, HENRY, Nicolas, et al. Eukaryotic plankton diversity in the sunlit ocean. *Science*, 2015, vol. 348, no 6237, p. 1261605.
- DECELLE, Johan, PROBERT, Ian, BITTNER, Lucie, et al. An original mode of symbiosis in open ocean plankton. *Proceedings of the National Academy of Sciences*, 2012, vol. 109, no 44, p. 18000-18005.
- EDGAR, Robert C. MUSCLE: multiple sequence alignment with high accuracy and high throughput. *Nucleic acids research*, 2004, vol. 32, no 5, p. 1792-1797.
- FAUST, Karoline, SATHIRAPONGSASUTI, J. Fah, IZARD, Jacques, et al. Microbial co-occurrence relationships in the human microbiome. *PLoS Computational Biology*, 2012, vol. 8, no 7, p. e1002606-e1002606.
- FIELDS, D. M., RUNGE, J. A., THOMPSON, C., et al. Infection of the planktonic copepod *Calanus finmarchicus* by the parasitic dinoflagellate, *Blastodinium spp*: effects on grazing, respiration, fecundity and fecal pellet production. *Journal of Plankton Research*, 2015, vol. 37, no 1, p. 211-220.
- FIGUEROA, Rosa Isabel, GARCÉS, Esther, MASSANA, Ramon, et al. Description, host-specificity, and strain selectivity of the dinoflagellate parasite *Parvilucifera sinerae* sp. nov. (Perkinsozoa). *Protist*, 2008, vol. 159, no 4, p. 563-578.

- GALLIENNE, Chris P. et ROBINS, David B. Is *Oithona* the most important copepod in the world's oceans?. *Journal of Plankton Research*, 2001, vol. 23, no 12, p. 1421-1432.
- GASCUEL, Olivier. BIONJ: an improved version of the NJ algorithm based on a simple model of sequence data. *Molecular biology and evolution*, 1997, vol. 14, no 7, p. 685-695.
- GOUY, Manolo, GUINDON, Stephane, et GASCUEL, Olivier. SeaView version 4: a multiplatform graphical user interface for sequence alignment and phylogenetic tree building. *Molecular biology and evolution*, 2010, vol. 27, no 2, p. 221-224.
- GUILLOU, Laure, VIPREY, Manon, CHAMBOUVET, A., et al. Widespread occurrence and genetic diversity of marine parasitoids belonging to Syndiniales (Alveolata). *Environmental Microbiology*, 2008, vol. 10, no 12, p. 3349-3365.
- GUO, Zhiling, LIU, Sheng, HU, Simin, et al. Prevalent ciliate symbiosis on copepods: high genetic diversity and wide distribution detected using small subunit ribosomal RNA gene. *PloS one*, 2012, vol. 7, no 9, p. e44847.
- KARSENTI, Eric, ACINAS, Silvia G., BORK, Peer, et al. A holistic approach to marine ecosystems biology. *PLoS biology*, 2011, vol. 9, no 10, p. e1001177.
- KÜHN, Stefanie, MEDLIN, Linda, et ELLER, Gundula. Phylogenetic position of the parasitoid nanoflagellate *Pirsonia* inferred from nuclear-encoded small subunit ribosomal DNA and a description of *Pseudopirsonia* n. gen. and *Pseudopirsonia mucosa* (Drebes) comb. nov. *Protist*, 2004, vol. 155, no 2, p. 143-156.
- LEGENDRE, Pierre et LEGENDRE, Louis. *Numerical Ecology*. Elsevier, 2012.
- LETUNIC, Ivica et BORK, Peer. Interactive Tree Of Life v2: online annotation and display of phylogenetic trees made easy. *Nucleic acids research*, 2011, p. gkr201.
- LIMA-MENDEZ, Gipsi, FAUST, Karoline, HENRY, Nicolas, et al. Determinants of community structure in the global plankton interactome. *Science*, 2015, vol. 348, no 6237, p. 1262073.
- PESANT, Stéphane, NOT, Fabrice, PICHERAL, Marc, et al. Open science resources for the discovery and analysis of Tara Oceans data. *Scientific Data*, 2015, vol. 2.
- POULIN, Robert. Network analysis shining light on parasite ecology and diversity. *Trends in parasitology*, 2010, vol. 26, no 10, p. 492-498.
- RAZOULS, Claude, DE BOVÉE, Francis, KOUWENBERG, Juliana, et al. Diversity and geographic distribution of marine planktonic copepods. Available from WWW:<<http://copepodes.obs-banyuls.fr/en>>[cited 2015-10-01], 2005-2015.

- SAIZ, Enric et CALBET, Albert. Copepod feeding in the ocean: scaling patterns, composition of their diet and the bias of estimates due to microzooplankton grazing during incubations. *Hydrobiologia*, 2011, vol. 666, no 1, p. 181-196.
- SCHMINKE, Horst Kurt. Entomology for the copepodologist. *Journal of Plankton Research*, 2007, vol. 29, no suppl 1, p. i149-i162.
- SIANO, Raffaele, MONTRESOR, Marina, PROBERT, Ian, *et al.* *Pelagodinium* gen. nov. and *P. bēii* comb. nov., a dinoflagellate symbiont of planktonic foraminifera. *Protist*, 2010, vol. 161, no 3, p. 385-399.
- SKOVGAARD, Alf, KARPOV, Sergey A., et GUILLOU, Laure. The parasitic dinoflagellates *Blastodinium* spp. inhabiting the gut of marine, planktonic copepods: morphology, ecology, and unrecognized species diversity. *Frontiers in microbiology*, 2012, vol. 3.
- SKOVGAARD, Alf, MASSANA, Ramon, SAIZ, Enric, *et al.* Parasitic species of the Genus *Blastodinium* (Blastodiniphyceae) are Peridinoid Dinoflagellates. *Journal of Phycology*, 2007, vol. 43, no 3, p. 553-560.
- SKOVGAARD, Alf et SALOMONSEN, Xenia M. *Blastodinium galatheanum* sp. nov. (Dinophyceae) a parasite of the planktonic copepod *Acartia negligens* (Crustacea, Calanoida) in the central Atlantic Ocean. *European Journal of Phycology*, 2009, vol. 44, no 3, p. 425-438.
- SMETACEK, Victor. Making sense of ocean biota: How evolution and biodiversity of land organisms differ from that of the plankton. *Journal of biosciences*, 2012, vol. 37, no 4, p. 589-607.
- SUNAGAWA, Shinichi, COELHO, Luis Pedro, CHAFFRON, Samuel, *et al.* Structure and function of the global ocean microbiome. *Science*, 2015, vol. 348, no 6237, p. 1261359.
- TILLMANN, Urban, ELBRÄCHTER, Malte, JOHN, Uwe, *et al.* *Azadinium obesum* (Dinophyceae), a new nontoxic species in the genus that can produce azaspiracid toxins. *Phycologia*, 2010, vol. 49, no 2, p. 169-182.
- TILLMANN, Urban, ELBRÄCHTER, Malte, KROCK, Bernd, *et al.* *Azadinium spinosum* gen. et sp. nov.(Dinophyceae) identified as a primary producer of azaspiracid toxins. *European Journal of Phycology*, 2009, vol. 44, no 1, p. 63-79.

Supplementary information

Copepod reference sequences OPB6 and OPB7

Two copepod specimens have been isolated from samples collected in the roadstead of Brest (France) with a plankton net (20µm mesh size) in September 2014. Prior to imaging, specimens were rinsed with artificial seawater, then DNA and membrane structures were stained for 60 minutes with 10µM Hoechst 33342 and 1.4µM DiOC6(3) (Life Technologies). Microscopy was conducted using a Leica SP5 (Leica Microsystems) confocal laser scanning microscope and a HC PL FLUOTAR 10x 0.3 DRY . The DiOC6 signal (ex488nm/em500-520nm) followed by the Hoechst signal (ex405 nm/em420-470nm).

Specimens were individually rinsed in filtered seawater, and stored at -20°C in absolute ethanol. DNA was extracted with MasterPure™ DNA/RNA purification kit (Epicenter) and PCR amplified using a specific forward primer (Cope18S1) and an universal-eukaryote reverse primer (Cope18S1: 5'-CGAAAGTTAGAGGYTCGAAGG-3' and reverse 1510R) from (de Vargas *et al.*, 2015). Purified amplicons were Sanger-sequenced with the ABI-PRISM Big Dye Terminator Sequencing kit (Applied Biosystems) using the 3130xl Genetic Analyzer, Applied Biosystems.

Obtained sequences are listed above:

>OPB6

```
ACCATAACATGCTGACTAGCGATCCGTAGCTGTTTCTATGTAGGCTCTACGGGAAGCTCCGGAAACCAAAGTTTGAGTT
CGGGGAAAGTATGGTCAAAGCTGAAACTAAAGGAATTGACGGAAGGGCACCAACCAGGAGTGGAGCCTCGGGCTTAATT
GACTCAACACGGGAAATCTACCAGGCCGGACACTGGAAGGATTGACAGATTGAGAGCTCTTCGATTAGTGGTGGTG
GTGCATGGCCGTTCTTAGTTGGAGTGAATTGCTGGTTAATTCCGATAACGAACGAGACTCTTCTGCTAAATAGGTTGC
CGTCTTTTGCCTAAACATTCTCTTAGAGAGACTGGCGCGCTAGCCGACGAGATTGAGCAATAACAGGTCTGTGATGC
CCTTAGATGTTCTGGGCTGCACACGCGCTACACTGAATGGATCAGCGTTTCCCTCCGAGAGGGACGGTAACCCGCTGA
ACCCCAITCGGGTAGGGATGGAGCTGCAATTATTCTCCGTGAACCAGGAATTCCAGTAAGCGCAAGTCATAAGCTTGCCTG
TGATTACGTCCCTGCCCTTGACACACCGCCCGCTGCTACTACCGATTGAACGTTTAGTGAGAAATCTGGATTCGACCTGTG
GGGTTCACTCCCACAGTGTGTCGGAGAAGTTTCAAACATTGAGCGTTAGAGGAAGTAAAGTCGAACAAGGTAGCTGTA
GGTGAACCTGCAGAAGG
```

>OPB7

```
CATGCTGACTAGCGATCCGTAGCTGTTTCTATGTAGGCTCTACGGGAAGCTCCGGAAACCAAAGTTTGAGTTCCGGGGG
AAAGTATGGTCAAAGCTGAAACTAAAGGAATTGACGGAAGGGCACCAACCAGGAGTGGAGCCTCGGGCTTAATTGACTCAA
CACGGGAAATCTCACCAGGCCGGACACTGGAAGGATTGACAGATTGAGAGCTCTTCGATTAGTGGTGGTGGTGCATG
GCCGTTCTTAGTTGGAGTGAATTGCTGGTTAATTCCGATAACGAACGAGAGCTCTTCTGCTAAATAGGTTGCCGTCTTT
TTGCGGTAAACATTCTCTTAGAGAGACTGGCGCGCTAGCCGACGAGATTGAGCAATAACAGGTCTGTGATGCCCTAGAT
GTTCTGGGCTGCACACGCGCTACACTGAATGGATCAGCGTTTCCCTCCGAGAGGGACGGTAACCCGCTGAACCCATT
```

CGTGGTAGGGATCGGAGCTGCAATTATTCTCCGTGAACCAGGAATTCCAGTAAGCGCAAGTCATAAGCTGCGTTGATTACG
TCCCTGCCCTTGACACACCGCCCCGCTGCTACTACCGATTGAACTGGAGAAATCTGGATTCGACCTCTGTGGGTTCAT
TCCCACAGTGTGTCGGAGAAGTTTCAAACATTGAGCGTTAGAGGAAGTAAAGTCGAACAAGGTAGCTGTAGGTGAAC
GCAGAAGG

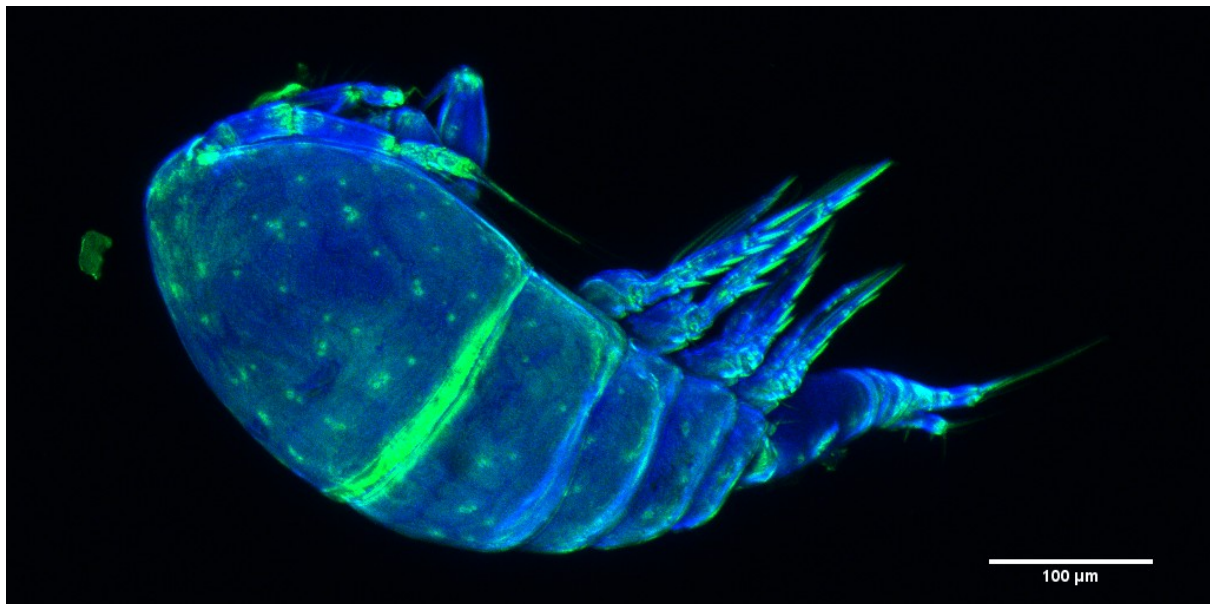


Figure S1: OPB6 specimen identified as *Oncaea* sp.

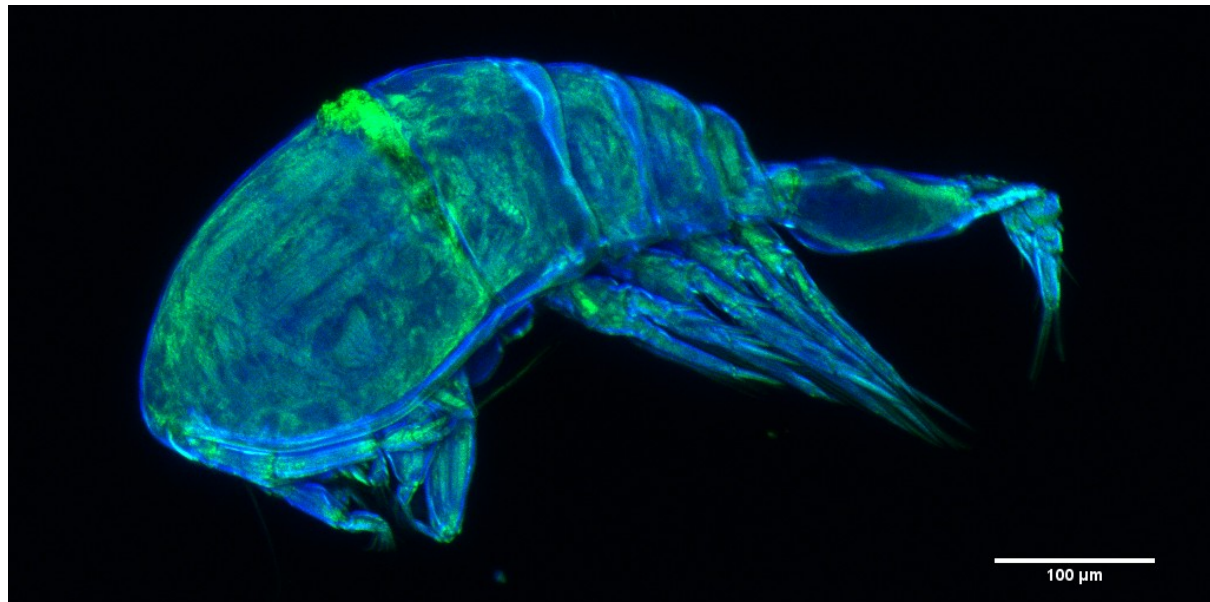


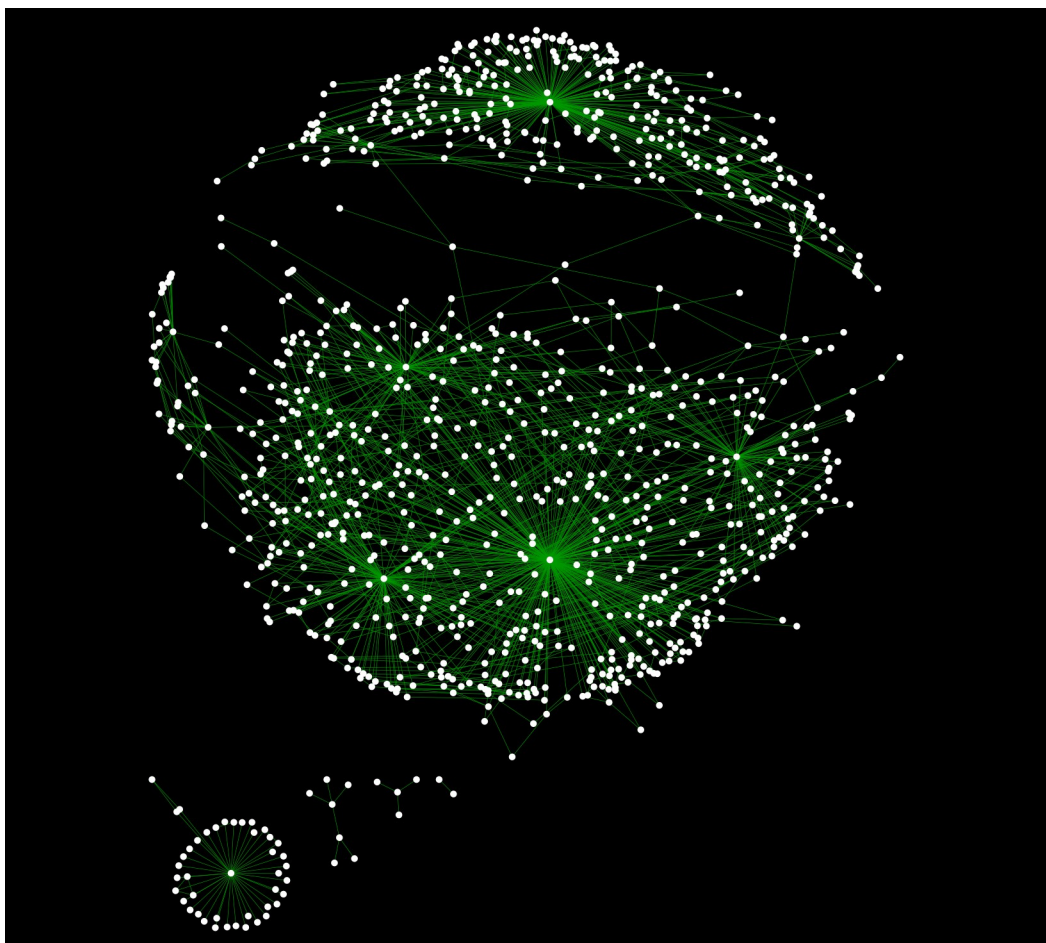
Figure S2: OPB7 specimen identified as *Oncaea* sp.

Bibliography from the Supplementary information

DE VARGAS, Colomban, AUDIC, Stéphane, HENRY, Nicolas, *et al.* Eukaryotic plankton diversity in the sunlit ocean. *Science*, 2015, vol. 348, no 6237, p. 1261605.

Chapitre III

Détection des symbioses eucaryotes planctoniques



Réseau d'haplotypes des metabarcodes *Tara Oceans* assignés au genre *Symbiodinium*.

Nous avons vu dans le premier chapitre que des réseaux de cooccurrences inférés à partir de données de metabarcoding permettaient de retrouver des interactions symbiotiques. Cependant, en l'état actuel des choses, le principal moyen à disposition pour différencier les associations statistiques correspondant à des interactions symbiotiques de celles correspondant à d'autres interactions biotiques est l'étude méticuleuse de l'assignation taxinomique des metabarcodes associés. Cette manière de procéder atteint très vite ses limites, étant donné que, dans le cadre des données de metabarcoding de *Tara Oceans*, moins de 1 % des metabarcodes sont identiques à des séquences de référence. Qui plus est, elle est chronophage et nécessite les compétences de spécialistes. L'étude de l'écologie du parasite *Blastodinium* au travers des données de metabarcoding nous montre qu'il est abondant dans les fractions qui correspondent à la taille de sa phase de dispersion mais également dans celle correspondant à sa phase parasitaire, alors que les organismes non symbiotiques étudiés (*Azadinium* spp., *Alexandrium* spp. et les copépodes) sont principalement retrouvés dans les fractions concordant avec leur taille d'organisme. Pour l'ensemble des metabarcodes assignés à l'ordre des Péridiniales (Figure 3), cette différence entre organismes symbiotiques (*Brandtодinium nutricula* et *Blastodinium* spp.) et organismes non symbiotiques (*Protoperidinium* spp. et *Scrippsiella* spp) est également observée.

Si l'on considère cette particularité comme étant commune à tous les symbiotes (non hôtes) du plancton, il est alors possible de distinguer les metabarcodes correspondant à des espèces symbiotiques des autres metabarcodes. En ne conservant que les associations comprenant un metabarcode considéré comme potentiellement symbiotique compte tenu de son abondance parmi les fractions de taille, la proportion d'associations correspondant réellement à une interaction symbiotique devrait être grandement augmentée. Ainsi on pourra accorder plus de confiance à ces associations statistiques, moins nombreuses, et entreprendre avec un taux de réussite potentiellement plus élevé la recherche de ces symbioses dans les échantillons biologiques.

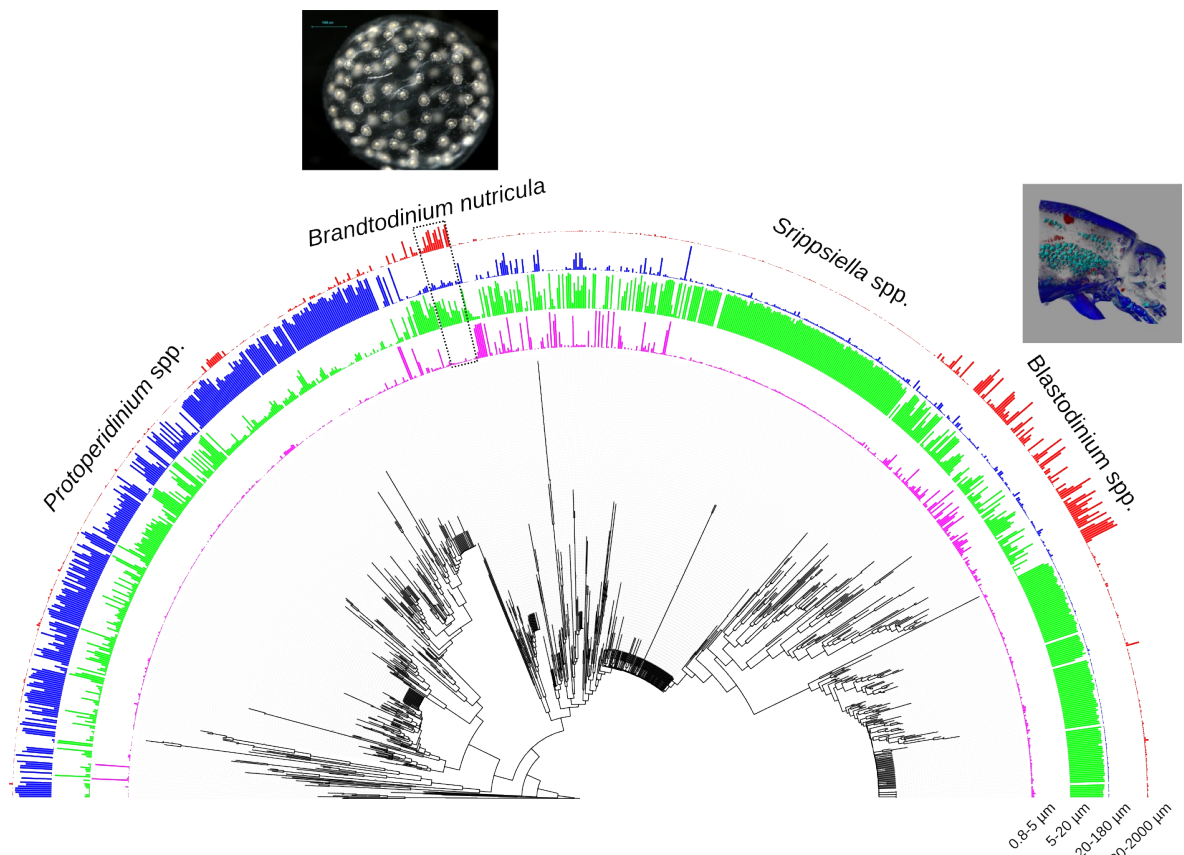


Figure 3: Arbre phylogénétique (Neighbor-joining) des metabarcodes (fragment V9) assignés aux Pérnidinales (Dinoflagellés) et représentés par plus de 300 lectures dans les données de metabarcoding *Tara Oceans*. Pour chaque metabarcode, les barres de couleurs représentent la répartition de son abondance dans les gammes de taille 0,8-5 µm (en violet), 5-20 µm (en vert), 20-180 µm (bleu) et 180-2000 µm (rouge). La longueur des barres est proportionnelle à une valeur comprise entre 0 et 1, calculée de la façon suivante ; pour une fraction de taille donnée et pour chaque metabarcode, l'abondance moyenne du metabarcode dans cette fraction de taille est divisée par la somme des abondances moyennes de chaque fraction de taille.

L'étude de la symbiose entre *Symbiodinium* et le cilié *Tiarina* montre que chacun des deux partenaires d'une association symbiotique peut être représenté par plusieurs metabarcodes. La diversité en metabarcodes associée à chacun des partenaires peut être assimilée à la spécificité de l'interaction. En effet une interaction symbiotique peu spécifique sera caractérisée par une diversité relativement importante de metabarcode chez l'hôte et ou le symbiose. Dans cette étude, pour chacun des partenaires, les metabarcodes ont des biogéographies différentes et le score d'association (rho de Spearman) est maximal lorsque l'on compare la somme des abondances des metabarcodes séquencés. Ce score, calculé pour 47 stations, croit de $\rho=0.59$ lorsque l'on considère seulement le metabarcode le plus abondant de chacun des partenaires, à $\rho=0.77$ quand on considère l'ensemble des metabarcodes. Cette interaction n'est pas retrouvée dans l'interactome global présenté dans le premier chapitre certainement du fait des seuils de détection stricts imposés (voir méthode Lima-Mendez *et al.*

2015). Cependant, en conservant les mêmes seuils de détection, on peut imaginer retrouver cette interaction en comparant les abondances des groupes génétiques regroupant exclusivement l'ensemble de la diversité des deux partenaires. Afin d'augmenter les chances de détection de symbioses grâce à des réseaux de cooccurrences, il serait souhaitable de définir, sans a priori, des groupes génétiques regroupant exclusivement l'ensemble de la diversité de partenaires en symbiose. Mais la spécificité des symbioses dans le plancton et donc la diversité génétique des partenaires impliqués sont variables. J'ai donc décidé dans cette partie d'effectuer un partitionnement génétique des metabarcodes à différents niveaux de résolution et de prendre en compte les metabarcodes et l'ensemble des groupes génétiques ainsi construit lors des mesures d'association. La spécificité d'une interaction symbiotique pourra être estimée en considérant la paire de groupes génétiques affichant le meilleur score d'association.

Le premier article intitulé « **Unveiling photosymbiotic associations across phylogenetic gradients in world-wide marine plankton based on massive eukaryotic rDNA metabarcoding** » décrit une approche originale permettant la détection de symbioses potentielles à partir d'un jeu de données de type metabarcoding. Cette approche repose sur deux méthodes. La première, consiste en un filtre visant à éliminer les groupes génétiques de metabarcodes dont la distribution de l'abondance le long de 4 fractions de tailles adjacentes (0.8-5, 5-20, 20-180 et 180-2000 µm) ressemble aux distributions théoriques reflétant le style de vie des organismes libres. Contrairement à ceux des symbiotes, les metabarcodes d'organismes libres seraient principalement retrouvés dans la ou les fractions concordants avec leur taille d'organisme libre et significativement moins abondants dans les autres. Son principal intérêt est de réduire considérablement dans les résultats le nombre de faux positifs, c'est à dire les associations significativement positives qui ne correspondent pas à un vrai cas de symbiose. La seconde méthode développée dans cet article est la construction de groupes génétiques définis à différents niveaux de résolution. Pour ce faire, deux méthodes de partitionnement génétiques sont utilisées. La première, Swarm (Mahé et al., 2014), est utilisée avec des valeurs de seuil local de partitionnement allant de 1 et 4. La seconde, Markov Cluster Algorithm (MCL), est appliquée à chaque groupe génétique défini par Swarm avec un seuil de 1 pour deux valeurs d'inflation (1.2 et 5). Ces groupes génétiques ont pour particularité d'être imbriqués à la manière de poupées russes, et appartiennent donc tous, à l'exception de ceux construits au plus bas niveau de résolution (Swarm avec un seuil de 4), à un unique niveau génétique parent, c'est à dire définis à un niveau de résolution inférieur. La

figure 4 représente un metabarcode et les groupes génétiques à trois différents niveau de résolution qui lui sont associés, en rouge, à l'intérieur du réseau d'haplotypes construit à partir des metabarcodes assignés au genre *Symbiodinium*. Cette représentation illustre parfaitement le caractère imbriqué de ces groupes génétiques.

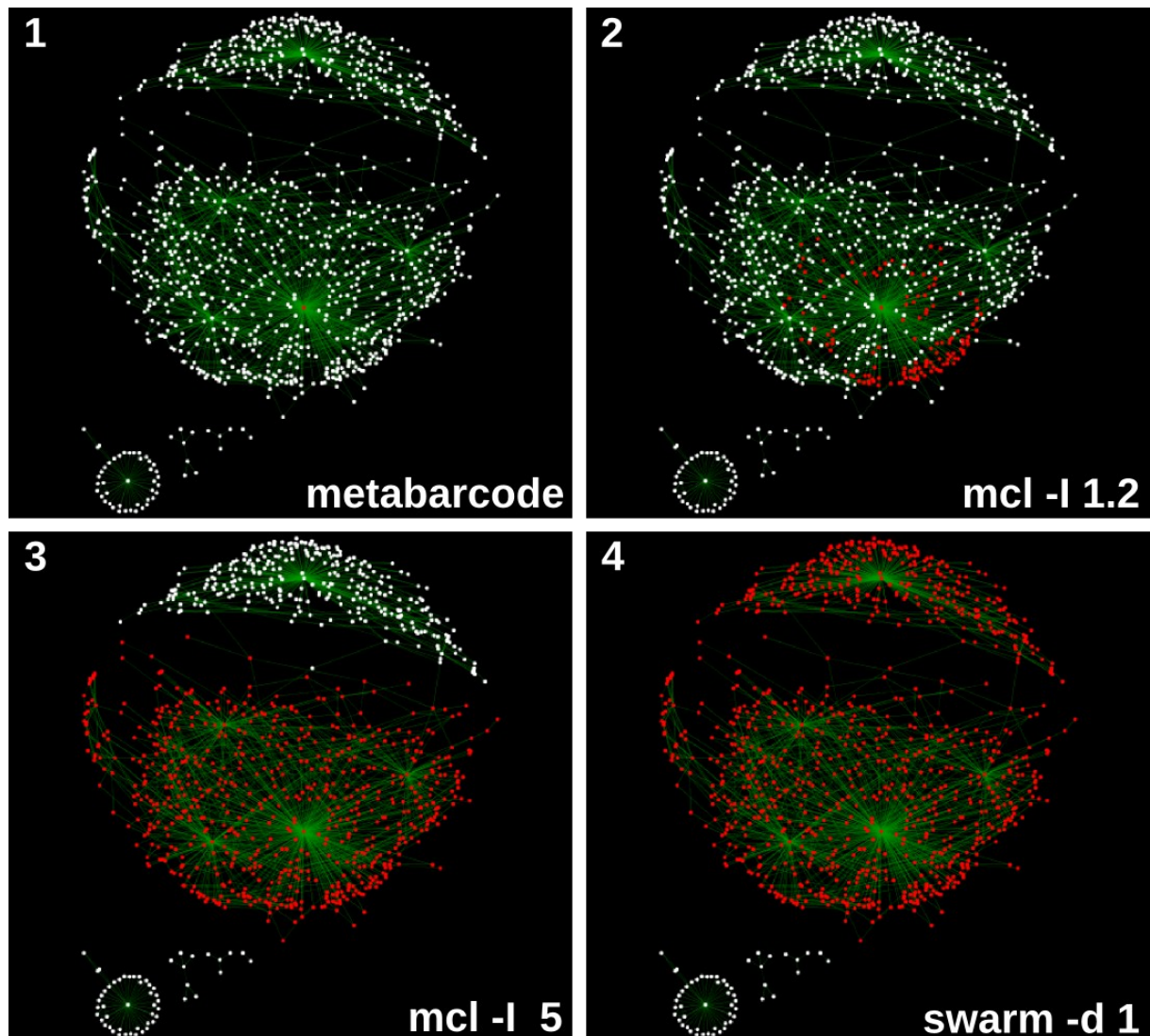


Figure 4: Réseaux d'haplotypes où les nœuds sont l'ensemble des metabarcodes (fragment V9) Tara Oceans assignés au genre *Symbiodinium*, et chaque arrête correspond à une mutation. En 1, le nœud rouge est le metabarcode le plus abondant assigné à *Symbiodinium*. En 2, 3 et 4, les groupes génétiques parents de ce metabarcode, respectivement construit avec le Markov Cluster Algorithm avec des valeurs d'inflation de 1,2 et 5 et avec Swarm avec un seuil de partitionnement local de 1, sont représentés en rouge.

Chaque metabarcode est alors affilié à une lignée de 6 groupes génétiques et l'ensemble des metabarcodes et des groupes génétiques parents rentrent en compte lors de la comparaison des abondances pour la détections d'associations significativement corrélées (ρ)

de Spearman). L'étude des scores des associations et du niveau de résolution des groupes génétiques nous renseigne alors sur la diversité génétique des hôtes et des symbiotes des symbioses potentielles détectées et donc sur leur spécificité. Dans cette article, l'approche est appliquée à la détection de photosymbioses planctoniques, c'est à dire que les abondances des groupes génétiques et metabarcodes assignés taxinomiquement à des lignées contenant des espèces ayant des chloroplastes permanents ont été comparées à celles de lignées contenant des espèces connues pour être hôtes de microalgues (les Retarias et les ciliés). La détection de photosymbioses connues de la littérature et de symbioses hautement probables à différents niveaux de spécificité soutiennent la pertinence de cette approche. Cette dernière permet également de retrouver la diversité décrite pour les deux partenaires de l'interaction entre *Symbiodinium* et *Tiarina* par Mordret *et al.* (2015) mais aussi d'identifier une nouvelle diversité de *Symbiodinium* (7 metabarcodes) impliquée dans cette symbiose.

Le second article, « **Parasites diversity and abundance in the *Tara* Oceans metabarcoding dataset challenge classic views on marine plankton ecology** » propose une vue globale de la diversité des parasites au sens large (vrais parasites et parasitoïdes) à travers l'analyse de 586 communautés planctoniques eucaryotes provenant de l'échantillonnage de 126 stations océaniques de tous les océans tropicaux à tempérés du globe. Cette étude montre, grâce à une annotation fonctionnelle des OTUs à partir de leur assignation taxinomique, que ces parasites représentent au moins 8% de la diversité totale des protistes du plancton océanique. Une part importante des OTUs (32%) n'a pas pu être assignée fonctionnellement du fait du manque de connaissances des cycles de vie de certaines lignées eucaryotes hyperdiversifiées dans le plancton, comme c'est le cas par exemple des diplonémides. L'approche présentée dans le premier article de ce chapitre a également été appliquée dans cette étude. Comme dans le cadre de l'étude des photosymbioses, elle permet de retrouver de nombreuses interactions déjà connues ce qui, une fois de plus, tend à la valider. De plus, le nombre important d'associations détectées entre les MALV-I (Syndiniales) et les acanthaires (radiolaria) suggère que les syndiniales seraient d'important régulateurs des populations d'acanthaires. Cette étude est encore préliminaire et nécessite des analyses phylogénétiques et écologiques afin d'obtenir une meilleure vision de la spécificité du parasitisme dans le plancton et définir la proportion des OTUs non assignées fonctionnellement qui pourrait être reliée à des parasites.

Unveiling photosymbiotic associations across phylogenetic gradients in world-wide marine plankton based on massive eukaryotic rDNA metabarcoding

Nicolas Henry, Johan Decelle, Daniel J. Richter, Stéphane Audic, Colomban de Vargas

EPEP - *Evolution des Protistes et des Ecosystèmes Pélagiques* - team, Sorbonne Universités, UPMC Univ Paris

06, UMR 7144, Station Biologique de Roscoff, 29680 Roscoff, France

CNRS, UMR 7144, Station Biologique de Roscoff, 29680 Roscoff, France

In preparation

Introduction

Acquisition of photosynthetic capability by the capture of endosymbiotic microalgae (photosymbiosis) or the sequestration of chloroplasts (kleptoplastidy) is a common phenomenon among phagotrophic protists in the oceanic plankton. Photosymbiosis, which tends to occur mainly in oligotrophic environments (Stoecker *et al.*, 2009; Decelle *et al.*, 2015), is thought to be mutualistic, wherein the heterotrophic host benefits from the photosynthetic products produced by one or more symbiotic microalgae, which in turn receive protection and nutrients recycled by the host (Trench, 1979; Davy *et al.*, 2012). In plankton, photosymbiosis generally involves large phagotrophic protists, such as foraminiferans and radiolarians, which host diverse microalgae like dinoflagellates (Dinophyceae), haptophytes and prasinophytes (Stoecker *et al.*, 2009). Kleptoplastidy is more common in productive ecosystems and is mainly performed by dinoflagellates and ciliates (Stoecker *et al.*, 2009). The magnitude of phototrophy acquisition by heterotrophic protists, a process whose distribution could challenge our view of planktonic ecosystem functioning, is poorly known. To fill this gap, we propose to study the diversity of the organisms implicated in this process.

Co-occurrence network-based analyses are widely used in environmental genomics (metabarcoding, metagenomics, metatranscriptomics), and can now be applied to the study of plankton community structures in the environment (Eiler *et al.*, 2012; Hunt and Ward, 2015). These methods were first used to characterize bacterial communities and were subsequently expanded to examine the other domains of life (archae, eukaryotes and viruses). In order to have a comprehensive understanding of the main factors governing the structure and function of communities, several previous efforts attempted to include genomic data from all four of

these domains to provide a global view of interactions both among and within them (Steele *et al.*, 2011; Chow *et al.*, 2014; Lima-Mendez *et al.*, 2015). Moreover, as the purpose of these methods is to detect co-occurring species, initial steps have been taken to expand them to encompass the detection of symbiosis *sensu lato*, which includes commensalism, mutualism and parasitism (de Bary, 1879; Chaffron *et al.*, 2010; Lima-Mendez *et al.*, 2015). Yet, the main challenge remains the detection of "true" symbiotic partnerships among thousands of associations that could be explained by other ecological processes (such as predation or sharing of a similar ecological niche). Validation of true partnerships may require a substantial amount of effort performed by specialists examining the taxonomic assignments of co-occurring genetic entities (by manual inspection). In addition, symbiotic relationships are very broad and occur along a continuum ranging from parasitism to mutualism without clearly delineated categories. Symbioses can be more or less specific (e.g. species-species), may change according to geography or, more generally, to environmental conditions, and can be facultative or obligate for one or the other partner (Decelle *et al.*, 2015).

One of the main difficulties in detecting photosymbiotic associations in the plankton from co-occurrence networks is the flexible specificity of these interactions (Decelle *et al.*, 2012a; Probert *et al.*, 2014). For example, in the case of the interaction between the haptophyte genus *Phaeocystis* and the Acantharia, whereas the *Phaeocystis* genus is found world-wide in association with acantharians, the identity of the symbiont species varies depending on geography (*P. cordata* in the Mediterranean Sea and *P. antarctica* in the Southern Ocean). As such, there is no specific interaction at the species level, implying that in the case of metabarcoding-based network, the metabarcodes of the host and the symbiont will not co-occur across all oceans, but will instead be restricted to a narrower geographic range. To address this problem, we developed a new method to compare the abundances of genetic entities across a phylogenetic gradient. Instead of comparing only the abundances of genetic entities resulting from one level of clustering (OTUs), as is generally done in a co-occurrence network based approach, our approach compares abundances of genetic groups formed by clustering metabarcodes at different resolution levels.

In metabarcodes generated from size-fractionated planktonic samples, planktonic organisms whose life cycles cause a significant variation in their organismal size can be detected as abundant in non-adjacent size fractions. For instance, symbionts (parasites and mutualists) involved in physical partnerships with their generally larger hosts may be found in larger size fractions than their dispersal/free-living stages would be. Therefore, it is possible

to differentiate *in hospite* and *ex hospite* stages by analyzing the data in this manner (Henry *et al.* in prep). Moreover, symbiotic organisms can be differentiated from non-symbiotic organisms based on their distribution among size fractions. The ability to distinguish symbiotic from non-symbiotic interaction patterns would greatly enhance our ability to distinguish associations which putatively involve symbionts from others in co-occurrence networks.

Here, we analysed the *Tara Oceans* metabarcoding dataset to evaluate the applicability of our method and to highlight potential new photosymbiotic interactions. We show that comparing abundances between multi-level genetic groups allows us to detect known interactions at their previously characterized level of specificity. In addition, we find many novel and highly probable associations, including a potential case of kleptoplastidy and a potential symbiosis involving environmental clades of Dinophyceae displaying characteristic symbiotic distributions amongst size fractions.

Material and methods

Data

Data used in this study are part of the *Tara Oceans* V9 metabarcoding dataset (de Vargas *et al.*, 2015; Karsenti *et al.*, 2011) extended to 126 stations. We analyze data consisting of V9 metabarcodes sequenced from 586 samples belonging to 121 stations (all oceans except the Arctic Ocean), four main organismal size fractions covering the majority of eukaryotic plankton diversity: *piconano*-plankton (0.8-5 μ m), *nano*-plankton (5-20 μ m), *micro*-plankton (20-180 μ m), and *meso*-plankton (180-2000 μ m), and 2 depths, subsurface (SUR) and Deep Chlorophyll Maximum (DCM). For a given sample and a given metabarcode, the number of reads assigned to the metabarcode divided by the total number of reads within the sample was used as a proxy for its abundance (de Vargas *et al.*, 2015).

Since the main goal of this study is the detection of photosymbioses and their specificity, we selected barcodes from the following lineages: (1) A group of putative photosymbionts (P) composed of lineages containing at least one planktonic species with permanent chloroplasts (de Vargas *et al.*, 2015), (i.e. Archaeplastida, Dinophyceae, Ochrophyta, Cryptophyta, Haptophyta, Chlorarachnea, Glaucophyta and Chromerids) and (2) a putative host group (H) composed of lineages containing species known to acquire

phototrophy through symbiosis or kleptoplastidy. We exclude Dinophyceae from the H group as some of them are known photosymbionts.

Multilevel genetic clustering

In order to investigate photosymbiotic associations across phylogenetic gradients, metabarcodes from both subsets were clustered in genetic groups with different levels of resolution. Metabarcodes were first grouped using swarm version 2.1.0 (Mahé *et al.*, 2014) with value of the local linking threshold (d) from 1 to 4 without chain-breaking. Then, each genetic group obtained using swarm with d equal to 1 (the finest level of clustering) was split in several groups using the Markov Cluster Algorithm (MCL) (Van Dongen, 2001) version 12-135 with two values of inflation (1.2 for the highest resolution and 5 for the lowest). MCL was performed on graphs in which each metabarcode represents a node and each edge represents one mutation. Genetic distance matrices used for graph construction were computed using sumatra version 1.0.10 (Mercier *et al.*, 2013). Following multilevel genetic clustering, each metabarcode (the smallest genetic entities) was associated with 6 higher-level genetic groups at decreasing levels of resolution.

Distribution profiles

The per sample abundance for each genetic group was computed by summing the abundances of its component metabarcodes that were assigned to reference sequences with a percentage of identity above 90% and present in more than 10% of *micro-* or *meso-*plankton samples. Only genetic groups present in more than 20% of *micro-* or *meso-*plankton samples were used for further analysis.

Based on the assumption that metabarcodes corresponding to free-living organisms are mainly found in the size fraction corresponding to the size of the organism itself and that the abundance of these metabarcodes should decrease progressively and significantly in both smaller and larger size fractions, it is possible to define a list of distribution profiles specific to free-living organisms (Figure 1A). In contrary to the free-living organisms, symbiont metabarcodes (parasites and mutualists) display a more particular distribution among size fractions (de Vargas *et al.*, 2015). This is the case for the parasitic genus *Blastodinium*, which infects copepods, that is mainly abundant in *piconano-* *nano-*plankton (dispersal stage) and in *meso-*plankton (infective stage) (Henry *et al.*, in prep).

We applied a filter to genetic groups from the P set in order to reduce the number of inappropriately inferred associations for non-symbiotic microalgae. To this end, for each genetic group, abundances between size fractions were compared using the Wilcoxon signed-rank test, as follows: are abundances from *piconano*-plankton significantly (p -value < 0.001) greater than abundances from *nano*-plankton? Are abundances from *nano*-plankton significantly greater than abundances from *piconano*- and *micro*-plankton? Are abundances from *micro*-plankton significantly greater than abundances from *nano*- and *meso*-plankton? And are abundances from *meso*-plankton significantly greater than abundances from *micro*-plankton? For each genetic group tested, p -values were adjusted using the False Discovery Rate (FDR) approach (Benjamini and Hochberg, 1995). Therefore, all genetic groups having a “free-living” like distribution (Figure 1A) were removed from the P group before calculating measures of association with the H group.

List of associations

Genetic group abundances were compared separately for *micro*- and *meso*-plankton samples between the P group and the H group and results for both size fractions were merged. Comparisons were conducted using Spearman's rho test after removing uninformative couples of zeros (Legendre and Legendre, 2012). The p -values were adjusted using the False Discovery Rate (FDR) approach (Benjamini and Hochberg, 1995). Only H-P pairs with a corrected p -value less than 0.001 and a Spearman's rho greater than 0.5 were considered to be associated. In order to avoid redundancy in the list of interactions, we kept only H-P pairs for which there were no other H-P pairs with a higher Spearman's rho for which both H and P belong to related genetic groups (parent, descendant or identical). In the case of phylogenetically related H-P pairs with equal Spearman's rho, the pair with the higher resolution genetic groups was kept. All metabarcodes used for abundance computation of genetic groups were considered as associated with the same partners as the genetic group to which they belonged. Circular visualizations to summarize associations were plotted using the R package circlize (Gu *et al.*, 2014).

Phylogenetic tree construction

Metabarcodes and V9 reference sequences used for phylogenetic analysis were aligned using MUSCLE v3.8.31 with default settings (Edgar, 2004). Neighbor-joining phylogenetic trees were constructed using the BioNJ algorithm (Gascuel, 1997) in Seaview (Gouy *et al.*,

2010). Observed divergences (percentage of residues differing between two sequences) were used as genetic distances and bootstrap supports were obtained from 1000 replicates. Trees containing metabarcodes and their associations were displayed using iTOL (Letunic and Bork, 2011). All other graphical visualizations and statistical analysis were performed using R (R Core Team, 2015).

Results and Discussion

Validity of filtering

Characterization of abundance distribution profiles allowed us to identify genetic groups consistent with a “free-living” lifestyle. Among 11,775 metabarcodes from the P group which appear in more than 10% of *micro-* and *meso-*plankton samples, 8,486 (72%) exclusively belong to genetic groups which have a “free-living” like distribution (Figure 1B). The highest proportions (78%) and number (8,467) of “free-living” metabarcodes are observed for Dinophyceae (both photo- and heterotrophs). Bacillariophyta, Haptophyta and undetermined Prasinophyceae Clade 7 also contain “free-living” metabarcodes but to a lower extent (1%, 17% and 50%, respectively). Very few cases of known protist/protist symbiosis involve diatoms, except as hosts of parasitoids (Scholz *et al.*, 2016) and as photosymbionts of some Dinophyceae species (Pienaar *et al.*, 2007). However, they display a very low proportion of metabarcodes with a “free-living” like distribution. Many diatom species which are able to make chains could be retained by a mesh size larger than a single individual during sampling. These diatoms would then be abundant in a broad range of size fractions, which explains why our method failed to filter them out. Moreover, the V9 metabarcode does not seem to be appropriate for resolving diatom species identity, as different diatom genera may share the same metabarcode (Figure 2A; also observed for Prymnesiophyceae). This implies that one metabarcode can reflect several species distributed across different size fractions.

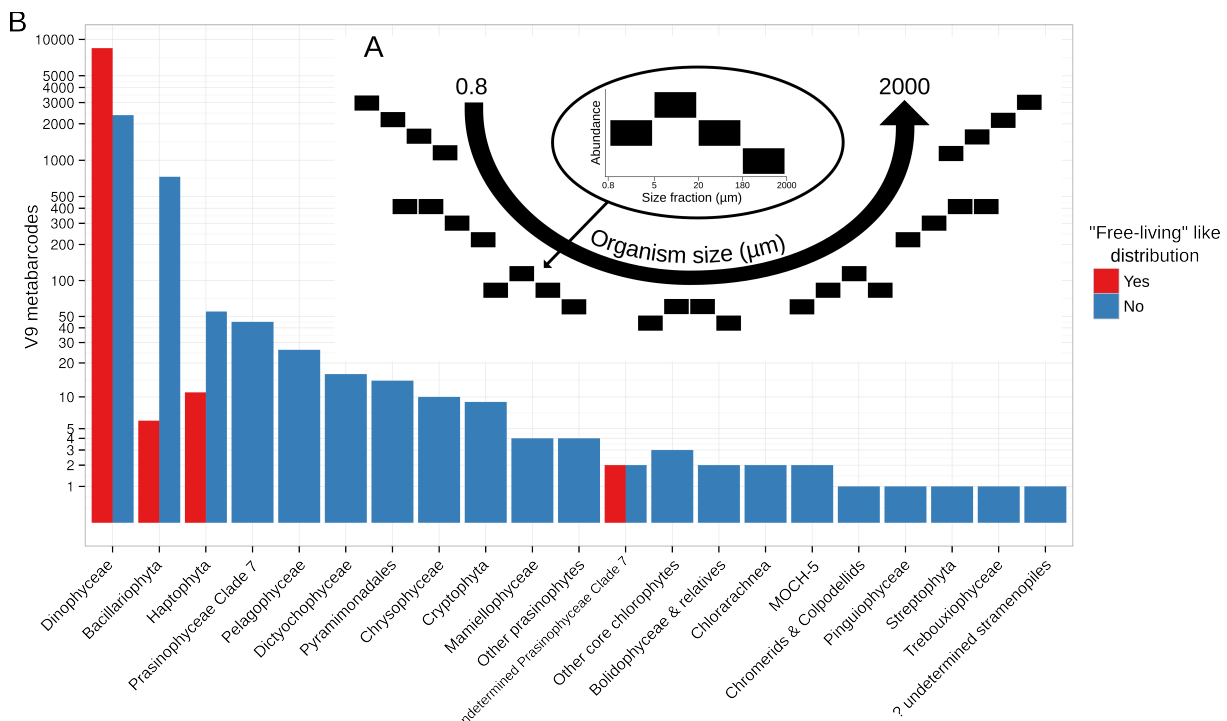


Figure 1: Size distribution profiles consistent with a “free-living” lifestyle among lineages containing species with permanent chloroplasts. **(A)** Enumeration of possible abundance distributions among size fractions for genetic groups characterized as entirely “free-living”. The list of profiles is ordered by the size of the organisms considered. Each square represents the abundance of a given genetic group in the size fraction corresponding to the position of the square along the x axis. For two adjacent squares, if one square is above the other, it indicates that its abundance is significantly higher. If both squares are at the same level, abundances are not significantly different. Each genetic group corresponding to one of these profiles is considered to be “free-living”. **(B)** Number of V9 metabarcodes present in more than 10% of micro- or meso-plankton samples assigned to a reference sequence with a percentage identity of 90% or greater and belonging to at least one genetic group present in more than 20% of micro- or meso-plankton samples. In blue, metabarcodes belonging to at least one genetic group not characterized as “free-living”. In red, metabarcodes which belong exclusively to “free-living” genetic groups.

Among Dinophyceae, the distribution of abundance profile types is not homogeneous at the order level (Figure 1C). The majority of orders contain a majority of “free-living” metabarcodes, except the Noctilucales, the Pyrocystales and the Suessiales, which display a higher proportion of non “free-living” metabarcodes (respectively 75%, 53% and 87%). The order Suessiales contains well-known symbiotic microalgal species such as *Symbiodinium* and *Pelagodinium*. Within the orders Noctilucales and Pyrocystales, there are species known to have particular life cycles (Elbrächter and Drebes, 1978; Fukuda and Endoh, 2006) alternating between large and small cells. In addition, the order Pyrocystales contains the parasitic species *Dissodinium pseudolunula*, which infects copepod eggs (Gómez *et al.*, 2009) and the species *D. elegans*, *Pyrocystis fusiformis* and *P. noctiluca* which populate the gelatinous capsule of the planktonic foraminiferan *Hastigerina pelagica* (Alldredge and Jones, 1973). The distribution of profile types is also heterogeneous at the genus level within the order

Peridiniales (Figure 1D). The genera *Scrippsiella* (which was recently separated into *Brandtodium* and *Scrippsiella*) and *Blastodinium* contain a large proportion of non “free-living” metabarcodes. Species from the genus *Blastodinium* are important parasites of copepods (Skovgaard *et al.*, 2012) and the species from the mutualistic genus *Brandtodium* have been found in association with diverse polycystine radiolarians (Probert *et al.*, 2014). Our filtering method cannot remove all free-living species, but, conversely, it is highly conservative with respect to symbiotic species, which is crucial for detection of symbiosis. Thus, the study of the distribution of metabarcodes can help to unveil the life style of organisms with metabarcodes of uncertain taxonomic affiliation.

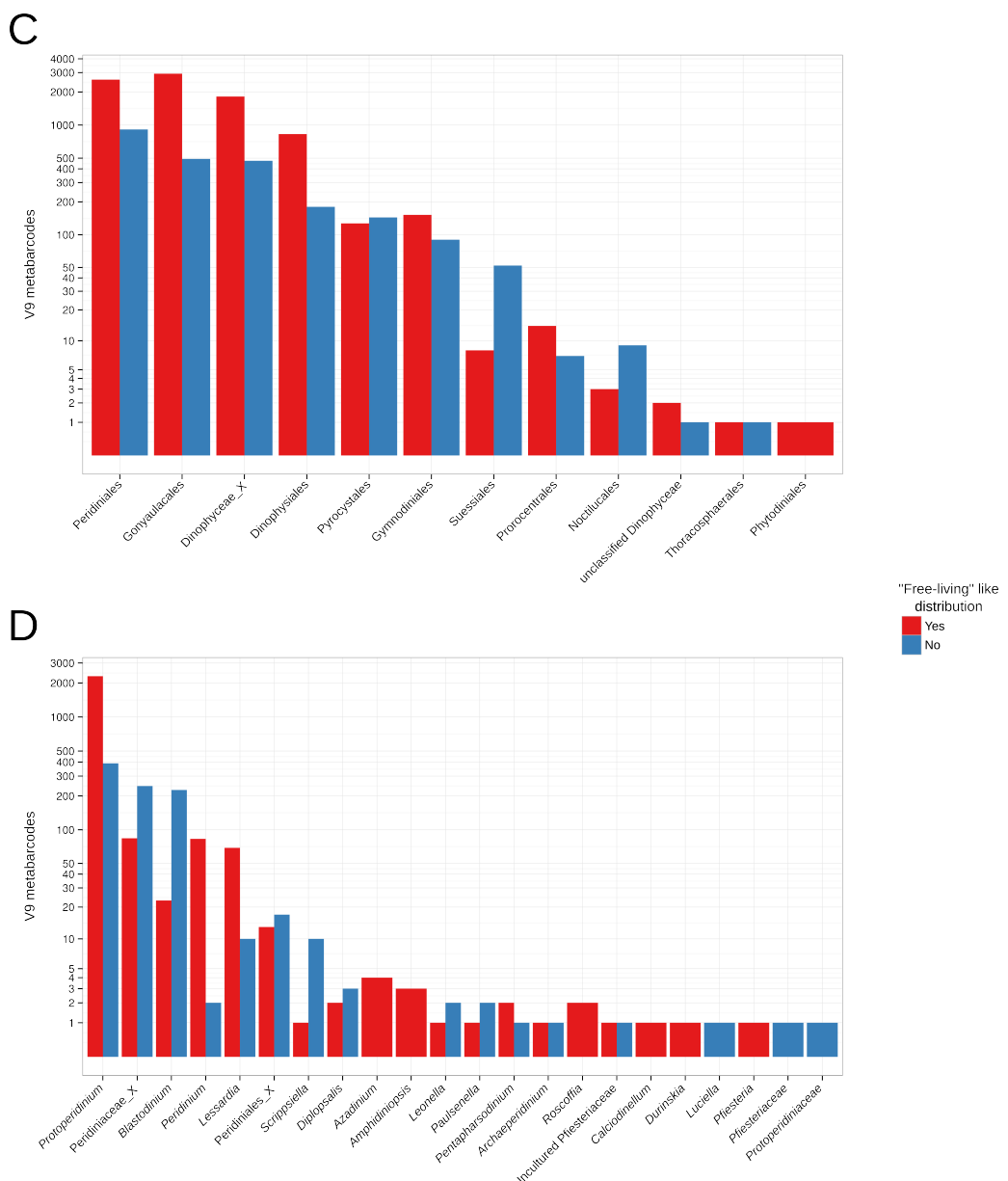


Figure 1 (continued): (C) “Free-living” like distribution among metabarcodes in the order Dinophyceae. (D) “Free-living” like distribution among Peridiniales genera metabarcodes.

Known symbionts

193 associations between 45 P and 165 H genetic groups were detected which, considering the number of individual metabarcodes constituting each genetic group, represent 3,555 interactions between 157 P and 554 H metabarcodes. Known photosymbionts from the literature (*Symbiodinium* sp., *Pelagodinium* sp. and *Gymnodinium* sp. ex *Spongotrochus glacialis*) are implicated in 39% (1,394) of the detected interactions, and involve 34% (54) of the P and 79% (438) of the H metabarcodes.

In addition, some members of Clade A within the genus *Symbiodinium* have been recently described as living in symbiosis within the ciliate *Tiarina* sp. (Protostomatea) in the oceanic plankton (Mordret *et al.*, 2015). In this study, we found that all associations involving *Symbiodinium* are with the ciliate *Tiarina* sp. (Figures 2B and 3A), suggesting that this ciliate may be the unique host of *Symbiodinium* in the plankton.

The genus *Pelagodinium*, known to be a symbiont of diverse foraminiferans and one acantharian species within clade B (Siano *et al.*, 2010; Decelle *et al.*, 2012b) was found not only to co-occur with planktonic foraminiferans related to the genera *Globigerinoides* and *Globigerinella*, but it was also found associated with *Tiarina* sp. (Protostomatea) and acantharians from the clades D, E et F (Figures 2B and 3). This may suggest these taxa share a similar ecological niche, such as the oligotrophic conditions found associated with the *Symbiodinium-Tiarina* symbiosis (Mordret *et al.*, 2015). In this case, interactions between *Pelagodinium* and acantharians within clade D (which are non symbiotic), E and F (which are symbiotic) could indicate only that they are both found in the same environment (likely an environment favorable to photosymbiosis). The *Gymnodinium* species found in association with the radiolarian *Spongotrochus glacialis* (Spumellaria (Ishitani *et al.*, 2014)) was detected here in association with collodarians, foraminiferans and acantharians but not with spumellarians (Figures 2B and 3). Further investigation is necessary to confirm the veracity of the associations we found involving *Gymnodinium* sp. ex *Spongotrochus glacialis*. As for *Pelagodinium*, these results could suggest that this symbiont establishes symbiotic relationships with several radiolarians and foraminiferans. Conversely, as also highlighted for *Pelagodinium*, these interactions could also be the result of indirect associations with environmental parameters.

A

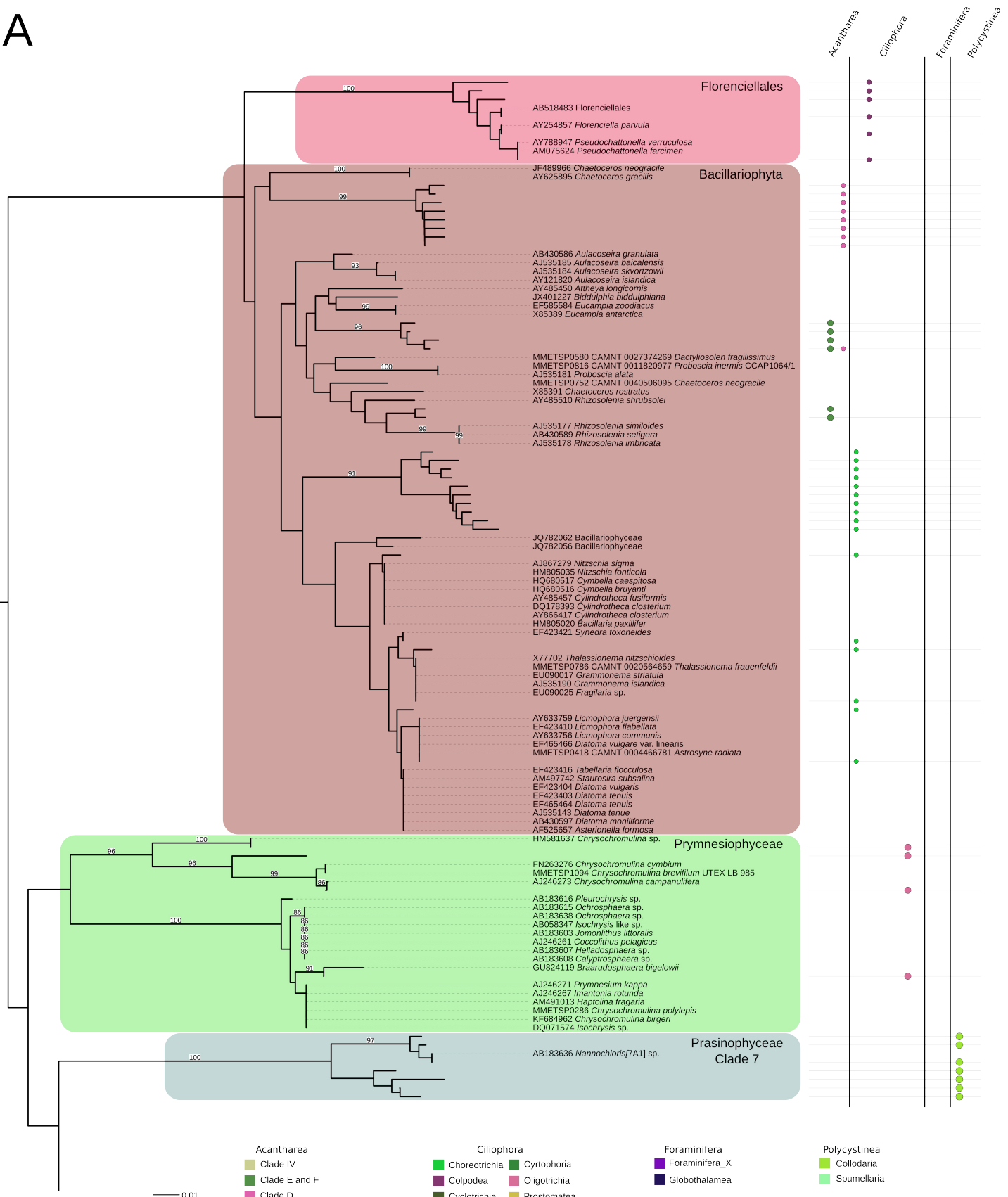


Figure 2: Neighbor-joining phylogenetic tree of photosymbiont group metabarcodes involved in at least one significant association, and related reference sequences. Numbers represent bootstrap values; values below 80% are not shown. Branch labels are GenBank accession numbers with species names. Colored circles at the leaves indicate host groups with which photosymbiont group metabarcodes are associated. The size of the circle is proportional to the number of associated host metabarcodes. **(A)** First part of the tree, containing Floreciellales, diatoms (Bacillariophyta), Prymnesiophyceae and Prasinophyceae Clade 7 metabarcodes. **(B)** Second part of the tree, containing Dinophyceae metabarcodes.

B

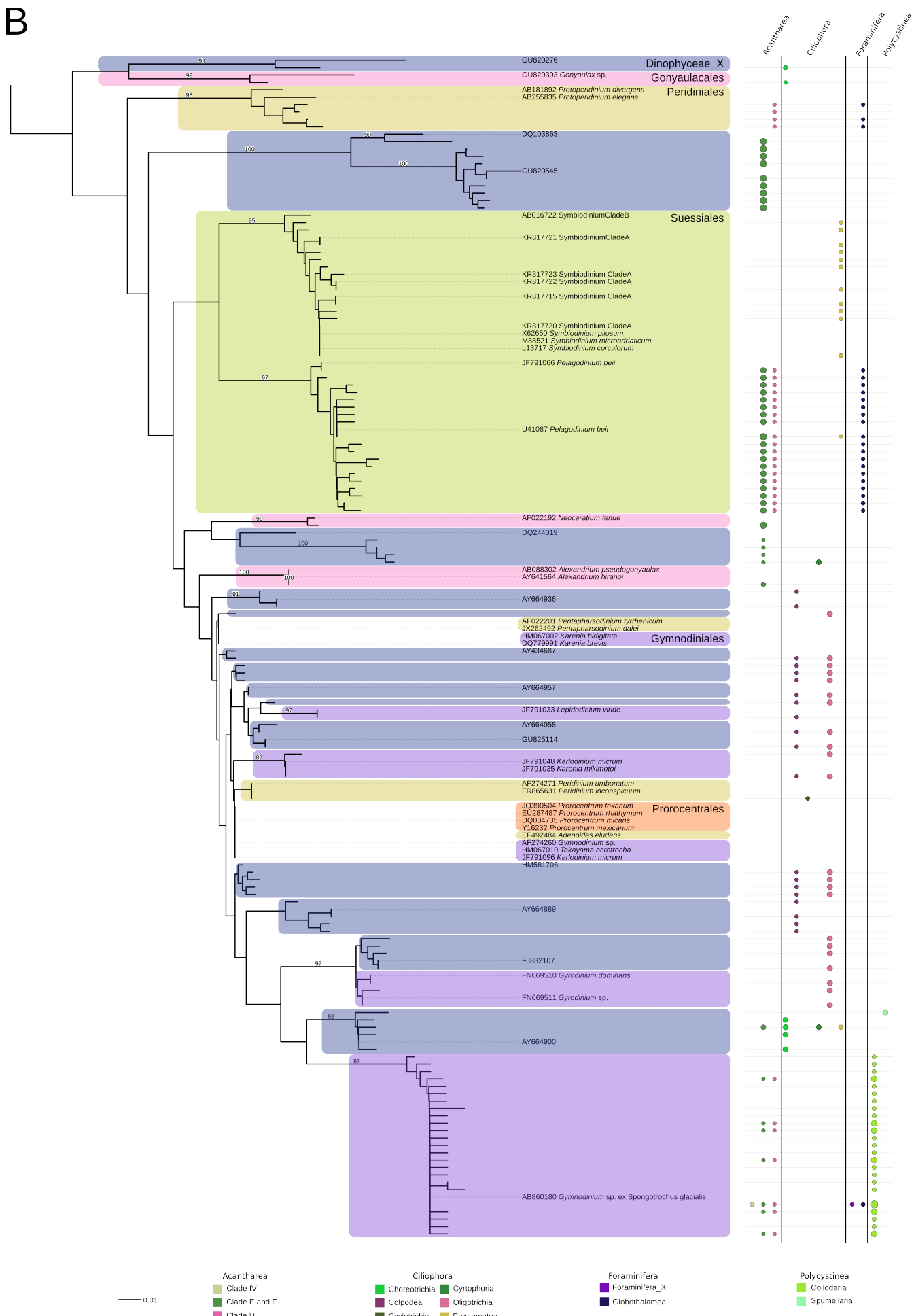


Figure 2 (continued)

The fact that we retrieved known photosymbionts with their hosts in our results, *e.g.* *Symbiodinium* clade A with *Tiarina* sp. (Mordret *et al.*, 2015) and *Pelagodinium bei*i with foraminiferans (Shaked and de Vargas, 2006; Siano *et al.*, 2010) can be considered as partially validating the method we propose. This implies that these photosymbiotic genetic groups are present at sufficient abundances in the *micro* and *meso*-plankton to be retained in our analysis and that their host-symbiont associations can be considered significant using classical statistical measures. However, known photosymbionts are also found associated with unexpected hosts. Rather than representing the discovery of new cases of photosymbiosis, these associations are likely only to reflect the difficulties in distinguishing associations resulting from both direct and indirect interactions.

The method we propose allowed us to increase the score of association (Spearman's rho) by comparing abundances at higher genetic "levels" than simply the metabarcode (level 7) (Figure 4). In the case of the association between *Tiarina* sp. and *Symbiodinium* Clade A, the best scores were obtained when comparing a level 7 (metabbarcode) H genetic group with a level 5 (MCL with inflation value 5) P genetic group (Figure 4A), which corresponds to two *Tiarina* sp. metabarcodes associated with 11 *Symbiodinium* Clade A metabarcodes. Mordret *et al.* (2015) characterized two different V9 sequences for the *Tiarina* sp. (two genotypes) host and five for the photosymbiont *Symbiodinium* Clade A. The 3 most abundant *Symbiodinium* Clade A metabarcodes, which represent 88% of the total abundance of the group, belong to the 5 *Symbiodinium* V9 sequences obtained by Mordret *et al.* (2015). The 8 remaining metabarcodes of the *Symbiodinium* Clade A genetic group could be other *Symbiodinium* genotypes that interact with *Tiarina* but which were not sampled by Mordret *et al.* (2015). This is the case for the fourth most abundant metabbarcode, which is particularly abundant in Red Sea (station 32, in yellow, Figure 4). Mordret *et al.* (2015) also characterized a specific *Symbiodinium* subclade interacting with *Tiarina* in the Red Sea (also in station 32) based on the study of its ITS2 and 28S sequences, but unfortunately the V9 sequence could not be obtained. We argue that this metabbarcode is truly in symbiosis with *Tiarina* sp. as, in this case, at least 93% of the abundance of the *Symbiodinium* group comes from metabarcodes with validated interactions with *Tiarina* sp. Thus, we detected this interaction at the right level of specificity, lending support to our approach of comparing the abundances of genetic groups defined at different levels of resolution.

A

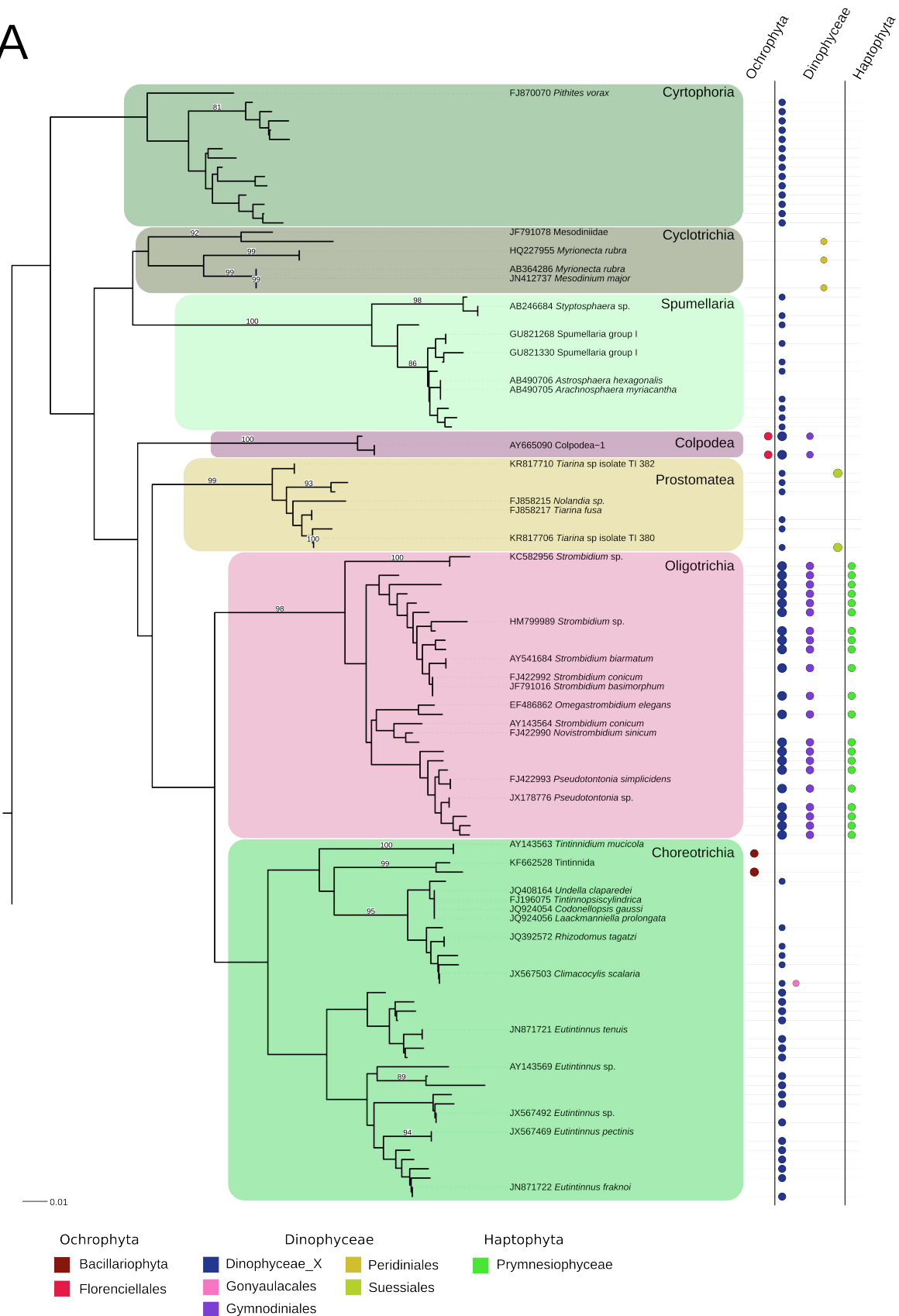
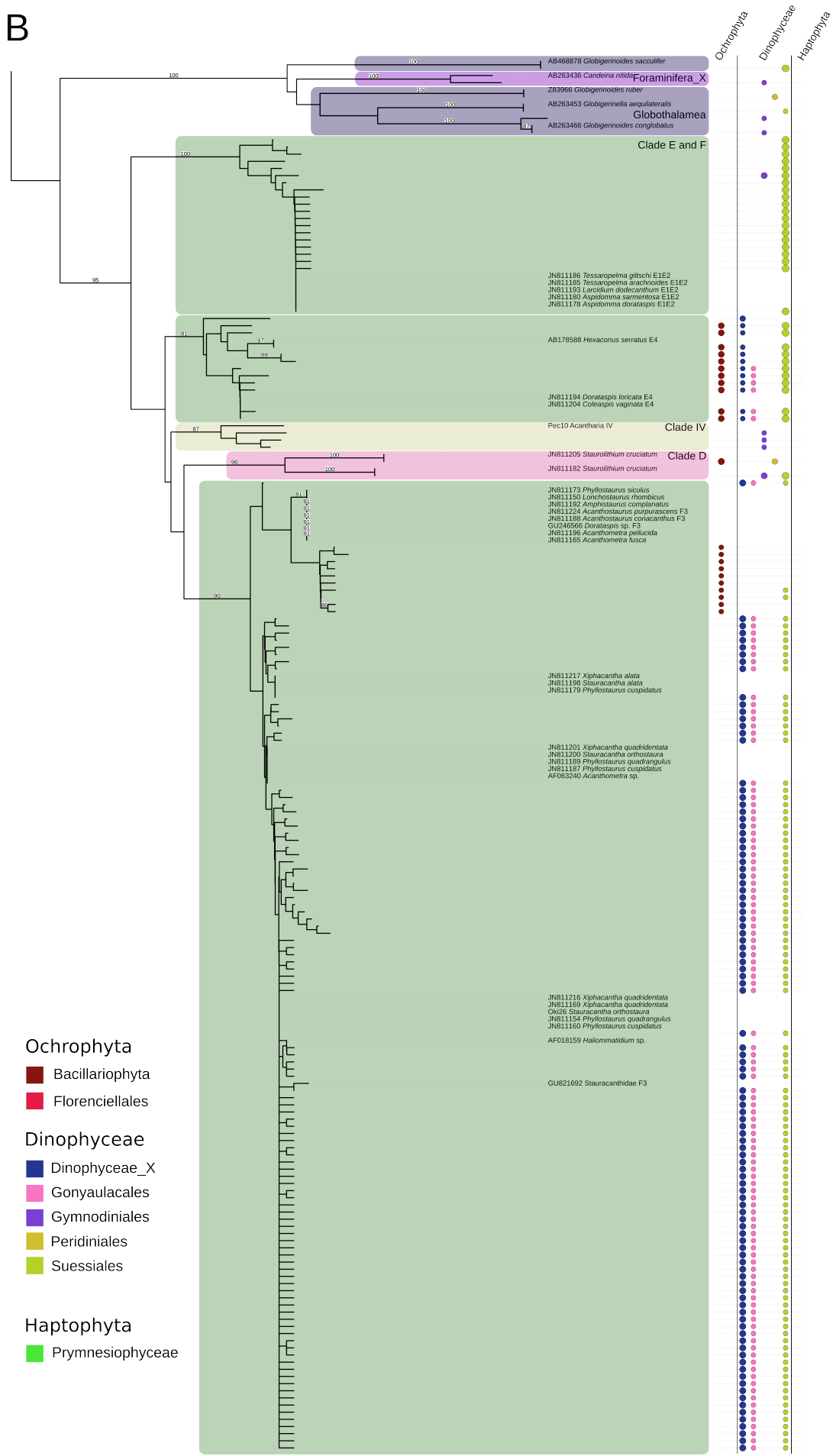


Figure 3: Neighbor-joining phylogenetic tree of host group metabarcodes (except collodarians) involved in at least one significant association, and related reference sequences. Numbers represent bootstrap values; values below 80% are not shown. Branch labels are GenBank accession numbers with species names. Colored circles at the leaves indicate photosymbiont groups with which host group metabarcodes are associated. The size of the circle is proportional to the number of associated photosymbiont metabarcodes. **(A)** First part of the tree, containing ciliate and spumellarian metabarcodes. **(B)** Second part of the tree, containing foraminiferan and acantharian metabarcodes.

B**Figure 3 (continued)**

Unfortunately, some photosymbiotic interactions with world-wide distributions do not appear in our results. This is the case for the interaction between *Brandtodium nutricula* (*Scrippsiella nutricula*), which is known to be the photosymbiont of a wide diversity of polycystines. The best score of association involving *Brandtodium* ($\rho=0.49$) is obtained comparing a *Brandtodium* level 5 genetic group (MCL with inflation value 5) with a collodarian level 2 genetic group (swarm -d 3). Whereas this level of specificity, wherein a low diversity of symbionts interacts with a high diversity of hosts, is consistent with previous observations (Probert *et al.*, 2014), this significant association ($p\text{-value} < 0.001$) was not retained by our method because its score of association (Spearman's ρ) was slightly below the threshold of 0.5. In addition, no genetic groups related to *Phaeocystis* with a non “free-living” like distribution are significantly associated ($p\text{-value} < 0.001$) to at least one genetic group from the H set, although this genus is known to occur world-wide in symbiosis with acantharians from Clade E and F (Decelle *et al.*, 2012a). The primary explanation for this observation is that *Phaeocystis* is able to form millimeters-long colonies (Chen *et al.*, 2002), and therefore its presence in larger size fractions cannot only be explained by its presence in hosts as a photosymbiont, thus preventing our abundance comparisons from capturing this interaction.

Hosts

Acantharians, ciliates and collodarians are the taxonomic groups of hosts which display the highest number of interactions with photosymbionts. Compared to collodarians, metabarcodes of ciliates and acantharians are connected with a larger diversity of metabarcodes belonging to the P group (Figure 5A).

We found a single association involving a chlorophyte. Seven metabarcodes assigned to the genus *Nannochloris* (Prasinophyceae clade 7A) are associated with 40 metabarcodes assigned to the collodarian genus *Acrosphaera* (Figure 2A). This association merits further investigation since two Prasinophyceae species, *Pedinomonas symbiotica* and *Pedinomonas noctilucae* have previously been described as photosymbionts of the Collodarian *Thalassolampe margarodes* (Cachon and Caram, 1979) and of the Dinoflagellate *Noctiluca scintillans* in the Indian Ocean (Sweeney, 1976), respectively. Validating this association could help to understand the role of the Prasinophyceae clade 7A in *micro-* and *meso-*plankton.

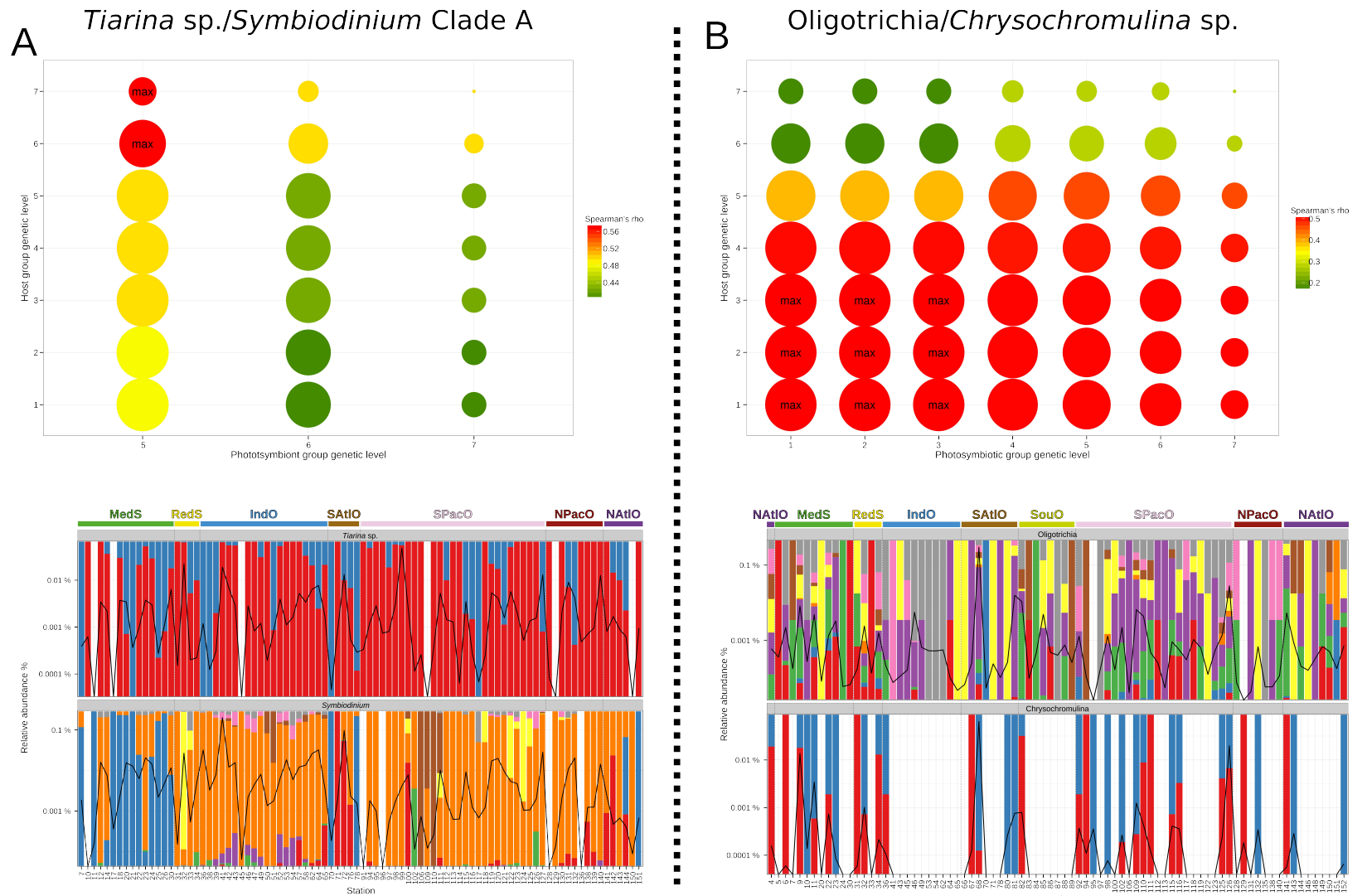


Figure 4: Specificity and biogeography of two interactions identified by our analysis: the known interaction between the ciliate *Tiarina* sp. and the Dinophyceae *Symbiodinium* Clade A (**A**), for which values of association and abundances were computed from *micro*-plankton samples (20–180 µm) and the association between oligotrich ciliates and *Chrysochromulina* (**B**), for which values of association and abundances were computed from *meso*-plankton samples (180–2000 µm). At the top, specificity of interaction is represented by colored circles. Each pair of photosymbiont and host group genetic levels (1: swarm -d 4; 2: swarm -d 3; 3: swarm -d 2; 4: swarm -d 1; 5: mcl -I 5; 6: mcl -I 1.2; 7: metabarcode) is represented by a dot displaying information about the association with the highest Spearman's rho, with larger values in red. The diameter of the circle is proportional to the number of host metabarcodes multiplied by the number of photosymbiont metabarcodes. At the bottom, we show the biogeography of the metacodes composing the pairs of genetic groups with the highest Spearman's rho. Black lines depict the relative abundance of the entire genetic group among stations. Color bars indicate the proportion of metabarcodes composing the group at each station, with one color for each of the eight most abundant metabarcodes, and grey indicating the proportion of all other metabarcodes. NAtlO: North Atlantic Ocean; MedS: Mediterranean Sea; RedS: Red Sea; IndO: Indian Ocean; SAatlO: South Atlantic Ocean; SouO: Southern Ocean; SPacO: South Pacific Ocean; NPacO: North Pacific Ocean.

Acantharians (mainly Clade E and F) are involved in a large number of associations with Suessiales (*Pelagodinium*), as was previously known, but they are also found in association with unidentified Dinophyceae (Dinophyceae_X) (Figure 5B). A highly divergent unidentified Dinophyceae clade (Dinophyceae_X), consisting of 2 sub-clades assigned only to environmental sequences (DQ103863 and GU820545) is found in interaction with 103 acantharian metabarcodes assigned to Stauracanthidae (Clade F) (Figure 2B and 3B). Metabarcodes from these 2 sub-clades also display a particular distribution among size fractions in stations where they are the most abundant in *micro-plankton* (20-180 µm), the size fraction for which we measured the score of association (Figure 6). They are generally more abundant in *piconano-plankton* (0.8-5 µm) and *micro-plankton* (20-180 µm) than in *nano-plankton* (5-20 µm). This kind of distribution is characteristic of symbiotic organisms which are detected in different size fractions depending on their life cycle stage (Henry *et al.* in prep). Depending on the size of the host, the symbiont may be nearly absent from intermediate size fractions (those between the size of the free-living stage of the symbiont and the size of the host). These unidentified Dinophyceae metabarcodes likely represent a small Dinophyceae (<5µm) which enters into symbiosis with free-living organisms from the *micro-plankton*. In previous studies, unidentified putative dinoflagellate parasites (Dinophyceae) was sequenced from individual radiolarian cells (Gast, 2006; Dolven *et al.*, 2007); as such, the unidentified clade we detected could also be parasitic.

Acantharians are also found associated with some diatoms. A diatom clade composed of 4 metabarcodes with no close reference sequence is associated with 12 acantharian metabarcodes (11 assigned to Clade E and one to Clade D), and one group of 2 diatom metabarcodes related to the genus *Rhizosolenia* are associated with 21 acantharian metabarcodes belonging to Clades E and F (Figures 2A and 3B). The statistical association between Clade E and F acantharians and rhizosolenid metabarcodes does not appear to be due to a symbiotic interaction: rhizosolenids diatoms are relatively large protists known to form chains and mats in oligotrophic waters (Kemp *et al.*, 1999), environments that are also populated by symbiotic acantharians (Decelle *et al.*, 2012a). Rhizosolenid metabarcodes do not have “free-living” like distributions and were retained in our abundance comparisons very likely because of their ability to form mats many times larger than the size of an individual cell.

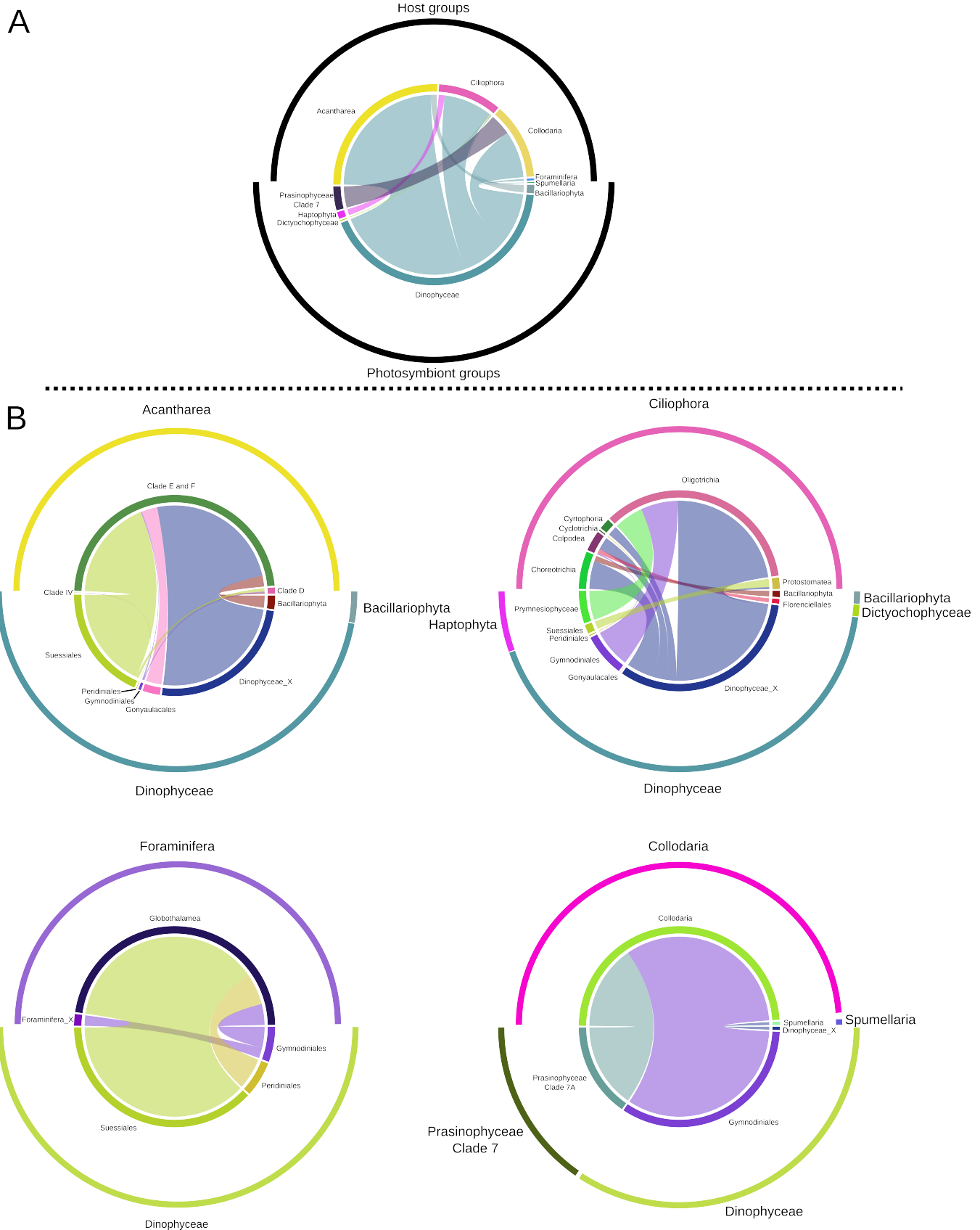


Figure 5: Global view of patterns of co-occurrence. **(A)** Positive and significant associations between host groups (top) and photosymbiont groups (bottom) summarized at a high taxonomic level. Sizes of ribbons are proportional to the number of associations detected between the metabarcodes. **(B)** Associations summarized at a lower taxonomic level. For better visualization, we generated circular visualizations for each group of hosts (acantharians, ciliates, foraminiferans and polycystines).

The ciliates are the only group associated with Florenciellales (Dictyochophyceae) and Prymnesiophyceae (Haptophyta). One group of 21 oligotrich ciliate metabarcodes is associated with 3 prymnesiophyceae metabarcodes (from 2 genetic groups) related to the genus *Chrysochromulina*. Moreover, one metabarcode assigned to several prymnesiophyceae genera (*Pleurochrysis*, *Ochrosphaera*, *Isochrysis*, *Jomonlithus*, *Coccolithus*, *Helladosphaera*, *Calyptrosphaera*, *Braarudosphaera*, *Prymnesium*, *Imantonia*, *Haptolina* and *Chrychromulina*) is associated with 19 of the 21 oligotrich metabarcodes described above. All of the 21 oligotrich metabarcodes are assigned to genera within the Strombidiidae (*Novistrombidium*, *Omegastrombidium*, *Strombidium*) and Tontoniidae (*Pseudotontiona*) (Figures 2A and 3A). Microalgae belonging to the Prymnesiophyceae, in particular *Chrysochromulina* spp., have been identified as the main source of chloroplasts for the kleptochloroplastic dinoflagellate *Dinophysis mitra* (Nishitani *et al.*, 2012). Like *Dinophysis accuminata*, which acquires cryptophyte chloroplasts by feeding via myzocytosis on the ciliate *Myrionecta rubra* (Nishitani *et al.*, 2010), *D. mitra* is thought to acquire chloroplasts by feeding on mixotrophic ciliates, presumably ciliates of the genera *Laboea*, *Tontonia* and *Strombidium* (Nishitani *et al.*, 2012). Our results suggest that *Chrysochromulina* chloroplasts could be an important source for the Strombiidae and Tontoniidae. However, further investigation is necessary to determine if *D. mitra* actually acquires its chloroplasts from these ciliates. These results also suggest that our method is able to detect cases of kleptoplastidy characterized by a low level of specificity (Figure 4B).

A group of 6 Dictyochophyceae metabarcodes related to the genera *Pseudochattonella* and *Florenceilla* is associated with a group of two Colpodea ciliate metabarcodes (Figures 2A and 3A), but Colpodea ciliates have not been described in the literature as harboring microalgae or performing kleptoplastidy.

As in our results for the acantharians, we also detected ciliates associated with diatoms (Figure 5). The association between 6 metabarcodes assigned to diatom species belonging to several Bacillariophyceae families (Bacillariaceae, Cymbellaceae, Fragilariaceae, Thalassionemataceae, Lichmophoraceae, Tabellariaceae) and one metabarcode assigned to *Tintinnidium mucicola* (Figures 2A and 3A) is particularly compelling because some tintinnid species, such as *Tintinnidium fluviatile*, are known to be able to agglutinate diatom frustules onto their lorica (Gold and Morales, 1976; Wasik *et al.*, 1996). Besides highlighting the potential diversity of diatoms that can be found on the lorica of one tintinnid species, this

result also suggests that diatom frustules composing the lorica still contain DNA that we were able to sequence and that, furthermore, these diatoms may continue living once attached.

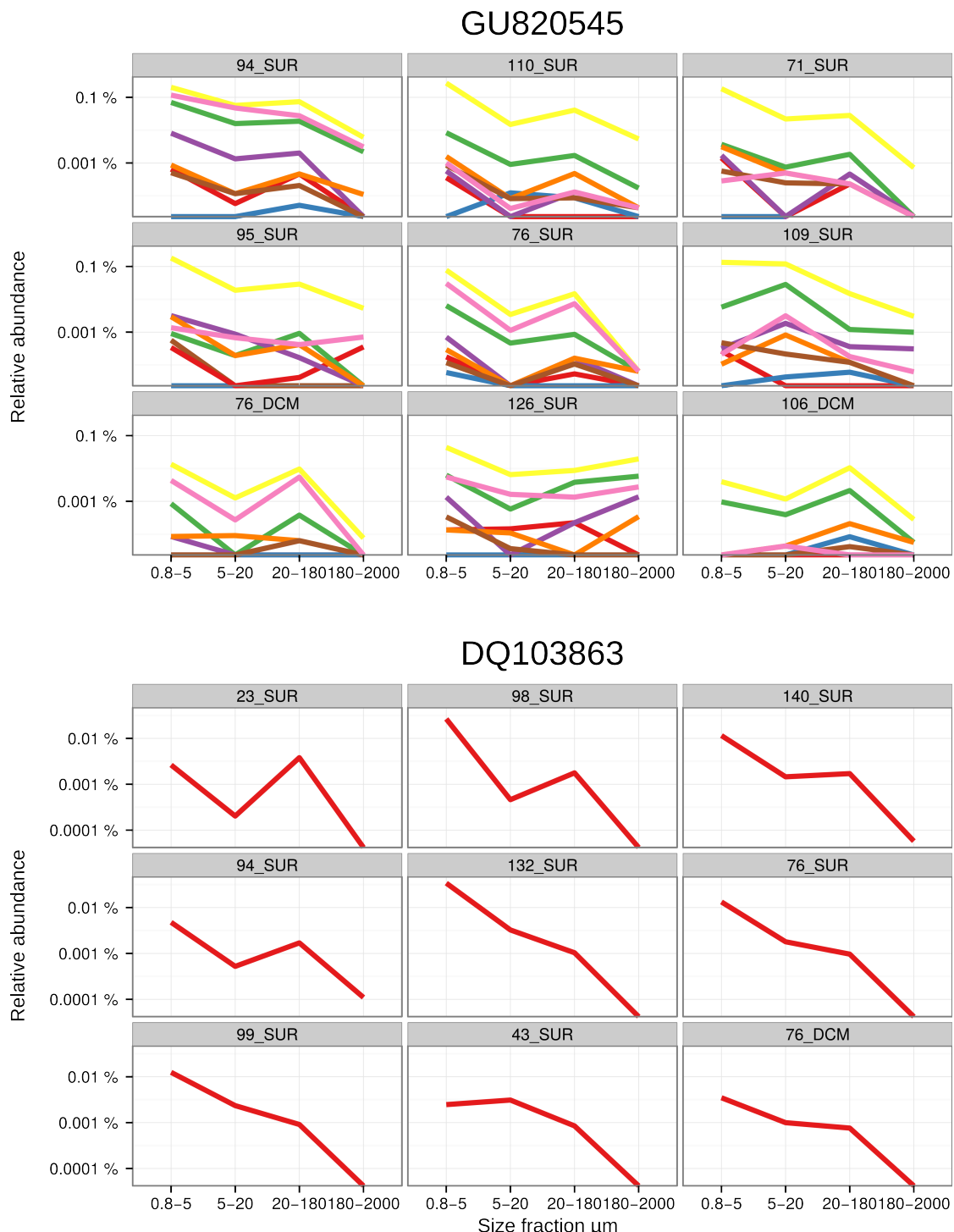


Figure 6: Distribution among size fractions by station/depth of uncultured Dinophyceae associated with acantharians in Clade F. Only the 9 station/depth pairs for which metabarcodes are the most abundant in the size fraction in which the association was detected (*micro-plankton samples (20-180 μm)*) are displayed here. (A) Relative abundances of the eight metabarcodes assigned to the Dinophyceae environmental reference sequence GU820545. (B) Relative abundances of the metabarcodes assigned to the Dinophyceae environmental reference sequence DQ103863.

The ciliates, with the exception of *Tiarina* sp., are found associated with a large number of unidentified Dinophyceae (Dinophyceae_X) and Gymnodiniales (Figure 5). Since a substantial fraction of these Dinophyceae metabarcodes are not closely related to named reference sequences, making conclusions about the nature of these associations is not straightforward. However, one association, likely related to a non-symbiotic interaction, should be noted here: a group of 7 metabarcodes related to the genus *Gyrodinium* (Gymnodiniales) and an environmental reference sequence (FJ832107) is associated with the same group of oligotrichs that is also associated with *Chrysochromulina* (see above) (Figures 2A and 3B). The ciliates from the families Strombidiidae and Tontoniidae are important grazers, like Dinophyceae species of the genus *Gyrodinium* (Sherr and Sherr, 2009 ;Löder *et al.*, 2011). Thus, this association could correspond to co-occurring grazers potentially feeding on similar prey.

Conclusion

Combining the characterization of distribution profiles among size fractions with the comparison of abundances across size fractions has the potential to detect both known and putative new photosymbiotic relationships within a size-fractionated metabarcoding dataset. In terms of computation time, these two aspects of our method are complementary. Whereas the multi-level genetic clustering increases the number of comparisons to be performed, removing genetic groups characterized by a “free-living” distribution reduces computational time. In addition to retrieving already known interactions, thereby validating our method, we have also discovered potential new photosymbioses in this study, providing compelling avenues for future research: the interactions we discovered should be validated experimentally by observing the symbiosis and by isolating and performing genotyping (barcoding) of both partners (Lima-Mendez *et al.*, 2015). Our approach represents a relatively fast way to decide how to direct microscopic observations of preserved biological samples when they are derived from a size fractionated metabarcoding dataset.

References

- ALLDREDGE, Alice L. et JONES, B. M. *Hastigerina pelagica*: foraminiferal habitat for planktonic dinoflagellates. *Marine Biology*, 1973, vol. 22, no 2, p. 131-135.

- BENJAMINI, Yoav et HOCHBERG, Yosef. Controlling the false discovery rate: a practical and powerful approach to multiple testing. *Journal of the Royal Statistical Society. Series B (Methodological)*, 1995, p. 289-300.
- CACHON, Monique et CARAM, Bernadette. A symbiotic green alga, *Pedinomonas symbiotica* sp. nov.(Prasinophyceae), in the radiolarian *Thalassolampe margarodes*. *Phycologia*, 1979, vol. 18, no 3, p. 177-184.
- CHAFFRON, Samuel, REHRAUER, Hubert, PERNTHALER, Jakob, *et al*. A global network of coexisting microbes from environmental and whole-genome sequence data. *Genome research*, 2010, vol. 20, no 7, p. 947-959.
- CHEN, Yue-Qin, WANG, Ning, ZHANG, Peng, *et al*. Molecular evidence identifies bloom-forming *Phaeocystis* (Prymnesiophyta) from coastal waters of southeast China as *Phaeocystis globosa*. *Biochemical Systematics and Ecology*, 2002, vol. 30, no 1, p. 15-22.
- CHOW, Cheryl-Emiliane T., KIM, Diane Y., SACHDEVA, Rohan, *et al*. Top-down controls on bacterial community structure: microbial network analysis of bacteria, T4-like viruses and protists. *The ISME journal*, 2014, vol. 8, no 4, p. 816-829.
- DAVY, Simon K., ALLEMAND, Denis, et WEIS, Virginia M. Cell biology of cnidarian-dinoflagellate symbiosis. *Microbiology and Molecular Biology Reviews*, 2012, vol. 76, no 2, p. 229-261.
- DE BARY, Anton. *Die erscheinung der symbiose*. Verlag von Karl J. Trübner, 1879.
- DE VARGAS, Colomban, AUDIC, Stéphane, HENRY, Nicolas, *et al*. Eukaryotic plankton diversity in the sunlit ocean. *Science*, 2015, vol. 348, no 6237, p. 1261605.
- DECCELLE, Johan, COLIN, Sébastien, et FOSTER, Rachel A. Photosymbiosis in marine planktonic protists. In : *Marine Protists*. Springer Japan, 2015. p. 465-500.
- DECCELLE, Johan, PROBERT, Ian, BITTNER, Lucie, *et al*. An original mode of symbiosis in open ocean plankton. *Proceedings of the National Academy of Sciences*, 2012a, vol. 109, no 44, p. 18000-18005.
- DECCELLE, Johan, SIANO, Raffaele, PROBERT, Ian, *et al*. Multiple microalgal partners in symbiosis with the acantharian *Acanthochiasma* sp.(Radiolaria).*Symbiosis*, 2012, vol. 58, no 1-3, p. 233-244.
- DOLVEN, Jane K., LINDQVIST, Charlotte, ALBERT, Victor A., *et al*. Molecular diversity of alveolates associated with neritic North Atlantic radiolarians. *Protist*, 2007, vol. 158, no 1, p. 65-76.

- EDGAR, Robert C. MUSCLE: multiple sequence alignment with high accuracy and high throughput. *Nucleic acids research*, 2004, vol. 32, no 5, p. 1792-1797.
- EILER, Alexander, HEINRICH, Friederike, et BERTILSSON, Stefan. Coherent dynamics and association networks among lake bacterioplankton taxa. *The ISME journal*, 2012, vol. 6, no 2, p. 330-342.
- ELBRÄCHTER, Malte et DREBES, Gerhard. Life cycles, phylogeny and taxonomy of *Dissodinium* and *Pyrocystis* (Dinophyta). *Helgoländer Wissenschaftliche Meeresuntersuchungen*, 1978, vol. 31, p. 347-366.
- FUKUDA, Yasuhiro et ENDOH, Hiroshi. New details from the complete life cycle of the red-tide dinoflagellate *Noctiluca scintillans* (Ehrenberg) McCartney. *European journal of protistology*, 2006, vol. 42, no 3, p. 209-219.
- GASCUEL, Olivier. BIONJ: an improved version of the NJ algorithm based on a simple model of sequence data. *Molecular biology and evolution*, 1997, vol. 14, no 7, p. 685-695.
- GAST, Rebecca J. Molecular phylogeny of a potentially parasitic dinoflagellate isolated from the solitary radiolarian, *Thalassicolla nucleata*. *Journal of Eukaryotic Microbiology*, 2006, vol. 53, no 1, p. 43-45.
- GOLD, Kenneth et MORALES, Eleanor A. Studies on the sizes, shapes, and the development of the lorica of agglutinated tintinnida. *The Biological Bulletin*, 1976, vol. 150, no 3, p. 377-392.
- GÓMEZ, Fernando, MOREIRA, David, et LÓPEZ-GARCÍA, Purificación. Life cycle and molecular phylogeny of the dinoflagellates *Chytriodinium* and *Dissodinium*, ectoparasites of copepod eggs. *European journal of protistology*, 2009, vol. 45, no 4, p. 260-270.
- GOUY, Manolo, GUINDON, Stephane, et GASCUEL, Olivier. SeaView version 4: a multiplatform graphical user interface for sequence alignment and phylogenetic tree building. *Molecular biology and evolution*, 2010, vol. 27, no 2, p. 221-224.
- HENRY, Nicolas, RICHTER, Daniel J., COLIN Sébastien, et al.. Size-fractionated global DNA metabarcoding reveals ecological significance of the planktonic dinoflagellate parasite *Blastodinium* in sunlit oceans. *In preparation*.
- HUNT, Dana E. et WARD, Christopher S. A network-based approach to disturbance transmission through microbial interactions. *Frontiers in microbiology*, 2015, vol. 6.

- ISHITANI, Yoshiyuki, UJIIÉ, Yurika, et TAKISHITA, Kiyotaka. Uncovering sibling species in Radiolaria: Evidence for ecological partitioning in a marine planktonic protist. *Molecular phylogenetics and evolution*, 2014, vol. 28, p. 215-222.
- KARSENTI, Eric, ACINAS, Silvia G., BORK, Peer, *et al.* A holistic approach to marine ecosystems biology. *PLoS biol*, 2011, vol. 9, no 10, p. e1001177.
- KEMP, Alan ES, PEARCE, Richard B., KOIZUMI, Itaru, *et al.* The role of mat-forming diatoms in the formation of Mediterranean sapropels. *Nature*, 1999, vol. 398, no 6722, p. 57-61.
- LEGENDRE, Pierre et LEGENDRE, Louis. *Numerical Ecology*. Elsevier, 2012.
- LETUNIC, Ivica et BORK, Peer. Interactive Tree Of Life v2: online annotation and display of phylogenetic trees made easy. *Nucleic acids research*, 2011, p. gkr201.
- LIMA-MENDEZ, Gipsi, FAUST, Karoline, HENRY, Nicolas, *et al.* Determinants of community structure in the global plankton interactome. *Science*, 2015, vol. 348, no 6237, p. 1262073.
- LÖDER, Martin GJ, MEUNIER, Cédric, WILTSHERE, Karen H., *et al.* The role of ciliates, heterotrophic dinoflagellates and copepods in structuring spring plankton communities at Helgoland Roads, North Sea. *Marine biology*, 2011, vol. 158, no 7, p. 1551-1580.
- MAHÉ, Frédéric, ROGNES, Torbjørn, QUINCE, Christopher, *et al.* Swarm: robust and fast clustering method for amplicon-based studies. *PeerJ*, 2014, vol. 2, p. e593
- MORDRET Solenn, ROMAC Sarah, HENRY Nicolas. The symbiotic life of *Symbiodinium* in the open ocean within a new species of calcifying ciliate (*Tiarina* sp.). *The ISME journal*, 2015, Press 1–13.
- NISHITANI, Goh, NAGAI, Satoshi, BABA, Katsuhisa, *et al.* High-level congruence of *Myrionecta rubra* prey and *Dinophysis* species plastid identities as revealed by genetic analyses of isolates from Japanese coastal waters. *Applied and environmental microbiology*, 2010, vol. 76, no 9, p. 2791-2798.
- NISHITANI, Goh, NAGAI, Satoshi, HAYAKAWA, Shiho, *et al.* Multiple plastids collected by the dinoflagellate *Dinophysis mitra* through kleptoplastidy. *Applied and environmental microbiology*, 2012, vol. 78, no 3, p. 813-821.
- MERCIER, Céline, BOYER, Frédéric, BONIN, Aurélie, *et al.* SUMATRA and SUMACLUST: fast and exact comparison and clustering of sequences. In :*Programs and Abstracts of the SeqBio 2013* Satoshi, HAYAKAWA, Shiho, *et al.* Multiple plastids collected

by the dinoflagellate *Dinophysis mitra* through kleptoplastidy. *Applied and environmental microbiology*, 2012, vol. 78, no 3, p. 813-821.

PIENAAR, Richard N., SAKAI, Hiroto, et HORIZUCHI, Takeo. Description of a new dinoflagellate with a diatom endosymbiont, *Durinskia capensis* sp. nov.(Peridiniales, Dinophyceae) from South Africa. *Journal of plant research*, 2007, vol. 120, no 2, p. 247-258.

PROBERT, Ian, SIANO, Raffaele, POIRIER, Camille, et al. *Blastodinium* gen. nov. and *B. nutricula* comb. nov.(Dinophyceae), a dinoflagellate commonly found in symbiosis with polycystine radiolarians. *Journal of Phycology*, 2014, vol. 50, no 2, p. 388-399.

R Core Team. R: A language and environment for statistical computing. R Foundation for Statistical Computing, Vienna, Austria, 2015

SCHOLZ, Bettina, GUILLOU, Laure, MARANO, Agostina V., et al. Zoosporic parasites infecting marine diatoms—A black box that needs to be opened. *Fungal Ecology*, 2016, vol. 19, p. 59-76.

SHAKED, Yonathan et DE VARGAS, Colombe. Pelagic photosymbiosis: rDNA assessment of diversity and evolution of dinoflagellate symbionts and planktonic foraminiferal hosts. *Marine Ecology Progress Series*, 2006, vol. 325, p. 59-71.

SHERR, Evelyn B. et SHERR, Barry F. Capacity of herbivorous protists to control initiation and development of mass phytoplankton blooms. *Aquatic Microbial Ecology*, 2009, vol. 57, no 3, p. 253.

SIANO, Raffaele, MONTRESOR, Marina, PROBERT, Ian, et al. *Pelagodinium* gen. nov. and *P. belli* comb. nov., a dinoflagellate symbiont of planktonic foraminifera. *Protist*, 2010, vol. 161, no 3, p. 385-399.

SKOVGAARD, Alf, KARPOV, Sergey A., et GUILLOU, Laure. The parasitic dinoflagellates *Blastodinium* spp. inhabiting the gut of marine, planktonic copepods: morphology, ecology, and unrecognized species diversity. *Frontiers in microbiology*, 2012, vol. 3.

STEELE, Joshua A., COUNTWAY, Peter D., XIA, Li, et al. Marine bacterial, archaeal and protistan association networks reveal ecological linkages. *The ISME journal*, 2011, vol. 5, no 9, p. 1414-1425.

STOECKER, Diane K., JOHNSON, Matthew D., DE VARGAS, Colombe, et al. Acquired phototrophy in aquatic protists. 2009.

SWEENEY, Beatrice M. *Pedinomonas noctilucae* (Prasinophyceae), The flagellate symbiotic in *Noctiluca* (Dinophyceae) in Southeast Asia. *Journal of phycology*, 1976, vol. 12, no 4, p. 460-464.

TRENCH, Robert K. The cell biology of plant-animal symbiosis. *Annual Review of Plant Physiology*, 1979, vol. 30, no 1, p. 485-531.

VAN DONGEN, Stijn Marinus. *Graph clustering by flow simulation*. 2001.

WASIK, Anna, MIKOLAJCZYK, Ewa, et LIGOWSKI, Ryszard. Agglutinated loricae of some Baltic and Antarctic Tintinnina species (Ciliophora). *Journal of plankton research*, 1996, vol. 18, no 10, p. 1931-1940. *workshop. Abstract*. 2013. p. 27-29.

Supplementary information

Table S01: Summary of the positive and significant associations. When the taxonomic assignment was not accurate enough to link a metabarcode to a genus, the “host genus” and “symbiont genus” fields indicate the next most precise taxonomic rank available.

Symbiont taxogroup	Symbiont group	Symbiont genus	Host taxogroup	Host group	Host genus	Number of associations
Bacillariophyta	Bacillariophyta	Bacillariophyceae	Ciliophora	Choreotrichia	<i>Tintinnidium</i>	5
Bacillariophyta	Bacillariophyta	Bacillariophyceae_X	Ciliophora	Choreotrichia	uncultured tintinnid ciliate	1
Bacillariophyta	Bacillariophyta	Bacillariophyta	Acantharea	Arthra_Symph	<i>Dorataspidae_E4</i>	16
Bacillariophyta	Bacillariophyta	Bacillariophyta	Ciliophora	Choreotrichia	uncultured tintinnid ciliate	5
Bacillariophyta	Bacillariophyta	Bacillariophyta	Acantharea	Arthra_Symph	<i>Acanthophracta_E3_X</i>	4
Bacillariophyta	Bacillariophyta	Bacillariophyta	Acantharea	Arthra_Symph	<i>Hexaconus</i>	2
Bacillariophyta	Bacillariophyta	<i>Biddulphia</i>	Acantharea	Arthra_Symph	<i>Dorataspidae_E4</i>	8
Bacillariophyta	Bacillariophyta	<i>Biddulphia</i>	Acantharea	Arthra_Symph	<i>Acanthophracta_E3_X</i>	2
Bacillariophyta	Bacillariophyta	<i>Biddulphia</i>	Acantharea	Arthra_Symph	<i>Hexaconus</i>	1
Bacillariophyta	Bacillariophyta	<i>Chaetoceros</i>	Ciliophora	Choreotrichia	uncultured tintinnid ciliate	1
Bacillariophyta	Bacillariophyta	<i>Dactyliosolen</i>	Acantharea	Arthra_Symph	<i>Dorataspidae_E4</i>	16
Bacillariophyta	Bacillariophyta	<i>Dactyliosolen</i>	Acantharea	Arthra_Symph	<i>Acanthophracta_E3_X</i>	4
Bacillariophyta	Bacillariophyta	<i>Dactyliosolen</i>	Acantharea	Arthra_Symph	<i>Hexaconus</i>	2
Bacillariophyta	Bacillariophyta	<i>Dactyliosolen</i>	Acantharea	Trizonaacantha_D	<i>Stauro lithium</i>	1
Bacillariophyta	Bacillariophyta	Mediophyceae	Ciliophora	Choreotrichia	uncultured tintinnid ciliate	3
Bacillariophyta	Bacillariophyta	<i>Proboscia</i>	Acantharea	Trizonaacantha_D	<i>Stauro lithium</i>	8
Bacillariophyta	Bacillariophyta	<i>Rhizosolenia</i>	Acantharea	Arthra_Symph	<i>Acanthometridae_F3</i>	9
Bacillariophyta	Bacillariophyta	<i>Rhizosolenia</i>	Acantharea	Arthra_Symph	<i>Dorataspidae_E4</i>	8
Bacillariophyta	Bacillariophyta	<i>Rhizosolenia</i>	Acantharea	Arthra_Symph	<i>Acanthophracta_E3_X</i>	2
Bacillariophyta	Bacillariophyta	<i>Rhizosolenia</i>	Acantharea	Arthra_Symph	<i>Acanthometridae_F3_X</i>	1
Bacillariophyta	Bacillariophyta	<i>Rhizosolenia</i>	Acantharea	Arthra_Symph	<i>Hexaconus</i>	1
Bacillariophyta	Bacillariophyta	<i>Synedra</i>	Ciliophora	Choreotrichia	<i>Tintinnidium</i>	1
Dictyochophyceae	Floreciellales	<i>Floreciella</i>	Ciliophora	Colpoda-1	Colpoda-1_X	8
Dictyochophyceae	Floreciellales	Floreciellales_X	Ciliophora	Colpoda-1	Colpoda-1_X	2
Dictyochophyceae	Floreciellales	<i>Pseudochattonella</i>	Ciliophora	Colpoda-1	Colpoda-1_X	2
Dinophyceae	Dinophyceae_X	AY434687_gen	Ciliophora	Oligotrichia	<i>Strombidium</i>	10
Dinophyceae	Dinophyceae_X	AY434687_gen	Ciliophora	Oligotrichia	<i>Pseudotontonia</i>	8
Dinophyceae	Dinophyceae_X	AY434687_gen	Ciliophora	Colpoda-1	Colpoda-1_X	2
Dinophyceae	Dinophyceae_X	AY434687_gen	Ciliophora	Oligotrichia	<i>Novistrombidium</i>	1
Dinophyceae	Dinophyceae_X	AY434687_gen	Ciliophora	Oligotrichia	<i>Omegastrombidium</i>	1
Dinophyceae	Dinophyceae_X	AY434687_gen	Ciliophora	Oligotrichia	<i>Strombidiidae</i>	1
Dinophyceae	Dinophyceae_X	AY664889_gen	Ciliophora	Colpoda-1	Colpoda-1_X	8
Dinophyceae	Dinophyceae_X	AY664900_gen	Ciliophora	Choreotrichia	<i>Eutintinnus</i>	72
Dinophyceae	Dinophyceae_X	AY664900_gen	Ciliophora	Cyrtophoria	<i>Pithites</i>	14
Dinophyceae	Dinophyceae_X	AY664900_gen	Acantharea	Arthra_Symph	<i>Dorataspidae_E4</i>	8
Dinophyceae	Dinophyceae_X	AY664900_gen	Spumellaria	Spumellaria	<i>Spum_group_I</i>	5
Dinophyceae	Dinophyceae_X	AY664900_gen	Ciliophora	Prostomatea_X	<i>Tiarina</i>	4
Dinophyceae	Dinophyceae_X	AY664900_gen	Spumellaria	Spumellaria	<i>Spum_group_I_X</i>	3
Dinophyceae	Dinophyceae_X	AY664900_gen	Acantharea	Arthra_Symph	<i>Acanthophracta_E3_X</i>	2
Dinophyceae	Dinophyceae_X	AY664900_gen	Spumellaria	Arthra_Symph	<i>Colepidae</i>	2
Dinophyceae	Dinophyceae_X	AY664900_gen	Acantharea	Arthra_Symph	<i>Styptosphaera</i>	2
Dinophyceae	Dinophyceae_X	AY664900_gen	Ciliophora	Prostomatea_X	<i>Hexaconus</i>	1
Dinophyceae	Dinophyceae_X	AY664900_gen	Spumellaria	Arthra_Symph	<i>Colpoda-1_X</i>	4
Dinophyceae	Dinophyceae_X	AY664936_gen	Ciliophora	Colpoda-1	<i>Strombidium</i>	10
Dinophyceae	Dinophyceae_X	AY664957_gen	Ciliophora	Oligotrichia	<i>Pseudotontonia</i>	8
Dinophyceae	Dinophyceae_X	AY664957_gen	Ciliophora	Oligotrichia	<i>Colpoda-1_X</i>	2
Dinophyceae	Dinophyceae_X	AY664957_gen	Ciliophora	Colpoda-1	<i>Novistrombidium</i>	1
Dinophyceae	Dinophyceae_X	AY664957_gen	Ciliophora	Oligotrichia	<i>Omegastrombidium</i>	1
Dinophyceae	Dinophyceae_X	AY664957_gen	Ciliophora	Oligotrichia	<i>Strombidiidae</i>	1
Dinophyceae	Dinophyceae_X	AY664957_gen	Ciliophora	Oligotrichia	<i>Strombidium</i>	90
Dinophyceae	Dinophyceae_X	AY664957_gen	Ciliophora	Oligotrichia	<i>Pseudotontonia</i>	72
Dinophyceae	Dinophyceae_X	AY664957_gen	Ciliophora	Oligotrichia	<i>Novistrombidium</i>	9
Dinophyceae	Dinophyceae_X	AY664957_gen	Ciliophora	Oligotrichia	<i>Omegastrombidium</i>	9
Dinophyceae	Dinophyceae_X	AY664957_gen	Ciliophora	Oligotrichia	<i>Strombidiidae</i>	9
Dinophyceae	Dinophyceae_X	AY664957_gen	Ciliophora	Colpoda-1	<i>Colpoda-1_X</i>	8
Dinophyceae	Dinophyceae_X	DQ103863_gen	Acantharea	Arthra_Symph	<i>Stauracanthidae_F3</i>	103
Dinophyceae	Dinophyceae_X	DQ244019_gen	Ciliophora	Cyrtophoria	<i>Pithites</i>	14
Dinophyceae	Dinophyceae_X	DQ244019_gen	Acantharea	Arthra_Symph	<i>Arthra_Symph</i>	4
Dinophyceae	Dinophyceae_X	GU820276_gen	Ciliophora	Choreotrichia	<i>Climacocylis</i>	4
Dinophyceae	Dinophyceae_X	GU820276_gen	Ciliophora	Choreotrichia	<i>Choreotrichia</i>	1
Dinophyceae	Dinophyceae_X	GU820545_gen	Acantharea	Choreotrichia	<i>Rhizodorus</i>	1
Dinophyceae	Dinophyceae_X	GU825114_gen	Ciliophora	Arthra_Symph	<i>Stauracanthidae_F3</i>	824
Dinophyceae	Dinophyceae_X	GU825114_gen	Ciliophora	Oligotrichia	<i>Strombidium</i>	10
Dinophyceae	Dinophyceae_X	GU825114_gen	Ciliophora	Oligotrichia	<i>Pseudotontonia</i>	8
Dinophyceae	Dinophyceae_X	GU825114_gen	Ciliophora	Colpoda-1	<i>Colpoda-1_X</i>	2
Dinophyceae	Dinophyceae_X	GU825114_gen	Ciliophora	Oligotrichia	<i>Novistrombidium</i>	1
Dinophyceae	Dinophyceae_X	GU825114_gen	Ciliophora	Oligotrichia	<i>Omegastrombidium</i>	1
Dinophyceae	Dinophyceae_X	GU825114_gen	Ciliophora	Oligotrichia	<i>Strombidiidae</i>	1

Table S01 (continued)

Symbiont taxogroup	Symbiont group	Symbiont genus	Host taxogroup	Host group	Host genus	Number of associations
Dinophyceae	Dinophyceae_X	<i>Gyrodinium</i>	Ciliophora	Oligotrichia	<i>Strombidium</i>	30
Dinophyceae	Dinophyceae_X	<i>Gyrodinium</i>	Ciliophora	Oligotrichia	<i>Pseudotontonia</i>	24
Dinophyceae	Dinophyceae_X	<i>Gyrodinium</i>	Ciliophora	Colpoda-1	<i>Colpoda_1_X</i>	6
Dinophyceae	Dinophyceae_X	<i>Gyrodinium</i>	Ciliophora	Oligotrichia	<i>Novistrombidium</i>	3
Dinophyceae	Dinophyceae_X	<i>Gyrodinium</i>	Ciliophora	Oligotrichia	<i>Oregastrobidium</i>	3
Dinophyceae	Dinophyceae_X	<i>Gyrodinium</i>	Ciliophora	Oligotrichia	<i>Strombiidae</i>	3
Dinophyceae	Dinophyceae_X	<i>Gyrodinium</i>	Ciliophora	Oligotrichia	<i>Strombidium</i>	20
Dinophyceae	Dinophyceae_X	Uncultured	Ciliophora	Oligotrichia	<i>Pseudotontonia</i>	16
Dinophyceae	Dinophyceae_X	Uncultured	Ciliophora	Oligotrichia	<i>Colpoda_1_X</i>	4
Dinophyceae	Dinophyceae_X	Uncultured	Ciliophora	Oligotrichia	<i>Novistrombidium</i>	2
Dinophyceae	Dinophyceae_X	Uncultured	Ciliophora	Oligotrichia	<i>Oregastrobidium</i>	2
Dinophyceae	Dinophyceae_X	Uncultured	Ciliophora	Oligotrichia	<i>Strombiidae</i>	2
Dinophyceae	Gonyaulacales	<i>Alexandrium_01</i>	Acantharea	<i>Arthra_Symph</i>	<i>Dorataspidae_E4</i>	6
Dinophyceae	Gonyaulacales	<i>Gonyaulax</i>	Ciliophora	Choreotrichia	<i>Climacoclysis</i>	1
Dinophyceae	Gonyaulacales	<i>Neoceratium</i>	Acantharea	<i>Arthra_Symph</i>	<i>Stauracanthidae_F3</i>	103
Dinophyceae	Gymnodinales	<i>Gymnodinium</i>	Collodaria	Collodaria	<i>Acrosphaera</i>	617
Dinophyceae	Gymnodinales	<i>Gymnodinium</i>	Acantharea	<i>Arthra_Symph</i>	<i>Arthra_Symph_E1E2</i>	7
Dinophyceae	Gymnodinales	<i>Gymnodinium</i>	Acantharea	Trizoneacantha_D	<i>Staurolithium</i>	7
Dinophyceae	Gymnodinales	<i>Gymnodinium</i>	Acantharea	<i>Acantharia_IV</i>	<i>Acantharia_IV_X</i>	3
Dinophyceae	Gymnodinales	<i>Gymnodinium</i>	Foraminifera	Globothalamea	<i>Globigerinoides</i>	2
Dinophyceae	Gymnodinales	<i>Gymnodinium</i>	Collodaria	Collodaria	<i>Collozoum</i>	1
Dinophyceae	Gymnodinales	<i>Gymnodinium</i>	Foraminifera	Foraminifera_X	<i>Foraminifera</i>	1
Dinophyceae	Gymnodinales	<i>Gymnodinium</i>	Ciliophora	Oligotrichia	<i>Strombidium</i>	30
Dinophyceae	Gymnodinales	<i>Gyrodinium_05</i>	Ciliophora	Oligotrichia	<i>Pseudotontonia</i>	24
Dinophyceae	Gymnodinales	<i>Gyrodinium_05</i>	Ciliophora	Oligotrichia	<i>Novistrombidium</i>	3
Dinophyceae	Gymnodinales	<i>Gyrodinium_05</i>	Ciliophora	Oligotrichia	<i>Oregastrobidium</i>	3
Dinophyceae	Gymnodinales	<i>Gyrodinium_05</i>	Ciliophora	Oligotrichia	<i>Strombiidae</i>	3
Dinophyceae	Gymnodinales	<i>Kareniaaceae_15</i>	Ciliophora	Oligotrichia	<i>Strombidium</i>	20
Dinophyceae	Gymnodinales	<i>Kareniaaceae_15</i>	Ciliophora	Oligotrichia	<i>Pseudotontonia</i>	16
Dinophyceae	Gymnodinales	<i>Kareniaaceae_15</i>	Ciliophora	Colpoda-1	<i>Colpoda_1_X</i>	2
Dinophyceae	Gymnodinales	<i>Kareniaaceae_15</i>	Ciliophora	Oligotrichia	<i>Novistrombidium</i>	2
Dinophyceae	Gymnodinales	<i>Kareniaaceae_15</i>	Ciliophora	Oligotrichia	<i>Oregastrobidium</i>	2
Dinophyceae	Gymnodinales	<i>Kareniaaceae_15</i>	Ciliophora	Oligotrichia	<i>Strombiidae</i>	2
Dinophyceae	Gymnodinales	<i>Lepidodinium</i>	Ciliophora	Colpoda-1	<i>Colpoda_1_X</i>	2
Dinophyceae	Peridiniales	<i>Peridinium_03</i>	Ciliophora	Cyclotrichia	<i>Mesodiniidae</i>	1
Dinophyceae	Peridiniales	<i>Peridinium_03</i>	Ciliophora	Cyclotrichia	<i>Myrionecta</i>	1
Dinophyceae	Peridiniales	<i>Peridinium_03</i>	Ciliophora	Cyclotrichia	<i>Globigerinoides</i>	2
Dinophyceae	Peridiniales	<i>Protoperidinium</i>	Foraminifera	Globothalamea	<i>Staurolithium</i>	2
Dinophyceae	Peridiniales	<i>Protoperidinium</i>	Acantharea	Trizoneacantha_D	<i>Staurolithium</i>	2
Dinophyceae	Peridiniales	<i>Protoperidinium_02</i>	Acantharea	Trizoneacantha_D	<i>Globigerinoides</i>	1
Dinophyceae	Peridiniales	<i>Protoperidinium_02</i>	Foraminifera	Globothalamea	<i>Arthra_Symph_E1E2</i>	380
Dinophyceae	Suessiales	<i>Pelagodinium</i>	Acantharea	<i>Arthra_Symph</i>	<i>Dorataspidae_E4</i>	152
Dinophyceae	Suessiales	<i>Pelagodinium</i>	Acantharea	<i>Arthra_Symph</i>	<i>Stauracanthidae_F3</i>	103
Dinophyceae	Suessiales	<i>Pelagodinium</i>	Acantharea	<i>Arthra_Symph</i>	<i>Acanthophracta_E3_X</i>	38
Dinophyceae	Suessiales	<i>Pelagodinium</i>	Foraminifera	Globothalamea	<i>Globigerinoides</i>	19
Dinophyceae	Suessiales	<i>Pelagodinium</i>	Acantharea	<i>Arthra_Symph</i>	<i>Hexaconus</i>	19
Dinophyceae	Suessiales	<i>Pelagodinium</i>	Acantharea	Trizoneacantha_D	<i>Staurolithium</i>	19
Dinophyceae	Suessiales	<i>Pelagodinium</i>	Acantharea	<i>Arthra_Symph</i>	<i>Acanthometridae_F3</i>	1
Dinophyceae	Suessiales	<i>Pelagodinium</i>	Acantharea	<i>Arthra_Symph</i>	<i>Acanthometridae_F3_X</i>	1
Dinophyceae	Suessiales	<i>Pelagodinium</i>	Foraminifera	Globothalamea	<i>Globigerinella</i>	1
Dinophyceae	Suessiales	<i>Pelagodinium</i>	Ciliophora	Prostomatea_X	<i>Tiarina</i>	1
Dinophyceae	Suessiales	<i>Pelagodinium</i>	Ciliophora	Prostomatea_X	<i>Tiarina</i>	2
Dinophyceae	Suessiales	<i>Symbiodiniaceae</i>	Ciliophora	Prostomatea_X	<i>Tiarina</i>	6
Dinophyceae	Suessiales	<i>Symbiodinium</i>	Ciliophora	Prostomatea_X	<i>Tiarina</i>	14
Dinophyceae	Suessiales	<i>Symbiodinium CladeA</i>	Ciliophora	Oligotrichia	<i>Strombidium</i>	20
Haptophyta	Prymnesiophyceae	<i>Chryschromulina</i>	Ciliophora	Oligotrichia	<i>Pseudotontonia</i>	16
Haptophyta	Prymnesiophyceae	<i>Chryschromulina</i>	Ciliophora	Oligotrichia	<i>Novistrombidium</i>	2
Haptophyta	Prymnesiophyceae	<i>Chryschromulina</i>	Ciliophora	Oligotrichia	<i>Oregastrobidium</i>	2
Haptophyta	Prymnesiophyceae	<i>Chryschromulina</i>	Ciliophora	Oligotrichia	<i>Strombiidae</i>	2
Haptophyta	Prymnesiophyceae	<i>Chryschromulina_X</i>	Ciliophora	Oligotrichia	<i>Strombidium</i>	10
Haptophyta	Prymnesiophyceae	<i>Chryschromulina_X</i>	Ciliophora	Oligotrichia	<i>Pseudotontonia</i>	8
Haptophyta	Prymnesiophyceae	<i>Chryschromulina_X</i>	Ciliophora	Oligotrichia	<i>Novistrombidium</i>	1
Haptophyta	Prymnesiophyceae	<i>Chryschromulina_X</i>	Ciliophora	Oligotrichia	<i>Oregastrobidium</i>	1
Haptophyta	Prymnesiophyceae	<i>Chryschromulina_X</i>	Ciliophora	Oligotrichia	<i>Strombiidae</i>	1
Haptophyta	Prymnesiophyceae	<i>Prymnesiophyceae</i>	Ciliophora	Oligotrichia	<i>Pseudotontonia</i>	8
Haptophyta	Prymnesiophyceae	<i>Prymnesiophyceae</i>	Ciliophora	Oligotrichia	<i>Strombidium</i>	8
Haptophyta	Prymnesiophyceae	<i>Prymnesiophyceae</i>	Ciliophora	Oligotrichia	<i>Novistrombidium</i>	1
Haptophyta	Prymnesiophyceae	<i>Prymnesiophyceae</i>	Ciliophora	Oligotrichia	<i>Oregastrobidium</i>	1
Haptophyta	Prymnesiophyceae	<i>Prymnesiophyceae</i>	Ciliophora	Oligotrichia	<i>Strombiidae</i>	1
Prasinophyceae Clade 7	Prasino_clade_7	<i>Nannochloris[7A1]</i>	Collodaria	Collodaria	<i>Acrosphaera</i>	280

Parasites diversity and abundance in the *Tara Oceans* dataset challenge classic views on marine plankton ecology

Cédric Berney, Nicolas Henry, Colomban de Vargas, Stéphane Audic

EPEP - *Evolution des Protistes et des Ecosystèmes Pélagiques* - team, Sorbonne Universités, UPMC Univ Paris

06, UMR 7144, Station Biologique de Roscoff, 29680 Roscoff, France

CNRS, UMR 7144, Station Biologique de Roscoff, 29680 Roscoff, France

In preparation

Abstract

Surveys of marine plankton biodiversity have so far been geographically restricted or have not accounted for the full range of plankton size. As part of the *Tara-Oceans* project, rDNA metabarcodes (the V9 region of 18S rDNA) were sequenced from size-fractionated plankton communities collected at 126 stations across tropical and temperate oceans, allowing for the first time an assessment of the entire eukaryotic biodiversity across a whole planetary biome. Here we use the data to explore the diversity and prevalence of protists with a parasitic/parasitoid life style in the open ocean plankton. Using the *V9_PR2* reference database derived from the 18S rDNA Protist Ribosomal Reference (PR2) database, we attributed broad ecological functions / symbiotic modes to taxonomically assigned protist metabarcodes, revealing that one third belongs to poorly known heterotrophic organisms whose exact life style is unknown. We then used abundance profiles and distributions across size-fractions to investigate the possible life style of these organisms, and identify potential new host-symbiont relationships between planktonic eukaryotes. OTUs from selected potential hosts were compared to OTUs belonging to both known parasites/parasitoids and organisms of unknown life style. Many of the significant associations that we recovered correspond to well-known symbiotic relationships (demonstrating the effectiveness of the approach) but we also uncovered a few intriguing novel associations between protist lineages. Overall, alveolates largely dominate open ocean plankton communities both in terms of global diversity and in terms of symbiotic associations with other eukaryotes. Our results also corroborate earlier suggestions that symbioses between eukaryotes are a key component of these communities and that models of plankton ecology should better integrate them.

Introduction

Symbiotic relationships between eukaryotic species where one organism benefits from the association at the expense of the other are widespread in all environments. Most lineages of eukaryotes are concerned, with both known parasitic and host species present across all eukaryotic supergroups (Poulin and Morand, 2000; Bass *et al.*, 2015). For the longest time, only few key parasitic taxa were given proper attention because of their direct medical or economic significance: parasites of humans, livestock, fisheries or crops are well studied, their life cycle is often fully elucidated, and more recently the main species have had their genome sequenced (Chaudhary and Roos, 2005; Stentiford *et al.*, 2014). Meanwhile, the global ecological and evolutionary significance of parasitism remains very poorly understood (Poulin, 2014). Often very little is known about the wider groups to which the few highly studied parasitic taxa belong, even though it is likely that they include a much larger diversity of yet undescribed parasites, globally playing key roles in ecosystems (the "parasitic dark matter", Bass *et al.*, 2015). This lack of knowledge is particularly acute for marine parasites, because marine diversity as a whole is much more incompletely known than terrestrial diversity (Rohde, 2002). One of the reasons behind this knowledge gap is the fact that the parasitic life style in itself makes these organisms difficult to study or even detect. Many parasites spend the majority of their life cycle within a host, and when infected hosts do not look or behave visibly differently from uninfected ones, parasitism remains inconspicuous. Global estimates of the diversity and prevalence of parasitic organisms in a given environment are thus impossible to achieve by direct observation as can usually be done for free-living organisms (Bass *et al.*, 2015). As a result, parasites are only now beginning to be included in ecological models at the level of whole ecosystems, despite the fact that their significance in food webs and ecosystem functions has been recognised since the turn of the century (Marcogliese and Cone, 1997; Windsor, 1998; Hudson *et al.*, 2006; Dobson *et al.*, 2008).

Over the last few decades, rapid advances in the fields of DNA isolation, amplification and sequencing have been revolutionising the ways in which we can address the biology, evolution, diversity and ecology of microbial eukaryotes. In particular, sequencing of ribosomal RNA genes from organisms within environmental samples (environmental rDNA surveys) has become a method of choice to apprehend the diversity of eukaryotes within a given habitat (Moreira and López-García, 2002; Berney *et al.*, 2004; Richards and Bass,

2005). Clear advantages of environmental rDNA surveys include the detection of cryptic or otherwise elusive organisms (including those for which classical morphological and culture approaches typically fail), large-scale sampling with fewer biases than specimen-based methods, and generation of data for molecular systematics and statistical ecological inferences; their potential for the study of parasitic organisms is therefore enormous (López-García and Moreira, 2008; Massana and Pedrós-Alió, 2008; Bass *et al.*, 2015). However, parasites often possess divergent genes/genomes, and may therefore escape detection in general environmental rDNA surveys using universal, eukaryote-wide PCR primers (Hartikainen *et al.*, 2014b; Bass *et al.*, 2015). Using lineage-specific PCR primers to obtain environmental rDNA libraries enriched in a given parasitic lineage has been shown to be highly efficient (Bråte *et al.*, 2010; Hartikainen *et al.*, 2014a), but it makes it impossible to compare directly diversity and abundance of different lineages in a given habitat. High-throughput sequencing technologies now make it possible to overcome this issue by significantly increasing the sequencing depth of amplicons within samples (metabarcoding approaches) and/or by generating metagenomic sequence datasets that are free from PCR-related biases. This most recent, "environmental genomics" revolution means that eukaryotic communities can now be addressed in their globality, including the rarest and most genetically divergent lineages.

In this study, we take advantage of the *Tara-Oceans* eukaryote V9 rDNA metabarcoding dataset to explore the global diversity and abundance of protists with a parasitic/parasitoid life style in the open ocean plankton, and try to identify potential new host-parasite associations. A functional annotation of taxonomically assignable protist metabarcodes reveals that one third belongs to poorly known heterotrophic organisms whose exact life style is unknown. We use abundance profiles and distributions across size-fractions to investigate the possible life style of these organisms, and identify potential new host-symbiont relationships among planktonic eukaryotes. Our results support the idea that symbioses between eukaryotes (a large majority of which involves alveolates) are a key component of open ocean plankton communities and should be better integrated into ecological models of plankton ecology and food webs.

Material and Methods

Data used in this study are part of the *Tara-Oceans* V9 metabarcoding dataset (Karsenti *et al.*, 2011; de Vargas *et al.*, 2015) extended to 126 stations (47 stations were

included in the initial dataset). Analyses were performed on metabarcodes obtained from 586 samples belonging to 121 stations, sampled at two depths (subsurface, mixed-layer waters, and the deep chlorophyll maximum at the top of the thermocline), and separated by serial filtration using plankton nets of various mesh-sizes into four main organismal size-fractions covering the majority of eukaryotic plankton diversity: *piconano*-plankton (0.8-5µm), *nano*-plankton (5-20µm), *micro*-plankton (20-180µm), and *meso*-plankton (180-2000µm). For a given sample and a given metabarcode, the number of reads assigned to the metabarcode divided by the total number of reads within that sample was used as a proxy for their abundance in further statistical analyses. Additional details on the methodology used to generate the data can be found in de Vargas et al. (2015).

A simple functional annotation of the metabarcoding data was performed to estimate the proportion of known parasitic protists in the sunlit ocean plankton. We followed an approach similar to that used in de Vargas et al. (2015) to associate metabarcodes to basic bio-ecological functions such as photo- versus heterotrophy, but focusing on the following three functional categories: (1) free-living life style, (2) parasitic, parasitoid, or amphizoic life style, and (3) unknown life style. First, each of the 91 taxogroups present in the *Tara*-Oceans data was attributed a main functional category. Then based on an extensive literature survey, we identified in each taxogroup all the sublineages (down to genera) known to have a different life style than that of the majority of organisms in that taxogroup. Taxogroups that contain a significantly higher proportion of environmental diversity than described members with a known life style (such as *Perkinsea* and *Diplonemida*) were categorised as having an unknown life style. Then within *Perkinsea* for instance the only two described genera (*Perkinsus* and *Parvilucifera*) were recorded as having a known (in this case parasitic) life style. *Tara* Oceans metabarcodes were then attributed a functional category based on their taxonomic assignment, provided that their closest hits among the reference barcodes were mono-functional; if not, they were annotated as having an unknown life style. This conservative, two-step approach was designed to avoid over- or under-estimating the prevalence of parasitic organisms in the dataset and minimise incorrect functional inferences for metabarcodes that are relatively distant from any reference barcode, especially within complex, poly-functional groups such as dinoflagellates.

The methodology used to investigate potential parasite-host associations across phylogenetic gradients was developed for a parallel study addressing photosymbiosis in the open ocean plankton (Henry et al., in prep.). Metabarcodes from both potential symbionts and

potential hosts were clustered into increasingly inclusive genetic groups (seven levels in total). The potential host groups we investigated were metazoans for comparisons in the *meso*-plankton, and the four main protist groups (diatoms, ciliates, dinoflagellates, and radiolarians) for comparisons in the *micro*-plankton. For both size-fractions, the potential symbiont group we tested comprised all protist lineages attributed to the functional categories 2 and 3 as explained above. However for comparisons in the *micro*-plankton, ciliates and dinoflagellates were excluded from the potential symbiont group because they were being tested as potential hosts. Then a filtering based on distribution profiles was applied to the genetic groups of potential symbionts to limit the number of false positives in our results (see Henry et al., in prep. for details concerning the filtering). Genetic groups abundances were compared separately for *micro*- and *meso*-plankton samples between the potential symbionts and the hosts and the results for both size fractions were analyzed separately.

Results and Discussion

Functional annotation of the V9 metabarcoding dataset reveals the extant of our ignorance of the ecology of planktonic protists

Results of the functional annotation are summarised in Figure 1 (see also Suppl. Table S1). About 60% of OTUs were attributed a free-living life style, with more than half of this proportion due to three of the most diverse and abundant taxogroups in the *Tara*-Oceans data: dinoflagellates, collodarians (Radiolaria), and diatoms. OTUs belonging to unquestionably parasitic, parasitoid, or amphizoic protists represented 8% of the total. The four main taxogroups concerned belong to alveolates: Apicomplexa (29% of the total parasites), MALV-I and MALV-II Syndiniales (19% and 18%, respectively), and parasitic dinoflagellates such as the very abundant genus *Blastodinium* (13%). The next most diverse taxogroups in that functional category belong to Amoebozoa (various lineages of amphizoic lobose amoebae, making up 6% of that category), opisthokonts (parasitic fungi and ichthyosporeans, making up 5% of that category), and Rhizaria (ascetosporean parasites such as *Paradinium* and paramyxids, making up 4% of that category). Other taxogroups that represent above 0.5% of the total parasites are also parasitic ciliates and perkinsids (alveolates), oomycetes and labyrinthulids (stramenopiles), phytomyxids (Rhizaria), and kinetoplastids (excavates).

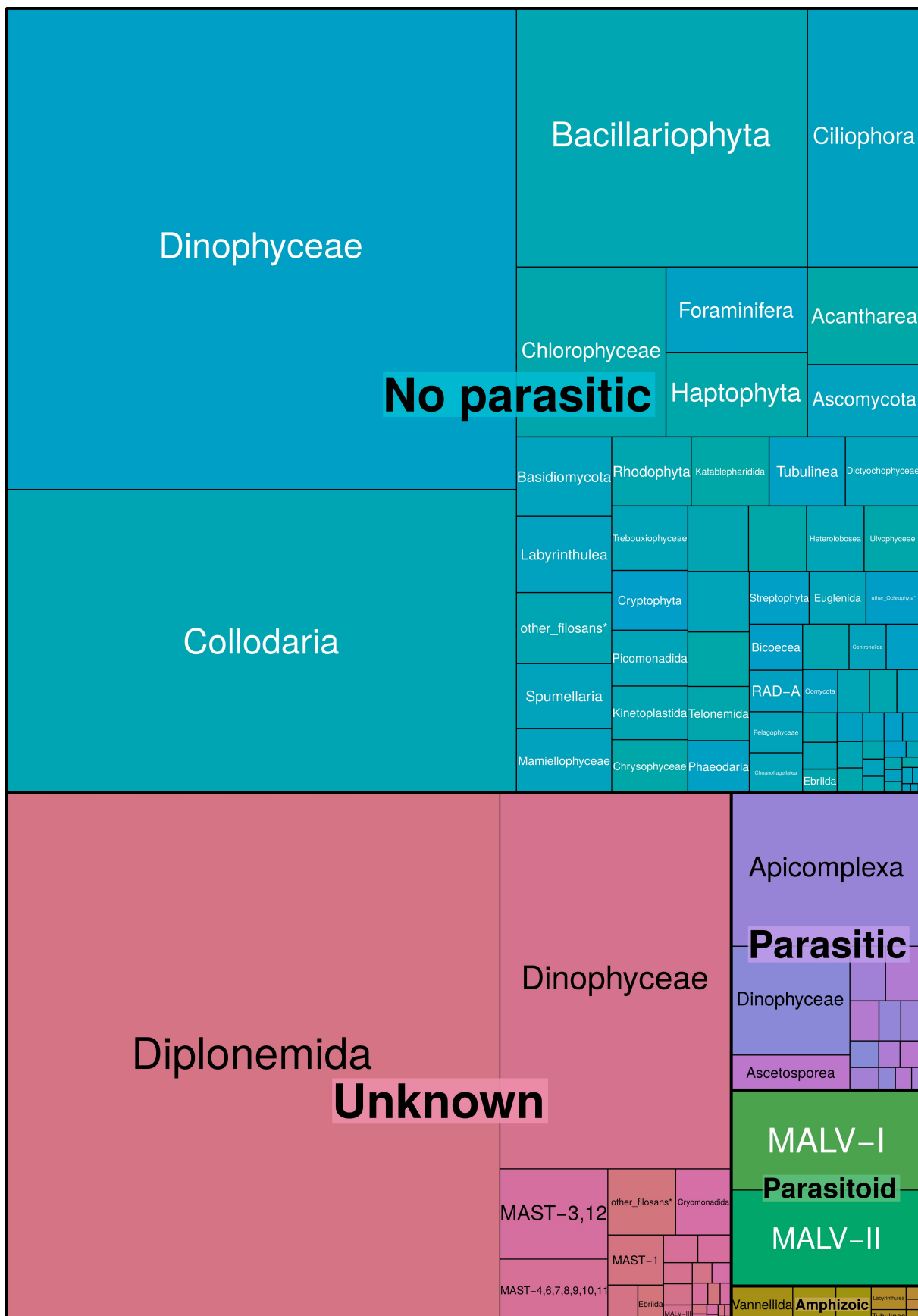


Figure 01: OTUs richness by taxogroups and functional annotation into three main categories: 1 - not parasitic life style (blue), 2 - parasitic (purple), parasitoid (green), or amphizoic (yellow) life style, and 3 - unknown life style (red). The size of the rectangles is proportional to the number of OTUs.

Strikingly, the remaining 32% of OTUs cannot be functionally annotated. This high proportion mainly reflects the generally high genetic distance that exists between OTUs and their closest morphologically described match in the reference database. Indeed a very high proportion of entries in *V9_PR2* consists of sequences from environmental surveys. Their phylogeny is known and they allow taxonomic annotation, but many belong to entirely novel lineages that contain no morphologically described organisms, therefore the life style of the organisms they come from is unknown. Significantly, this is the case for the entirety of the second most diverse protist taxogroup in the *Tara Oceans* data, diplomonads. Although their assignment to diplomonads is beyond any doubt from a phylogenetic point of view, all concerned OTUs and reference sequences form an environmental clade that is clearly separate from *Diplonema*, *Rhynchopus*, and *Hemistasia*, the only three described genera in that group for which sequences are available (Yabuki and Tame, 2015). As a result, the life style of these open ocean planktonic diplomonads remains hypothetical; most of them are probably free-living predators, but some could be parasitic/parasitoid (Lara *et al.*, 2009; Lukeš *et al.*, 2015). This is also the case for the significant proportion of dinoflagellate OTUs that were attributed to the unknown category because their closest match in *V9_PR2* are environmental sequences of unknown life style, as well as for OTUs attributed to environmental lineages among Stramenopiles (the MASTs). Other significant lineages in the unknown category comprise various cercozoans such as cryomonads or ebridians, whose known possible life styles range from predators to parasites/parasitoids.

Investigating symbiotic associations across phylogenetic gradients to identify potential new parasitic lineages and parasite-host pairs

Figure 2 shows the results of our analysis of distribution profiles for the 12,544 metabarcodes belonging to lineages attributed to the functional categories 2 and 3 and which appear in more than 10% of *micro-* and *meso*-plankton samples. 4,166 metabarcodes (33%) have a distribution profile compatible with a possible symbiont life style (blue bars in Fig. 2). This result is congruent with the fact that many of these lineages comprise organisms of relatively small size (for instance kinetoplastid flagellates or ascomycete yeasts) that are not expected to be found in the two larger size-fractions unless they are closely associated with a larger organism present in these size-fractions. The remaining 8,378 metabarcodes (67%) exclusively belong to genetic groups which have a “free-living” like distribution (red bars in Fig. 2); they were therefore excluded from later analyses. A majority of them belongs to only three lineages: Dinophyceae (72% of metabarcodes with a distribution profile expected to be

specific to free-living organisms), ciliates (51%), and diplonemids (73%). Such a result is not unexpected for these taxogroups. The corresponding metabarcodes were attributed an unknown function because they are only distantly related to reference sequences of identified organisms. However we expect a significant proportion of them to correspond to free-living organisms, present in the two larger size-fractions simply because they are larger cells.

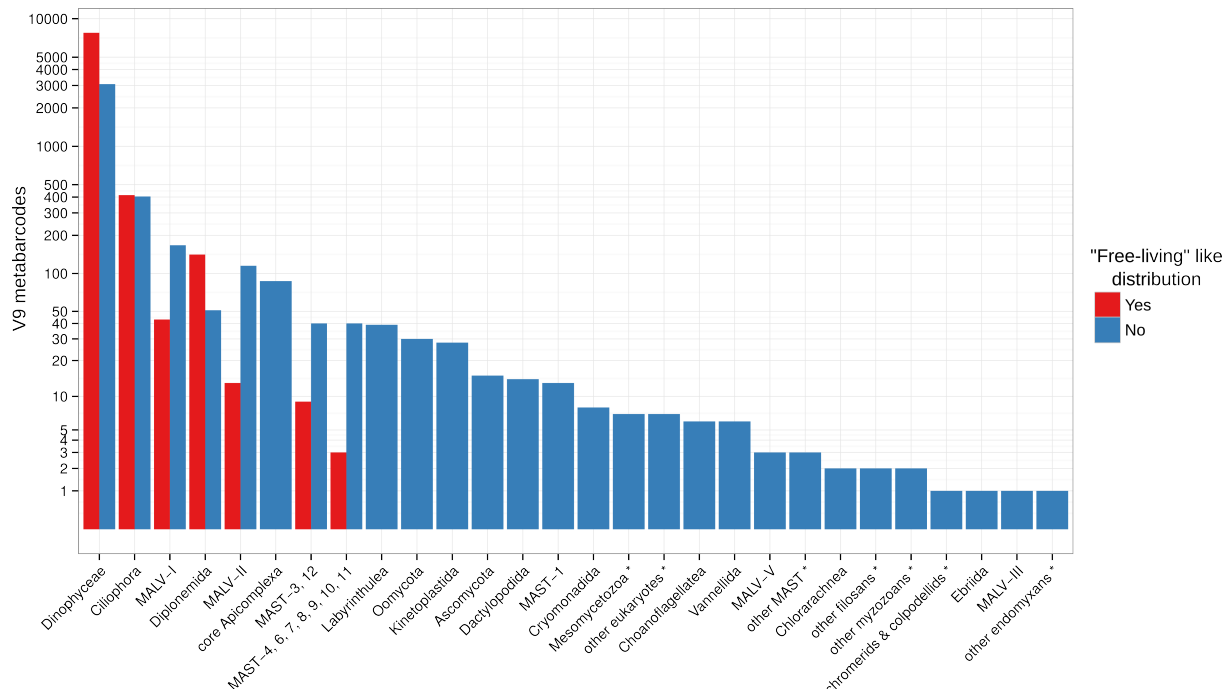


Figure 02: Proportion of size distribution profiles that are consistent with a “free-living” life style among lineages containing species in functional categories 2 (parasitic, parasitoid, or amphizoic life style) and 3 (unknown life style). For all taxogroups, the bars represent numbers of V9 metabarcodes present in more than 10% of micro- or meso-plankton samples, assigned to a reference sequence with a percentage identity of 90% or greater, and belonging to at least one genetic group present in more than 20% of micro- or meso-plankton samples. In red, number of metabarcodes which exclusively belong to genetic groups with a “free-living” distribution profile. In blue, number of metabarcodes belonging to at least one genetic group not characterized as “free-living”.

Figure 3 presents a global view of the patterns of co-occurrence that were recovered in our analyses. In the *meso*-plankton (Fig. 3A; see also Suppl. Table S3), metazoan hosts positively associated to potential symbionts were almost exclusively comprised of copepods, an unsurprising result given that they account for the vast majority of the diversity and abundance of metazoans in the whole *Tara*-Oceans dataset (de Vargas et al., 2015). Copepods were found to be associated in majority with the dinoflagellate genera *Blastodinium* and *Chytriodinium* but also with gregarine Apicomplexa of the order Cephaloidophorida (related to the genus *Thiriotia*) and with the ciliate genus *Vampyrophrya*. A small amount of positive associations was found between copepods and *Amoebophrya* (MALV-II), *Syndinium* and *Hematodinium* (MALV-IV), and neobodonid Kinetoplastida. Other metazoan hosts that

produced significant associations with potential symbionts include Eumalacostraca metabarcodes with *Syndinium* and *Vampyrophrya*, Appendicularia metabarcodes with *Vampyrophrya*, and Siphonophora metabarcodes with the dinoflagellate *Pyrocystis*. In the *micro-plankton* (Fig. 3B; see also Suppl. Table S2), protist hosts positively associated to potential symbionts were predominantly comprised of dinoflagellates, again an unsurprising result given that they are by far the most diverse eukaryotes in the whole *Tara-Oceans* dataset (de Vargas *et al.*, 2015). Dinoflagellates were found to be associated almost exclusively with metabarcodes of MALV-II (*Amoebophrya* and relatives), but also with metabarcodes of undetermined MALV-I and a few stramenopile metabarcodes (Labyrinthulea and MAST-1 lineage). Diatoms were next as the hosts with the highest number of positive associations with potential symbionts. Various diatoms (both centric and pennate) were found to be significantly associated with an enigmatic basal environmental lineage of choanoflagellates with no described member. It corresponds to two reference sequences (clones MB04.9 and SGYW634, GenBank accession numbers FJ176220 and KJ760652, respectively) previously found in Pacific Ocean samples (Cheung *et al.*, 2008; Lie *et al.*, 2014). Other protist hosts that produced significant associations with potential symbionts include Acantharea with diverse MALV-I and a few MALV-II and labyrinthulean metabarcodes, and tintinnid ciliates with a few MALV-I, MALV-II, and diplomirimid metabarcodes.

The effectiveness of the approach used in this study to identify symbiont-host associations is supported by the fact that well documented cases of symbiotic relationships in the open ocean plankton were recovered. This holds true for many cases of known host-parasite relationships, as evidenced by the strong associations observed in the *meso-plankton* between copepods and parasites such as the dinoflagellates *Blastodinium* (Skovgaard *et al.*, 2012) and *Chytriodinium* (Gómez *et al.*, 2009), the MALV-IV genus *Syndinium* (Skovgaard *et al.*, 2005), the ciliate *Vampyrophrya* (Grimes and Bradbury, 1992), or gregarine apicomplexans of the order Cephaloidophorida (Rueckert *et al.*, 2011), and in the *micro-plankton* between dinoflagellate hosts and MALV-II Syndiniales (Guillou *et al.*, 2008). This is true as well for mutualistic photosymbioses that are the main focus of a parallel study (Henry *et al.*, in prep.). However, it is worth noting that the approach in itself does not allow discrimination between the various possible types of symbiotic associations that can exist between a host and its symbiont along the gradient from mutualism to commensalism to parasitism. Therefore, not all of the associations we detected are expected to represent cases of parasitism. This is the case in particular for the strong association observed in the *micro-*

plankton between diatoms and an environmental lineage of choanoflagellates. Freshwater planktonic diatoms are known to sometimes have small bacterivorous choanoflagellates and bicoecids attached to them (Carrias *et al.*, 1998; Šimek *et al.*, 2004) and we believe the same epiphytic relationship may exist in the open ocean plankton between diatoms and this environmental choanoflagellate lineage. Significant scores could also be obtained for associations that are only indirect, for instance through an intermediate organism that is both the symbiont of a larger host and the host of a smaller symbiont.

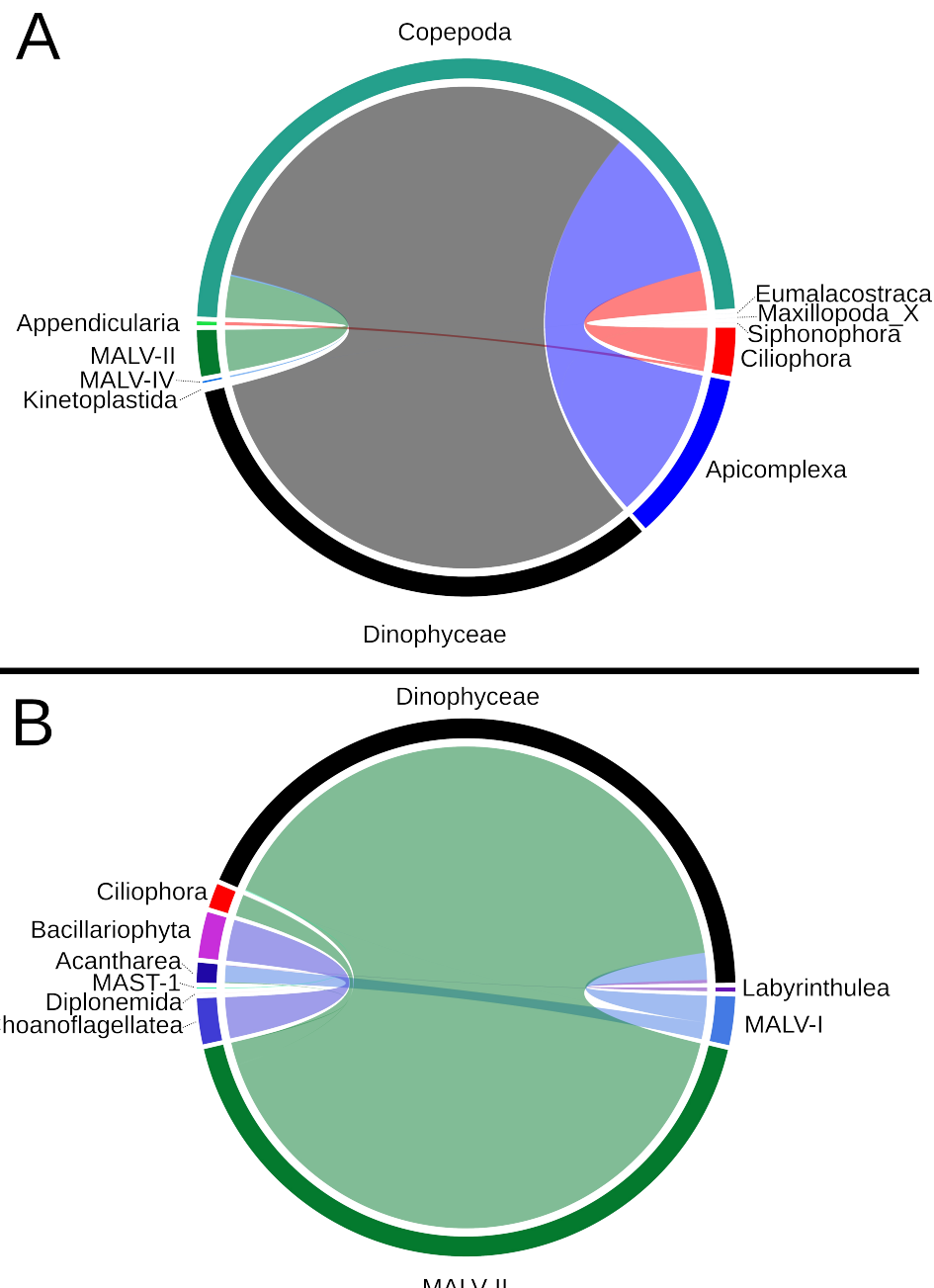


Figure 03: Global view of the patterns of co-occurrence that were recovered in our analyses for the meso-plankton (A) and the micro-plankton (B). Positive and significant associations between host groups (top) and putative symbiont groups (bottom) are represented at the level of taxogroups.

Inversely, the approach we have used will necessarily miss potential symbioses of interest because of the selection process that we used. For instance, we eliminated metabarcodes that showed a distribution profile supposedly typical of a free-living organism. Therefore in cases where a parasite/parasitoid would be about the same size as its host and restricted to the same size-fraction at all stages of its life cycle, it could not be detected. In addition, for now in the *meso*-plankton we focused only on metazoans as potential hosts and did not investigate large protists present in that size-fraction. Finally, to ensure statistically significant results we restricted our search for symbiont-host associations to genetic groups that were present in at least 20% of the samples. This implies that we are missing associations between hosts and symbionts that involve rarer organisms. This could explain why many documented host-parasitic relationships involving protists that we know to be present in the *Tara*-Oceans dataset were not recovered. For instance, many lineages of cercozoans (Rhizaria) are known parasites of various eukaryotes; in particular cryomonads like *Cryothecomonas* spp. can be parasitoids of diatoms (Thaler and Lovejoy, 2012), while ascetosporeans like *Paradinium* spp. are parasites of copepods (Skovgaard and Daugbjerg, 2008) and paramyxean like *Marteilia* spp. are parasites of benthic molluscs that infect planktonic copepods as obligatory intermediate hosts (Audemard *et al.*, 2002). These lineages are present and relatively diverse in the dataset (see Figure 1), but were not abundant enough to be tested. Finally, it is important to keep in mind that associations can only be detected when the infective stage of the parasite and the host co-occur in the samples. The *Tara* Oceans sampling was mostly done in the open ocean, but some of the potential parasites identified in the dataset could have predominantly benthic or coastal hosts (for instance perkinsids infecting bivalves; e.g. Chambouvet *et al.*, 2014). In that case the observed parasites may only represent "lost" dispersal stages that never actually meet the host they need to complete their life cycle.

Towards a better integration of parasites and parasitoids in ecological models

Many of the significant associations that we recovered correspond to well-known symbiotic relationships, as mentioned above. However we also uncovered a few intriguing novel associations between protist lineages that will warrant further scrutiny. The putatively entirely parasitic MALV-I and MALV-II alveolate lineages so far contain only few described members: *Ichthyodinium* (a parasite of fish; Skovgaard *et al.*, 2009) and *Euduboscquella* (a parasite of ciliates; Coats *et al.*, 2012; Harada *et al.*, 2007) belong to MALV-I, while *Amoebophrya* (a parasite of dinoflagellates; Guillou *et al.*, 2008) belongs to MALV-II.

However, the known genetic diversity of both lineages extends far beyond these three genera. Previous studies have shown that various radiolarian groups (Spumellaria, Nassellaria and Phaeodarea) can be associated with a large diversity of alveolates symbionts belonging to these two MALV lineages (Bråte *et al.*, 2012; Dolven *et al.*, 2007). Surprisingly, our results suggest that a stronger association can actually be found in the open ocean plankton between MALV-I symbionts and another clade of radiolarians, the Acantharea, which so far had not been linked to alveolate symbionts.

Associations involving labyrinthulean OTUs (with dinoflagellates and Acantharea) are also interesting: very little is known of these osmoheterotrophic, mostly marine and substrate-bound stramenopiles in planktonic habitats (Collado-Mercado *et al.*, 2010). Another stramenopile lineage showed up in our associations: the environmental MAST-1, correlating with dinoflagellates. Little is known of this stramenopile lineage, other than its members are aplastidic (heterotrophic) and some have been shown to be bacterial grazers (Massana *et al.*, 2014). Perhaps the most interesting association we uncovered is that between tintinnid ciliates and diplonemids, as the latter are the second most diverse group of protists in the open ocean plankton but have an unknown life style. This association does only concern a limited number of diplonemid metabarcodes, however, suggesting that if cases of parasitism exist among these planktonic diplonemids, they are exceptions rather than the rule. More likely the majority of these small flagellates are predators of algae. Another intriguing association uncovered in this study is that involving copepods and neobodonid Kinetoplastida, as these are so far not known to contain parasitic members (Simpson *et al.*, 2006). Finally, in the micro-plankton the second most abundant association we recovered (after that between MALV-II parasites and their dinoflagellate hosts) was that between diatoms and an environmental lineage of choanoflagellates, that we interpret as epiphytic mutualists or commensals. This association doesn't seem to be specific, because the concerned choanoflagellate metabarcodes correlated indiscriminately with both centric and pennate diatoms; it could however be quite widespread in the open ocean plankton.

Although parasitic/parasitoid organisms are found in all eukaryotic supergroups and all of them are represented in the *Tara-Oceans* dataset, myzozoan alveolates (which include dinoflagellates, apicomplexans and their relatives) clearly dominate this functional category in the open ocean plankton. This could be seen as a consequence of a key adaptive feature of Myzozoa, the apical complex, which ancestrally made these organisms able to feed by myzocytosis, i.e. by insertion of the cell apex into the surface of the prey cell to suck out their

cytoplasmic contents into food vacuoles, as opposed to the more widespread engulfment of whole cells by phagocytosis (Schnepf and Deichgräber, 1984; Cavalier-Smith and Chao, 2004). The apical complex was independently modified multiple times during myzozoan diversification in lineages that acquired a parasitic/parasitoid life style to become structures allowing infection of the host cell, as observed for instance in perkinsids, Syndiniales, and apicomplexans (Leander and Keeling, 2003; Gubbels and Duraisingham, 2012). This defining morphological feature of myzozoan alveolates thus seems to have enabled them to explore new life styles along the gradient from predators to parasites or parasitoids more successfully than any other major group of eukaryotes, at least in the plankton. It may also explain in part the very wide phylogenetic range of their possible preyhosts (from other alveolates to radiolarians and metazoans). The huge diversity and abundance of myzozoan OTUs in the *Tara-Oceans* dataset confirms earlier results hinting at the unrecognised ecological importance of these alveolates in marine habitats (Guillou *et al.*, 2008; Lie *et al.*, 2014).

Known types of symbiotic relationships between planktonic eukaryotes are numerous and sometimes elude classification into discrete categories such as mutualists, commensals, and parasites. Perhaps they would be more usefully considered as possible states along at least two overlapping gradients, one ranging from mutually beneficial symbioses to single-sided symbioses, and the other ranging from predator-prey relationships to parasitoid-host relationships (Taylor, 1982; Coats, 1999). The evolutionary success of planktonic lineages comprising relatively large organisms such as copepods, radiolarians, dinoflagellates, and diatoms must have enabled a huge diversification of smaller organisms that prey on them, parasitize them, live in mutually beneficial symbioses with them, or in some cases simply live on them commensally. Inversely, the various small symbionts, parasitoids, or predators that can be associated with these large organisms imply that multiple, contrasting evolutionary forces kept driving their diversification. These reflections, together with our results and that of a parallel study on photosymbioses (Henry *et al.*, in prep.), generally corroborate earlier suggestions that symbioses between eukaryotes are a key component of open ocean plankton communities, and that models of plankton ecology should better integrate them (Marcogliese and Cone, 1997; Hudson *et al.*, 2006; Gleason *et al.*, 2014; Bass *et al.*, 2015; Scholz *et al.*, 2016). This is especially true for parasites of marine planktonic eukaryotes, which are believed to play a key part in the regulation of host populations and general ecosystem equilibrium (Guillou *et al.*, 2008; Gleason *et al.*, 2013, 2015; Jephcott *et al.*, 2016), but remain critically less studied than other types of symbionts.

References

- AUDEMARD, Corinne, LE ROUX, Frédérique, BARNAUD, Antoine, *et al.* Needle in a haystack: involvement of the copepod *Paracartia grani* in the life-cycle of the oyster pathogen *Marteilia refringens*. *Parasitology*, 2002, vol. 124, no 03, p. 315-323.
- BASS, David, STENTIFORD, Grant D., LITTLEWOOD, D. T. J., *et al.* Diverse Applications of Environmental DNA Methods in Parasitology. *Trends in parasitology*, 2015, vol. 31, no 10, p. 499-513.
- BERNEY, Cédric, FAHRNI, José, et PAWLOWSKI, Jan. How many novel eukaryotic 'kingdoms'? Pitfalls and limitations of environmental DNA surveys. *BMC biology*, 2004, vol. 2, no 1, p. 13.
- BRÅTE, Jon, KRABBERØD, Anders K., DOLVEN, Jane K., *et al.* Radiolaria associated with large diversity of marine alveolates. *Protist*, 2012, vol. 163, no 5, p. 767-777.
- BRÅTE, Jon, LOGARES, Ramiro, BERNEY, Cédric, *et al.* Freshwater Perkinsea and marine-freshwater colonizations revealed by pyrosequencing and phylogeny of environmental rDNA. *The ISME journal*, 2010, vol. 4, no 9, p. 1144-1153.
- CARRIAS, Jean-François, AMBLARD, Christian, QUIBLIER-LLOBERAS, Catherine, *et al.* Seasonal dynamics of free and attached heterotrophic nanoflagellates in an oligomesotrophic lake. *Freshwater Biology*, 1998, vol. 39, no 1, p. 91-101.
- CAVALIER-SMITH, Thomas et CHAO, Ema E. Protalveolate phylogeny and systematics and the origins of Sporozoa and dinoflagellates (phylum Myzozoa nom. nov.). *European Journal of Protistology*, 2004, vol. 40, no 3, p. 185-212.
- CHAMBOUVET, Aurélie, BERNEY, Cédric, ROMAC, Sarah, *et al.* Diverse molecular signatures for ribosomally 'active' Perkinsea in marine sediments. *BMC microbiology*, 2014, vol. 14, no 1, p. 110.
- CHAUDHARY, Kshitiz et ROOS, David S. Protozoan genomics for drug discovery. *Nature biotechnology*, 2005, vol. 23, no 9, p. 1089-1091.
- CHEUNG, Man Kit, CHU, Ka Hou, LI, Chi Pang, *et al.* Genetic diversity of picoeukaryotes in a semi-enclosed harbour in the subtropical western Pacific Ocean. *Aquatic Microbial Ecology*, 2008, vol. 53, no 3, p. 295.
- COATS, D. Wayne. Parasitic Lite Styles of Marine Dinoflagellates. *Journal of Eukaryotic Microbiology*, 1999, vol. 46, p. 402-409.

- COATS, D. Wayne, BACHVAROFF, Tsvetan R., et DELWICHE, Charles F. Revision of the Family Duboscquellidae with Description of *Euduboscquella crenulata* n. gen., n. sp. (Dinoflagellata, Syndinea), an Intracellular Parasite of the Ciliate *Favella panamensis* Kofoed & Campbell. *Journal of Eukaryotic Microbiology*, 2012, vol. 59, no 1, p. 1-11.
- COLLADO-MERCADO, Enixy, RADWAY, JoAnn C., et COLLIER, Jackie L. Novel uncultivated labyrinthulomycetes revealed by 18S rDNA sequences from seawater and sediment samples. *Aquatic Microbial Ecology*, 2010, vol. 58, no 3, p. 215.
- DE VARGAS, Colomban, AUDIC, Stéphane, HENRY, Nicolas, et al. Eukaryotic plankton diversity in the sunlit ocean. *Science*, 2015, vol. 348, no 6237, p. 1261605.
- DOBSON, Andy, LAFFERTY, Kevin D., KURIS, Armand M., et al. Homage to Linnaeus: How many parasites? How many hosts?. *Proceedings of the National Academy of Sciences*, 2008, vol. 105, no Supplement 1, p. 11482-11489.
- DOLVEN, Jane K., LINDQVIST, Charlotte, ALBERT, Victor A., et al. Molecular diversity of alveolates associated with neritic North Atlantic radiolarians. *Protist*, 2007, vol. 158, no 1, p. 65-76.
- GLEASON, Frank H., JEPHCOTT, Thomas G., KÜPPER, Frithjof C., et al. Potential roles for recently discovered chytrid parasites in the dynamics of harmful algal blooms. *Fungal Biology Reviews*, 2015, vol. 29, no 1, p. 20-33.
- GLEASON, Frank H., LILJE, Osu, MARANO, Agostina V., et al. Ecological functions of zoosporic hyperparasites. *Frontiers in Microbiology*, 2014, vol. 5, p. 244.
- GLEASON, Frank H., VAN OGTROP, Floris, LILJE, Osu, et al. Ecological roles of zoosporic parasites in blue carbon ecosystems. *Fungal Ecology*, 2013, vol. 6, no 5, p. 319-327.
- GÓMEZ, Fernando, MOREIRA, David, et LÓPEZ-GARCÍA, Purificación. Life cycle and molecular phylogeny of the dinoflagellates *Chytriodinium* and *Dissodinium*, ectoparasites of copepod eggs. *European journal of protistology*, 2009, vol. 45, no 4, p. 260-270.
- GRIMES, Barbara Hartley et BRADBURY, Phyllis Clarke. The biology of *Vampyrophrya pelagica* (Chatton & Lwoff, 1930), a histophagous apostome ciliate associated with marine calanoid copepods. *The Journal of protozoology*, 1992, vol. 39, no 1, p. 65-79.
- GUBBELS, Marc-Jan et DURAISINGH, Manoj T. Evolution of apicomplexan secretory organelles. *International journal for parasitology*, 2012, vol. 42, no 12, p. 1071-1081.

- GUILLOU, Laure, VIPREY, Manon, CHAMBOUVET, A., *et al.* Widespread occurrence and genetic diversity of marine parasitoids belonging to Syndiniales (Alveolata). *Environmental Microbiology*, 2008, vol. 10, no 12, p. 3349-3365.
- HARADA, Ai, OHTSUKA, Susumu, et Horiguchi, Takeo. Species of the parasitic genus *Duboscquella* are members of the enigmatic Marine Alveolate Group I. *Protist*, 2007, vol. 158, no 3, p. 337-347.
- HARTIKAINEN, Hanna, ASHFORD, Oliver S., BERNEY, Cédric, *et al.* Lineage-specific molecular probing reveals novel diversity and ecological partitioning of haplosporidians. *The ISME journal*, 2014a, vol. 8, no 1, p. 177-186.
- HARTIKAINEN, Hanna, STENTIFORD, Grant D., BATEMAN, Kelly S., *et al.* Mikrocystids are a broadly distributed and divergent radiation of parasites in aquatic invertebrates. *Current Biology*, 2014b, vol. 24, no 7, p. 807-812.
- HENRY, Nicolas, DECELLE, Johan, RICHTER Daniel J., *et al..* Unveiling photosymbiotic associations across phylogenetic gradients in world-wide marine plankton based on massive eukaryotic rDNA metabarcoding. *In preparation.*
- HUDSON, Peter J., DOBSON, Andrew P., et LAFFERTY, Kevin D. Is a healthy ecosystem one that is rich in parasites?. *Trends in Ecology & Evolution*, 2006, vol. 21, no 7, p. 381-385.
- JEPHCOTT, Thomas G., ALVES-DE-SOUZA, Catharina, GLEASON, Frank H., *et al.* Ecological impacts of parasitic chytrids, syndiniales and perkinsids on populations of marine photosynthetic dinoflagellates. *Fungal Ecology*, 2016, vol 19, p. 47-58.
- KARSENTI, Eric, ACINAS, Silvia G., BORK, Peer, *et al.* A holistic approach to marine ecosystems biology. *PLoS biol*, 2011, vol. 9, no 10, p. e1001177.
- LARA, Enrique, MOREIRA, David, VERESHCHAKA, Alexander, *et al.* Pan-oceanic distribution of new highly diverse clades of deep-sea diplonemids. *Environmental microbiology*, 2009, vol. 11, no 1, p. 47-55.
- LEANDER, Brian S. et KEELING, Patrick J. Morphostasis in alveolate evolution. *Trends in Ecology & Evolution*, 2003, vol. 18, no 8, p. 395-402.
- LIE, Alle AY, LIU, Zhenfeng, HU, Sarah K., *et al.* Investigating microbial eukaryotic diversity from a global census: insights from a comparison of pyrotag and full-length sequences of 18S rRNA genes. *Applied and environmental microbiology*, 2014, vol. 80, no 14, p. 4363-4373.

- LÓPEZ-GARCÍA, Purificación et MOREIRA, David. Tracking microbial biodiversity through molecular and genomic ecology. *Research in microbiology*, 2008, vol. 159, no 1, p. 67-73.
- LUKEŠ, Julius, FLEGONTOVA, Olga, et HORÁK, Aleš. Diplonemids. *Current Biology*, 2015, vol. 25, no 16, p. R702-R704.
- MARCOGLIESE, David J. et CONE, David K. Food webs: a plea for parasites. *Trends in Ecology & Evolution*, 1997, vol. 12, no 8, p. 320-325.
- MASSANA, Ramon, DEL CAMPO, Javier, SIERACKI, Michael E., et al. Exploring the uncultured microeukaryote majority in the oceans: reevaluation of ribogroups within stramenopiles. *The ISME journal*, 2014, vol. 8, no 4, p. 854-866.
- MASSANA, Ramon et PEDRÓS-ALIÓ, Carlos. Unveiling new microbial eukaryotes in the surface ocean. *Current opinion in microbiology*, 2008, vol. 11, no 3, p. 213-218.
- MOREIRA, David et LÓPEZ-GARCÍA, Purificación. The molecular ecology of microbial eukaryotes unveils a hidden world. *Trends in microbiology*, 2002, vol. 10, no 1, p. 31-38.
- POULIN, Robert. Parasite biodiversity revisited: frontiers and constraints. *International journal for parasitology*, 2014, vol. 44, no 9, p. 581-589.
- POULIN, Robert et MORAND, Serge. The diversity of parasites. *Quarterly Review of Biology*, 2000, p. 277-293.
- RICHARDS, Thomas A. et BASS, David. Molecular screening of free-living microbial eukaryotes: diversity and distribution using a meta-analysis. *Current opinion in microbiology*, 2005, vol. 8, no 3, p. 240-252.
- ROHDE, Klaus. Ecology and biogeography of marine parasites. *Advances in Marine Biology*, 2002, vol. 43, p. 1-83.
- RUECKERT, Sonja, SIMDYANOV, Timur G., ALEOSHIN, Vladimir V., et al. Identification of a divergent environmental DNA sequence clade using the phylogeny of gregarine parasites (Apicomplexa) from crustacean hosts. *PloS one*, 2011, vol. 6, no 3, p. e18163-e18163.
- SCHNEPF, E. et DEICHGRÄBER, G. “Myzocytosis”, a kind of endocytosis with implications to compartmentation in endosymbiosis. *Naturwissenschaften*, 1984, vol. 71, no 4, p. 218-219.
- SCHOLZ, Bettina, GUILLOU, Laure, MARANO, Agostina V., et al. Zoosporic parasites infecting marine diatoms—A black box that needs to be opened. *Fungal Ecology*, 2016, vol. 19, p. 59-76.

- ŠIMEK, Karel, JEZBERA, Jan, HORNÁK, Karel, et al. Role of diatom-attached choanoflagellates of the genus *Salpingoeca* as pelagic bacterivores. *Aquatic microbial ecology*, 2004, vol. 36, no 3, p. 257-269.
- SIMPSON, Alastair GB, STEVENS, Jamie R., et LUKEŠ, Julius. The evolution and diversity of kinetoplastid flagellates. *Trends in parasitology*, 2006, vol. 22, no 4, p. 168-174.
- SKOVGAARD, Alf, MASSANA, Ramon, BALAGUÉ, Vanessa, et al. Phylogenetic position of the copepod-infesting parasite *Syndinium turbo* (Dinoflagellata, Syndinea). *Protist*, 2005, vol. 156, no 4, p. 413-423.
- SKOVGAARD, Alf et DAUGBJERG, Niels. Identity and systematic position of *Paradinium poucheti* and other *Paradinium*-like parasites of marine copepods based on morphology and nuclear-encoded SSU rDNA. *Protist*, 2008, vol. 159, no 3, p. 401-413.
- SKOVGAARD, Alf, KARPOV, Sergey A., et GUILLOU, Laure. The Parasitic Dinoflagellates Blastodinium spp. Inhabiting the Gut of Marine, Planktonic Copepods: Morphology, Ecology, and Unrecognized Species Diversity. *Frontiers in Microbiology*, 2012, vol. 3, p. 305.
- SKOVGAARD, Alf, MENESSES, Isabel, et ANGÉLICO, Maria Manuel. Identifying the lethal fish egg parasite *Ichthyodinium chabardi* as a member of Marine Alveolate Group I. *Environmental microbiology*, 2009, vol. 11, no 8, p. 2030-2041.
- STENTIFORD, Grant D., FEIST, Stephen W., STONE, David M., et al. Policy, phylogeny, and the parasite. *Trends in parasitology*, 2014, vol. 30, no 6, p. 274-281.
- TAYLOR, F. J. R. Symbioses in marine microplankton. *Ann. Inst. Oceanogr.(Paris)*, 1982, vol. 58, p. 61-91.
- THALER, Mary et LOVEJOY, Connie. Distribution and diversity of a protist predator *Cryothecomonas* (Cercozoa) in Arctic marine waters. *Journal of Eukaryotic Microbiology*, 2012, vol. 59, no 4, p. 291-299.
- WINDSOR, Donald A. Controversies in parasitology, Most of the species on Earth are parasites. *International journal for parasitology*, 1998, vol. 28, no 12, p. 1939-1941.
- YABUKI, Akinori et TAME, Akihiro. Phylogeny and Reclassification of *Hemistasia phaeocysticola* (Scherffel) Elbrächter & Schnepf, 1996. *Journal of Eukaryotic Microbiology*, 2015, vol. 62, no 3, p. 426-429.

Supplementary information

Table S01: OTUs richness by taxogroups and functional annotation into three main categories (see Figure 1).

Category	Taxogroup	OTUs
1 - free-living life style	Alveolata - Dinophyceae	28,615
1 - free-living life style	Rhizaria - Collodaria	18,032
1 - free-living life style	Stramenopiles - Bacillariophyta	8,788
1 - free-living life style	Alveolata - Ciliophora	3,428
1 - free-living life style	Archaeplastida - Chlorophyceae	2,965
1 - free-living life style	Rhizaria - Foraminifera	1,414
1 - free-living life style	incertae sedis - Haptophyta	1,389
1 - free-living life style	Rhizaria - Acantharea	1,293
1 - free-living life style	Opisthokonts - Ascomycota	960
1 - free-living life style	Opisthokonts - Basidiomycota	884
1 - free-living life style	Stramenopiles - Labyrinthulea	847
1 - free-living life style	Rhizaria - other filosans*	789
1 - free-living life style	Rhizaria - Spumellaria	725
1 - free-living life style	Archaeplastida - Mamiellophyceae	712
1 - free-living life style	Archaeplastida - Rhodophyta	639
1 - free-living life style	incertae sedis - Katablepharidida	627
1 - free-living life style	Amoebozoa - Tubulinea	613
1 - free-living life style	Stramenopiles - Dictyochophyceae	609
1 - free-living life style	Archaeplastida - Trebouxiophyceae	573
1 - free-living life style	incertae sedis - Cryptophyta	530
1 - free-living life style	incertae sedis - Picomonadida	495
1 - free-living life style	Excavates - Kinetoplastida	476
1 - free-living life style	Stramenopiles - Chrysophyceae	470
1 - free-living life style	Rhizaria - RAD-B (Sticholonche & relatives)	465
1 - free-living life style	Archaeplastida - other core chlorophytes	444
1 - free-living life style	Excavates - Heterolobosea	441
1 - free-living life style	Archaeplastida - Ulvophyceae	436
1 - free-living life style	Rhizaria - Nassellaria & Eucyrtidium*	435
1 - free-living life style	Archaeplastida - Prasinophyceae clade 7	391
1 - free-living life style	incertae sedis - Telonemida	389
1 - free-living life style	Rhizaria - Phaeodaria	374
1 - free-living life style	Archaeplastida - Streptophyta	368
1 - free-living life style	Excavates - Euglenida	350
1 - free-living life style	Stramenopiles - other Ochrophyta*	339
1 - free-living life style	Stramenopiles - Bicoecea	286
1 - free-living life style	Rhizaria - RAD-A	258
1 - free-living life style	Stramenopiles - Pelagophyceae	255
1 - free-living life style	Opisthokonts - Choanoflagellatea	248
1 - free-living life style	Amoebozoa - Macromycetozoa	246
1 - free-living life style	incertae sedis - Centrohelida	197
1 - free-living life style	Rhizaria - Chlorarachnea	185
1 - free-living life style	Stramenopiles - Oomycota	177
1 - free-living life style	Archaeplastida - Pyramimonadales	160
1 - free-living life style	Archaeplastida - other prasinophytes	138
1 - free-living life style	Rhizaria - Cryomonadida	122
1 - free-living life style	incertae sedis - apusozoans*	119
1 - free-living life style	Rhizaria - other endomyxans*	108
1 - free-living life style	Rhizaria - Ebrida	95
1 - free-living life style	Alveolata - chromerids & colpodellids*	86
1 - free-living life style	Opisthokonts - Chytridiomycota	79
1 - free-living life style	Stramenopiles - Bolidophyceae & relatives	74
1 - free-living life style	Stramenopiles - other heterotrophic stramenopiles*	70
1 - free-living life style	Amoebozoa - other Lobosa	61
1 - free-living life style	Amoebozoa - Variosea	61
1 - free-living life style	Stramenopiles - Phaeophyceae	45
1 - free-living life style	Stramenopiles - MOCH-3	43
1 - free-living life style	Opisthokonts - other low er Fungi*	41
1 - free-living life style	Stramenopiles - Raphidophyceae	41
1 - free-living life style	Amoebozoa - Vannellida	28
1 - free-living life style	Stramenopiles - MOCH-1, 2	26
1 - free-living life style	Stramenopiles - Pinguiphycaceae	25
1 - free-living life style	Amoebozoa - Dactylopodida	23

Table S01 (continued)

Category	Taxogroup	OTUs
1 - free-living life style	Stramenopiles - MOCH-5	23
1 - free-living life style	Alveolata - other myzozoans*	20
1 - free-living life style	Stramenopiles - MOCH-4	16
1 - free-living life style	Excavates - Jakobida	9
1 - free-living life style	incertae sedis - other eukaryotes*	8
1 - free-living life style	Opisthokonts - Mesomycetozoa*	2
1 - free-living life style	Rhizaria - RAD-C	1
2 - parasitic, parasitoid, or amphizoic life style	Alveolata - core Apicomplexa	3,402
2 - parasitic, parasitoid, or amphizoic life style	Alveolata - MALV-I + MALV-IV	2,215
2 - parasitic, parasitoid, or amphizoic life style	Alveolata - MALV-II	2,125
2 - parasitic, parasitoid, or amphizoic life style	Alveolata - Dinophyceae	1,506
2 - parasitic, parasitoid, or amphizoic life style	Rhizaria - Ascetospora	485
2 - parasitic, parasitoid, or amphizoic life style	Amoebozoa - Vannellida	264
2 - parasitic, parasitoid, or amphizoic life style	Opisthokonts - Mesomycetozoa*	227
2 - parasitic, parasitoid, or amphizoic life style	Opisthokonts - Microsporidiomycota	226
2 - parasitic, parasitoid, or amphizoic life style	Amoebozoa - Dactylopodida	185
2 - parasitic, parasitoid, or amphizoic life style	Alveolata - Ciliophora	154
2 - parasitic, parasitoid, or amphizoic life style	Amoebozoa - other Lobosa	152
2 - parasitic, parasitoid, or amphizoic life style	Alveolata - Perkinsa	118
2 - parasitic, parasitoid, or amphizoic life style	Stramenopiles - Oomycota	102
2 - parasitic, parasitoid, or amphizoic life style	Stramenopiles - Labyrinthulea	96
2 - parasitic, parasitoid, or amphizoic life style	Opisthokonts - other low er Fungi*	89
2 - parasitic, parasitoid, or amphizoic life style	Opisthokonts - Ascomycota	76
2 - parasitic, parasitoid, or amphizoic life style	Rhizaria - Phytomyxea & relatives	66
2 - parasitic, parasitoid, or amphizoic life style	Excavates - Kinetoplastida	65
2 - parasitic, parasitoid, or amphizoic life style	Amoebozoa - Tubulinea	54
2 - parasitic, parasitoid, or amphizoic life style	Stramenopiles - Pirsonia lineage	44
2 - parasitic, parasitoid, or amphizoic life style	Alveolata - other myzozoans*	43
2 - parasitic, parasitoid, or amphizoic life style	Rhizaria - other filosans*	26
2 - parasitic, parasitoid, or amphizoic life style	Rhizaria - Cryomonadida	13
2 - parasitic, parasitoid, or amphizoic life style	Excavates - Heterolobosea	6
2 - parasitic, parasitoid, or amphizoic life style	Amoebozoa - Variosea	1
2 - parasitic, parasitoid, or amphizoic life style	Opisthokonts - Cristidiscoidea	1
2 - parasitic, parasitoid, or amphizoic life style	Opisthokonts - Cryptomycota	1
2 - parasitic, parasitoid, or amphizoic life style	Excavates - Diplonemida	30,509
2 - parasitic, parasitoid, or amphizoic life style	Alveolata - Dinophyceae	10,159
2 - parasitic, parasitoid, or amphizoic life style	Stramenopiles - MAST-3, 12	1,137
3 - unknown life style	Stramenopiles - MAST-4, 6, 7, 8, 9, 10, 11	803
3 - unknown life style	Rhizaria - other filosans*	523
3 - unknown life style	Rhizaria - Cryomonadida	430
3 - unknown life style	Stramenopiles - MAST-1	325
3 - unknown life style	incertae sedis - other eukaryotes*	132
3 - unknown life style	Rhizaria - Ebriida	113
3 - unknown life style	Opisthokonts - Choanoflagellatea	111
3 - unknown life style	Stramenopiles - other MASTs*	108
3 - unknown life style	Alveolata - Perkinsa	71
3 - unknown life style	Rhizaria - other endomycxans*	71
3 - unknown life style	Alveolata - MALV-III	60
3 - unknown life style	Alveolata - MALV-V	47
3 - unknown life style	Stramenopiles - MAST-16, 22, 24	46
3 - unknown life style	Excavates - Kinetoplastida	39
3 - unknown life style	Opisthokonts - Cristidiscoidea	31
3 - unknown life style	Rhizaria - Chlorarachnea	28
3 - unknown life style	Rhizaria - Phytomyxea & relatives	16
3 - unknown life style	Opisthokonts - Cryptomycota	15
3 - unknown life style	Amoebozoa - other Lobosa	13
3 - unknown life style	Amoebozoa - environmental lineage LKM74	11
3 - unknown life style	Alveolata - Ciliophora	9
3 - unknown life style	Alveolata - other myzozoans*	9
3 - unknown life style	Amoebozoa - Dactylopodida	5
3 - unknown life style	Rhizaria - Ascetospora	4
3 - unknown life style	Alveolata - chromerids & colpodellids*	1

Table S02: Summary of the positive and significant associations found for the meso-plancton (see Figure 3A). When the taxonomic assignment was not accurate enough to link a metabarcode to a genus, the “host genus” and “symbiont genus” fields indicate the next most precise taxonomic rank available.

Symbiont taxogroup	Symbiont genus	Host taxogroup	Host genus	Number of associations
Ciliophora	<i>Gymnodinioides</i>	Appendicularia	Appendicularia_X	146
Ciliophora	<i>Gymnodinioides</i>	Copepoda	<i>Oncaeaa</i>	54
Ciliophora	<i>Hyalophysa</i>	Copepoda	<i>Gaetanus</i>	124
Ciliophora	<i>Hyalophysa</i>	Copepoda	Calanoida	107
Ciliophora	<i>Hyalophysa</i>	Copepoda	Calanidae	49
Ciliophora	<i>Hyalophysa</i>	Copepoda	<i>Neocalanus</i>	11
Ciliophora	<i>Hyalophysa</i>	Copepoda	<i>Euchaeta</i>	2
Ciliophora	Oligohymenophorea	Copepoda	<i>Oncaeaa</i>	18
Ciliophora	<i>Paracineta</i>	Copepoda	<i>Euchaeta</i>	18
Ciliophora	<i>Paracineta</i>	Copepoda	<i>Gaetanus</i>	1
Ciliophora	<i>Vampyrophrya</i>	Copepoda	<i>Acartia</i>	6,414
Ciliophora	<i>Vampyrophrya</i>	Copepoda	Calanoida_X	5,988
Ciliophora	<i>Vampyrophrya</i>	Copepoda	<i>Temora</i>	5,085
Ciliophora	<i>Vampyrophrya</i>	Copepoda	Calanidae	4,122
Ciliophora	<i>Vampyrophrya</i>	Copepoda	Paracalanidae_X	2,631
Ciliophora	<i>Vampyrophrya</i>	Appendicularia	Appendicularia_X	2,190
Ciliophora	<i>Vampyrophrya</i>	Copepoda	<i>Oncaeaa</i>	1,602
Ciliophora	<i>Vampyrophrya</i>	Copepoda	Calanoida	427
Ciliophora	<i>Vampyrophrya</i>	Copepoda	<i>Euchaeta</i>	74
Ciliophora	<i>Vampyrophrya</i>	Copepoda	<i>Neocalanus</i>	30
Ciliophora	<i>Vampyrophrya</i>	Maxillopoda	Maxillopoda	20
Ciliophora	<i>Vampyrophrya</i>	Maxillopoda	Maxillopoda_X	20
Ciliophora	<i>Vampyrophrya</i>	Copepoda	<i>Subeucalanus</i>	10
Ciliophora	<i>Vampyrophrya</i>	Eumalacostraca	Eumalacostraca	8
Ciliophora	<i>Vampyrophrya</i>	Copepoda	<i>Paracalanus</i>	1
core Apicomplexa	Piroplasmida_X	Copepoda	Paracalanidae_X	147
core Apicomplexa	Piroplasmida_X	Copepoda	Calanoida	16
core Apicomplexa	Piroplasmida_X	Copepoda	Calanidae	2
core Apicomplexa	Piroplasmida_X	Copepoda	<i>Neocalanus</i>	1
core Apicomplexa	Thiriotia_lineage	Copepoda	<i>Oncaeaa</i>	1,839
core Apicomplexa	Thiriotia_lineage	Copepoda	Copepoda_X	1,250
core Apicomplexa	Thiriotia_lineage	Copepoda	Copepoda	12
core Apicomplexa	Thiriotia_lineage_X	Copepoda	<i>Oncaeaa</i>	58,848
core Apicomplexa	Thiriotia_lineage_X	Copepoda	Copepoda_X	40,000
core Apicomplexa	Thiriotia_lineage_X	Copepoda	Copepoda	384
Dinophyceae	<i>Blastodinium</i>	Copepoda	Copepoda	123,602
Dinophyceae	<i>Blastodinium</i>	Copepoda	<i>Corycaeus</i>	46,134
Dinophyceae	<i>Blastodinium</i>	Copepoda	<i>Oncaeaa</i>	18,880
Dinophyceae	<i>Blastodinium</i>	Copepoda	Copepoda_X	11,250
Dinophyceae	<i>Blastodinium</i>	Copepoda	Calanoida_X	183
Dinophyceae	<i>Blastodinium</i>	Copepoda	<i>Acartia</i>	68
Dinophyceae	<i>Blastodinium</i>	Copepoda	Calanoida	43
Dinophyceae	<i>Blastodinium</i>	Copepoda	Paracalanidae_X	41
Dinophyceae	<i>Blastodinium</i>	Copepoda	Calanidae	24
Dinophyceae	<i>Blastodinium</i>	Copepoda	<i>Subeucalanus</i>	3
Dinophyceae	Blastodinium_02	Copepoda	<i>Oncaeaa</i>	3,678
Dinophyceae	Blastodinium_02	Copepoda	Copepoda_X	2,500
Dinophyceae	Blastodinium_02	Copepoda	Copepoda	24
Dinophyceae	<i>Chytriodinium</i>	Copepoda	<i>Oncaeaa</i>	2,892
Dinophyceae	<i>Chytriodinium</i>	Copepoda	Calanidae	814
Dinophyceae	<i>Chytriodinium</i>	Copepoda	<i>Acartia</i>	728
Dinophyceae	<i>Chytriodinium</i>	Copepoda	Paracalanidae_X	570
Dinophyceae	<i>Chytriodinium</i>	Copepoda	Calanoida	46
Dinophyceae	<i>Chytriodinium</i>	Copepoda	Calanoida_X	18
Dinophyceae	<i>Chytriodinium</i>	Copepoda	<i>Neocalanus</i>	6
Dinophyceae	<i>Chytriodinium</i>	Maxillopoda	Maxillopoda	4
Dinophyceae	<i>Chytriodinium</i>	Maxillopoda	Maxillopoda_X	4
Dinophyceae	<i>Gymnodinium</i>	Copepoda	Calanoida_X	11,784
Dinophyceae	<i>Gymnodinium</i>	Copepoda	<i>Acartia</i>	4,896

Table S02 (continued)

Symbiont taxogroup	Symbiont genus	Host taxogroup	Host genus	Number of associations
Dinophyceae	<i>Gymnodinium</i>	Copepoda	Paracalanidae_X	3,576
Dinophyceae	<i>Gymnodinium</i>	Copepoda	Copepoda	1,367
Dinophyceae	<i>Gymnodinium</i>	Copepoda	Calanoida	576
Dinophyceae	<i>Gymnodinium</i>	Copepoda	<i>Oncaeaa</i>	432
Dinophyceae	<i>Gymnodinium</i>	Copepoda	Calanidae	48
Dinophyceae	<i>Gymnodinium</i>	Copepoda	<i>Neocalanus</i>	24
Dinophyceae	<i>Pelagodinium</i>	Copepoda	<i>Oncaeaa</i>	34,941
Dinophyceae	<i>Pelagodinium</i>	Copepoda	Copepoda	26,201
Dinophyceae	<i>Pelagodinium</i>	Copepoda	Copepoda_X	23,750
Dinophyceae	<i>Pelagodinium</i>	Copepoda	Calanidae	430
Dinophyceae	<i>Pelagodinium</i>	Copepoda	<i>Acartia</i>	428
Dinophyceae	<i>Pelagodinium</i>	Copepoda	Calanoida_X	187
Dinophyceae	<i>Pelagodinium</i>	Copepoda	Paracalanidae_X	153
Dinophyceae	<i>Pelagodinium</i>	Copepoda	Calanoida	43
Dinophyceae	<i>Pelagodinium</i>	Copepoda	<i>Candacia</i>	5
Dinophyceae	<i>Pelagodinium</i>	Copepoda	<i>Neocalanus</i>	3
Dinophyceae	<i>Pelagodinium</i>	Maxillopoda	Maxillopoda	2
Dinophyceae	<i>Pelagodinium</i>	Maxillopoda	Maxillopoda_X	2
Dinophyceae	<i>Pelagodinium</i>	Copepoda	<i>Subeucalanus</i>	1
Dinophyceae	Peridiniales	Copepoda	<i>Oncaeaa</i>	4,609
Dinophyceae	Peridiniales	Copepoda	Calanidae	405
Dinophyceae	Peridiniales	Copepoda	Paracalanidae_X	34
Dinophyceae	Peridiniales	Copepoda	Calanoida	3
Dinophyceae	Peridiniales	Maxillopoda	Maxillopoda	2
Dinophyceae	Peridiniales	Maxillopoda	Maxillopoda_X	2
Dinophyceae	Peridiniales	Copepoda	<i>Neocalanus</i>	2
Dinophyceae	Peridiniales	Copepoda	Calanoida_X	1
Dinophyceae	<i>Pyrocystis</i>	Copepoda	Calycophorae	68
Dinophyceae	<i>Pyrocystis</i>	Siphonophora	Siphonophora	1
Kinetoplastida	<i>Neobodo</i>	Copepoda	<i>Corycaeus</i>	7
Kinetoplastida	<i>Neobodo</i>	Copepoda	<i>Euchaeta</i>	7
MALV-IV	<i>Hematodinium</i>	Copepoda	<i>Gaetanus</i>	248
MALV-IV	<i>Hematodinium</i>	Copepoda	Calanoida	214
MALV-IV	<i>Hematodinium</i>	Copepoda	<i>Neocalanus</i>	18
MALV-IV	<i>Hematodinium</i>	Copepoda	<i>Euchaeta</i>	4
MALV-IV	<i>Syndinium</i>	Copepoda	Calanidae	405
MALV-IV	<i>Syndinium</i>	Copepoda	Calanoida_X	65
MALV-IV	<i>Syndinium</i>	Copepoda	<i>Acartia</i>	54
MALV-IV	<i>Syndinium</i>	Eumalacostraca	Eumalacostraca	53
MALV-IV	<i>Syndinium</i>	Copepoda	<i>Oncaeaa</i>	25
MALV-IV	<i>Syndinium</i>	Copepoda	Calanoida	9
MALV-IV	<i>Syndinium</i>	Maxillopoda	Maxillopoda	2
MALV-IV	<i>Syndinium</i>	Maxillopoda	Maxillopoda_X	2
MALV-IV	<i>Syndinium</i>	Copepoda	<i>Neocalanus</i>	2
MALV-IV	<i>Syndinium</i>	Copepoda	Copepoda	1
MALV-IV	<i>Syndinium</i>	Copepoda	Paracalanidae_X	1
MALV-II	<i>Amoebophrya</i>	Copepoda	<i>Oncaeaa</i>	5,517
MALV-II	<i>Amoebophrya</i>	Copepoda	Copepoda_X	3,750
MALV-II	<i>Amoebophrya</i>	Copepoda	Copepoda	36
MALV-II	Malv_II_clade_04_X	Copepoda	<i>Oncaeaa</i>	11,034
MALV-II	Malv_II_clade_04_X	Copepoda	Copepoda_X	7,500
MALV-II	Malv_II_clade_04_X	Copepoda	Copepoda	72

Table S03: Summary of the positive and significant associations found for the microplancton (see Figure 3B). Same convention as in Table S02 for the “host genus” and “symbiont genus” fields.

Symbiont taxogroup	Symbiont genus	Host taxogroup	Host genus	Number of associations
Choanoflagellatea	Choanozoa_U1_X1	Bacillariophyta	Bacillariophyceae	471
Choanoflagellatea	Choanozoa_U1_X1	Bacillariophyta	Mediophyceae	342
Choanoflagellatea	Choanozoa_U1_X1	Bacillariophyta	<i>Chaetoceros</i>	288
Choanoflagellatea	Choanozoa_U1_X1	Bacillariophyta	<i>Planktoniella</i>	174
Choanoflagellatea	Choanozoa_U1_X1	Bacillariophyta	Bacillariophyceae_X	153
Choanoflagellatea	Choanozoa_U1_X1	Bacillariophyta	<i>Thalassiosira</i>	111
Choanoflagellatea	Choanozoa_U1_X1	Bacillariophyta	<i>Pseudo-nitzschia</i>	78
Choanoflagellatea	Choanozoa_U1_X1	Bacillariophyta	Rhizosolenids_X	63
Choanoflagellatea	Choanozoa_U1_X1	Bacillariophyta	<i>Proboscia</i>	57
Choanoflagellatea	Choanozoa_U1_X1	Bacillariophyta	<i>Eucampia</i>	39
Choanoflagellatea	Choanozoa_U1_X1	Bacillariophyta	Bacillariophyta	30
Choanoflagellatea	Choanozoa_U1_X1	Bacillariophyta	<i>Fragilaropsis</i>	27
Choanoflagellatea	Choanozoa_U1_X1	Bacillariophyta	<i>Rhizosolenia</i>	27
Choanoflagellatea	Choanozoa_U1_X1	Bacillariophyta	<i>Guinardia</i>	21
Choanoflagellatea	Choanozoa_U1_X1	Bacillariophyta	<i>Synedra</i>	21
Choanoflagellatea	Choanozoa_U1_X1	Bacillariophyta	Mediophyceae_X	18
Choanoflagellatea	Choanozoa_U1_X1	Bacillariophyta	<i>Navicula</i>	15
Choanoflagellatea	Choanozoa_U1_X1	Bacillariophyta	<i>Corethron</i>	9
Choanoflagellatea	Choanozoa_U1_X1	Bacillariophyta	<i>Cymbella</i>	9
Choanoflagellatea	Choanozoa_U1_X1	Bacillariophyta	<i>Dactyliosolen</i>	9
Choanoflagellatea	Choanozoa_U1_X1	Bacillariophyta	<i>Skeletonema</i>	9
Choanoflagellatea	Choanozoa_U1_X1	Bacillariophyta	Bacillariophytina	6
Choanoflagellatea	Choanozoa_U1_X1	Bacillariophyta	<i>Biddulphia</i>	6
Choanoflagellatea	Choanozoa_U1_X1	Bacillariophyta	<i>Cylindrotheca</i>	6
Choanoflagellatea	Choanozoa_U1_X1	Bacillariophyta	<i>Haslea</i>	6
Choanoflagellatea	Choanozoa_U1_X1	Bacillariophyta	<i>Leptocylindrus</i>	6
Choanoflagellatea	Choanozoa_U1_X1	Bacillariophyta	<i>Pleurosigma</i>	6
Choanoflagellatea	Choanozoa_U1_X1	Bacillariophyta	Rhizosolenids	6
Choanoflagellatea	Choanozoa_U1_X1	Bacillariophyta	<i>Amphiprora</i>	3
Choanoflagellatea	Choanozoa_U1_X1	Bacillariophyta	<i>Cyclophora</i>	3
Choanoflagellatea	Choanozoa_U1_X1	Bacillariophyta	<i>Ditylum</i>	3
Choanoflagellatea	Choanozoa_U1_X1	Bacillariophyta	<i>Lithodesmium</i>	3
Choanoflagellatea	Choanozoa_U1_X1	Bacillariophyta	<i>Minidiscus</i>	3
Choanoflagellatea	Choanozoa_U1_X1	Bacillariophyta	<i>Odontella</i>	3
Choanoflagellatea	Choanozoa_U1_X1	Bacillariophyta	<i>Raphoneis</i>	3
Choanoflagellatea	Choanozoa_U1_X1	Bacillariophyta	<i>Salpingella</i>	5
Diplonemida	Diplonemida_X	Ciliophora	uncultured tintinnid ciliate	5
Diplonemida	Diplonemida_X	Ciliophora	<i>Peridinium_03</i>	69
Labyrinthulea	Labyrinthulea	Dinophyceae	Dinophyceae	12
Labyrinthulea	Labyrinthulea	Dinophyceae	Dorataspidae_E4	8
Labyrinthulea	Labyrinthulea	Dinophyceae	<i>Gyrodinium</i>	3
Labyrinthulea	Labyrinthulea	Acantharea	Acanthophracta_E3_X	2
Labyrinthulea	Labyrinthulea	Acantharea	<i>Hexaconus</i>	1
Labyrinthulea	Labyrinthulea	Dinophyceae	Peridiniales	1
Labyrinthulea	<i>Thraustochytrium</i>	Dinophyceae	Peridinium_03	69
Labyrinthulea	<i>Thraustochytrium</i>	Dinophyceae	Dinophyceae	12
Labyrinthulea	<i>Thraustochytrium</i>	Acantharea	Dorataspidae_E4	8
Labyrinthulea	<i>Thraustochytrium</i>	Dinophyceae	<i>Gyrodinium</i>	3
Labyrinthulea	<i>Thraustochytrium</i>	Acantharea	Acanthophracta_E3_X	2
Labyrinthulea	<i>Thraustochytrium</i>	Acantharea	<i>Hexaconus</i>	1
Labyrinthulea	<i>Thraustochytrium</i>	Dinophyceae	Peridiniales	1
MALV-I	Malv_I_clade_1_X	Acantharea	<i>Heteracon</i>	16
MALV-I	Malv_I_clade_1_X	Acantharea	Conaconidae_C3	13
MALV-I	Malv_I_clade_1_X	Acantharea	Conaconidae_C1	3
MALV-I	Malv_I_clade_1_X	Bacillariophyta	<i>Proboscia</i>	3
MALV-I	Malv_I_clade_1_X	Acantharea	Stauracanthidae_F3	3
MALV-I	Malv_I_clade_1_X	Acantharea	Chaunacanthida_C	2
MALV-I	Malv_I_clade_1_X	Acantharea	Acanthometridae_F3	1
MALV-I	Malv_I_clade_1_X	Acantharea	Acanthometridae_F3_X	1

Table S03 (continued)

Symbiont taxogroup	Symbiont genus	Host taxogroup	Host genus	Number of associations
MALV-I	Malv_I_clade_1_X	Acantharea	<i>Litholophus</i>	1
MALV-I	Malv_I_clade_2_X	Ciliophora	<i>Salpingella</i>	4
MALV-I	Malv_I_clade_3_X	Dinophyceae	<i>Peridinium_03</i>	345
MALV-I	Malv_I_clade_3_X	Dinophyceae	<i>Gymnodinium</i>	217
MALV-I	Malv_I_clade_3_X	Dinophyceae	<i>Dinophyceae</i>	184
MALV-I	Malv_I_clade_3_X	Acantharea	<i>Arthra_Symply_E1E2</i>	160
MALV-I	Malv_I_clade_3_X	Acantharea	<i>Heteracon</i>	128
MALV-I	Malv_I_clade_3_X	Acantharea	<i>Conaconidae_C3</i>	104
MALV-I	Malv_I_clade_3_X	Dinophyceae	AY664956_gen	43
MALV-I	Malv_I_clade_3_X	Dinophyceae	<i>Gyrodinium</i>	31
MALV-I	Malv_I_clade_3_X	Dinophyceae	AY664890_gen	24
MALV-I	Malv_I_clade_3_X	Acantharea	<i>Conaconidae_C1</i>	24
MALV-I	Malv_I_clade_3_X	Acantharea	<i>Acanthometridae_F3</i>	18
MALV-I	Malv_I_clade_3_X	Acantharea	<i>Chaunacanthida_C</i>	16
MALV-I	Malv_I_clade_3_X	Dinophyceae	<i>Peridiniales</i>	13
MALV-I	Malv_I_clade_3_X	Dinophyceae	AY664961_gen	10
MALV-I	Malv_I_clade_3_X	Dinophyceae	AY664900_gen	8
MALV-I	Malv_I_clade_3_X	Acantharea	<i>Litholophus</i>	8
MALV-I	Malv_I_clade_3_X	Acantharea	<i>Dorataspidae_E4</i>	6
MALV-I	Malv_I_clade_3_X	Dinophyceae	AY664964_gen	5
MALV-I	Malv_I_clade_3_X	Acantharea	<i>Acanthometridae_F3_X</i>	2
MALV-I	Malv_I_clade_3_X	Dinophyceae	<i>Gonyaulax</i>	2
MALV-I	Malv_I_clade_3_X	Acantharea	<i>Stauracanthidae_F3</i>	2
MALV-I	Malv_I_clade_4_X	Dinophyceae	<i>Peridinium_03</i>	69
MALV-I	Malv_I_clade_4_X	Dinophyceae	<i>Gymnodinium</i>	27
MALV-I	Malv_I_clade_4_X	Dinophyceae	<i>Dinophyceae</i>	25
MALV-I	Malv_I_clade_4_X	Acantharea	<i>Dorataspidae_E4</i>	8
MALV-I	Malv_I_clade_4_X	Dinophyceae	<i>Gyrodinium</i>	5
MALV-I	Malv_I_clade_4_X	Dinophyceae	AY664890_gen	3
MALV-I	Malv_I_clade_4_X	Dinophyceae	<i>Prorocentrum</i>	3
MALV-I	Malv_I_clade_4_X	Acantharea	<i>Acanthophracta_E3_X</i>	2
MALV-I	Malv_I_clade_4_X	Dinophyceae	AY664957_gen	2
MALV-I	Malv_I_clade_4_X	Dinophyceae	<i>Peridiniales</i>	2
MALV-I	Malv_I_clade_4_X	Dinophyceae	AY664956_gen	1
MALV-I	Malv_I_clade_4_X	Acantharea	<i>Hexaconus</i>	1
MALV-I	Malv_I_clade_5_X	Dinophyceae	<i>Dinophyceae</i>	8
MALV-I	Malv_I_clade_5_X	Dinophyceae	<i>Gyrodinium_05</i>	6
MALV-I	Malv_I_clade_5_X	Dinophyceae	AY664957_gen	2
MALV-I	Malv_L_X	Acantharea	<i>Stauracanthidae_F3</i>	300
MALV-I	Malv_L_X	Dinophyceae	<i>Pelagodinium</i>	285
MALV-II	Amoebophrya	Dinophyceae	AY664900_gen	8,832
MALV-II	Amoebophrya	Dinophyceae	<i>Dinophyceae</i>	2,688
MALV-II	Amoebophrya	Dinophyceae	<i>Peridinium_03</i>	2,208
MALV-II	Amoebophrya	Dinophyceae	<i>Gyrodinium</i>	1,312
MALV-II	Amoebophrya	Ciliophora	<i>Eutintinnus</i>	576
MALV-II	Amoebophrya	Dinophyceae	<i>Noctiluca</i>	320
MALV-II	Amoebophrya	Dinophyceae	<i>Peridiniales</i>	128
MALV-II	Amoebophrya	Dinophyceae	AY664890_gen	96
MALV-II	Amoebophrya	Dinophyceae	AY665026_gen	96
MALV-II	Amoebophrya	Dinophyceae	<i>Karlodinium</i>	96
MALV-II	Amoebophrya	Dinophyceae	<i>Prorocentrum</i>	96
MALV-II	Amoebophrya	Dinophyceae	AY664956_gen	64
MALV-II	Amoebophrya	Dinophyceae	AY664957_gen	32
MALV-II	Amoebophrya	Dinophyceae	<i>Azadinium</i>	32
MALV-II	Amoebophrya	Dinophyceae	<i>Blastodinium</i>	32
MALV-II	Amoebophrya	Dinophyceae	EF527108_gen	32
MALV-II	Amoebophrya	Dinophyceae	<i>Gymnodiniales</i>	32
MALV-II	Amoebophrya	Dinophyceae	Uncultured-X	32
MALV-II	Amoebophrya	Acantharea	<i>Conaconidae_C3</i>	23

Table S03 (continued)

Symbiont taxogroup	Symbiont genus	Host taxogroup	Host genus	Number of associations
MALV-II	Malv_II_clade_04	Dinophyceae	AY664900_gen	2,484
MALV-II	Malv_II_clade_04	Dinophyceae	Dinophyceae	756
MALV-II	Malv_II_clade_04	Dinophyceae	<i>Peridinium_03</i>	621
MALV-II	Malv_II_clade_04	Dinophyceae	<i>Gyrodinium</i>	369
MALV-II	Malv_II_clade_04	Ciliophora	<i>Eutintinnus</i>	162
MALV-II	Malv_II_clade_04	Dinophyceae	<i>Noctiluca</i>	90
MALV-II	Malv_II_clade_04	Dinophyceae	Peridiniales	36
MALV-II	Malv_II_clade_04	Dinophyceae	AY664890_gen	27
MALV-II	Malv_II_clade_04	Dinophyceae	AY665026_gen	27
MALV-II	Malv_II_clade_04	Dinophyceae	<i>Karlodinium</i>	27
MALV-II	Malv_II_clade_04	Dinophyceae	<i>Prorocentrum</i>	27
MALV-II	Malv_II_clade_04	Dinophyceae	AY664956_gen	18
MALV-II	Malv_II_clade_04	Dinophyceae	AY664957_gen	9
MALV-II	Malv_II_clade_04	Dinophyceae	<i>Azadinium</i>	9
MALV-II	Malv_II_clade_04	Dinophyceae	<i>Blastodinium</i>	9
MALV-II	Malv_II_clade_04	Dinophyceae	EF527108_gen	9
MALV-II	Malv_II_clade_04	Dinophyceae	Gymnodiniales	9
MALV-II	Malv_II_clade_04	Dinophyceae	Uncultured-X	9
MALV-II	Malv_II_clade_04	Acantharea	Conaconidae_C3	3
MALV-II	Malv_II_clade_04_X	Dinophyceae	AY664900_gen	5,244
MALV-II	Malv_II_clade_04_X	Dinophyceae	Dinophyceae	1,596
MALV-II	Malv_II_clade_04_X	Dinophyceae	<i>Peridinium_03</i>	1,311
MALV-II	Malv_II_clade_04_X	Dinophyceae	<i>Gyrodinium</i>	779
MALV-II	Malv_II_clade_04_X	Ciliophora	<i>Eutintinnus</i>	342
MALV-II	Malv_II_clade_04_X	Dinophyceae	<i>Noctiluca</i>	190
MALV-II	Malv_II_clade_04_X	Dinophyceae	Peridiniales	76
MALV-II	Malv_II_clade_04_X	Dinophyceae	AY664890_gen	57
MALV-II	Malv_II_clade_04_X	Dinophyceae	AY665026_gen	57
MALV-II	Malv_II_clade_04_X	Dinophyceae	<i>Karlodinium</i>	57
MALV-II	Malv_II_clade_04_X	Dinophyceae	<i>Prorocentrum</i>	57
MALV-II	Malv_II_clade_04_X	Dinophyceae	AY664956_gen	38
MALV-II	Malv_II_clade_04_X	Dinophyceae	AY664957_gen	19
MALV-II	Malv_II_clade_04_X	Dinophyceae	<i>Azadinium</i>	19
MALV-II	Malv_II_clade_04_X	Dinophyceae	<i>Blastodinium</i>	19
MALV-II	Malv_II_clade_04_X	Dinophyceae	EF527108_gen	19
MALV-II	Malv_II_clade_04_X	Dinophyceae	Gymnodiniales	19
MALV-II	Malv_II_clade_04_X	Dinophyceae	Uncultured-X	19
MALV-II	Malv_II_clade_04_X	Acantharea	Conaconidae_C3	15
MALV-II	Malv_II_clade_22_X	Acantharea	Dorataspidae_E4	7
MALV-II	Malv_II_X	Dinophyceae	<i>Gymnodinium</i>	7
MAST-1	MAST_1B_X	Dinophyceae	<i>Prorocentrum</i>	3
MAST-1	MAST_1B_X	Dinophyceae	AY664957_gen	2
MAST-1	MAST_1D_X	Dinophyceae	<i>Prorocentrum</i>	15
MAST-1	MAST_1D_X	Dinophyceae	Dinophyceae	12
MAST-1	MAST_1D_X	Dinophyceae	<i>Gyrodinium_05</i>	12
MAST-1	MAST_1D_X	Dinophyceae	AY664957_gen	10

Conclusion et perspectives

Les symbiotes au sens large (parasites ou mutualistes) sont des acteurs majeurs des écosystèmes planctoniques (Skovgaard, 2014; Decelle *et al.*, 2015). Les parasites, et plus particulièrement les parasitoïdes, redistribuent l'énergie au sein de ces systèmes à la manière des virus, et constituent, une force majeure permettant la remise à disposition de la matière organique accumulée par des organismes protégés des prédateurs grâce à des protections physiques (frustules des diatomées) ou chimiques (composés allélopathiques, composés secondaires) (Kagami *et al.*, 2007; Chambouvet *et al.*, 2008). De par leur abondance, leurs phases de dispersion peuvent représenter une part importante de l'alimentation de différents prédateurs planctoniques (copépodes, ciliés, dinoflagellés) (Salomon *et al.*, 2009; Siano *et al.*, 2011). Les photosymbiontes (mutualistes) quant à eux, permettent à des organismes hétérotrophes, généralement de grande taille, d'obtenir une partie de leur énergie par le biais de la photosynthèse (Decelle *et al.*, 2012; Probert *et al.*, 2014). Des géants du plancton de quelques millimètres (collodaires) participent alors de manière non négligeable à la production primaire et aux flux de carbone, particulièrement dans les environnements oligotrophes (Michaels *et al.*, 1995; Dennett *et al.*, 2002).

Les études présentées dans ce manuscrit mettent en évidence l'importante diversité et abondance des organismes en symbiose (de Vargas *et al.*, 2015b) dans le plancton (hôtes et symbiotes) mais illustrent aussi l'ampleur du manque de connaissance à leur sujet. L'étude par réseaux de cooccurrences des organismes des communautés planctoniques apparaît comme une manière rapide de détecter des associations symbiotiques (Lima-Mendez *et al.*, 2015). En effet, les symbiotes étant généralement de petite taille, leur présence dans les grandes fractions de taille serait en toute logique entièrement expliquée par la présence de leur hôtes. Cependant, du fait de la complexité des modes de vies symbiotiques et du nombre potentiel d'interactions, il s'avère être très difficile de détecter de nouvelles symbioses grâce aux réseaux de cooccurrences sans adaptation de la méthode au préalable. Les principaux obstacles à la détection de symbioses sont l'impossibilité de différencier une association symbiotique de la simple coprésence de deux organismes n'ayant aucun contact physique (niche écologique similaire) et la présence dans le plancton de symbioses peu spécifiques (Decelle *et al.*, 2012).

Le premier obstacle peut être surmonté en étudiant l'assignation taxinomique des deux entités statistiquement associées. Il est alors possible de retrouver des symbiotes ou des hôtes déjà connus et d'émettre des hypothèses sur la véracité des associations les impliquant avec des partenaires jusque là non décris comme étant en symbiose. Mais cette démarche est fastidieuse, particulièrement lorsqu'il s'agit d'analyser plusieurs milliers d'associations (Lima-Mendez *et al.*, 2015). De plus, lorsque le réseau de cooccurrences a été généré à partir de données de metabarcoding, il est délicat et réducteur de travailler avec l'assignation taxinomique car une proportion non négligeable des metabarcodes (correspondant aux nœuds dans le réseau) est génétiquement très éloignée de séquences de référence (de Vargas *et al.*, 2015b), ce qui produit des assignations imprécises, pas toujours au niveau du genre ou de l'espèce. Une idée développée dans la troisième partie de ce manuscrit permettrait de surmonter ce problème. En effet, les symbiotes, du fait de leurs cycles de vie, présentent une distribution particulière le long des fractions de taille. Le genre *Blastodinium* (dinoflagellé) parasite de copépodes en est un parfait exemple. Il est particulièrement présent dans le *piconano*-plancton (0,8-5 µm) et le *nano*-plancton (5-20 µm) correspondant à sa phase libre mais aussi dans le *meso*-plancton (180-2000 µm), fraction de taille dans laquelle ces hôtes (copépodes adultes) sont particulièrement abondants (Skovgaard *et al.*, 2012; Henry *et al.* in prep.). Il semble alors possible de différencier automatiquement les symbiotes des autres organismes en analysant la distribution des metabarcodes le long des fractions de taille (Figure 9). Il est cependant indispensable de travailler avec un jeu de données issu d'une étude par metabarcoding d'échantillons environnementaux soigneusement séparés par fraction de taille. Alors que cela semble relativement aisé pour des échantillons provenant d'environnements aquatiques, il peut s'avérer plus difficile d'appliquer ce fractionnement à d'autres types d'environnement comme les sols. Dans son état actuel la méthode proposée dans ce manuscrit pour étudier la distribution des metabarcodes parmi les fractions de taille (très conservative pour les symbiotes) ne permet pas de différencier les symbiotes des organismes ayant des cycles ou mode de vie leur permettant d'être abondants dans plusieurs fractions de taille (formation de colonies, production de gamètes) (Figure 5). Cette méthode nécessite donc d'être affinée afin de capturer au mieux les symbiotes et donc d'éliminer au maximum le nombre d'association non symbiotiques d'un réseau de cooccurrences.

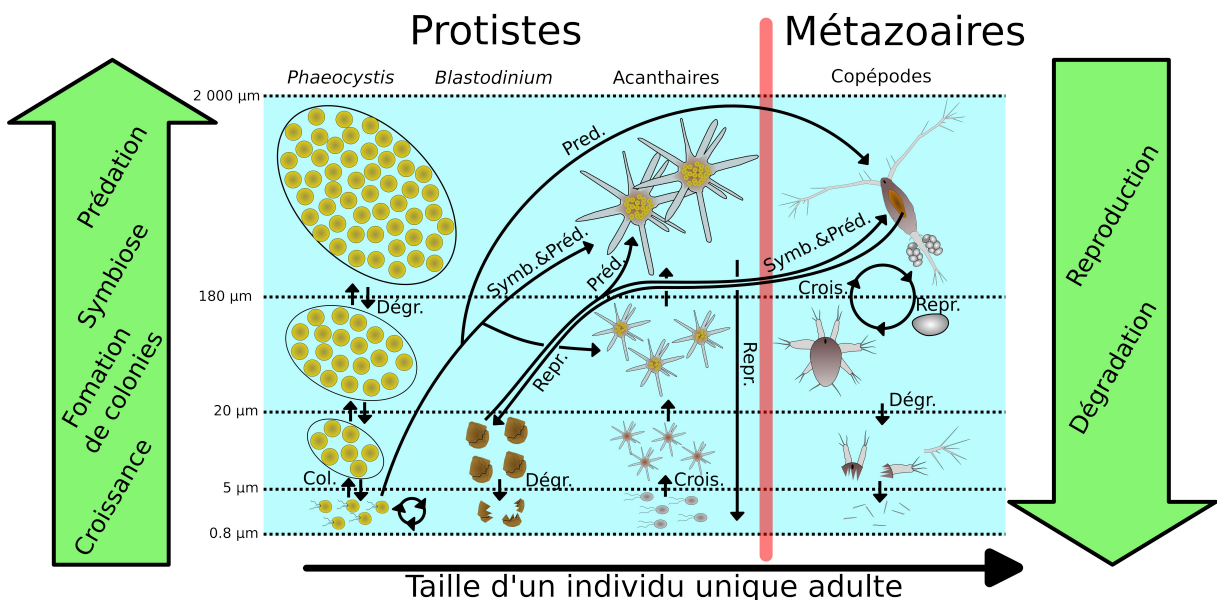


Figure 5: Principaux processus expliquant la détection de metabarcodes dans différentes fractions de taille (ici, le fractionnement de taille utilisé dans le cadre de *Tara Oceans*) représentés grâce à la microalgue haptophyte *Phaeocystis* (symbiose mutualiste d'acanthaires), le dinoflagellé *Blastodinium* (parasite de copépodes), les radiolaires acanthaires et les copépodes. Les principaux processus expliquant le passage à une fraction de taille supérieure sont la croissance (Crois.), la formation de colonies (Col.), la symbiose (Symb.) et la préation (Préd.) et les principaux processus expliquant le passage à une fraction de taille inférieure sont la reproduction (Repr.) et la dégradation (Degr.).

Afin de surmonter le second obstacle, c'est à dire la présence de symbioses peu spécifiques dans le plancton, une solution a également été proposée dans la troisième partie du manuscrit. Il s'agit, lors de l'inférence d'un réseau de cooccurrences de comparer l'abondance de groupes génétiques définis à différents niveaux de résolution. Cette méthode permet par exemple dans le cas de la symbiose entre *Symbiodinium* et *Tiarina* sp. de détecter cette association au niveau de spécificité observé lors de la description de la symbiose. Cette méthode permet de capturer le niveau de spécificité d'une interaction et le score d'association qui lui est associé. Elle permet ainsi de révéler des interactions peu spécifiques qui passent inaperçues lorsque l'on compare les abondances de metabarcodes ou d'OTUs issus d'un clustering résolutif (97 %, 99 %, swarm -d 1).

Les solutions présentées dans ce manuscrit ne sont que les prémisses d'une méthode d'inférence de réseaux de cooccurrences alliant écologie (étude des cycles de vie) et phylogénie (comparaison de groupes génétiques à différents niveaux de résolution) dédiée à la détection de symbioses et de leur histoire évolutive. Les études menées dans le cadre de la théorie des réseaux concernent de plus en plus l'analyses des réseaux multiplexes combinant plusieurs types d'interactions (Kivelä *et al.*, 2013; Boccaletti *et al.*, 2014) et proposent ainsi des solutions permettant la détection de communautés au sein de ces réseaux en prenant en

compte tous les types d'interaction (Tang *et al.*, 2012). A partir d'un jeu de données de type metabarcoding il est possible de construire des réseaux génétiques où chaque nœud correspond à un metabarcode et chaque arrête correspond à une ou plusieurs mutations. Deux réseaux génétiques, un pour les hôtes potentiels et un pour les symbiotes potentiels, peuvent être reliés par les cooccurrences détectées entre les metabarcodes de chaque groupe (hôtes et symbiotes) (Figure 6). L'étude des communautés composant ce réseau multiplexe ainsi obtenu permettrait d'apprécier les processus co-évolutifs inhérents aux associations symbiotiques détectées.

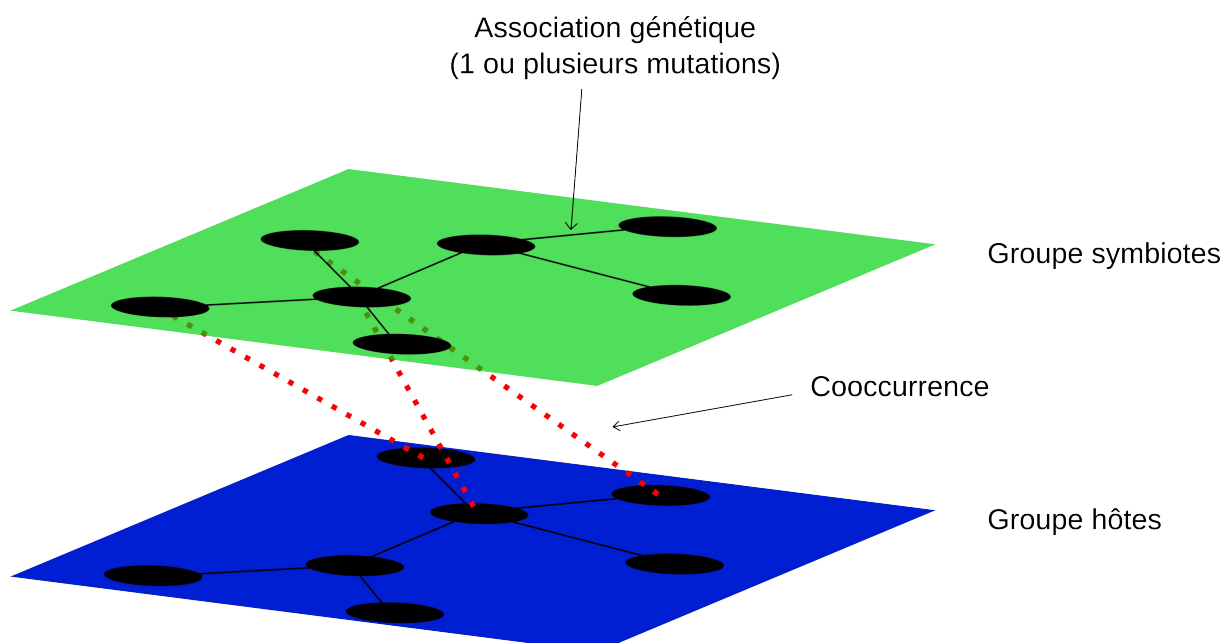


Figure 6: Exemple de réseau multiplexe prenant en compte deux types d'interactions (génétique et écologique)

A partir du début du XX^{ème} siècle, une diversité importante de parasites planctoniques a été décrite morphologiquement (Apstein, 1911; Chatton, 1920 ;Cachon, 1964). Une partie de ces parasites a continué à être étudiée grâce à des approches moléculaires permettant ainsi de confirmer leur position dans l'arbre du vivant et de mieux connaître leur écologie, mais un certain nombre de parasites reste encore trop peu connu. C'est le cas par exemple des parasites de Radiolaires, pour lesquels un nombre important d'espèces de différents genres (*Amoebophrya*, *Apodinium*, *Atlanticellodium*, *Keppenodinium*, *Oodinium*, *Solenodinium*, *Syndinium*) appartenant aux syndiniales et aux blastodiniales a été uniquement décrit morphologiquement (Cachon and Cachon, 1987). Sans références génétiques il est délicat de confirmer leur assignation taxinomique. Par contre ces anciennes observations sont à mettre en relation avec l'observation récente chez des individus uniques de radiolaires d'un nombre important de séquences assignées à des dinoflagellés et des syndiniales (MALV I et MALV

II))(Dolven *et al.*, 2007; Bråte *et al.*, 2012). Ces séquences proviennent-elles d'organismes parasitant l'individu séquencé ou s'agit-il de proies? Cette question mérite une attention toute particulière, car l'étude des parasites de radiolaires permettrait de mieux comprendre la dynamique des populations de ces géants du plancton. De nouvelles méthodes de détection de symbioses par réseaux de cooccurrences seront un atout majeur pour enrichir notre connaissance des parasites des radiolaires. De manière générale, il apparaît judicieux de profiter de la richesse d'anciennes observations afin d'axer les analyses dans leur sens. Ceci permettrait d'accélérer la description des symbioses planctoniques et de valoriser ces connaissances qui risquent de tomber dans l'oubli.

La généralisation de l'utilisation du metabarcoding pour l'étude de la composition et de la structure des communautés naturelles est l'occasion de décrire de nouvelles symbioses. En plus de l'expédition *Tara Oceans* (2009-2013) ayant permis l'échantillonnage de 210 stations réparties dans tous les océans du globe, des initiatives institutionnelles et citoyennes, comme le projet Ocean Sampling Day (Kopf *et al.*, 2015) permettent d'augmenter significativement l'effort d'échantillonnage des océans. Les données de metabarcoding ainsi générées constituent un trésor pour quiconque cherche à dévoiler les rouages du fonctionnement des écosystèmes planctoniques. L'utilisation de méthodes de détection de symbioses par réseaux de cooccurrences sur des jeux de données provenant de l'échantillonnage de plusieurs centaines voir milliers de stations réparties dans le temps et l'espace permettrait assurément la description de nouvelles symbioses, car les associations sont d'autant plus faciles à détecter que le nombre de points de mesure est élevé. L'utilisation du metabarcoding sur des échantillons fractionnés par taille provenant de suivis temporels permettrait de mieux connaître l'écologie des organismes symbiotiques. En effet, les organismes symbiotiques du plancton sont généralement observés à la fois sous leur forme libre et leur forme symbiotique. À partir du moment où l'on arrive à savoir quelles fractions de taille correspondent à chacune de ces phases, il est possible de suivre dans le temps leur évolution. Ceci est particulièrement intéressant dans le cas des parasites pour lesquels les dynamiques d'infection sont encore assez peu connues.

Bibliographie

Références citées dans l'introduction, les objectifs, les parties de transition et la conclusion.

AMARAL-ZETTLER, Linda A., MCCLIMENT, Elizabeth A., DUCKLOW, Hugh W., *et al.* A method for studying protistan diversity using massively parallel sequencing of V9 hypervariable regions of small-subunit ribosomal RNA genes. *PLoS One*, 2009, vol. 4, no 7, p. e6372.

ANDERSON, O. ROGER. The radiolarian symbiosis. *Algal Symbiosis: A Continuum of Interaction Strategies*, 1983, p. 69-89.

APSTEIN, Carl, Parasiten von *Calanus finmarchicus*. Wissenschaftliche Meeresuntersuchungen. Abt. Kiel., 1911, vol. 13, p. 205-223.

AZAM, Farooq, FENCHEL, Tom, FIELD, John G, *et al.* The ecological role of water-column microbes in the sea. *Estuaries*, 1983, vol. 50, no 2.

DE BARY, Anton. *Die erscheinung der symbiose*. Verlag von Karl J. Trübner, 1879.

BENJAMINI, Yoav et HOCHBERG, Yosef. Controlling the false discovery rate: a practical and powerful approach to multiple testing. *Journal of the Royal Statistical Society. Series B (Methodological)*, 1995, p. 289-300.

BLAXTER, Mark, MANN, Jenna, CHAPMAN, Tom, *et al.* Defining operational taxonomic units using DNA barcode data. *Philosophical Transactions of the Royal Society of London B: Biological Sciences*, 2005, vol. 360, no 1462, p. 1935-1943.

BOCCALETTI, Stefano, BIANCONI, G., CRIADO, R., *et al.* The structure and dynamics of multilayer networks. *Physics Reports*, 2014, vol. 544, no 1, p. 1-122.

BRÅTE, Jon, KRABBERØD, Anders K., DOLVEN, Jane K., *et al.* Radiolaria associated with large diversity of marine alveolates. *Protist*, 2012, vol. 163, no 5, p. 767-777.

BROWN, Morton B. 400: A method for combining non-independent, one-sided tests of significance. *Biometrics*, 1975, p. 987-992.

BURNS, Carolyn W. Parasitic regulation in a population of *Boeckella hamata* Brehm (Copepoda: Calanoida). *Freshwater biology*, 1989, vol. 21, no 3, p. 421-426.

CACHON, Jean. Contribution à l'étude des périodiniens parasites. Cytologie, cycles évolutifs. *Annales des Sciences Naturelles - Zoologie et Biologie Animale*, 1964, vol. 6, p. 1-158.

- CACHON, Jean et CACHON, Monique. Parasitic dinoflagellates. *The biology of dinoflagellates*, 1987, vol. 21, p. 571-610.
- CARON, David A., COUNTWAY, Peter D., SAVAI, Pratik, et al. Defining DNA-based operational taxonomic units for microbial-eukaryote ecology. *Applied and environmental microbiology*, 2009, vol. 75, no 18, p. 5797-5808.
- CHAMBOUVET, Aurelie, MORIN, Pascal, MARIE, Dominique, et al. Control of toxic marine dinoflagellate blooms by serial parasitic killers. *Science*, 2008, vol. 322, no 5905, p. 1254-1257.
- CHATTON, Édouard. Les Péridiniens parasites: Morphologie, reproduction, éthologie. *Archives de zoologie expérimentale et générale*, 1920, vol 59, p. 1–475.
- DAUGBJERG, Niels, JENSEN, Maria Hastrup, et HANSEN, Per Juel. Using nuclear-encoded LSU and SSU rDNA sequences to identify the Eukaryotic Endosymbiont in *Amphisolenia bidentata* (Dinophyceae). *Protist*, 2013, vol. 164, no 3, p. 411-422.
- DAVIDSON, Keith. The challenges of incorporating realistic simulations of marine protists in biogeochemically based mathematical models. *Acta Protozoologica*, 2014, vol. 53, no 1, p. 129.
- DECAESTECKER, Ellen, DECLERCK, Steven, DE MEESTER, Luc, et al. Ecological implications of parasites in natural Daphnia populations. *Oecologia*, 2005, vol. 144, no 3, p. 382-390.
- DECCELLE, Johan. New perspectives on the functioning and evolution of photosymbiosis in plankton: Mutualism or parasitism?. *Communicative & integrative biology*, 2013, vol. 6, no 4, p. e24560.
- DECCELLE, Johan, COLIN, Sébastien, et FOSTER, Rachel A. Photosymbiosis in marine planktonic protists. In : *Marine Protists*. Springer Japan, 2015. p. 465-500.
- DECCELLE, Johan, PROBERT, Ian, BITTNER, Lucie, et al. An original mode of symbiosis in open ocean plankton. *Proceedings of the National Academy of Sciences*, 2012, vol. 109, no 44, p. 18000-18005.
- DENNELL, Mark R., CARON, David A., MICHAELS, Anthony F., et al. Video plankton recorder reveals high abundances of colonial Radiolaria in surface waters of the central North Pacific. *Journal of Plankton Research*, 2002, vol. 24, no 8, p. 797-805.

- Text W2, Figure W3. In :DE VARGAS, Colomban, AUDIC, Stéphane, HENRY, Nicolas, et al. *Companion Website to the article: "Eukaryotic plankton diversity in the sunlit ocean"*. [en ligne]. 2015a. Disponible à l'adresse: <http://taraoceans.sb-roscoff.fr/EukDiv/>
- DE VARGAS, Colomban, AUDIC, Stéphane, HENRY, Nicolas, et al. Eukaryotic plankton diversity in the sunlit ocean. *Science*, 2015b, vol. 348, no 6237, p. 1261605.
- DÍEZ, Beatriz, PEDRÓS-ALIÓ, Carlos, et MASSANA, Ramon. Study of genetic diversity of eukaryotic picoplankton in different oceanic regions by small-subunit rRNA gene cloning and sequencing. *Applied and environmental microbiology*, 2001, vol. 67, no 7, p. 2932-2941.
- DOLVEN, Jane K., LINDQVIST, Charlotte, ALBERT, Victor A., et al. Molecular diversity of alveolates associated with neritic North Atlantic radiolarians. *Protist*, 2007, vol. 158, no 1, p. 65-76.
- FALKOWSKI, Paul. Ocean science: the power of plankton. *Nature*, 2012, vol. 483, no 7387, p. S17-S20.
- FAUST, Karoline et RAES, Jeroen. Microbial interactions: from networks to models. *Nature Reviews Microbiology*, 2012, vol. 10, no 8, p. 538-550.
- FAUST, Karoline, SATHIRAPONGSASUTI, J. Fah, IZARD, Jacques, et al. Microbial co-occurrence relationships in the human microbiome. *PLoS computational biology*, 2012, vol. 8, no 7, p. e1002606-e1002606.
- FLYNN, Kevin J., STOECKER, Diane K., MITRA, Aditee, et al. Misuse of the phytoplankton–zooplankton dichotomy: the need to assign organisms as mixotrophs within plankton functional types. *Journal of Plankton Research*, 2012, p. fbs062.
- GOBILLARD, Marie-Odile. *Cephaloidophora petiti* sp. n., Grégarine parasite de Copépodes pélagiques de la région de Banyuls (note préliminaire). *Vie et Milieu Suppl*, 1964, vol. 17, p. 107-113.
- GUILLOU, Laure, BACHAR, Dipankar, AUDIC, Stéphane, et al. The Protist Ribosomal Reference database (PR2): a catalog of unicellular eukaryote small sub-unit rRNA sequences with curated taxonomy. *Nucleic acids research*, 2013, p. gks1160.
- GUO, Zhiling, LIU, Sheng, HU, Simin, et al. Prevalent ciliate symbiosis on copepods: high genetic diversity and wide distribution detected using small subunit ribosomal RNA gene. *PloS one*, 2012, vol. 7, no 9, p. e44847.

- HEBERT, Paul DN, CYWINSKA, Alina, BALL, Shelley L., et al. Biological identifications through DNA barcodes. *Proceedings of the Royal Society of London B: Biological Sciences*, 2003, vol. 270, no 1512, p. 313-321.
- HO, Ju-shey et PERKINS, Penny S. Symbionts of marine copepoda: an overview. *Bulletin of marine science*, 1985, vol. 37, no 2, p. 586-598.
- JEPHCOTT, Thomas G., ALVES-DE-SOUZA, Catharina, GLEASON, Frank H., et al. Ecological impacts of parasitic chytrids, syndiniales and perkinsids on populations of marine photosynthetic dinoflagellates. *Fungal Ecology*, 2016, vol 19, p. 47-58.
- JI, Yinqiu, ASHTON, Louise, PEDLEY, Scott M., et al. Reliable, verifiable and efficient monitoring of biodiversity via metabarcoding. *Ecology letters*, 2013, vol. 16, no 10, p. 1245-1257.
- JOHNSON, Matthew D., OLDACH, David, DELWICHE, Charles F., et al. Retention of transcriptionally active cryptophyte nuclei by the ciliate *Myrionecta rubra*. *Nature*, 2007, vol. 445, no 7126, p. 426-428.
- JOHNSON, Nancy C., GRAHAM, J.-H., et SMITH, F. Andrew. Functioning of mycorrhizal associations along the mutualism–parasitism continuum*. *New phytologist*, 1997, vol. 135, no 4, p. 575-585.
- KAGAMI, Maiko, DE BRUIN, Arnout, IBELINGS, Bas W., et al. Parasitic chytrids: their effects on phytoplankton communities and food-web dynamics. *Hydrobiologia*, 2007, vol. 578, no 1, p. 113-129.
- KIVELÄ, Mikko, ARENAS, Alex, BARTHELEMY, Marc, et al. Multilayer networks. *Journal of Complex Networks*, 2014, vol. 2, no 3, p. 203-271.
- KOIKE, Kazuhiko et TAKISHITA, Kiyotaka. Anucleated cryptophyte vestiges in the gonyaulacalean dinoflagellates *Amylax buxus* and *Amylax triacantha* (Dinophyceae). *Phycological research*, 2008, vol. 56, no 4, p. 301-311.
- KOPF, Anna, BICAK, Mesude, KOTTMANN, Renzo, et al. The ocean sampling day consortium. *GigaScience*, 2015, vol. 4, no 1, p. 1-5.
- KURIS, Armand M., HECHINGER, Ryan F., SHAW, Jenny C., et al. Ecosystem energetic implications of parasite and free-living biomass in three estuaries. *Nature*, 2008, vol. 454, no 7203, p. 515-518.
- LAMPITT, R. S., SALTER, I., et JOHNS, D. Radiolaria: major exporters of organic carbon to the deep ocean. *Global Biogeochemical Cycles*, 2009, vol. 23, no 1.

- LIDICKER, William Z. A clarification of interactions in ecological systems. *BioScience*, 1979, vol. 29, no 8, p. 475-477.
- LIMA-MENDEZ, Gipsi, FAUST, Karoline, HENRY, Nicolas, et al. Determinants of community structure in the global plankton interactome. *Science*, 2015, vol. 348, no 6237, p. 1262073.
- LÓPEZ-GARCÍA, Purificación, RODRIGUEZ-VALERA, Francisco, PEDRÓS-ALIÓ, Carlos, et al. Unexpected diversity of small eukaryotes in deep-sea Antarctic plankton. *Nature*, 2001, vol. 409, no 6820, p. 603-607.
- MADHU, Nikathithara V., JYOTHIBABU, Retnamma, MAHESWARAN, Padinjaratte A., et al. Enhanced chlorophyll a and primary production in the northern Arabian Sea during the spring intermonsoon due to green *Noctiluca scintillans* bloom. *Marine Biology Research*, 2012, vol. 8, no 2, p. 182-188.
- MAHÉ, Frédéric, ROGNES, Torbjørn, QUINCE, Christopher, et al. Swarm: robust and fast clustering method for amplicon-based studies. *PeerJ*, 2014, vol. 2, p. e593.
- DE MEEÙS, Thierry et RENAUD, François. Parasites within the new phylogeny of eukaryotes. *Trends in parasitology*, 2002, vol. 18, no 6, p. 247-251.
- MICHAELS, Anthony F., CARON, David A., SWANBERG, Neil R., et al. Planktonic sarcodines (Acantharia, Radiolaria, Foraminifera) in surface waters near Bermuda: abundance, biomass and vertical flux. *Journal of Plankton Research*, 1995, vol. 17, no 1, p. 131-163.
- MOON-VAN DER STAAY, Seung Yeo, DE WACHTER, Rupert, et VAULOT, Daniel. Oceanic 18S rDNA sequences from picoplankton reveal unsuspected eukaryotic diversity. *Nature*, 2001, vol. 409, no 6820, p. 607-610.
- MORDRET Solenn, ROMAC Sarah, HENRY Nicolas. The symbiotic life of *Symbiodinium* in the open ocean within a new species of calcifying ciliate (*Tiarina* sp.). *The ISME journal*, 2015, Press 1-13.
- NOWACK, Eva CM et MELKONIAN, Michael. Endosymbiotic associations within protists. *Philosophical Transactions of the Royal Society B: Biological Sciences*, 2010, vol. 365, no 1541, p. 699-712.
- OHTSUKA, Susumu, HORA, Mariko, SUZAKI, Toshinobu, et al. Morphology and host-specificity of the apostome ciliate *Vampyrophrya pelagica* infecting pelagic copepods in the Seto Inland Sea, Japan. *Marine Ecology Progress Series*, 2004, vol. 282, p. 129-142.

- VAN OMMEREN, Ron J. et WHITHAM, Thomas G. Changes in interactions between juniper and mistletoe mediated by shared avian frugivores: parasitism to potential mutualism. *Oecologia*, 2002, vol. 130, no 2, p. 281-288.
- PARK, Myung Gil, YIH, Wonho, et COATS, D. Wayne. Parasites and phytoplankton, with special emphasis on dinoflagellate infections1. *Journal of Eukaryotic Microbiology*, 2004, vol. 51, no 2, p. 145-155.
- PROBERT, Ian, SIANO, Raffaele, POIRIER, Camille, et al. *Brandtodinium* gen. nov. and *B. nutricula* comb. Nov.(Dinophyceae), a dinoflagellate commonly found in symbiosis with polycystine radiolarians. *Journal of Phycology*, 2014, vol. 50, no 2, p. 388-399.
- RASCONI, Serena, NIQUIL, Nathalie, et SIME-NGANDO, Télesphore. Phytoplankton chytridiomycosis: community structure and infectivity of fungal parasites in aquatic ecosystems. *Environmental microbiology*, 2012, vol. 14, no 8, p. 2151-2170.
- RAZOULS, Claude, DE BOVÉE, Francis, KOUWENBERG, Juliana, et al. Diversity and geographic distribution of marine planktonic copepods. Available from WWW:<<http://copepodes.obs-banyuls.fr/en>>[cited 2015-10-01], 2005-2015.
- SALOMON, Paulo S., GRANÉLI, Edna, NEVES, Maria HCB, et al. Infection by *Amoebophrya* spp. parasitoids of dinoflagellates in a tropical marine coastal area. *Aquatic microbial ecology*, 2009, vol. 55, no 2, p. 143-153.
- SCHOLZ, Bettina, GUILLOU, Laure, MARANO, Agostina V., et al. Zoosporic parasites infecting marine diatoms—A black box that needs to be opened. *Fungal Ecology*, 2016, vol. 19, p. 59-76.
- SHAKED, Yonathan et DE VARGAS, Colomban. Pelagic photosymbiosis: rDNA assessment of diversity and evolution of dinoflagellate symbionts and planktonic foraminiferal hosts. *Marine Ecology Progress Series*, 2006, vol. 325, p. 59-71.
- SIANO, Raffaele, ALVES-DE-SOUZA, C., FOULON, E., et al. Distribution and host diversity of Amoebophryidae parasites across oligotrophic waters of the Mediterranean Sea. *Biogeosciences*, 2011, vol. 8, no 2, p. 267-278.
- SKOVGAARD, Alf. Dirty tricks in the plankton: Diversity and Role of Marine Parasitic Protists: diversity and role of marine parasitic protists. *Acta Protozoologica*, 2014, vol. 53, no 1, p. 51-62.

- SKOVGAARD, Alf, KARPOV, Sergey A., et GUILLOU, Laure. The parasitic dinoflagellates *Blastodinium* spp. inhabiting the gut of marine, planktonic copepods: morphology, ecology, and unrecognized species diversity. *Frontiers in microbiology*, 2012, vol. 3.
- SMETACEK, Victor. Making sense of ocean biota: How evolution and biodiversity of land organisms differ from that of the plankton. *Journal of biosciences*, 2012, vol. 37, no 4, p. 589-607.
- STEELE, John H. *The structure of marine ecosystems*. 1974.
- STOECKER, Diane K., JOHNSON, Matthew D., DE VARGAS, Colomban, *et al.* Acquired phototrophy in aquatic protists. *Aquatic Microbial Ecology*, 2009, vol. 57, p. 279-310.
- TABERLET, Pierre, COISSAC, Eric, POMPANON, Francois, *et al.* Towards next-generation biodiversity assessment using DNA metabarcoding. *Molecular Ecology*, 2012, vol. 21, no 8, p. 2045-2050.
- TANG, Lei, WANG, Xufei, et LIU, Huan. Community detection via heterogeneous interaction analysis. *Data Mining and Knowledge Discovery*, 2012, vol. 25, no 1, p. 1-33.
- TRENCH, R. K. The cell biology of plant-animal symbiosis. *Annual Review of Plant Physiology*, 1979, vol. 30, no 1, p. 485-531.
- WALKUSZ, W. et ROLBIECKI, L. Epibionts (Paracineta) and parasites (Ellobiopsis) on copepods from Spitsbergen (Kongsfjorden area). *Oceanologia*, 2007, vol. 49, no 3.
- WINDSOR, Donald A. Controversies in parasitology, Most of the species on Earth are parasites. *International journal for parasitology*, 1998, vol. 28, no 12, p. 1939-1941.
- WORDEN, Alexandra Z., FOLLOWS, Michael J., GIOVANNONI, Stephen J., *et al.* Rethinking the marine carbon cycle: Factoring in the multifarious lifestyles of microbes. *Science*, 2015, vol. 347, no 6223, p. 1257594.

Liste des figures

Figures de l'introduction, des objectifs, des parties de transition et de la conclusion.

Figure 1: Réseau des associations symbiotiques entre eucaryotes du plancton marin décrites dans la littérature.....	18
Figure 2: Diversité génétique et biogéographie des metabarcodes séquencés à partir des individus de <i>Tiarina</i> et de <i>Symbiodinium</i> en symbiose.....	83
Figure 3: Arbre phylogénétique (Neighbor-joining) des metabarcodes (fragment V9) assignés aux Péridiniales (Dinoflagellés) et leur distribution parmi les fractions de taille.....	149
Figure 4: Réseaux d'haplotypes de <i>Symbiodinium</i> illustrant le caractère imbriqué des groupes génétiques construits à différents niveaux de résolution.....	151
Figure 5: Principaux processus expliquant la détection de metabarcodes dans différentes fractions de taille.....	209
Figure 6: Exemple de réseau multiplex prenant en compte deux types d'interactions (génétique et écologique).....	210

Glossaire

- **Barcode/Metabbarcode:** Marqueur génétique utilisé dans une étude de (meta)barcoding. Ce terme peut également faire référence une séquence unique de ce marqueur.
- **DNA barcoding:** Méthode taxinomique utilisant un court marqueur génétique de l'ADN d'un organisme afin de définir son appartenance à une espèce.
- **DNA metabarcoding:** DNA barcoding appliqué à un assemblage de populations.
- **OTU:** Operational Taxonomic Unit, Unité Taxonomique Opérationnelle en français. Définition opérationnelle d'une espèce ou d'un groupe d'espèces souvent utilisée lorsque seules des données de séquences d'ADN sont disponibles.
- **Photosymbiose:** Symbiose, généralement mutualiste, impliquant un partenaire photosynthétique.

Annexes

Liste des communications orales

Communications orales:

- OCEANOMICS annual meeting – Octobre 2015 – Roscoff, France - “Unveiling photosymbiotic associations and their specificity in world-wide marine plankton based on massive rDNA metabarcoding.”
- Ateliers en Ecologie Evolutive (Evolution de la symbiose)– Janvier 2014 – Plouzané, France: “The use of NGS metabarcoding to unveil host-parasite relationships in marine world plankton.”
- 2nd Colloque de Génomique Environnementale – Novembre 2013 – Rennes, France: “The use of NGS metabarcoding to unveil host-parasite relationships in marine world plankton.”
- Journées de l’École Doctorale Diversité du Vivant – Octobre 2013 – Roscoff, France: “Mise en évidence de symbioses dans le plancton marin grâce au metabarcoding.”
- Tara Oceans retreat – Mai 2013 – Roscoff, France: “Highlighting biological interactions in plankton using numerical ecology tools on metabarcodes.”
- Journées thématiques du GPLF – Octobre 2012 – La Rochelle, France: “Etude de la physiologie et de l'enkystement d'un dinoflagellé toxique, *Alexandrium minutum* Halim.”

Posters:

- Conférence Jacques Monod "Biologie marine éco-systémique" _ Juin 2015 _ Roscoff, France: “Unveiling symbiotic relationships in marine world plankton based on massive rDNA metabarcoding.”

- Gen2Bio _ Mars 2015 _ La Baule, France: “Eukaryotic plankton diversity in the sunlit ocean.”

Résumé :

Les symbioses ont un rôle majeur dans le fonctionnement et l'équilibre des écosystèmes. Dans les océans, qui couvrent près de 70 % de la surface de la planète, vivent une multitude d'organismes incapables de lutter contre les courants et la plupart sont microscopiques, il s'agit du plancton. Les organismes du plancton, comme ceux d'autres écosystèmes, entretiennent des symbioses, mais la nature et l'ampleur de ces interactions sont encore mal connues dans le plancton du fait la petite taille de ces organismes et de la difficulté d'échantillonnage des écosystèmes planctoniques, surtout dans les zones les plus éloignées des côtes. Les principaux objectifs de cette thèse sont de donner un aperçu global de la place occupée par ces symbioses dans le plancton et de proposer des méthodes originales permettant leur détection. Les travaux présentés dans ce manuscrit s'appuient sur l'analyse des données générées lors de l'expédition *Tara Oceans* (2009-2013) pendant laquelle 210 stations océaniques ont été échantillonnées à travers le monde. Ils concernent plus précisément le jeu de données environnemental obtenu grâce au séquençage à haut débit (Illumina) de la région hypervariable V9 (130 nucléotides) de la sous-unité 18S de l'ADN ribosomique des organismes eucaryotes (metabarcoding). Dans un premier temps, un état des lieux de la diversité et de la structure des communautés du *pico-nano-micro-mesoplancton* (0,8-2000 µm) eucaryote de la zone photique des océans tempérés à tropicaux est réalisé. Il met en évidence la place importante occupée par les symbiotes au sein de ces communautés. Ensuite, l'étude de deux cas de symbiose (*Blastodinium-Copépodes* et *Symbiodinium-Tiarina*) montre les difficultés inhérentes à la détection de couples symbiotiques à partir d'un jeu de données issue d'études par metabarcoding du plancton (flexibilité de la spécificité des symbioses dans le plancton), mais aussi la possibilité de distinguer les différentes phases de vie des symbiotes (libres et symbiotiques) lorsque les échantillons étudiés ont été fractionnés. Enfin, un ensemble de méthodes est proposé afin d'améliorer l'efficacité de la détection de symbioses dans le cadre d'études par réseau de cooccurrences des communautés planctoniques. L'analyse de la distribution des metabarcodes le long des fractions de taille (*piconano-* (0.8-5 µm), *nano-* (5-20 µm), *micro-* (20-180 µm), et *meso-plancton* (180-2000 µm)) permet de différencier ceux provenant d'organismes symbiotiques de ceux d'organismes libres, sans a priori. De plus la comparaison de l'abondance de groupes génétiques définis à différents niveaux de résolution permet de détecter des associations symbiotiques peu spécifiques et d'apprécier leur niveau de spécificité.

Mots clés : symbiose, plancton, metabarcoding

Molecular ecology of eukaryotic symbioses in the planktonic ecosystems of the oceanic photic zone

Abstract :

The oceans, which cover nearly 70 % of the earth's surface, is host to a myriad of mostly microscopic organisms that drift with the currents and are collectively called plankton. As in other ecosystems, symbioses play a major role in the functioning and equilibrium of the plankton. But the exact nature and strength of those symbiotic interactions are still poorly known, not only due to the small size of most planktonic organisms, but also because of the inherent difficulty of sampling planktonic ecosystems, especially in the high-seas. The main goals of this thesis are to give a global view of the importance of planktonic symbioses and to propose novel methods for their detection. The work presented in this manuscript is based on analyses of data generated during the *Tara Oceans* expedition (2009-2013), during which sea water was collected and size fractionated by filtration at 210 sampling locations distributed across the world's oceans. The data analyses presented herein mostly focus on an environmental metabarcoding dataset obtained from next-generation sequencing (Illumina) of the V9 hypervariable region (~130 nucleotides long) of the 18S small ribosomal subunit of eukaryotic organisms. We begin by assessing the diversity and structure of pico-, nano-, micro and meso-planktonic eukaryotic communities (0.8-2000 µm) in the photic zone of tropical to temperate sea regions. Then, we present two cases of symbioses (*Blastodinium-Copepods* and *Symbiodinium-Tiarina*) to illustrate both the difficulties encountered when trying to detect symbiotic relationships using metabarcoding data due to varying specificities of symbiotic relationships, but also the potential solutions offered by size-fractionated sampling to distinguish between the different stages of the life cycle of symbiotic organisms (free living and symbiotic stages). Finally, we propose a set of methods to improve the detection of symbioses by studying the co-occurrence of organisms in planktonic communities: we use the distribution of metabarcodes along size fractions ((*piconano-* (0.8-5 µm), *nano-* (5-20 µm), *micro-* (20-180 µm), and *meso-plancton* (180-2000 µm)) to distinguish likely free living organisms from those that have a symbiotic life style, and we compare the abundance of genetic groups constructed by clustering metabarcodes at different resolution levels, which allows us to detect interactions occurring above the species level and to evaluate their level of specificity.

Keywords : symbiosis, plankton, metabarcoding